THE INTEGRATION OF COMPUTATIONAL AND SPECTROSCOPIC INFORMATION FOR HYDROGEN BONDED SYSTEMS

JASON MARK PRICE

A submission presented in partial fulfilment of the requirements of the University of Glamorgan/Prifysgol Morgannwg for the degree of Doctor of Philosophy

This research was carried out in collaboration with Chemical Design Ltd., Oxfordshire and The Rutherford Appleton Laboratory, Didcot

December 2000

Certificate of Research

This is to certify that, except where specific reference is made, the work described in this thesis is the result of the candidate. Neither this thesis, nor any part of it, has been presented, or is currently submitted, in candidature for any degree at any other University.

Signed ..... *Candidate*

Signed ..... *Director of Studies*

Date ...30 Jan 2001.....

COPYRIGHT STATEMENT

I declare that the work contained in this thesis is my own.

Publications arising from this work are appended with this thesis.

ACKNOWLEDGMENTS

I would like to express my gratitude to the University of Glamorgan for the studentship that allowed me to study and submit this PhD thesis.

I am also extremely grateful to my PhD supervisors, Dr. Rhobert Lewis, Dr Brian Jones and Professor John Dixon, for their support, insight and advice.

I would also like to thank my Director of Studies, Professor Bill George for his continual and limitless patience, his enthusiasm for the subject and his friendship over the last six years. I wish him the very best of everything for the future.

I would also like to thank Sal, the laboratory technician, for his friendship, and everyone else within the University who have provided help in some way.

Only when you finish a work such as this do you realise exactly how much the burden is felt by those close to you. For tolerating this PhD thesis and me for the last couple of years, when I know I have not been an easy person to live with, I would like to express my deepest thanks to my Mum and Dad. I love you both so much. Thank you for keeping the faith, folks!

This PhD thesis is dedicated to my nephews, James and Gianluca, for sunshine every day, perspective and the realisation that I have done the right thing, that there *is* light at the end of the tunnel.

"At it's beginning I felt no real hope of finding the light; now it glimmers dimly, encouragingly, but intermittently in the hall of mirrors around me. I suppose if we ever knew exactly where the light was coming from getting there would be easy..."

Brian May, 20th July 1992.

ABSTRACT

The infrared spectra of methanol as dilute solutions in CCl_4 and in the vapour phase have been measured between 2500 and 4000 cm^{-1} and between 1000 and 1100 cm^{-1} in order to better understand the nature of the hydrogen bonding equilibria present. The integrated absorption coefficient of the monomeric O-H stretching mode is calculated as $(2.157 \pm 0.025)\times10^4$ m mol^{-1} and the proportion of the components associated with the three principal bands and a fourth weaker band estimated. Seven possible components were considered which were monomer, closed cyclic and open chain dimers, trimers and tetramers. *Ab initio* calculations were carried out on these components using six basis sets up to the restricted Hartree Fock 6-311++G(3df,3pd) level. Relevant calculated infrared wavenumber and intensity values, O-H...O bond lengths and hydrogen bonding energies are reported. The cyclic dimer is shown to be a transition state with the open dimer forming a stable minimum energy form. In the case of the trimer and tetramer the hydrogen bonding energy is calculated to be respectively 12 and 32 kJ mol^{-1} greater in the cyclic form than in the open form with good agreement at the RHF6-31G(d) and RHF 6-31++G(d,p) levels. The experimental and theoretical results are consistent with an equilibrium involving monomer, open dimer, cyclic trimer and cyclic tetramer.

Also, *ab initio* calculations are reported for HCl complexes of H_2CO, CH_3HCO, $(CH_3)_2CO$, HCN, CH_3CN, C_2H_5CN, HCOCN and CH_3COCN. Comparison with experimentally determined values of hydrogen bond energy, HCl wavenumber shifts and bond lengths for the four smallest complexes suggest a suitable method and basis set is B3LYP/6-311++G(2d,2p). In the case of CH_3HCO there are two possible isomers in which the HCl is *cis* and *trans* to the aldehydic H atom (low and high energy forms respectively). The two bi-functional complexes each have three possible isomers; HCl may bond to the nitrile group, to the carbonyl group *cis* to the nitrile or to the carbonyl group *trans* to the nitrile . Calculated values of hydrogen bond energy; harmonic HCl, CO and CN stretching modes; hydrogen bond lengths and other associated lengths and angles are reported for all seven mono- and all six bi-functional complexes and compared with experimentally determined values, when known. These properties are predicted in other cases including those of the newly described high energy complex of CH_3HCO, and those of three newly described complexes of both HCOCN and CH_3COCN.

CONTENTS

Chapter 1

Introduction

Chapter 2

Experimental Methods of FT-IR Spectroscopy

Chapter 3

Computational Chemistry

Chapter 4

Software Description

Chapter 5

Hydrogen Bonded Forms of Methanol – Infrared Spectra and *Ab Initio* Calculations

Chapter 6

An *Ab Initio* Study of medium strength Hydrogen Bonding of Mono- and Bi-Functional Carbonyl and Nitrile Complexes with Hydrogen Chloride.

Chapter 7

Conclusions and Suggested Further Work.

Chapter 1

Introduction.

1.1 An overview of the project.

Computational chemistry has evolved in parallel with the ever-increasing power of modern desktop computers. A result of this is the development of *ab initio* calculation techniques for analysing molecular structures. *Ab initio*, translated from the Latin, literally means "from the beginning", and these calculations are based on the fundamental postulates of Quantum Mechanics. This theoretical structural information is invaluable to the experimentalist, as it allows predictions to be made on the outcome of reactions, and the geometrical implications at the molecular level.

Hydrogen bonding, usually observed where a hydrogen atom acts as a bridge between two electronegative atoms, has many implications in nature. It is the reason why water is a liquid at room temperature, and is responsible for the replication of DNA. It is not really understood, due to the many variables that affect H-bonding.

Molecular modelling of H-bonded complexes, whether they are intra- or intermolecularly bonded, can be achieved, to a certain extent, with the Chem-X software. A conformational analysis of such complexes can be performed to find the idealised structure at the global energy minimum. However, for a more detailed approach, an *ab initio* package, such as Gaussian, will be required. This is capable of finding localised minima, as well as the global minimum, and will thus provide a more generalised picture of the various conformations allowed in the H-bonded complexes.

It is hoped that eventually, methods such as FT-IR spectroscopy will provide experimental verification of the validity of the calculations, so that such calculations may be used in parallel with the experiment, combining quantum mechanical ideas with laboratory measurements. Presented here is a study of hydrogen bonded methanol complexes and medium strength hydrogen bonding (mono- and bi-functional carbonyl and

nitrile complexes). It is hoped that the calculations will provide a greater insight into these systems, and that the readily available experimental data will validate the work.

1.2 Hydrogen Bonding.

1.2.1 Initial ideas of Hydrogen Bonding.

The idea of hydrogen bonding (H-bonding) began as a proposal by Werner in 1902 that ammonium hydroxide is the "addition product" of water and ammonia[1]:

$$H_3N \cdots H{-}OH \rightleftharpoons H_3N{-}H \cdots OH$$

(··· denotes a hydrogen bond)

In 1911, Knorr described the structure of acetoacetic ester in terms of tautomerism involving an enol form, stabilised by hydrogen bonding, and a keto form[2]:

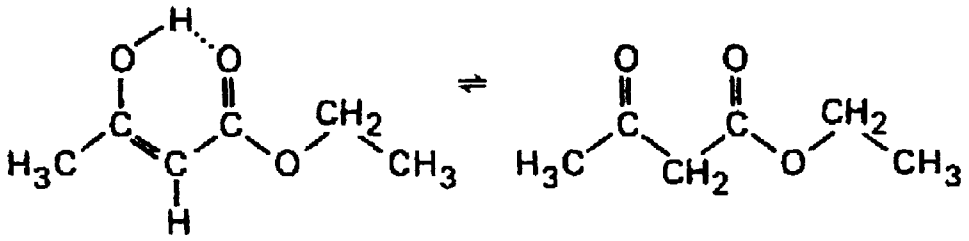

And in 1914, Pfeiffer discovered the cyclic dimer structure of carboxylic acid complexes[3]:

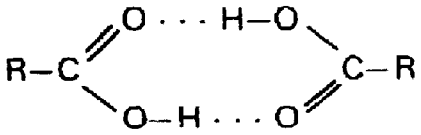

In 1916, G N Lewis formulated a theory of bonding that embodied a vast amount of empirical chemical information[4]. He saw that many compounds could be understood by applying the fact that they strived to achieve inert-gas-like electron distribution by sharing electrons, two at a time, forming an octet of electrons in the valence shell. The electrons not used for bonding existed as "lone pairs".

In 1920, Latimer and Rodebush concluded that if a H atom is held between 2 octets, then a weak bond is constituted[5]. They also mentioned that water was made up of a "chains and quasi-crystalline network" where large aggregates of molecules continually break up and reform under the influence of thermal agitation.

1.2.2 A definition of hydrogen bonding.

Hydrogen bonding can be viewed as an example of the reaction between a Lewis acid, AH, and a Lewis base, B[6]:

$$AH + B \rightarrow AH \cdots B$$

A simple operational definition is: "A hydrogen bond exists when a hydrogen atom is bonded to more than one atom."[7]. Vinogradov and Linnell[8] take this definition further by stating: "Hydrogen bonding occurs between a proton donor group, AH, and a proton acceptor group, B, where A is an electronegative atom and the acceptor group is a lone pair of an electronegative atom or a π electron orbital of a multiple bond system".

Pimental and McClellan[9] provide the definitive description: "A hydrogen bond exists between a functional group, AH, and an atom or group of atoms, B, in the same or different molecule when :-

a) there is evidence of bond formation

b) there is evidence that this new bond linking AH and B specifically involves the hydrogen atom already bonded to A."

This definition implies that hydrogen bonding can occur between atoms that are not particularly electronegative or with hydrogen atoms covalently bound to non-electronegative atoms such as carbon.

1.2.3 The criteria for hydrogen bonding.

In order for the formation of a H-bond to occur, certain criteria must be met:

1) There must be sufficient polar separation between the H atom and the strongly electronegative atom involved in the bonding process[10,11]. This is generally achieved by the fact that the H atom is usually covalently bound to another highly electronegative atom, which causes an uneven charge distribution within the bond, resulting in the formation of a polar covalent bond:

$$^{\delta-}A\text{——}H^{\delta+}$$

2) The implication of (1) is that the H-bonded complex is clearly an electrostatic interaction[12], formed between the slightly positive proton donor and slightly negative proton acceptor groups.

3) Hydrogen bonding is generally a weak interaction, typically in the range of 4-40 $kJmol^{-1}$ [13]. If the proton donor group and the axis of the lone pair orbital are co-linear, then this produces the strongest H-bonds[14]. The strength of a H-bond is approximately 10 times less than the strength of the corresponding covalent bond[13], but significantly higher than a van der Waals interaction. Table 1.1[15] outlines this comparison, also highlighting the bi-fluoride ion $[F\cdots H\cdots F]^-$ which has the strongest H-bonds :

Hydrogen Bonded Species	Hydrogen Bond Strength ($kJ\ mol^{-1}$)	Corresponding Covalent Bond Strength ($kJ\ mol^{-1}$)
$HS—H\cdots SH_2$	-7	-363
$H_2N—H\cdots NH_3$	-17	-386
$HO—H\cdots OH_2$	-22	-459
$F—H\cdots FH$	-29	-565
$HO—H\cdots Cl^-$	-55	-428
$[F\cdots H\cdots F]^-$	-165	-565

Table 1.1 – A comparison of the strengths of hydrogen and covalent bonds.

4) In many H-bonded complexes, A—H ··· B, the atoms A and B are significantly closer than the sum of their van der Waal radii. The hydrogen atom is small and is unique in the fact that its atomic core consists solely of its nucleus (a proton), without any inner-shell electrons. This implies that there is an intense positive electrostatic field experienced by the highly electronegative atom B, resulting in AH bonding closer to B because of the strong electrostatic attraction. Observations suggest that the total bond length contraction due to H-bond formation is equal to or greater than twice the van der Waal radius of the hydrogen atom[13].

5) Intermolecular hydrogen bonding is an associative phenomenon. It results in a decrease in the total number of free molecules and an increase in the average molecular mass.

Hydrogen bonds can exist in the solid and liquid phases, as well as in solution. Also in the gas phase, compounds that form particularly strong H-bonds may still be associated. An important feature of H-bonding is that at ordinary temperatures, only a fraction of the molecules are generally associated. At equilibrium, while a certain number of new complexes are continually being formed, so an equal number are being continually broken down due to the kinetic energy of the motion of the interacting molecules[13].

All molecules may be classified into one of four possible categories depending on their H-bonding ability:

1) Molecules with one or more donor groups (acids) and no acceptor groups.

2) Molecules with one or more acceptor groups (bases) and no donor groups.

3) Molecules with both donor and acceptor groups.

4) Molecules without any donor or acceptor groups.

Molecules that are classified under category 4 would not be expected to form H-bonds. Table 1.2 outlines these categories with examples of molecules showing the acceptor and/or donor sites. Note that chloroform is depicted as a strong donor, even though it can act as a weak acceptor, and that any interactions involving carbon tetrachloride are weak enough to regard the molecule as having no acceptor or donor sites.

Category	1	2	3	4	
Molecule Name	Chloroform	Acetone	Water	Carbon Tetrachloride	Key: (a) – site of proton acceptor (d) – site of proton donor
Molecular Diagram	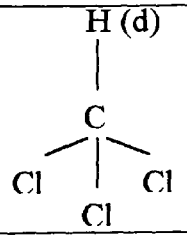	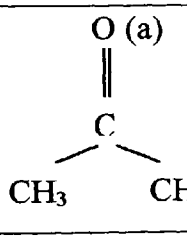	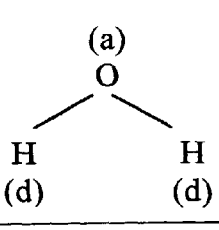	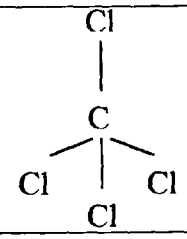	

Table 1.2 – Classifying molecules for hydrogen bonding.

1.2.4 Types of hydrogen bond.

Hydrogen bonding occurs in one of two forms – intermolecular or intramolecular.

1.2.4.1 Intermolecular hydrogen bonding.

Intermolecular hydrogen bonding involves the association of two or more separate molecules of the same or different compounds. It can occur in the form of polymeric chains (Fig 1.1) or rings (Fig 1.2). Molecules of categories 1, 2 and 3 (see Table 1.2) are capable of this form of H-bonding as combinations of: 1 & 2, 1 &3, 2 & 3 or 3 & 3. It is the more common of the two forms of H-bonding.

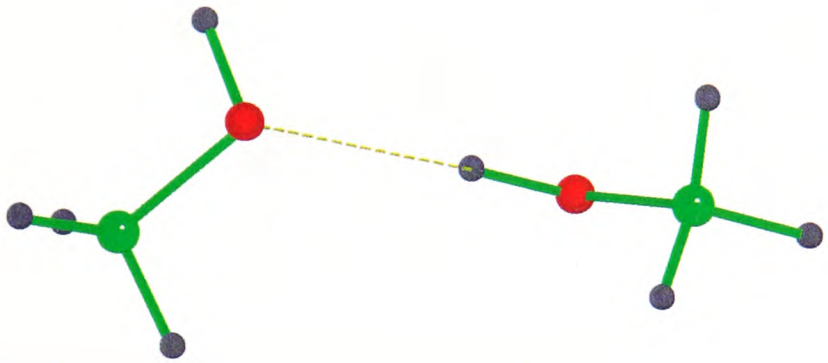

Fig 1.1 – The open dimeric chain of two intermolecularly hydrogen bonded methanol molecules.

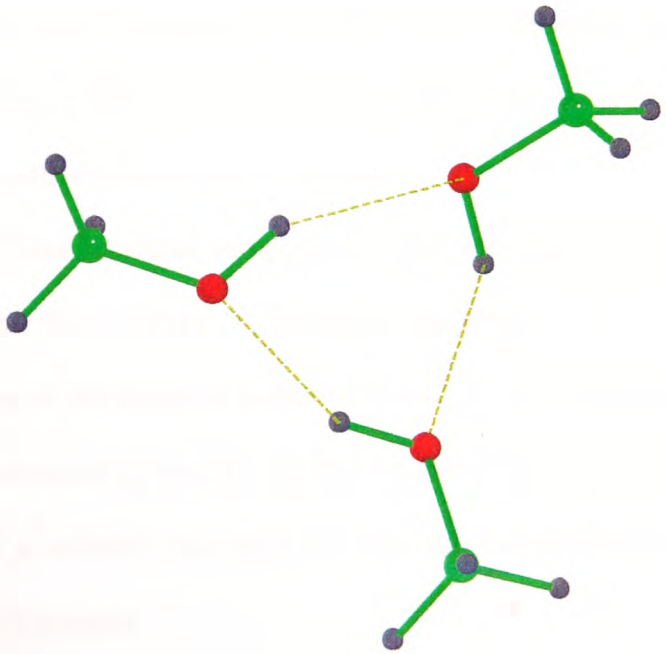

Fig 1.2 – The closed trimeric ring of three intermolecularly hydrogen bonded methanol molecules.

1.2.4.2 Intramolecular hydrogen bonding.

This form occurs when the hydrogen bonding occurs within a molecule. The molecule must be able to exhibit a favourable spatial, and thus an energetically minimal, configuration for this form to occur. This form of H-bonding can only occur in category 3 molecules (Fig 1.3). Intramolecular H-bonds are usually weaker than their intermolecular counterparts and are less sensitive to temperature and concentration changes.

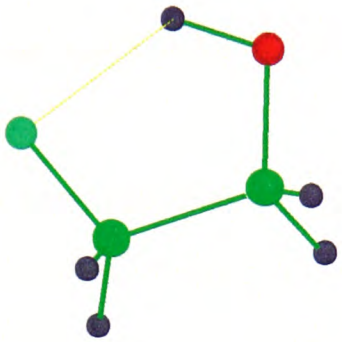

Fig 1.3 – Intramolecular hydrogen bonding for 2- fluoroethanol.

1.3 Techniques for analysing hydrogen bonded complexes.

Since 1920 there have been many methods for investigating the structures of molecules[5]. Such evidence has been gathered from x-ray diffraction, neutron diffraction crystallography, microwave, infrared (and Raman), visible and ultra-violet spectroscopy, and nuclear magnetic resonance (NMR) spectroscopy.

X-ray diffraction[16] has provided some useful data regarding H-bonded systems, but is not capable of resolving the position of the hydrogen atoms accurately. As a result, it generates an overall value of the distance between A and B, not the distance, and thus the hydrogen bond length, between H and B. However, when the sum of the two van der Waals radii for A and B is notably less than the sum for non-bonded atoms, a hydrogen bond may be assumed to be present.

More recently, however, neutron diffraction methods have enabled the location of the hydrogen atom to be determined directly[17]. Despite this apparent improvement in the

analysis of H-bonded compounds, x-ray and neutron diffraction techniques are only applicable to crystalline solids and for other phases, spectroscopic methods must be employed. The types of spectra which have been used for the detection of H-bonding include microwave[18], infrared, Raman, UV, visible and NMR.

If a H-bonded system contains a suitable chromophore which is perturbed by the H-bond formation, then UV and visible spectroscopy may be utilised to analyse the system[19,20]. As a general rule, hydrogen bonding causes a red (bathochromic) shift when chromophores act as proton donors and a blue (hypsochromic) shift when chromophores act as proton acceptors.

Proton NMR has been important to studies of H-bonded systems[21,22], and it provides an indication of a shift (to lower fields usually) of the proton involved in the H-bonded complex[23]. This shift indicates that the proton experiences less shielding from the surrounding electrons and hence a lower electron density around the hydrogen nucleus. Only one peak intermediate between those for pure A—H and A—H···B is observed.

For liquid and vapour states and solution analysis, Raman and infrared spectrometry provide two of the best methods of detecting H-bonded complexes. In the non-hydrogen-bonded state, the A—H stretching band is quite sharp in weak solution or the vapour state. In more concentrated solutions or the liquid phase, when the hydrogen bonded complex A—H···B is formed, the A—H stretching band shifts to a lower wavenumber value and also broadens[24]. Also the grouping of the polar species causes a large change in the dipole moment as the complex vibrates, leading to a strong infrared absorption. It must also be noted that the vibrations of the complexes which preserve the centre of symmetry, if present, as they vibrate are infrared inactive (and thus undetectable via IR spectroscopy), but Raman active (and thus detectable via Raman spectroscopy).

1.4 Vibrational spectra of hydrogen bonded systems.

One of the most prominent effects of H-bonding is to cause considerable changes to the spectra of the interacting compounds[25]. The main varieties of vibration are shown in Fig 1.4[26]. Four modes are involved in a hydrogen bond. The low frequency stretching and bending modes of the hydrogen bond, ν_σ and ν_β respectively, and the high frequency stretching and bending modes of the A-H bond, ν_S and ν_B respectively. These are the characteristic normal modes of vibration for a hydrogen bonded system[27].

Fig 1.4 – Vibrational modes of a hydrogen bonded complex.

The following changes occur to the normal vibrational modes after H-bond formation:

1) **The ν_B mode**. The bending frequency increases, since the hydrogen bond restricts the motion, i.e. stiffens the bend, increasing the force constant[13].

2) **The ν_β mode.** The H-bond stretch is most often coupled to the skeletal modes in large molecules and appears in rather populated areas, so even its detection is quite difficult without resorting to deuteration.

3) **The ν_σ mode**. This is at the far IR, and is generally out of the range of most IR spectrometers. Hydrogen bonds are relatively weak, so have low force constants and thus the frequency of vibration is low

4) **The ν_S mode**. This vibrational mode provides the most accessible information about the H-bonded complex:

   i) The frequency of vibration decreases on formation of the H-bond and is usually the key indicator of H-bond formation. It is assumed that the shift depends only on changes in the A-H bond, due to the proton acceptor B, but

considering the shift as a weakening of the A-H bond is an over simplification, since the observed value of the A-H band depends on the dynamics of the whole H bonded complex.

ii) The intensity of the A-H band increases on H-bond formation. It is as important in H-bonding as the shift (but the intensity measurements are limited to the liquid systems and relatively weak bonds). The intensity of IR absorption depends on the change of dipole moment during the vibration[25,28,29]. A proton in a hydrogen bond is in a much more polar environment than when unbound (due to the electronegativity of the surrounding atoms), so there is an increase in dipole moment. Since the dipole moment increases, so the intensity of ν_S increases. The intensity enhancement of the A-H band is dependent on the change in polarity of the A-H bond and the redistribution of charge within the whole complex.

iii) Broadening of the A-H band is the third piece of evidence of H bonding (and is often an indicator of H bond strength). The broadening of the A-H band is often accompanied by the appearance of sub maxima. Several mechanisms are thought to contribute to the band broadening, and the problem is a complex one with most of the approaches lacking in generality, but are discussed below.

1.4.1 The broadening of the A-H band.

Several factors contribute the broadening of the A-H stretching band[30]:

1) The presence of polymeric hydrogen bonded species might broaden the band, since they will introduce shifts of different magnitudes, creating overlapping bands. It would be difficult to know which species (or whether more than one species) is contributing to a particular band.

2) Fermi resonance with overtones in the region of the A-H band could contribute to the broadening. Evidence that Fermi resonance is not the origin of the breadth or

structure of the band has been verified for the dimer $(CH_3)_2O\cdots HCl$ and the deuterated form $(CD_3)_2O\cdots HCl$[31]. The possibility for Fermi resonance was found to be different in each case, but the dimer spectra were identical. This eliminates the possibility of broadening due to the structure of the band.

3) Unresolved rotational fine structure.

4) Anharmonic coupling between the A-H band and low frequency vibrations, such as the H···B stretching band. Such coupling would give a series of sum and difference bands of the form: $\nu_S \pm n\nu_\sigma$ where n is an integer[32]. When the H-bond is formed, the A···B distance contracts causing a decrease in the A-H force constant. Thus the A-H vibration is modulated by the A-H···B vibration[33] and hence the simple A-H band is replaced by a series of sub-bands not normally resolved. The band has a strong central peak at ν_S flanked by side bands of $\nu_S+n\nu_\sigma$ and $\nu_S-n\nu_\sigma$[34,35].

In polyatomic molecules, overtones may be observed with wave number values that are approximately twice those of the corresponding fundamentals. Also sum or difference combinations may appear at wave number values, which are approximately the sum or difference of wave number values of the component fundamentals. These are examples of binary combinations. Ternary combinations may be formed in similar ways with an increase in the number of possible combinations. The symmetry of any combination band may be determined by combining the symmetry properties of its components. This determines the activity of the combinations in the IR and Raman spectrum. If a binary combination and a fundamental mode belong to the same symmetry species and have similar wave number values, interaction can occur leading to a pair of bands with comparable intensity values.

1.5 The properties of hydrogen bonded conplexes.

From experimental evidence[36,37], it appears that the sites of high electron density, the lone pairs or π bonds on the acceptor, B, provide the point of hydrogen bonding. For the lone pair situation, the A-H molecule also aligns along the direction that the classical

notion of lone pairs dictates. Much controversy underlies the lone pair "rabbit ears" ideology as to whether the electrons actually do form this configuration. Millen has shown[38], in his electron density plot, that initially there is clear evidence of the two lone pairs characteristically associated with water. But as we get further from the molecule, the plot becomes more spherical, and the electron density plot becomes more homogeneous. If the idea that the lone pairs dictate the geometry of the complexes is to be believed, then the electron density plot must always show signs of the increased electron density at the lone pair site. In the case of π bonds, the A-H molecule aligns perpendicularly to the bond, intersecting the axis. If both lone pairs and π bonds are available for bonding, the A-H molecule bonds to the lone pair, again following the geometry of the lone pair system.

On a more macroscopic level, hydrogen bonding can modify the physical and chemical properties of a compound or solution. The mass, size, shape and atomic arrangement, as well as the electronic structure of the functional group can be affected.

Intramolecular H-bonding affects many chemical properties, and is responsible for the large amount of enol present in certain tautomeric equilibria.

For example, 2,4-pentanedione tautomers:

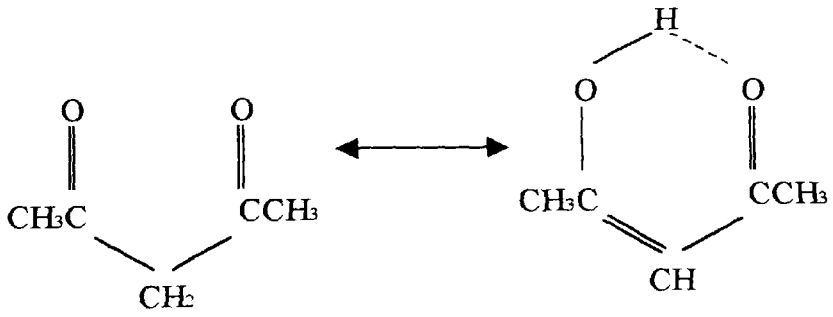

Keto form (20%) Enol form (80%)

Intermolecular H-bonding raises the boiling and melting point of many H-bonded substances (e.g. water) because extra energy is required to break the H-bonds. If H-bonding is possible between a solute and a solvent, then this greatly increases the solubility, resulting in large solubilities where none would be expected. For example,

glucose, a large molecule but with many O-H functional groups, is readily soluble in water Conversely, cyclohexane cannot form H-bonds and is subsequently insoluble in water.

Chapter 2

Experimental methods of FT-IR spectroscopy.

2.1 Modern FT-IR Spectroscopy.

The Fourier Transform Infra Red (FT-IR) spectrometer is based on the Michelson interferometer (Fig 2.1). A beam of radiation from a source, S, is focussed on a beam splitter at 45°. The beam splitter is constructed of a material that, at 45°, allows half the beam to be transmitted to a moving mirror, and half to be reflected to a fixed mirror. The beam reflected by the moving mirror travels back to the beam splitter, where the reflected beam is split again. This time, the reflected half of the beam travels through the sample and is ultimately focussed onto a detector, D. The beam reflected by the fixed mirror also travels back to the beam splitter. Here, the transmitted half of the reflected beam passes through the sample and is focussed onto D[39,40,41].

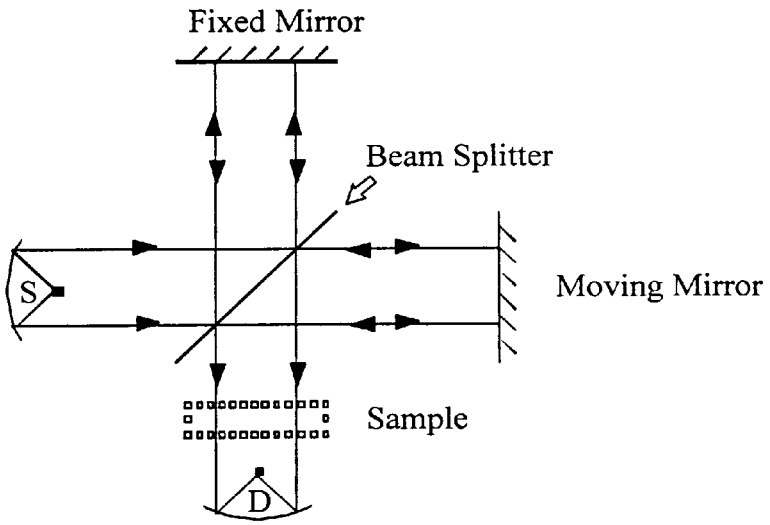

Fig 2.1 – Schematic diagram of the Michelson interferometer.

Spectroscopy is performed by the interference of the reflected beams at the beam splitter, where they recombine. The intensity of the interference beam is a function of the optical path difference between the two recombining beams for a particular frequency of the source. Only constructive interference will allow the recombined beam to pass through the beam splitter and subsequently on through the sample to the detector. The moving mirror allows the alteration of the optical path difference and using a prism to split the

source into an infinite number of different beams effectively alters the frequency of the source. When the interference beam reaches the sample, changes are induced into the beam, which are received by the detector.

The mathematics to convert the interference pattern into a spectrum is quite formidable and so a computer handles the final stage of the FT-IR spectroscopy process. However, the essential equations relate the intensity falling on the detector, $I(\delta)$, to the spectral power density at a particular wavenumber, $\bar{\nu}$, given by $B(\bar{\nu})$ are:

$$I(\delta) = \int_0^{+\infty} B(\bar{\nu}) \cos 2\pi\bar{\nu}.d\bar{\nu} \qquad \text{and} \qquad B(\bar{\nu}) = \int_{-\infty}^{+\infty} I(\delta) \cos 2\pi\bar{\nu}\delta.d\delta$$

These two equations are known as a Fourier Transform (FT) pair (hence "FT-IR Spectroscopy") and are fully interconvertible. The first describes the variation in power density as a function of difference in path length, which is an interference pattern. The second describes a variation of intensity as a function of wavenumber, and is a spectrum. Each can be converted from one to the other via the mathematical process of Fourier Transformation[42].

2.1.1 Advantages of FT-IR spectroscopy.

The interferometer technique used in FT-IR spectroscopy has the following advantages:

1) It provides information about the entire spectral range during scanning, where as dispersive spectroscopy provides information only about a narrow wavenumber region governed by the exit slit width at any given time.

2) Dispersive techniques require long, narrow slits to achieve an adequate resolution, where as an interferometer can operate with a large circular aperture. Quantitatively, up to 200 times more power can be gleaned from an interferometer compared to a good dispersive instrument[43].

3) The interferometer can have large resolving powers achieved by large mirror movements[44].

2.1.2 Disadvantage of FT-IR spectroscopy.

The main disadvantage of FT-IR spectroscopy is that it is a single beam technique. This means that it is always necessary to compare the sample spectrum to a predetermined background spectrum after the measurement has been made, rather than continually comparing the sample spectrum to the background as it is being recorded, as a double beam dispersive instrument would.

2.2 The role of the computer in FT-IR spectroscopy.

The initial function of the computer (PC) will be the acquisition of the desired IR spectrum from the spectrometer. Here the PC's primary function is the mathematical conversion of the interferogram to a spectrum using the Fourier Transform pair as outlined in 2.1. The PC is also responsible for the background subtraction from the spectrum, as well as the physical controlling of the scanning process by which the spectrum is obtained.

The computer may also be used to convert the spectrum into a readily transferable electronic format for transfer across computer networks, electronic publishing or for further spectral manipulations such as peak-fitting[45].

2.3 Infrared absorption theory.

The absorption frequency of infrared (IR) radiation depends on the molecular vibrational frequency, whilst the absorption intensity of that radiation relies on how efficiently a photon of IR radiation can be absorbed by the molecule. The ease of absorption depends on the change in dipole moment resulting from natural molecular vibration. The dipole moment is defined as the magnitude of the charge in the dipole multiplied by the separation of the charge (Fig 2.2).

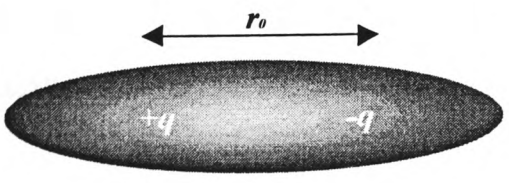

If there is a charge separation of $(+q) - (-q)$ over a distance r_0, then the dipole moment, μ, is: $\mu=|q|\ r_0$

Fig 2.2 – Schematic diagram of a dipole demonstrating charge separation.

In a complex molecule this simplified view of a dipole moment can be preserved if the positive charge represents the entire charge at the centre of charge for the nuclei, and the negative charge represents the entire charge at the centre of charge for the electrons. Note that these centres of charge coincide with the corresponding centres of mass[24,40,41].

As the IR radiation approaches the dipolar molecule, the molecule experiences a force from the electric field of the photons. Since the wavelength of the radiation is greater than the size of the molecule, the electric field of the photons can be considered uniform over the entire molecule. The force exerted by the electric field will attract or repel the positive charge of the dipolar molecule and repel or attract the negative charge – i.e. the opposite charges will experience opposite forces from the electric field. Thus the oscillating electric field from the photons of the IR radiation will induce an oscillating force on the molecule which in turn causes an oscillation of the dipole moment of the molecule at the same frequency as the IR radiation.

At particular frequencies, the oscillating dipole will have a tendency to stimulate a vibration of the nucleus, and these molecular vibrations also cause a change in dipole moment. The more the dipole moment changes during a vibration, the easier it is for the electric field (from the IR photons) to activate that vibration. If a molecular vibration causes no change in the dipole moment, then a forced dipole moment oscillation cannot activate that vibration.

This can be summarised in the selection rule:

In order to absorb infrared radiation, a molecule must undergo a net change in dipole moment as a result of its vibrational motion.

Only under these conditions can the molecule interact with the electric field of the IR radiation photons and modify its vibrational motion. Fig 2.3 shows how the dipole oscillates in the IR radiation electric field.

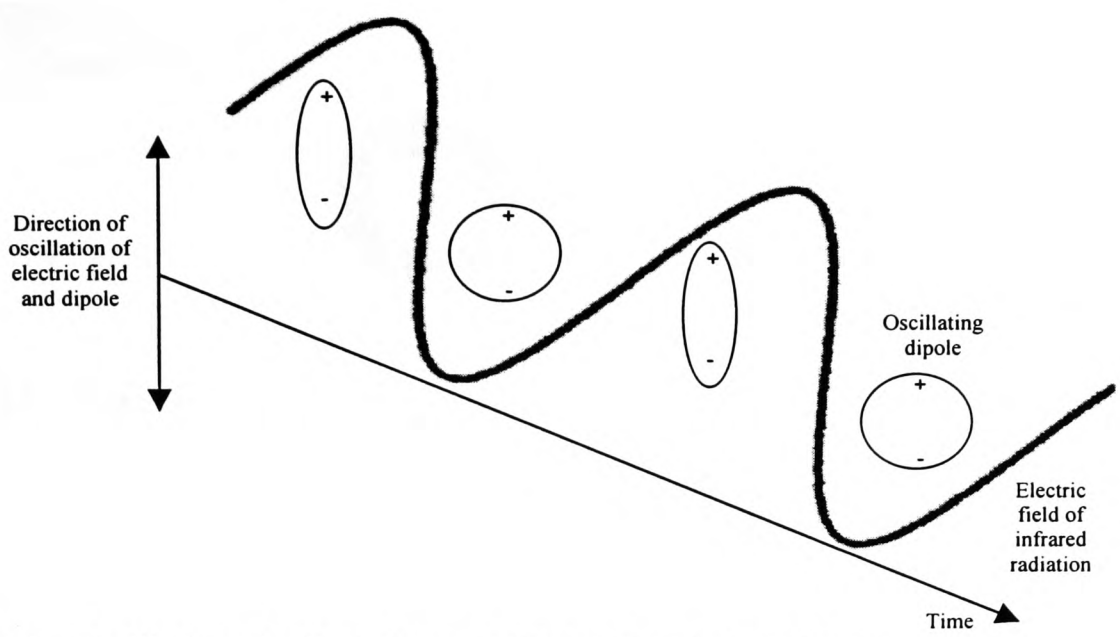

Fig 2.3 – Oscillation of a dipole in an oscillating electric field from IR radiation.

2.4 The diatomic molecule.

For a simplistic picture, consider a heteronuclear (i.e. made of two different atoms) diatomic molecule. The atoms can be thought of as two different masses, m_1, m_2, joined by a spring, the bond (Fig 2.4).

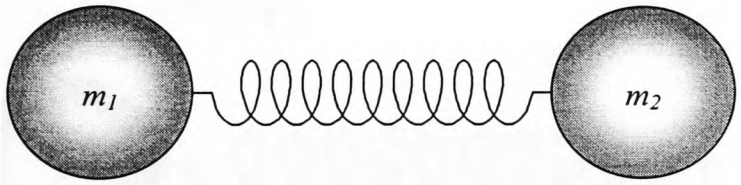

Fig 2.4 - Schematic diagram of a diatomic molecule

This system can be reduced further to a single mass attached to a spring, where the new mass is defined as the reduced mass, μ, and is defined as[46]:

$$\mu = \frac{m_1 m_2}{m_1 + m_2} \qquad \text{Eq. 2.1}$$

2.4.1 The classical mechanics approach to the diatomic molecule.

Suppose the extension of the spring is x at equilibrium (Fig 2.5), then according to Hooke's Law, the force acting on the reduced mass system, F, is given by[47]:

$$F = -kx \qquad \text{Eq. 2.2}$$

Where k is the force constant of the spring (or "springiness" of the bond).

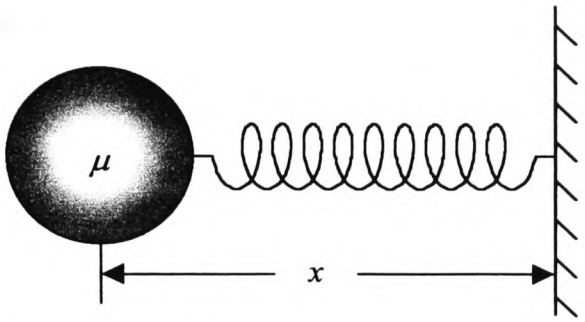

Fig 2.5 – Reduced mass system at equilibrium.

Suppose that the reduced mass system is displaced by dx (i.e. the spring is stretched – Fig 2.6), then the work done, dV, in performing this displacement is:

$$dV = -Fdx = kx.dx \qquad \text{Eq. 2.3}$$

Thus the total work done stretching the spring from 0 to x is:

$$\int_0^{V_0} dV = \int_0^x kx.dx \qquad \text{Eq. 2.4}$$

Which gives the total potential energy of the system:

$$V_0 = \frac{kx^2}{2} \qquad \text{Eq. 2.5}$$

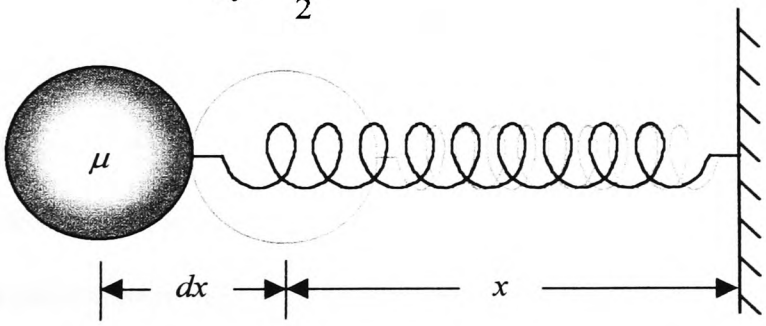

Fig 2.6 – Displacement of the reduced mass system.

If the system is then allowed to return to its equilibrium state, it will have a velocity, $\dot{x}$, and a resultant kinetic energy, T, given by[48]:

$$T = \frac{\mu \dot{x}^2}{2} \qquad \text{Eq. 2.6}$$

Note that $\dot{x}$ is the relative velocity between m_1 and m_2 (NB: $\dot{x} = \dot{x}_{m_1} - \dot{x}_{m_2}$).

For this system, the Lagrangian, L, is given by[49]:

$$L=T-V \qquad \text{Eq. 2.6}$$

Substituting equations 2.4 and 2.5 into equation 2.6 gives:

$$L = \frac{\mu \dot{x}^2}{2} - \frac{kx^2}{2} \qquad \text{Eq. 2.7}$$

Now, Lagrange's equation is defined to as[50]:

$$\frac{d}{dt}\frac{\partial L}{\partial \dot{x}} - \frac{\partial L}{\partial x} = 0 \qquad \text{Eq. 2.8}$$

Now: $\frac{\partial L}{\partial \dot{x}} = \mu \dot{x}$ and $\frac{\partial L}{\partial x} = -kx$ therefore $\frac{d}{dt}\frac{\partial L}{\partial \dot{x}} = \mu \ddot{x}$ and so from equation 2.8:

$$\ddot{x} = -\frac{k}{\mu}x \qquad \text{Eq. 2.9}$$

Equation 2.9 is the equation for simple harmonic motion[51]. Therefore, the frequency, ν_m, of the motion is:

$$\nu_\mu = \frac{1}{2\pi}\sqrt{\frac{k}{\mu}} \qquad \text{Eq. 2.10}$$

This is, in the classical sense, the frequency of the oscillations induced by the electric field of the IR radiation in the dipolar molecule. Clearly, this idea could be extended to dipolar polyatomic molecules of n atoms. Note that the vibrations in the n atomic system would be harmonic.

2.4.2 The quantum mechanics approach to the diatomic molecule.

The one-dimension time independent Schrödinger equation of a harmonic oscillator, such as the oscillating dipole, is:

$$\frac{d^2\psi}{dx^2} + \frac{2\mu}{\hbar^2}(E - V_0)\psi = 0 \qquad \text{Eq. 2.11}$$

Where $V_0 = \frac{1}{2}kx^2$ (as for the classical case), E is the total energy of the system and ψ is the wavefunction of the system, and has no real physical significance, other than providing a basis for calculating real-world properties of the system[52]. If we let

$$y = \left(\frac{\sqrt{k\mu}}{\hbar}\right)^{1/2} x = \sqrt{\frac{2\pi\mu\nu_m}{\hbar}}x \qquad \text{and} \qquad \alpha = \frac{2E}{\hbar}\sqrt{\frac{\mu}{k}} = \frac{2E}{h\nu_m} \qquad \text{Eq. 2.12}$$

where y and α are dimensionless quantities and ν_m is the classical frequency of the oscillations, then equation 2.11 becomes:

$$\frac{d^2\psi}{dy^2} + (\alpha + y^2)\psi = 0 \qquad \text{Eq. 2.13}$$

This equation has mathematical properties such that solutions are only possible when:

$$\alpha = 2v + 1 \qquad ; v = 0, 1, 2, 3, \ldots$$

Where v is as defined and is called the vibrational quantum number. Combining this with equation 2.12, leads to the total energy of the system being given by:

$$E_n = (v + ½)h\nu_\mu \qquad ; v = 0, 1, 2, 3, \ldots \qquad \text{Eq. 2.14}$$

Again, these ideas can be extended to polyatomic molecules. The conclusions that can be drawn from the comparison of classical and quantum mechanics are:

1) Classically, the energy of the harmonic oscillator is a continuous quantity (Eq. 2.5), varying as the distance from the equilibrium point varies. Quantum mechanically, only certain specific energies are allowed, and they are multiples of the frequency of the oscillations (Eq. 2.14).

2) Under classical analysis, the lowest energy of the system allowed is zero. However, quantum mechanically, there is a minimum energy of the system, the zero point energy, given by: $E_0 = ½h\nu_\mu$.

A more rigorous treatment of the solution of Schrödinger's equation for the harmonic oscillator is presented in Appendix A.

2.5 Absorption of infrared radiation.

Consider a dipolar diatomic molecule vibrating with in a quantum energy well with energy:

$$E_m = (v + ½)h\nu_\mu \qquad \text{Eq. 2.15}$$

Let us assume that the dipolar diatomic molecule absorbs one photon of IR radiation, frequency, ν_γ, whose energy is $E_\gamma = h\nu_\gamma$.

The increase in vibrational energy experienced by the molecule, ΔE_m is:

$$\Delta E_m = E_\gamma = h\nu_\gamma \qquad \text{Eq. 2.16}$$

If we also assume that the absorption causes a transition in quantum state i.e. $v \rightarrow v+1$, then:

$$E_{m+1} = \{(v+1)+½\}h\nu_\mu \qquad \text{Eq. 2.17}$$

Hence the increase in the molecular energy is:

$$\begin{aligned} \Delta E_m &= E_{m+1} - E_m \\ &= \{(v+1)+½\}h\nu_\mu - (v+½)h\nu_\mu \\ &= h\nu_\mu \end{aligned} \qquad \text{Eq. 2.18}$$

Comparing equations 2.18 and 2.16, it is obvious that:

$$\nu_\gamma = \nu_\mu \qquad \text{Eq. 2.19}$$

Therefore, if the photon has the right energy to increase the vibrational quantum number by 1, then it must have a frequency equal to that of the classical vibrational frequency of the molecule. Thus the absorption of infrared radiation is a quantum mechanical phenomenon.

The intensity of an infrared band associated with a transition from a lower level, i, to a higher level, j, is proportional to the square of the transition moment[53], $P_{i\rightarrow j}$ i.e.:

$$Intensity \propto \left(P_{i\rightarrow j}\right)^2 \qquad \text{where:} \qquad P_{i\rightarrow j} = \int_{-\infty}^{+\infty} \psi_i p_x \psi_j dx \qquad \text{Eq. 2.20}$$

Here, ψ_i and ψ_j are the wavefunctions of the i and j states and p_x is the dipole moment in the x direction.

Note that the comparison of classical and quantum mechanical methods has assumed simple harmonic motion of the diatomic molecular vibrations. This is an over simplification, since anharmonic motion has not been considered, but for small amplitude oscillations, anharmonic motion can be approximated by harmonic motion.

2.6 The infrared spectrum.

The IR region of the electromagnetic spectrum extends from the end of the red of the visible spectrum (Fig 2.7). It is split into three regions:

1) **Near infrared** - This provides the range of wavenumbers (defined as the reciprocal of the wavelength) from 15,800 to 1200 cm^{-1} (quartz beamsplitter) or 15,800 to 2700 cm^{-1} (Calcium Fluoride beamsplitter).

2) **Mid infrared** - This provides the range 5000 to 220 cm^{-1} (Calcium Iodide beamsplitter) or 1000 to 370 cm^{-1} (Potassium Bromide beamsplitter). This is the most common used in FT-IR spectroscopy. It provides the most information about the functional groups present. It can be divided into two main parts: The "group frequency" and the "fingerprint" regions.

   The "group frequency" (4000 –1300 cm^{-1}) vibrations are easily associated with specific functional groups. The "fingerprint" (1300 – 400 cm^{-1}) vibrations are associated with vibrations of the molecule as a whole.

3) **Far infrared** – A Mylar beamsplitter provides the range 400 to 50 cm^{-1}. The vibrations associated with this region are torsions and other motions of heavy atoms.

2.7 Infrared sources and detectors.

In FT-IR spectroscopy, the main source used is a voltage stabilised, air cooled ceramic (Globar) operated at 1400K[40].

The main detectors used are pyroelectric and photoconducting devices. Triglycine Sulphate (TGS) is a pyroelectric substance used in the construction of FT-IR spectroscopy detectors. TGS instruments that operate in the mid and near IR region have Calcium Iodide windows, where as those that operate in the far IR region have plastic windows.

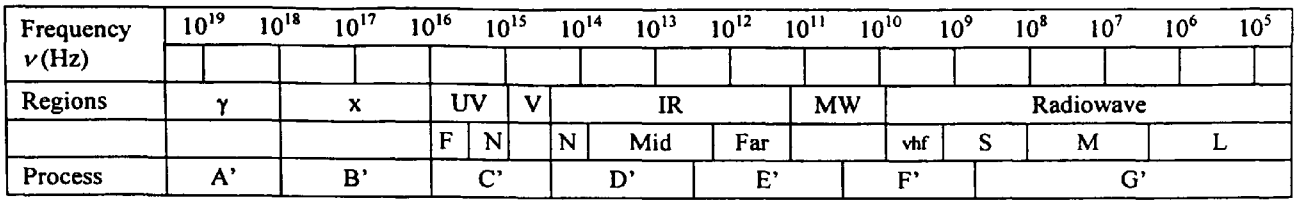

Key:

γ	γ - Rays
x	x - Rays
UV	Ultraviolet
V	Visible
IR	Infrared
MW	Microwave
F	Far
N	Near
vhf	Very high frequency
S	Short wavelength
M	Medium wavelength
L	Long wavelength

A'	Atomic nuclei excited
B'	Inner electronic transitions
C'	Outer electronic transitions
D'	Molecular vibrations
E'	Molecular vibrations
F'	Electron spin resonance
G'	Nuclear magnetic resonance

Fig 2.7 – The electromagnetic spectrum.

Chapter 3

Computational chemistry.

3.1 Introduction.

Computational chemistry is a relatively new discipline, and has evolved in parallel with the continually increasing power of computers. The challenges for computational chemistry are to characterise and predict the structure and stability of chemical systems, to estimate energy differences between different states, and to explain reaction pathways at the atomic level. Meeting these challenges reliably and effectively could eliminate time consuming and costly trial experiments.

There are two broad areas of computational chemistry dedicated to the structure and reactivity of molecular species – molecular mechanics and electronic structure methods. Both techniques perform the same basic types of calculation, but from different theoretical approaches:

1) Geometry optimisation.

The co-ordinates of each of the atoms are adjusted to minimise the overall molecular energy of the molecule, resulting in the most stable form. Geometry optimisations rely on calculating the first derivative of the energy function, with respect to the atomic motions, and finding a stationary value. To categorise the stationary value, the second derivative is then analysed. The process is repeated until a suitable energy minimised state is reached and then the calculation ends producing the optimised geometry of the molecule.

2) Vibrational Spectra.

Calculation of the second derivative of the energy function, with respect to the atomic motions, allows the calculation of the vibrational frequencies of the molecular structure. This in turn allows a spectrum to be generated so that the identifying bands can be analysed, and other useful data determined.

3.2 Molecular Mechanics.

Molecular mechanics simulations rely on the laws on classical mechanics to predict the properties and structures of molecules. Each particular molecular mechanics method is characterised by its own specific force field. The calculations do not treat the electrons as a part of the molecular system explicitly. Instead they perform calculations based on the nuclear interactions, implicitly incorporating the electrons in the force fields through parameterisation.

Consequently, there are limitations to this technique:

1) Each force field is limited to providing good results only for the molecules for which it was parameterised. This implies that there is no universal force field that can be used generally for all molecular systems.

2) The over simplification of the treatment of the electrons implies that molecular mechanics cannot describe systems where electronic effects predominate, such as the formation or breaking of molecular bonds.

However, the approximation allows the calculations to be simplified and means that the computational requirements are minimal. It also means that very large systems comprising thousands of atoms can be comfortably managed. Many computer programs utilise this method of computational chemistry, such as: HyperChem, MM3, Quanta, Sybyl, Alchemy and Chem-X (which will be detailed in chapter 4).

3.3 Electronic structure methods.

These techniques of computing the physical and chemical properties of molecular structures utilise quantum mechanics, notably the application of Schrödinger's equation and the derivation of numerical solutions to the many-bodied problem that it describes. There are two main classes of methodology for determining the solutions, which *are semi-empirical*, and *ab initio* methods. The latter forms the basis of this work, and will be described.

3.3.1 Theoretical discussion.

3.3.1.1 Solving Schrödinger's equation.

Any description of molecular properties starts from the Time Dependent Schrödinger equation[54]:

$$\hat{\mathcal{H}}\,\Phi = i\hbar\frac{\partial\Phi}{\partial t} \qquad \text{Eq. 3.1}$$

where: $\Phi \equiv \Phi(\underline{\mathbf{r}}_l, \underline{\mathbf{R}}_m, t)$

Here $\underline{\mathbf{r}}_l$ and $\underline{\mathbf{R}}_m$ denote the Cartesian co-ordinates for the lth electron and mth nucleus respectively, and t is time. The full Hamiltonian for a system of N nuclei and n electrons is:

$$\hat{\mathcal{H}} = \hat{T}_N + \hat{T}_E + \hat{V} \qquad \text{Eq. 3.2}$$

Where:

$$\hat{T}_N = -\frac{\hbar^2}{2}\sum_{k=1}^{N}\frac{1}{M_k}\nabla_k^2 \qquad \text{Eq. 3.3}$$

This is the total nuclear kinetic energy.

$$\hat{T}_E = -\frac{\hbar^2}{2m_0}\sum_{i=1}^{n}\nabla_i^2 \qquad \text{Eq. 3.4}$$

This is the total electronic kinetic energy.

$$\hat{V} = e_0^2\left\{\underbrace{\sum_{k=1}^{N-1}\sum_{l>k}^{N}\frac{Z_k Z_l}{R_{kl}}}_{\text{nucleus/nucleus}} + \underbrace{\sum_{i=1}^{n-1}\sum_{j>i}^{n}\frac{1}{R_{ij}}}_{\text{electron/electron}} - \underbrace{\sum_{k=1}^{N}\sum_{i=1}^{n}\frac{Z_k}{R_{ki}}}_{\text{nucleus/electron}}\right\} \qquad \text{Eq. 3.5}$$

This is the total interaction potential energy.

R_{ab} is the distance between particles a and b.

M_k, $Z_k e_0$ are the mass and charge of nucleus k.

m_0, e_0 are the mass and charge of an electron.

Note: The indices k and l refer to nuclei, while i and j refer to electrons

The next stage is to adopt the Born-Oppenhiemer condition[55]. This is the separation of the motion of the electrons from the motion of the nuclei. The consequence of the approximation is that the electron wavefunction can be calculated for any specific static nuclear framework.

The approximation is based on the great differences between the masses of the electrons and nuclei. The consequence of this difference is that the nuclei move so slowly that the electrons can adjust their distribution instantaneously to take into account the changing potential. The practical effect is that the arbitrary, fixed locations of the nuclei can be selected and the electronic wavefunctions calculated for each one of them. The nuclei can then be moved to new positions, and the electronic calculation repeated. Therefore, it is possible to calculate the energy for all possible arrangements of the nuclei and find the one corresponding to the lowest energy, which is identified as the equilibrium shape of the molecule. Thus the wave function, Φ, can be separated into the time dependent part (the slow nuclei) and the time independent part (the fast electrons)[56].

Thus:

$$\Phi(\underline{\mathbf{r}},\underline{\mathbf{R}},t)=\psi(\underline{\mathbf{r}},\underline{\mathbf{R}})\phi(\underline{\mathbf{R}},t) \qquad \text{Eq. 3.6}$$

From Eq. 3.2, this leads to two coupled partial differential equations:

$$\hat{\mathcal{H}}'\psi(\underline{\mathbf{r}},\underline{\mathbf{R}})=E(\underline{\mathbf{R}})\psi(\underline{\mathbf{r}},\underline{\mathbf{R}}) \qquad \text{Eq. 3.7}$$
$$\left\{\hat{\mathcal{H}}'=\hat{T}_E+\hat{V}\right\}$$

$$\left[\hat{T}_N+E(\underline{\mathbf{R}})\right]\phi(\underline{\mathbf{R}},t)=i\hbar\frac{\partial\phi(\underline{\mathbf{R}},t)}{\partial t} \qquad \text{Eq. 3.8}$$

Clearly, Eq. 3.7 is the time independent Schrödinger equation for the electrons, and Eq. 3.8 is the time dependent form for the nuclei.

The solution for Eq. 3.7 provides the total energy $E(\underline{\mathbf{R}})$ of the system, and since the potential energy only varies with position and not time, we can assume that ϕ separates as below:

$$\phi(\underline{\mathbf{R}},t)=\chi(\underline{\mathbf{R}})e^{-i\lambda t} \qquad \text{Eq. 3.9}$$

This is the steady state solution of Eq. 3.8[57]. Hence the amplitude of $\phi(\underline{\mathbf{R}},t)$, i.e. $\chi(\underline{\mathbf{R}})$, can be found by solving the eigenvalue equation:

$$\left[\hat{T}_N + E(\underline{\mathbf{R}})\right]\chi(\underline{\mathbf{R}}) = \lambda\chi(\underline{\mathbf{R}}) \qquad \text{Eq. 3.10}$$

Where λ are the eigenenergies of the wavefunction $\phi(\underline{\mathbf{R}},t)$.

But the Schrödinger equation cannot be solved analytically for any molecules other than the $(H_2)^+$ ion (many body problem). However, approximate solutions can be found assuming that the molecular orbitals are a linear combination of the atomic orbitals of a similar nature[58].

An electron wavefunction, $\psi(\underline{\mathbf{r}})$, is a function of the Cartesian coordinates of the electron (i.e. $r \equiv x\underline{\mathbf{e}}_x + y\underline{\mathbf{e}}_y + z\underline{\mathbf{e}}_z$). To describe the co-ordinates of the electron completely, we must include a "spin co-ordinate", ξ. This can have two values for an electron: $\xi = \pm ½$ and measures spin angular momentum along the positive z axis. This leads to a spin wave function, $\alpha(\xi)$, such that:

$$\begin{aligned}\alpha(\xi = +½) &= 1\\ \alpha(\xi = -½) &= 0\end{aligned} \qquad \text{Eq. 3.11}$$

By symmetry, there is also a spin wave function, $\beta(\xi)$, along the negative z axis:

$$\begin{aligned}\beta(\xi = +½) &= 0\\ \beta(\xi = -½) &= 1\end{aligned} \qquad \text{Eq. 3.12}$$

Thus the complete wavefunction for the electron is:

$$\psi_e(\underline{\mathbf{r}},\xi) = \psi(\underline{\mathbf{r}})\alpha(\xi) + \psi(\underline{\mathbf{r}})\beta(\xi) \qquad \text{Eq. 3.13}$$

This implies that one possible solution to the Schrödinger equation for an n electron system would be the product of the wavefunctions in Eq. 13 for all n electrons[59]:

$$\begin{aligned}\Psi_{PRODUCT} &= \psi_1(\underline{\mathbf{r}}_1,\xi_1)\psi_2(\underline{\mathbf{r}}_2,\xi_2)\ldots\psi_n(\underline{\mathbf{r}}_n,\xi_n)\\ &= \prod_{i=1}^{n}\psi_i(\underline{\mathbf{r}}_i,\xi_i)\end{aligned} \qquad \text{Eq. 3.14}$$

But this does not have the property of antisymmetry. If the co-ordinates of electrons i and j are interchanged in this wavefunction, the result is not equal to multiplying by -1,

the basis of asymmetry[60,61]. To ensure antisymmetry, the spin orbital wavefunctions are arranged in a determinantal wavefunction:

$$\Psi_{DET} = \sqrt{n!}\begin{vmatrix} \prod_{i=1}^{n}\psi_i(\underline{\mathbf{r}}_1,\xi_1) \\ \prod_{i=1}^{n}\psi_i(\underline{\mathbf{r}}_2,\xi_2) \\ \vdots \\ \prod_{i=1}^{n}\psi_i(\underline{\mathbf{r}}_n,\xi_n) \end{vmatrix} \qquad \text{Eq. 3.15}$$

The factor $\sqrt{n!}$ is a normalising factor ensuring that the probability of finding an electron in space is unity:

$$\int\cdots\int\Psi^*_{DET}\Psi_{DET}\,d\underline{\tau}_1\cdots d\underline{\tau}_n = 1 \qquad \text{Eq. 3.16}$$

Eq. 16 is called the *Slater Determinant* and provides the basis for the Hartree-Fock theory[62,63].

3.3.1.2 Basis set expansions.

However, the wavefunction for the i^{th} electron is not a simple mathematical function, and so is represented by the Linear Combination of Atomic Orbital, or LCAO, theories that exist. Generally we say that ψ_i can be expressed as the linear sum of N single electron wavefunctions, or basis functions[64]:

$$\psi_i = \sum_{\mu=1}^{N} c_{\mu i}\phi_\mu \qquad \text{Eq. 3.17}$$

Where $c_{\mu i}$ is the expansion coefficient, allowing ϕ_μ to define a complete orthonormal basis set of basis functions.

These wavefunctions have been defined by having symmetry properties of atomic orbitals and are classed as *s*, *p*, *d*, *f*, ... depending on their angular properties. Two types of atomic orbital are widely used. Slater Type Orbitals (STOs) and Gaussian Type Orbitals. STOs have exponential radial parts, and thus have radial symmetry. They are labelled like hydrogen orbitals - *1s*, *2s*, $2p_x$, $2p_y$, $2p_z$ ... and are of the following form:

$$\phi_{1s} = \left(\frac{\zeta_1^3}{\pi}\right)^{1/2} \exp(-\zeta_1 r)$$

$$\phi_{2s} = \left(\frac{\zeta_2^5}{96\pi}\right)^{1/2} r \exp\left(\frac{-\zeta_2 r}{2}\right)$$

$$\phi_{2p_x} = \left(\frac{\zeta_2^5}{32\pi}\right)^{1/2} x \exp\left(\frac{-\zeta_2 r}{2}\right)$$

etc...

Note that ζ_1 and ζ_2 are constants that determine the size of the orbitals. STOs are not, however, well suited to numerical work, and are thus superseded by the Gaussian Type Orbitals. These are powers of the *x*- *y*- and *z*- co-ordinates of the electron in question, multiplied by $\exp(-\alpha r^2)$, where α is the constant of orbital size (c.f. ζ_1 and ζ_2), and are of the following form:

$$g_s(\alpha, r) = \left(\frac{2\alpha}{\pi}\right)^{3/4} \exp\left(-\alpha r^2\right)$$

$$g_x(\alpha, r) = \left(\frac{128\alpha^5}{\pi^3}\right)^{1/4} x \exp\left(-\alpha r^2\right)$$

$$g_y(\alpha, r) = \left(\frac{128\alpha^5}{\pi^3}\right)^{1/4} y \exp\left(-\alpha r^2\right)$$

$$g_z(\alpha, r) = \left(\frac{128\alpha^5}{\pi^3}\right)^{1/4} z \exp\left(-\alpha r^2\right)$$

$$g_{xx}(\alpha, r) = \left(\frac{2048\alpha^2}{9\pi^3}\right)^{1/4} x^2 \exp\left(-\alpha r^2\right)$$

$$g_{yy}(\alpha, r) = \left(\frac{2048\alpha^2}{9\pi^3}\right)^{1/4} y^2 \exp\left(-\alpha r^2\right)$$

$$g_{zz}(\alpha, r) = \left(\frac{2048\alpha^2}{9\pi^3}\right)^{1/4} z^2 \exp\left(-\alpha r^2\right)$$

$$g_{xy}(\alpha,r)=\left(\frac{2048\alpha^2}{9\pi^3}\right)^{1/4} xy\exp\left(-\alpha r^2\right)$$

$$g_{xz}(\alpha,r)=\left(\frac{2048\alpha^2}{9\pi^3}\right)^{1/4} xz\exp\left(-\alpha r^2\right)$$

$$g_{yz}(\alpha,r)=\left(\frac{2048\alpha^2}{9\pi^3}\right)^{1/4} yz\exp\left(-\alpha r^2\right)$$

etc...

Note the g_s is an *s*-type orbital, and g_x, g_y, g_z are *p*-type orbitals, due to their angular symmetries, but the remainder only constitute orbitals as a result of superposition[65].

Thus a linear combination of Gaussian functions can be used to describe the basis functions, so for an *s*-type basis function:

$$\phi_\mu = \sum_s d_{\mu s} g_s \qquad \text{Eq. 3.18}$$

Where ϕ_μ are called contracted Gaussians, g_s are called primitive Gaussians, and $d_{\mu s}$ are the contraction constants (second order tensors) [66]. Note that ϕ_μ is said to be a minimal basis set, i.e. the smallest set of atomic orbitals from which useful molecular orbitals can be built. It is a Slater Type Orbital created by the superposition of Gaussian Type Orbitals. Gaussian Type Orbitals are preferred to Slater Type Orbitals because they can be explicitly evaluated without any numerical integration.

3.3.2 Electronic orbitals.

An orbital, in the classical sense is usually thought of as the "orbit" of an electron around the nucleus. This is true to some extent. One definition is that an orbital is the volume of space in which there is a 95% chance of finding the electron. Note that there is a 5% chance of the electron being outside the orbital.

3.3.2.1 The probability function.

The probability is found from the probability density function (pdf), $P(\underline{\mathbf{r}})$, defined as so that $P(\underline{\mathbf{r}})d\underline{\mathbf{r}}$ is the probability of finding the electron at any location between $\underline{\mathbf{r}}$ and

$\underline{r}+d\underline{r}$. By integrating the probability density $|\psi_i|^2 = \psi_i^* \psi_i$ over the volume element we get[67]:

$$P(\underline{r})d\underline{r} = |\psi_i|^2 .4\pi|\underline{r}|^2 .d\underline{r} \qquad \text{Eq. 3.19}$$

Fig 3.1 shows a plot of $P(\underline{r})$ against $\underline{r}$ for the 1s wavefunction. It is within the peak that the 95 % chance of finding the electron is. At a distance r^*, we have a maximum. This provides the most probable location of the electron. The value of r^* is 0.053 nm, the Bohr Radius, as the Bohr model predicts[68]. Note that in Fig 3.2, the plot for the 2s orbital contains the 1s orbital. These ideas can be extended for the p,d,f etc orbitals[67].

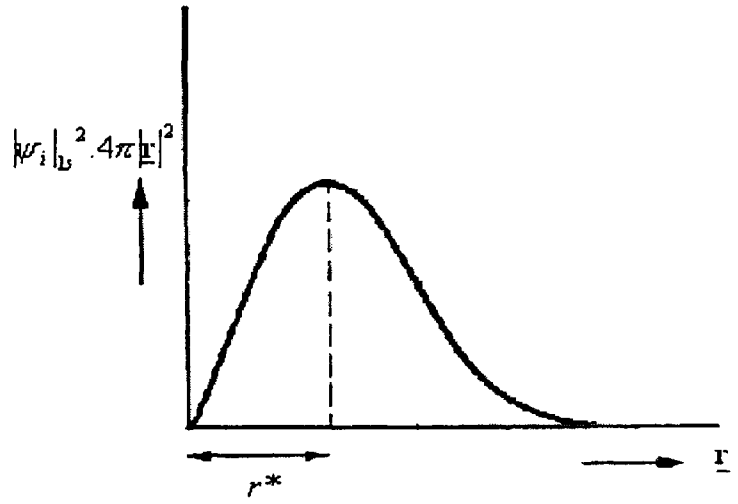

Fig 3.1 – Probability density plot for an electron in a 1s orbital.

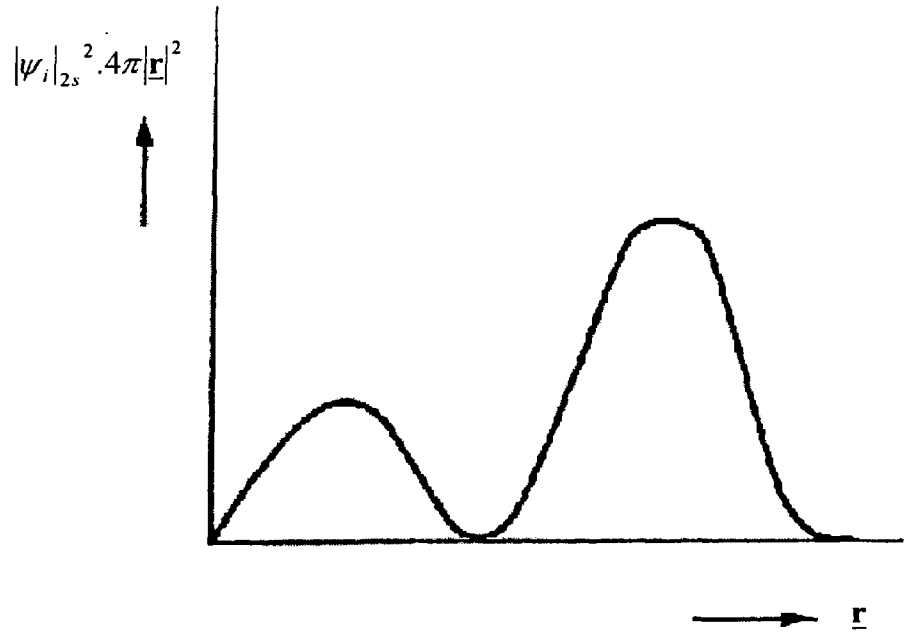

Fig 3.2 – Probability density plot for an electron in a 2s orbital.

3.3.3 Limitations of the *ab initio* method.

The ab initio calculations are capable of handling any atom type, including metals. They can produce useful information about structure, vibrational frequencies and energies of molecules and transition states in both the ground and excited states. However, they neglect the effects of electron correlation which make them insufficient for modelling certain systems e.g. the energetics of reactions and bond dissociation[69].

3.3.3.1 The basis set superposition error.

When we examine H-bonded complexes, we often consider the energy of the H-bond as the difference between the energy of the complex and the sum of the energies of the free molecules[70] i.e.:

$$E_{H-Bond} = E_{Complex} - n\left(E_{Free\,Molecule}\right) \qquad ;n = 1,2,3... \qquad \text{Eq. 3.20}$$

Consider a dimer A–H···B. The standard calculation of the energy of the complex is calculated from the union of the monomer basis sets[71]:

$$\phi_{\mu_{A-H\cdots B}} = \phi_{\mu_{A-H}} \oplus \phi_{\mu_B} \qquad \text{Eq. 3.21}$$

And the H-bond energy is calculated, as above, but each energy has its own basis:

$$E_{H-Bond} = E_{A-H\cdots B}\left(\phi_{\mu_{A-H}} \oplus \phi_{\mu_B}\right) - E_{A-H}\left(\phi_{\mu_{A-H}}\right) - E\left(\phi_{\mu_B}\right) \qquad \text{Eq. 3.22}$$

This energy contains, in addition to the effect of the interaction, the result of the basis set extension for each monomer. This is called the basis set superposition error (BSSE).

To eliminate this the Counterpoise Method of correction must be used[72]. The idea behind this is to use the union of the monomer basis sets when calculating the properties of the monomers. To do this for A–H, first calculate the properties of the dimer, but remove the electrons from B, and set the nuclear charge of B to zero. This means that the electrons of A effectively take up their dimer positions but only undergo monomer-type interactions. The same method is then applied to B.

Thus:

$$E_{Corrcted} = E_{A-H\cdots B}(\phi_{\mu_{A-H}} \oplus \phi_{\mu_B}) - E_{A-H}(\phi_{\mu_{A-H}} \oplus \phi_{\mu_B}) - E_B(\phi_{\mu_{A-H}} \oplus \phi_{\mu_B}) \quad \text{Eq. 3.23}$$

Now if we assume that:

$$E_{Corrected} = E_{H-Bond} + \delta \quad \text{Eq. 3.24}$$

Where δ is the correction, we see that

$$\delta = \{E_{A-H}(\phi_{\mu_{A-H}}) - E_{A-H}(\phi_{\mu_{A-H}} \oplus \phi_{\mu_B})\} + \{E_B(\phi_{\mu_B}) - E_B(\phi_{\mu_{A-H}} \oplus \phi_{\mu_B})\} \quad \text{Eq. 3.25}$$

Consider two monomers X and Y (Fig 3.3). On forming the H-bonded dimer, the electrons interact causing the electron cloud to distort (Fig 3.4). The Counterpoise Method of correction of the H-bond energy effectively treats each monomer as though it had the distorted electron cloud (Fig 3.5). This treatment removes the basis set extension for each monomer, and providing a more realistic value for the energy of the hydrogen bond alone.

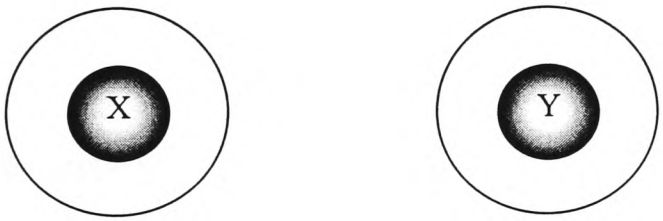

Fig 3.3 – Schematic diagram of two monomers, X and Y, shown as nuclei surrounded by an electron cloud.

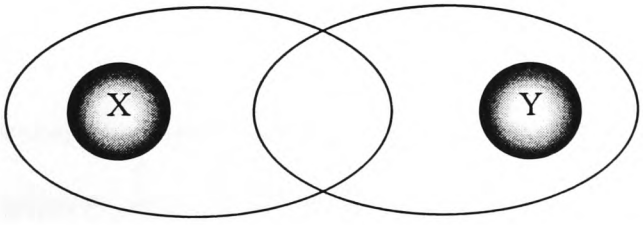

Fig 3.4 – Schematic diagram of the hydrogen bonded dimer X···Y.

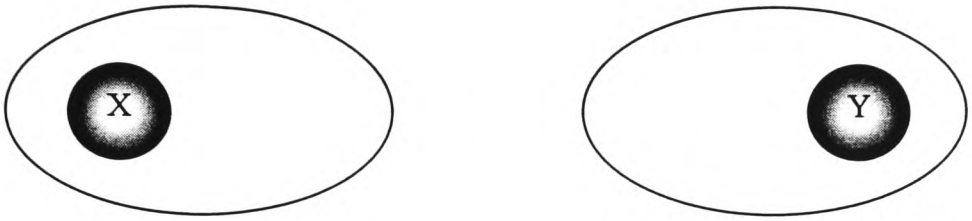

Fig 3.5 – How the Counterpoise Correction method views the electron clouds of the monomers X and Y.

3.3.3.2 Frequency anomalies.

The *ab initio* method calculates the frequencies assuming harmonic behaviour in the PE function around the minimum where the energy calculation has converged. In reality, polyatomic molecules vibrate anharmonically broadening the harmonic band, making it difficult to resolve. By scaling the calculated frequencies to about 90% of their original value helps to compensate for this and small errors introduced by the calculation methods employed[73].

However, generalising the scaling is difficult. The amount of anharmonicity contained within a vibrational frequency varies from bond to bond and from molecule to molecule.

3.3.3.3 Performing the calculations.

The overall problem of analysing the physical and chemical properties of molecules using *ab initio* calculations is a computational one, requiring quite powerful and fast computers to perform such calculations. Many computer programs utilise this method of computational chemistry, but Gaussian is probably the most widely used (which will be detailed in chapter 4).

Even with the use of Supercomputers, a calculation might take several days. The initial structural information needs to be vigilantly scrutinised and laboriously entered into the computer to obtain sensible "real world" results, and the output data needs to be carefully considered to ensure that the correct conclusions about the molecular system being studied are drawn.

Chapter 4

Software description.

4.1 Primary software packages.

The subsequent sections provide brief descriptions of the main software packages used for the calculations in the work that follows.

4.1.1 Chem-X.

Chemical Design's Chem-X is a Windows based molecular modelling package, employing molecular mechanics techniques to generate the structural parameters. It allows the user to create and manipulate large molecules, such as collagen, without losing any functionality with much smaller molecules. Chem-X has two main strengths as a molecular modelling package: The ability to generate conformers (and produce potential energy maps from the conformers) and the ability to create databases of molecules, allowing pharmacophore searches and conformer storage. It also allows the molecules to be saved in various formats for direct transfer to other packages. The main formats used are: DBS database (the molecular database format mentioned above), CSSR format (useful for storing small molecules and are formatted text files, so they can be altered using a suitable text editor) and PDB Brookhaven protein database format (in widespread use; suitable for other molecule types as well as proteins, and are, again, formatted text files). Other file types include: North, Tribble, SMILES and MACCS MOL formats[74].

When a molecule is created, Chem-X builds the molecule using in-built values for bond lengths and angles. This can result in erroneous molecular shapes. However, Chem-X allows the user to alter bond lengths and angles at will, so the molecule can be tailored to the user's requirements. Once the geometry has been set, it can then be optimised. There are two molecular mechanics options for geometry optimisation. The Van der Waals (VdW) method adjusts the conformation by varying bond torsion angles only, whilst the molecular mechanics energy (MME) optimiser refines the full x- y- and z- co-ordinates.

The VdW optimiser is often a useful precursor to the MME method. After the optimisation has been performed, both the VdW and MM energies of the system can be calculated[75].

Within Chem-X, the VdW and MM energies are defined as[76]:

$$E_{MM} = E_{VdW} + V_b + V_a + V_{oop} + V_r \qquad \text{Eq. 4.1}$$

$$E_{VdW} = V_{nb} + V_{tor} + V_{el} + V_{hb} \qquad \text{Eq. 4.2}$$

Where each term is an energy corresponding thus: V_b = bond strain; V_a = angle strain; V_{oop} = out of plane bending; V_r = restraints; V_{nb} = non-bonded interactions; V_{tor} = torsions; V_{el} = electrostatic; V_{hb} = hydrogen bonding.

One disappointing aspect of Chem-X is its treatment of hydrogen bonded systems. A H-bond has an energy contribution which is defined by Chem-X as[(77)]:

$$V_{hb} = 1.31\left(\frac{C}{r^A} - \frac{D}{r^B}\right) \qquad \text{Eq. 4.3}$$

where *A, B, C, D* are all constants.

This is just a standard Lennard-Jones expression for potential energy. However, the repulsive polarisation energy between the H-bonded atoms is too high to obtain good geometries which approximate experimental observations. As a result, a scaling factor called the *hydrogen-bonding factor*, is used to scale the equilibrium distance in the energy calculations, and has a default value of 1.31[78]. Chem-X also does not seem to have the ability to decide whether a system should have a H-bond or not, leaving the user to specify this absolutely.

The package can import spectra in a non-standard SPK format. Chemical Design have, however, written a conversion routine called JCAMPDX, which converts spectra from the JCAMP-DX format to the SPK format. The imported spectra can be stored in a molecular database alongside the molecule it represents, but no manipulation of the spectra is allowed.

Whilst the Chem-X package does provide some useful molecular modelling facilities (especially the generation of molecular structures to provide a foundation for the Gaussian calculations), it is felt that the main use of the software is the creation and manipulation of pharmacophore databases.

4.1.2 Gaussian 94, 92.

The Gaussian 94 (and previously 92) package from Gaussian Inc., is a Windows based *ab initio* calculation package. It allows the user to enter information about a molecule, in the form of internal co-ordinates, a Z-Matrix, or directly as Cartesian co-ordinates, specifying only the atom types and the bonding order. To speed-up calculations, the user can also provide estimates of bond lengths and angles. Gaussian 94 (G94) can also convert many different file types into Z-Matrices, including Cartesian co-ordinates, MOPAC, and PDB. Clearly, this allows molecules built with Chem-X to be directly imported to Gaussian, without the user having to create a suitable Z-Matrix, or guess good initial values for the structural parameters, thus simplifying the use of Gaussian[79].

The program can then generate, by numerical calculations based on the Schrödinger equation and the quantum mechanical postulates, an energy minimised geometry of the specified molecule. The output file generated is quite verbose, and contains useful data about the molecule, such as dipole moments, thermochemical data, and the infrared harmonic frequencies and intensities. An example of an output file, together with its corresponding input file is given in Appendix B for illustration purposes.

The calculation method, together with a basis set must be specified in the Z-Matrix. It is up to the user's discretion, which types should be implemented, and experience provides an informed choice. In an ideal world, we would just specify the atoms, and G94 would calculate all the possible energy minimised structures complete with all spectroscopic and thermochemical data required. However, this is not possible. One reason is that G94 optimises the geometry with respect to the energy i.e. finds an energy minimum for the structure by varying the geometry. Calculating the energy plot for molecules with

many degrees of freedom (>3) is a complex problem. So finding the global minimum is not an easy task, and can result in G94 homing in on a local minimum. The local minima can represent other conformations of the structure, not necessarily the most stable. Saddle points are places on the energy plot consisting of the superposition of minima and maxima, and are considered to be *transition states*[81]. It should also be noted that G94 does not work with absolute bonds, but by looking at the possible orbital configurations, decides on whether there is a high probability of bonding taking place. It is therefore incapable of stating whether bonding should be single, double, triple or resonant hybrids (e.g. benzene). It is left to the user to deduce the bond type, although analysing at the calculated bond lengths will decide.

Thus G94 requires starting point geometry, preferably close to the optimised geometry. This not only allows G94 to converge on the global minimum, but also decreases the amount of computational time, and Chem-X provides this requirement.

The accuracy of *ab initio* results, when compared to experimental values, is not very high and varies quite considerably for different calculations on the same system. The conclusion drawn from this observation is that agreement is often due to the cancellation of errors, and deciding on the calculation method and basis set, requires some forethought on behalf of the user.

4.1.2.1 Gaussian 94 Z-Matrices.

Gaussian 94 requires the user to input molecular data in the form of a Z-Matrix (Fig 4.1)[80]

#<calculation type>/<basis set> <calculation function>

<charge>,<multiplicity>

<first atom>

<second atom>,<bonding atom>,<bond length>

<third atom>,<bonding atom>,<bond length>,<forms angle with>,<bond angle>

<fourth atom>,<bonding atom>,<bond length>,<forms angle with>,<bond angle>,<forms torsion with>,<torsional angle>

And so on...

Fig 4.1 – The format of a G94 Z-Matrix.

4.1.2.2 Gaussian 94 calculation types.

The calculation type can be full Hartree-Fock (HF), spin restricted HF (RHF), spin unrestricted HF (UHF); second, third, fourth order Møller-Plesset perturbation theory energy correction, (MP2,3,4) or Density Functional Methods (detailed in Appendix B), (B3LYP) among others[82]:

1) **RHF** – The spin restricted Hartree-Fock calculation is the most commonly used calculation method. It assumes that the total electronic spin is zero i.e. all the electrons are paired up, as per the Pauli Exclusion Principle (i.e. every α electron is paired with its β counterpart). This assumption helps to speed-up the calculation.

2) **UHF** – The spin unrestricted HF calculation is used when studying ions etc, that can contain an unpaired electron.

3) **MP2, 3, 4** – This provides a 2^{nd}, 3^{rd}, 4^{th} order perturbation theory correction to the energy calculation. This calculation is very processor intensive, and takes a considerable amount of time.

4) **B3LYP** – This method provides a correction for electron correlation. This helps to correct the overestimation of the vibrational frequencies of the molecular structure. Again, this method is processor intensive, but less so than MP2, 3, 4.

4.1.2.3 Gaussian 94 basis set types.

As stated in Chapter 3, the basis set provides the mathematical description of the orbitals within a system, which in turn combine to approximate the total electronic wavefunction. Large basis sets more accurately approximate the orbitals by imposing fewer restrictions on the electrons in space. Ideally, since an electron has a finite probability of being anywhere in space, we should use an infinite basis set expansion. However, this impractical for the calculations.

There are several types of basis sets that can be used for the calculations:

1) Minimal basis sets (MBS).

These contain the minimal number of basis functions needed to describe each atom.

For example:

H: 1s

C: 1s, 2s, $2p_x$, $2p_y$, $2p_z$

etc

MBS use fixed size orbitals. They are entered into G94 as: STO-*k*G. This implies that all the electrons shells consist of Slater-type orbitals, each written in terms of *k* Gaussian functions[83].

The STO-3G s a MBS. It comprises 3 Gaussian functions per basis function (hence 3G). The basis functions are Slater Type Orbitals (hence STO), so the STO-3G basis set approximates STOs with Gaussian functions, as mentioned in chapter 3.

2) Split valence basis sets (SVBS).

One way to improve the approximation is to increase the number of basis functions per atom.

For example:

H: 1s, 1s'

C: 1s, 2s, 2s', $2p_x$, $2p_y$, $2p_z$, $2p_x'$, $2p_y'$, $2p_z'$

The primed and unprimed orbitals differ in size.

SVBS are entered into G94 as: *l*-*mn*G. This implies that each inner-shell is represented by a single function, which in turn is a combination of *l* Gaussian primitives, and that the valence shell orbitals are represented by one contracted basis function written in terms of *m* primitive Gaussian functions, and one diffuse basis function written in terms of *n* primitive Gaussian functions[84].

For example: The 3-21G SVBS uses 3 Gaussian functions per basis function for inner orbitals, and 2 sizes of basis functions for each valence orbital, 1 basis function described by 2 Gaussian function, the other described by 1 Gaussian function.

3) Polarised basis sets (PBS).

SVBS allow the orbitals to change size but not shape. Polarising the basis set helps to overcome this. They are denoted by adding (*x*,*y*) after the SVBS. For example: 6-31G(d,p) (equivalent to 6-31G**) allows d-type functions to be added to heavy atoms, and p-type functions to be added to H atoms. This allows G94 to contend with ideas like hybridisation of orbitals where, for example, sp^3 orbitals are formed on carbon by mixing filled 2s orbitals and partially filled 2p orbitals[85].

4) Diffuse functions (DF)

Diffuse functions can be thought of as large versions of s- and p-type functions, as opposed to standard valence size functions. They allow orbitals to occupy a larger region of space. Basis sets with DFs are important for systems where the electrons can exist quite far from the nucleus e.g. lone pairs, anions etc. They are denoted by adding "+"s after the SVBS. For example: *l-mn*++G, where the first + adds DFs to heavy atoms, and the second to H atoms[(85)]. It is debatable whether adding DFs to H atoms improves the accuracy of the calculations.

4.1.2.4 Gaussian 94 calculation functions.

The calculation function is that which the user wishes G94 to perform e.g. OPT (structure optimisation), FREQ=ANAL, (analytical calculation of the IR and Raman normal mode frequencies and intensities (no anharmonicity)).

4.1.2.5 Gaussian 94 charge specification.

The charge is as expected: 0 for a neutral molecule, +1 for a singly charged cation etc.

4.1.2.6 Gaussian 94 multiplicity specification.

The multiplicity refers to the electron spin angular momentum vector, $\underline{\mathbf{S}}$, in terms of the α and β spin states of the electrons of the molecule in question[86]. It is defined as:

$$\underline{\mathbf{S}} = 2.\sum_{i_{\alpha,\beta}} s_i + 1 \qquad \text{Eq. 4.4}$$

where: $s_{1_\alpha} = +½$ and $s_{1_\beta} = -½$ Eq. 4.5

For a neutral molecule such as H_2, $\sum_{i_{\alpha,\beta}} s_i = 0$, so the multiplicity would be 1, but for the OH radical, whose overall charge is 0, $\sum_{i_{\alpha,\beta}} s_i = 1$, so the multiplicity would be 2.

4.1.2.7 Gaussian 94 molecular structure specification.

As stated previously, the initial molecular structure can be specified as either internal co-ordinates, or as Cartesians, from some arbitrary point. Which ever are chosen, G94 automatically converts them into Cartesians whose origin is the centre of mass of the molecule.

4.1.2.8 Gaussian 94 basis set limitations.

Not all basis sets are suitable for all elements of the Periodic Table. Table 4.1 identifies which basis sets are applicable to different ranges of elements[87].

Basis set	STO-3G	3-21G	6-21G	4-31G	6-31G	6-311G
Element range	H – Xe	H – Xe	H – Cl	H – Ne	H – Cl	H – Br

Table 4.1 – Identifying the range of elements covered by a basis set.

4.1.3 Initial calculations.

As stated previously, a sample input file for the CON···HCl complex, complete with its corresponding output file is presented in Appendix B.

Initial calculations compared a variety of basis sets and calculation types for HF and HCN, and also compared the molecular mechanics methods of Chem-X with the *ab initio* methods of Gaussian for the intramolecularly hydrogen bonded 2-Fluoroethanol, and the intermolecularly bonded HCN···HF complex. However, it is felt that these results are a preliminary aside to the main work that follows, and can thus be found detailed in Appendix C.

4.2 Secondary software packages.

The following packages provided additional support to the main software.

4.2.1 Galactic *GRAMS*.

The Galactic *GRAMS* software is a popular Spectroscopy analysis package. It is written in Array Basic, which means it can be modified to the users requirements, and also allows the user to write his/her own modules which can run within the package. An example of this is the Spectral Search Module, which is an optional routine available from Galactic. Once installed it is accessed through *GRAMS*, and can search a wide variety of libraries including Sprouse, Nicolet-Aldrich and Sadtler. The *GRAMS* software also imports and exports over 100 different instrument data formats, including JCAMP-DX and two-column ASCII text, and because of the modular approach of the software, new formats can be added as needed.

Once a spectrum has been imported, then it can be manipulated in many ways, allowing curve fitting, deconvolution and spectral searches to be performed and the resulting data can be exported to a word processor for inclusion into reports etc.

4.2.1.1 Curve fitting with *GRAMS*.

Curve fitting is a powerful application of *GRAMS*. It can fit a number of ideal peaks to measured data, deconvoluting broad bands into the separate peaks that make the band. It has the following capabilities[88]:

1) It can apply different methods of curve fitting: Gaussian, Voigt, Lorentzian, Log Normal, Pearson VII, Mixed Gaussian-Lorentzian.
2) Different baselines can be included: Offset, Linear, Quadratic, Cubic.
3) Only computing resources limit the number of peaks that can be fitted – i.e. hundreds of peaks may be fitted to thousands of data points.
4) An initial estimate of the number of peaks and their position may be calculated using the AutoFit function.

5) An interactive peak selector allows fast and flexible selection of the initial parameters in real time.

6) All parameters may be optionally constrained.

The algorithm of non-linear curve fitting used is the Levenburg-Marquardt method[89]. It was found, by trial and error, that the Voigt function provided the best from of deconvoluion. The function is defined as[88]:

$$f_V(x) = \frac{\int_{-\infty}^{+\infty} \frac{a_0 \exp(-y^2)}{a_3^2 + \left\{\left(\frac{X - a_1}{a_2}\right) - y\right\}^2} dy}{\int \frac{\exp(-y^2)}{a_3^2 + y^2} dy} \qquad \text{Eq. 4.6}$$

where: a_0=height; a_1=position; a_2=Gaussian width; a_3=Lorentzian width.

4.2.2 Animol.

Animol is a Windows based package written by Innovative Software. It has been designed as an illustrative tool, linking the vibrational normal modes of a molecule to the resulting infrared spectrum it would produce.

The main virtue of the package is that it can import the infra-red harmonic frequencies and intensities from the Gaussian output file, display the spectrum on the screen, and then export the spectrum in a format that can be readily imported into *GRAMS*. In *GRAMS*, this theoretical spectrum can then be fully analysed.

4.2.3 Rasmol.

Rasmol is a Freeware package for Windows, written by Roger Sayle at Glaxo. Its main use is molecular rendering and can display molecules in several formats such as ball and stick, space fill, and ribbons and strands for proteins. It can export the chosen design to CompuServe GIF, Bitmap BMP or Postscript, for incorporation into reports. It supports the Brookhaven PDB and Alchemy file formats.

4.2.4 Microsoft Office.

This suite of standard office productivity tools provides the usual word-processing and spreadsheet capabilities, for general document manipulation.

4.3 Tertiary software packages.

This selection of software consists mainly of small utilities and applets, providing additional assistance.

4.3.1 JCAMPDX.

JCAMPDX is a small MS-DOS conversion routine by Chemical Design for converting JCAMP-DX files to the SPK format required by Chem-X.

4.3.2 Listasc.

This is a small MS-DOS program by Perkin-Elmer for converting the binary SP spectrum files produced by their 1440 spectrometer to two-column ASCII text. This text can then be imported into GRAMS, or even a spreadsheet package for display and manipulation.

4.3.3 PeakFit.

PeakFit is an MS-DOS based curve-fitting package, which can be used to analyse spectra. It only accepts Lotus 1-2-3 files, so conversion is required. It incorporates many advanced non-linear curve fitting functions, such as Gaussian, Lorentzian and Voigt. However, being an MS-DOS package, means that much of the functionality that Windows has (e.g. OLE, DDE) is lost, plus GRAMS easily supersede it.

4.4 Spectroscopic File Transfer Protocols

Computers are now widely used within the field of science and, as a result, the users usually require their experimental data to be transferred over the various computer networks that now exist. Certain standards (called protocols) need to be set by both the sender and receiver if the transfer is to be successful, and the data usable.

4.4.1 JCamp-DX

Spectroscopic data has recently been subjected to standardisation by MacDonald and Wilks[90], and the result is the JCamp-DX format. This file type consists of ASCII text in a header/data format. The header contains all of the necessary information about the measurement ranges for wavenumber and absorbance, as well as peripheral information about the instrument, date, and owner etc. The data following the header has a wavenumber value followed by several absorbance values, separated either by "+" or single spaces. Fig. 4.2 shows a typical DX file for one band in the benzene spectrum, and Fig. 4.3 shows this band as imported into *GRAMS*.

```
##TITLE= BENZENE 0.025 mm CELL. BAND RANGE 1100-905 cm-1
##JCAMP-DX= 4.10
##DATA TYPE= INFRARED SPECTRUM
##ORIGIN= BIO-RAD DIGILAB FTS50
##OWNER= SHAUN O'NEILL
##DATE= 90/02/09
##TIME= 13:07:04
##CREATED= Fri Feb 09 13:07:04 1990
##SPECTROMETER/DATA SYSTEM= Digilab Data system=3250
##XUNITS= 1/CM
##YUNITS= ABSORBANCE
##RESOLUTION= 4.0
##FIRSTX= 9.02683764e+02
##LASTX= 1.10135135e+03
##FIRSTY= -1.140267774e-02
##MAXY= 8.430289328e-01
##MINY= -2.213525400e-02
##XFACTOR= 1.92881146e+00
##YFACTOR= 1.862645149e-09
##NPOINTS= 104
##XYDATA= (X++(Y..Y))
468-6121766-6528578-6991656-7371402-7758902-8134432-8588962-9065912-9468926
477-9851472-10115622-10388762-10747136-11044434-11284876-11528954-11702978
485-11747350-11844452-11883774-11734282-11520162-11343218-11209842-10971858
```

```
493-10582016-10130006-9549656-8789154-7924348-6942524-5799222-4563398-3508236
502-2866934-2430346-2353074-2476424-2400928-2380850-2290766-2023100-1609692
511-835870 509046 2368794 3829752 4145582 3963760 4044556 4564634 5610604
520 7537924 10778000 15701046 21241542 23826166 23273704 23416980 26081706
528 31570804 40505622 54381564 75810522 108636692 158035770 229025060
535 321125922 414939022 452597712 381859334 266070032 172599276 111686866
542 74208942 50927972 35923094 25685474 18546888 13536804 9822122 7014350
550 4872016 3172896 1778640 566638-512162-1387046-2126150-2782530-3261706
559-3606274-3965792-4284546-4604918-4843236-4987570-5145748-5308050-5446376
568-5590840-5751124-5829130-5780230
##END=
```

Fig 4.2 - JCamp-DX file for the benzene band at 1035 cm^{-1}

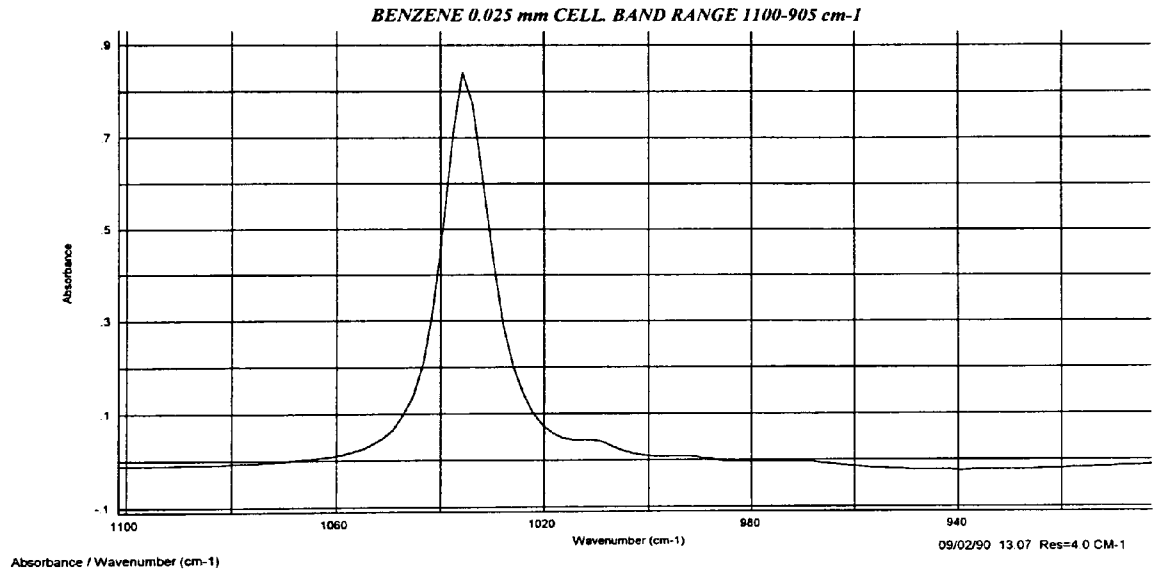

Fig 4.3 - Spectrum of the 1035cm^{-1} band of benzene.

This data format, being ASCII text, can be easily edited in a favourite text editor/word processor, allowing the user to delete unwanted spectral bands etc. Care must be taken, however, as some of the header parameters specifying details of the data must also be changed. A JCamp-DX file can also be easily transmitted to other users via LANs, e-mail, and ultimately, the Internet.

4.4.2 JCamp-DT

The main problem with JCamp-DX is that the files tend to be quite large, and also the native data cannot be directly incorporated into documents for electronic publishing. Thus a binary format, JCamp-DT has been developed to overcome these problems[91]. The main drawback with this format is that the user is unable to view or edit the data, but the data can be transferred over computer networks with greater ease.

4.4.3 JCamp-BDX

This file type is Robert MacDonald's compromise between the DX and DT types[92]. The file structure comprises of an ASCII header with the data in binary. So while the data cannot be edited, the details of it can be viewed as required. Again, transfer over computer networks can be made with relative ease.

4.4.4 UU Encoding and Base 64 Encoding

These are two popular methods of encoding files to be transmitted over computer networks, especially globally. These techniques were developed because sometimes the binary files transmitted contained codes that were reserved by the networks, and could result in premature closing of a connection, even though the codes were perfectly valid binary instructions. UU encoding was developed first to counteract this, and converts the binary data into ASCII so that the reserved codes are not used. Once a UU encoded file is received, it needs to be UU decoded before the information can be used. Base 64 encoding was developed to over come certain limitations within the UU method. It is supported by MIDE, even though UU encoding is the more popular technique. Again, it converts binary to ASCII, avoiding the reserved codes within the ASCII character set.

Chapter 5

Hydrogen Bonded Forms of Methanol - Infrared Spectra and *Ab Initio* Calculations.

5.1 Introduction.

Methanol, arguably the next higher homologue of water, has been studied in relation to equilibria between various hydrogen bonded forms in solution[93,94], as vapour[95,96,97,98,99] and by matrix isolation.[100,101] Infrared spectroscopy is a sensitive measure of different hydrogen bonded forms and, in principle, methanol may have an infinite number of open (linear or chain) and cyclic (closed) inter-molecularly hydrogen bonded forms in all phases. A quantitative study of methanol was carried out by Liddel and Becker[93] who review earlier controversies on the nature and amounts of the various hydrogen bonded forms as between cyclic and open polymeric structures. They assign bands centred at 3643, 3528 and 3332 cm^{-1} for spectra in solution in CCl_4 to monomer, dimer and polymer respectively. Using both temperature and dilution variations they conclude that the band centred at 3528 cm^{-1} probably arose from a cyclic dimer and the band centred at 3332 cm^{-1} arose from open polymers. Bellamy and Pace[94] argued for the inverse assignment. They suggested that the band at 3528 cm^{-1} should be assigned to an open dimer and that at 3332 cm^{-1} to a cyclic trimer. They argue that a cyclic polymer would have abnormally strong hydrogen bonds because an oxygen atom of an O-H group engaged in hydrogen bond formation would be more basic than an oxygen atom in an open dimer and similarly the hydrogen in the cyclic polymer would be more acidic than in the open dimer. Cyclic hydrogen-bonded systems are common in biological situations including those associated with genetical reproduction. These factors may, therefore, explain the very large shift (311 cm^{-1}) of the methanol band attributed to the cyclic trimer or higher cyclic polymers compared with that attributed to the open dimer (115 cm^{-1}). These conclusions are also supported by matrix isolation studies of methanol by Barnes, Hallam and Jones[96] which suggest that the dimer of methanol is open chain rather than cyclic. It was further presumed that trimer and tetramer are largely open chain although

bands were also tentatively assigned to cyclic tetramer by analogy with gas studies by Inskeep et al[98]. The species present in methanol vapour have been estimated from vapour density measurements by Cheam, Farnham and Christian[101] to be monomer, dimer and trimer with no evidence for higher polymeric forms and with estimated equilibria constants favouring trimer up to pressures of 90 Torr. Huisken and Stemmler[102] carried out photodissociation studies on methanol clusters in a continuous supersonic beam with a crossed pulsed CO_2 laser. They observed evidence for two forms of methanol in dimer but only one form in trimer and higher polymers. This is further evidence for an open dimer but closed trimer and higher ring structures.

Recent measurements on higher alcohols provide additional general information on structure of hydrogen-bonded complexes in mono functional O-H systems. Dipole moment measurements[103] of ethanol in various non-polar solvents were interpreted in terms of monomer, open-dimer, cyclic-tetramer association and the enthalpies of the dimer and tetramer structures determined. Near infrared measurement[104] of pentanols in solution in heptane were interpreted in terms of monomer-dimer equilibria at low concentrations, monomer-dimer-tetramer at intermediate concentrations and involving octamers at higher concentrations: dielectric measurements suggested an open dimer, a cyclic tetramer and an open octamer. Heat capacity measurements[105] of aromatic alcohols and phenols in n-heptane solution were interpreted in terms of monomer, dimers, trimers and tetramers. Near-infrared, nmr, viscosity and self-diffusion measurements of octan-1-ol as a liquid and in solution in decane[106] indicated a cyclic tetramer as the predominant species at the concentrations and temperatures obtaining. Mid-infrared measurements[107] of the fundamental O-H stretching mode of medium-length chain alcohols in n-decane solutions were subjected to multivariate analysis which suggested the monomers dominated at low concentrations but cyclic polymers, in particular the tetramer, dominated at high concentrations in the conditions with only small amounts of open polymers.

Theoretical considerations of the components of hydrogen bonded equilibria of methanol are sparse but *ab initio* calculations[108] at the STO-3G level indicate that all polymers greater than dimer were more stable as cyclic rather than open structures. Higher level calculations[109] using the Hartree-Fock 6-311++G(2d,2p) basis sets have been carried out on the cyclic trimer with comparisons with monomer and open dimer.

The present work provides new experimental information on the hydrogen bonded equilibria in methanol in both vapour phase and in solution in CCl_4 by quantitative measurements of the O-H stretching modes (also with some observed effects of hydrogen bonding on the C-O stretching modes). New theoretical information is also presented from *ab initio* calculations of the vibrational frequencies and intensities, geometrical parameters and energies for monomeric methanol and cyclic and open dimer, trimer and tetramer methanol structures using the Gaussian 94 package incorporating six basis sets as representations of molecular orbitals up to RHF6-311++G(3df,3pd) for the monomer, 6-311++G(d,p) for the cyclic and open dimer and 6-31++G(d,p) for the cyclic and open tetramer.

5.2 Experimental work.

Methanol and carbon tetrachloride were BDH Analar grade reagents and spectra were recorded on a Perkin Elmer Spectrum 2000 FT-IR spectrometer at a temperature of 298 K. Wavenumber values were checked as within ± 1 cm^{-1} with HCl gas calibration. The signal-to-noise was measured at intervals as up to 9000 using the instrumental recommended settings

5.2.1 Results.

5.2.1.1 Solution of methanol in CCl_4.

For the following work, I am indebted to Md. Fokhray Hossain for the experimental and some of the computational work.

The spectra of a series of solutions for C/%v/v between 0.10 and 0.80 were recorded between 2500 and 4000 cm^{-1} at 4 cm^{-1} resolution ratioed against solvent using 64

scans. Additionally a pseudo-double beam shuttle arrangement was used to obtain spectra (Fig. 5.1) in which the sample and matching solvent cell were cycled in the spectrometer beam. The rato and shuttle methods yielded similar results.

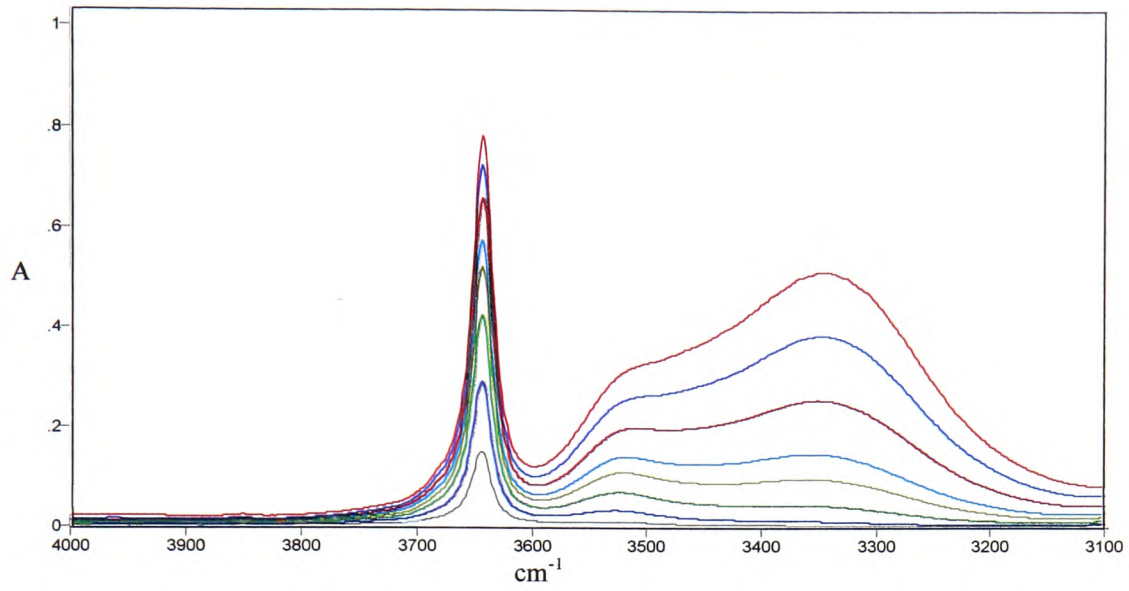

Fig. 5.1 - Infrared spectra of methanol in carbon tetrachloride solution (0.10-0.80 %v/v).

The integrated absorbances, $A_0(cm^{-1})$, of overlapping bands centred at a particular wavenumber value are determined by standard curve resolution packages, as discussed in Chapter 4. Decreasing concentration leads to reduction in the intensity of the band centred near 3358 cm^{-1} (this is a broad band corresponding to that reported at 3332 cm^{-1} by Liddel and Becker[93] with whom these results are qualitatively consistent) but initial increase in the intensity of the band centred at 3517 cm^{-1} followed by a decrease and ultimately only the band at 3644 cm^{-1} is observed. Additional to these bands a shoulder is apparent at 3438 cm^{-1} which will be discussed later in relation to a similar band in the vapour state. This region of the spectrum reveals large changes in O-H stretching modes arising from hydrogen bonding. Measurable changes were also observed in the 900-1200 cm^{-1} region. The C-O stretching mode of methanol as a dilute solution is observed at 1022 cm^{-1}. In more concentrated solution this is shifted to 1027 cm^{-1} and is likely to be a C-O stretching mode in one or more hydrogen bonded complexes

The calculation of the integrated absorption coefficient, ε_0, of the monomer is determined from measurements of integrated band areas, A_0, as a function of concentrations c at path-length, l, which are related by the Beer-Lambert expression:

$$A_o = \int \log_{10} \frac{I_0}{I} dv = \varepsilon_0 cl$$

The plot of A_0/c against c is shown in Fig 5.2 and provides the limiting value of $\varepsilon_0 l$ ($\varepsilon_0 l$ = 53.393 cm^{-1} $(\%v/v)^{-1}$ with correlation coefficient of -0.9883) for the monomer form of methanol at infinite dilution. The value of the integrated absorption coefficient obtained in the present work is $(2.157 \pm 0.025)\times10^4$ m mol^{-1}. This is slightly higher than the value obtained by Lidell and Becker[93] of 2.04×10^4 m mol^{-1} (in comparable units).

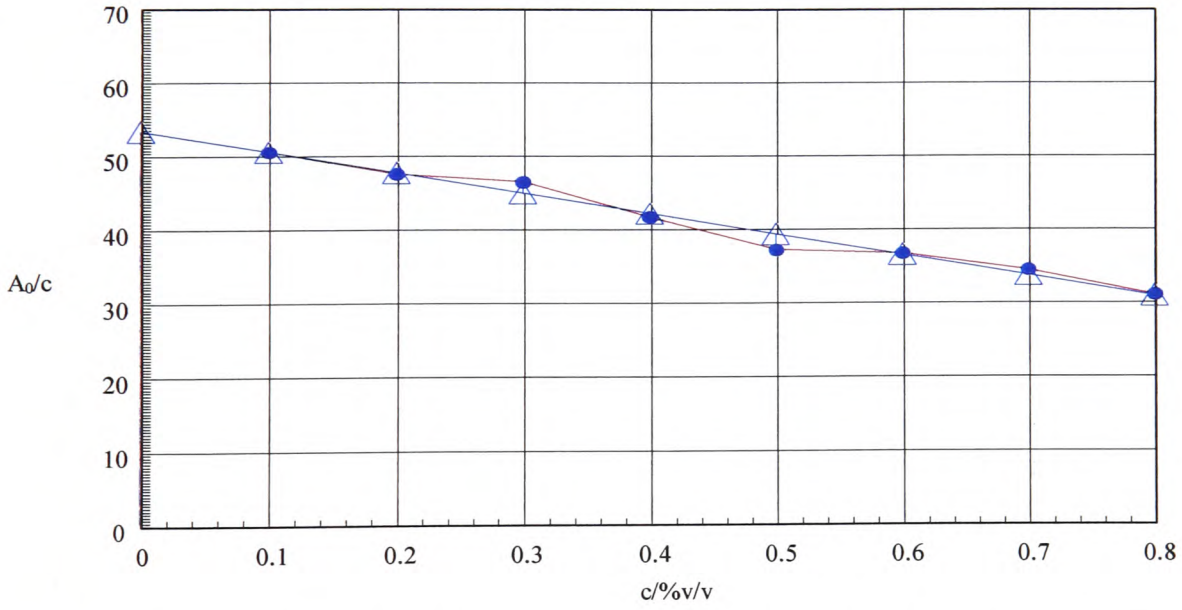

Fig. 5.2 - Determination of limiting value of integrated absorption coefficient.

The determination of ε_0 for methanol monomer permits estimation of the concentration of this species at each concentration C(3644) as shown in Table 5.1. This permits a determination of the total bonded form at each concentration by subtraction of the calculated monomer concentration from the total concentration. The integrated absorbance of the two main overlapping band associated with hydrogen bonded forms A_0(3517) and A_0(3358) was estimated by curve resolution as discussed in Chapter 4.

Evidence for a third band at 3438 cm^{-1} was obtained at higher concentration and the absorbance of this band, $A_0(3438)$, was estimated at 0.60 %v/v and 0.70 %v/v and is included in Table 5.1. It is possible that one or more of the bands associated with hydrogen-bonded forms arise from more than one species and the integrated absorption coefficients of each hydrogen-bonded forms cannot be explicitly determined. However, if the sweeping assumption is made that all hydrogen bonded forms have the same integrated absorption coefficient, these can be estimated for the component(s) associated with the bands at 3517, 3438 and 3358 cm^{-1} and the concentrations of the forms estimated in each solution as C(3517), C(3438) and C(3358). These values are reported in Table 5.1.

Table 5.1 - Integrated absorbance values $\{(A_0(\cdots.)/cm^{-1}\}$ and estimated concentrations $\{C(\cdots.)/\%v/v\}$ of monomeric and hydrogen bonded forms of methanol at specified wavenumber values.

C(Total)	$A_0(3644)$	C(3644)	$A_0(3517)$	C(3517)	$A_0(3438)$	C(3438)	$A_0(3358)$	C(3358)
0.10	5.06	0.095	0.872	0.005	0	0	0	0
0.20	9.52	0.178	5.599	0.021	0	0	0	0
0.30	13.96	0.261	8.325	0.019	0	0	8.34	0.019
0.40	16.69	0.313	14.092	0.038	0	0	18.71	0.049
0.50	18.60	0.348	17.109	0.054	0	0	30.54	0.097
0.60	22.05	0.413	11.489	0.029	12.31	0.029	54.47	0.130
0.70	24.15	0.452	11.385	0.025	19.80	0.043	81.70	0.179
0.80	24.88	0.466	31.082	0.069	0	0	119.44	0.265

5.2.1.2 Vapour phase.

Methanol has been studied less extensively as a gas than in solution and previous work by Inskeep et al[98]. has not provided quantitative information on hydrogen bonding. The O-H stretching mode has been studied at high resolution[95] and the series of Q branches centred at 3681.5 cm^{-1} assigned to rotational-torsional levels from which

molecular constants of methanol were determined for the monomer state but no assignments were made for higher polymeric forms.

Fig 5.3(a) shows the spectrum of methanol gas and provides comparable information to that for solution in Fig 5.1. Three bands are attributed to corresponding bands which were observed in solution and attributed to monomer and different hydrogen-bonded polymer forms. Fig 5.3(b) shows the bands attributed to polymeric forms obtained by subtraction methods and shows the variation with pressure.

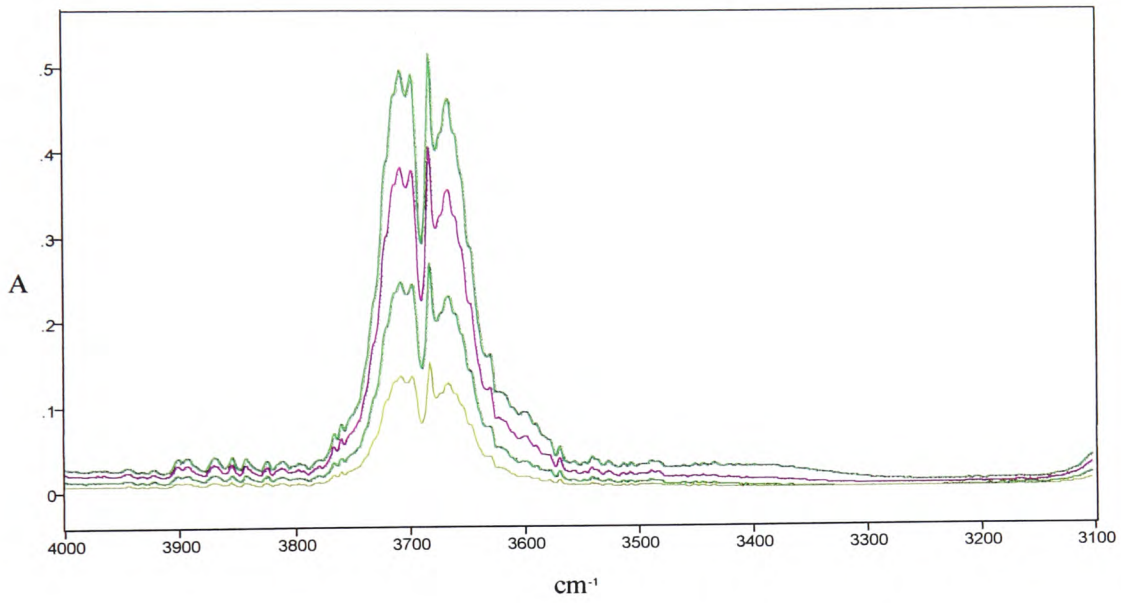

Fig. 5.3(a) - Infrared spectra of methanol vapour (25, 50, 75, 100 torr).

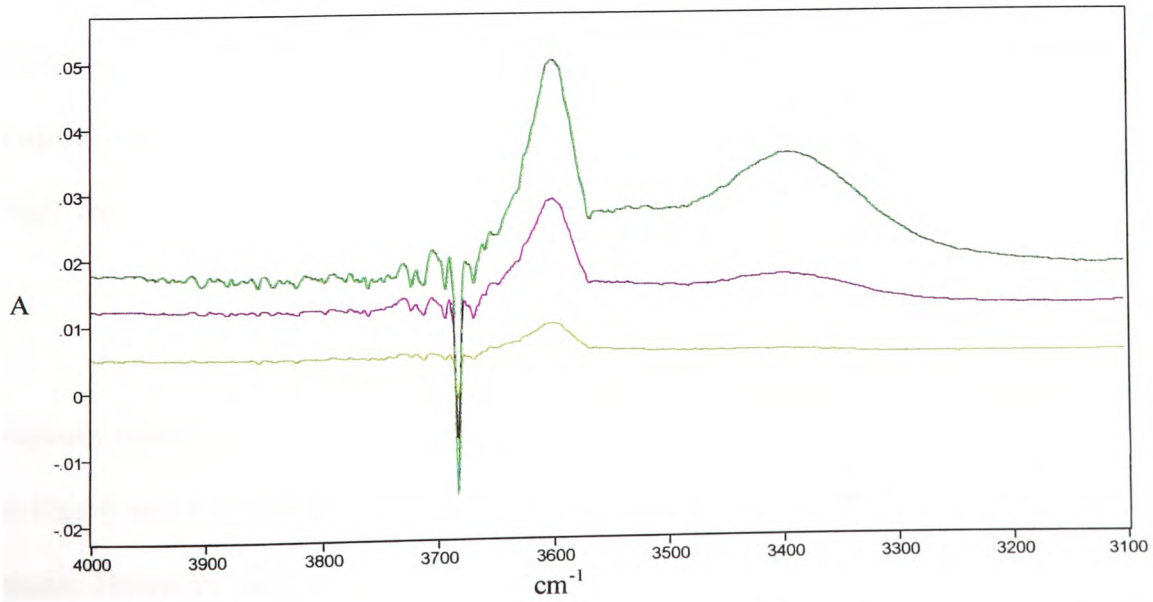

Fig. 5.3(b) - Subtraction of ir spectrum of methanol at 25 torr from spectra at 50, 75, 100 torr.

In the region associated with O-H stretching motion in both solution and vapour phases there are three prominent bands which have similar dependencies with concentration and pressure and two weaker features. There is only one such detectable band in the region associated with C-O stretching modes. In both phases the prominent band in the O-H region at highest wavenumber (Band 2) is favoured at low concentration or pressure and the band at lowest wavenumber (Band 5) is favoured at high concentration or pressure. The prominent intermediate band (Band 3) initially gains in intensity as the concentration or pressure decreases at the expense of Bands 3 and 4, which weaken. Further reduction in methanol concentration or pressure leads to the diminution of Band 3 and the increase in Band 2. The weaker features are Bands 1 and 4 which are shoulders on the high wavenumber sides of Bands 2 and 5. Bands 6 and 7 are associated with C-O stretching vibrations.

The essential question posed from observation of spectra of methanol in solution and vapour state is the assignment and characterisation of the molecular species associated with these bands. They may be summarised:

Phase /Band	**1**	**2**	**3**	**4**	**5**	**6**	**7**
CCl_4 solution/cm^{-1}	3672	3644	3517	3438	3358	1022	1027
Shift/cm^{-1}	+28	0	-127	- 206	-286	0	+5
Vapour/cm^{-1}	3895[7]	3681	3595	3500	3392	1033	1057
Shift/cm^{-1}	+214	0	-85	-181	-289	0	+24

It may be assumed that these apparently corresponding bands in the solution and vapours states are assigned to the same species. In principle the nine calculated structures in Figs 4 and 5 and a number of others would be in rapid equilibria in solution and vapour phase. However the balance of evidence in the present and previous work suggests that Band 3 is assigned to the hydrogen bonded O-H of an open dimer, Band 5 is assigned to a

cyclic trimer or tetramer and Band 2 is assigned to a monomer with possible overlap from the free O-H of an open dimer.

The assignment of Band 2 to overlapping O-H groups is, in principle, amenable to experimental verification. Firstly by possibly deconvoluting relevant overlapping bands with slightly different wavenumbers. Such methods are applicable with more confidence in the solution state because of the more complex band contour in the vapour state. In the present work the low sensitivity at low concentrations precluded separation of bands with separations less than 5 cm^{-1} but there appeared to be a weak feature described as Band 1. However this did not show a concentration dependence consistent with a monomer/polymer equilibrium and is therefore likely to arise from a combination band between the O-H stretching mode and a low frequency motion. Similar assignments can been made in the vapour state. Here the wavenumber separation is much greater in the vapour than solution phase and the origins of the components may be different. Secondly the concentration dependence of absorbance would be expected to show an enhanced intensity from terminal O-H groups of open chain polymers at higher concentrations. The assignment of Band 3 to an open dimer would be expected to lead to an enhancement of Band 2 in the concentration range where Band 3 is prominent. The graph shown in Fig 5.2 is approximately linear within experimental error but measurements at higher accuracy could possibly be fitted to curves representing overlapping O-H groupings from monomer and one or more open polymers.

Band 5 has been variously assigned to a cyclic trimer or tetramer as discussed earlier. The experimental infrared information cannot readily discriminate between different cyclic forms but the weight of other evidence favours the cyclic trimer in solution and vapour but cannot rule out the partial existence of cyclic tetramer or other cyclic forms. Similarly Band 4 may be associated with the same or different cyclic forms of methanol.

5.3 *Ab Initio* work.

The theoretical calculation methods employed were Hartree Fock, Moller Plesset and Density Functional Theory. The calculations using the Hartree Fock method were carried out using the Gaussian 94w package operating on a Viglen PC Pentium 2 (266 MHz, 64 MB RAM, 3GB hard drive space). Calculations by Gaussian methods using the Moller Plesset (MP2) and the Density Functional Theory (B3LYP) methods were frequently too large for the PC and were carried out by remote access to the Columbus and Magellan facilities at the Rutherford Appleton Laboratory using the DEC 8400 supercomputer.

5.3.1 Results.

Calculations by all three methods were carried out using ten basis sets and the properties for methanol determined. The stable model was taken as that in which the methyl hydrogen atoms are staggered with respect to the O-H group. This corresponds to the planar C_s point group and the 12 vibrations split into 9 a′ and 3a′ vibrations. Selected geometrical, spectroscopic, thermodynamic results and the dipole moments for the Hartree Fock method are summarised in Table 5.2 for ten basis sets.

The basis sets correspond to different levels of approximation for molecular orbitals and higher basis sets are composed of greater numbers of basis functions. The number of basis functions for each basis set is included in Table 5.2. This Table selects the O-H and C-O stretching vibrations which are the most characteristic of alcohols and reports the calculated wavenumber value together with the calculated IR and Raman intensities in arbitrary units for all ten basis sets at the Hartree Fock level. Table 5.3 reports all twelve normal vibrations of methanol for the smallest and largest basis sets used for the three methods, HF, MP2 and B3LYP. Here the calculated wavenumber values are compared with the measured values reported by Serrallach, Meyer and Gunthard [110]. The co-ordinates of the output model from any Gaussian calculation are readily transferred into

a standard PDB (protein database) file which may then be exported to a package such as Chem-X and the model displayed as in Fig. 5.4(a) and Fig. 5.4(b).

The calculated structures of the cyclic forms shown in Fig 5.4(a) indicate the following point groups and spectral activities (neglecting the effect of different conformations through rotations of the methyl groups which are likely to be small). The trimer structure, as shown, strictly has no rotation or reflection symmetry elements. However it is conceivable that the methyl groups are able to flip between each side of the ring. If these equilibria were sufficiently rapid the trimer would belong to the C_{3v} point group (or possibly the D_{3h} point group). The cyclic tetramer has unusual symmetry properties in terms of a 4-fold alternating reflection -rotation axis. This corresponds to the S_4 point group. This gives rise to an active pair of degenerate O-H stretching modes for the cyclic tetramer at a calculated wavenumber value 3581 cm^{-1} at the higher basis set used. The corresponding active near-degenerate pair for the trimer are at 3648 and 3644 cm^{-1} . This indicates the effect of departure from C_{3v} symmetry in terms of splitting the degeneracy which would otherwise obtain by only 4 cm^{-1} calculated at the 6-31++G(d,p) level or 2 cm^{-1} at the 6-31G(d) level and with corresponding small differences in calculated intensities of the components of the near-degenerate pairs:

$(CH_3OH)_n$	**Dimer(n=2)**	**Trimer(n=3)**	**Tetramer(n=4)**
Point Group	C_{2h}	C_{3v} (approx)	S_4
O-H stretch	a_g(inactive)	a_1(active)	a(inactive)
IR- activity	a_u(active)	e (active)	b(active)
			e(active)

The calculated wavenumber shifts of the cyclic dimer relative to the monomer using four different basis sets are between 12 and 23 cm^{-1} for the a_u mode. This suggests hydrogen bonding would be weak in this structure. The calculated shifts for the cyclic trimer are similar for both basis sets used. The calculated band approximating to an a_1 mode at a shift near 120 cm^{-1} is of calculated weak intensity but the near degenerate pair

near 100 cm^{-1} in shift are calculated to be intense bands and are assigned to Bands 4 or 5. In the case of the cyclic tetramer the inactive *a* mode has the largest calculated shift with the degenerate pair of *e* modes displaying calculated shifts near 164 cm^{-1} with large calculated intensities for both basis sets and the *b* mode displaying a shift near 145 cm^{-1} of low intensity. The degenerate pair of *e* modes could also be assigned to Band 4 or 5.

The calculated shift values could indicate the cyclic trimer and tetramer were assigned to Bands 4 and 5 respectively but *ab initio* calculations of hydrogen bonded systems are not yet well developed and can not be used with confidence at this level of detail. The shift values for hydrogen-bonded O-H open structures shown in Table 4 are smaller than for the corresponding cyclic structures in Table 3 in accord with the proposition that cyclic structures of this kind are more stable. The open dimer is assigned to Band 3 with calculated shifts of between 56 and 69 cm^{-1} compared with an observed shift of 85 cm^{-1} in the vapour state. The calculated shifts for the open trimer and tetramer are between 76 and 156 cm^{-1}. This would suggest that if higher open polymers were present they would reveal bands with slightly larger shifts than those assigned to open dimer. The restricted (closed shell) RHF method used in the present work is the default method where there are no unpaired electrons (odd numbers of electrons, excited states or bond dissociation). The (2d,2p) basis set is higher than (d,p) used in the present work for polymeric forms by virtue of inclusion of polarisation functions for two sets of d functions on the carbon and oxygen atoms and two sets of p functions on the hydrogen atoms. The present work included the RHF/6-311+G(d) and the RHF/6-311++G(d,p) basis sets for monomer and cyclic and linear dimer but was limited to the lower basis sets for the trimer and tetramer. These calculations showed good agreements with corresponding basis sets of within 16 cm^{-1} for O-H stretching mode shifts (and in many cases much closer agreement, Tables 3 and 4). In terms of hydrogen bonding the O-H···O distances are particularly interesting and are reported in Table 5 (cyclic structures) and Table 6 (open structure). The cyclic dimer is calculated as having the largest distance at 2.3Å or greater which is

significantly larger than that of the open dimer at 2.0Å with little change over the four basis sets reported in each case. The trimers and tetramers do show calculated values which vary with basis set more in the cyclic forms than in the open forms. The larger value for the cyclic dimer is consistent with the apparent lack of stability and failure to achieve a minimum energy value under the conditions applied experimentally and theoretically. These agreements suggested that the use of the RHF/6-31G basis set with added diffusion and polarisation functions was adequate for the trimer and tetramer molecules.

The structure of all nine molecules is determined after optimisation for each of the four basis sets used and the values are included in Figs 5.4(a) and 5.5(b) at the RHF6-31++G(d,p) level. The hydrogen bonding energy ($E_{H\ Bond}$) is assumed to be the energy of the hydrogen bonded complex ($E_{Electronic}$) minus the corresponding sum of the energy values of the unbonded components and is included in Tables 5 and 6. The average values for the cyclic dimer (17.8 kJ mol $^{-1}$) and open dimer (21.8 kJ mol^{-1}) are similar. As stated earlier the cyclic dimer appears to be a transition state and the open dimer is assigned to Band 3. The $E_{H\ Bond}$ values for the cyclic trimer are greater (more negative) than those of the open structure by 13.2 and 10.4 kJ mol^{-1} at the two basis sets used whilst the values for the tetramer are greater for the cyclic forms than the open forms by 34.0 and 29.3 kJ mol^{-1}. These values are consistent with greater stability of the ring structures compared with the open structures by an average value of 12 and 32 kJ mol^{-1} for trimer and tetramer respectively. However in terms of calculated hydrogen bonded energy per bond the cyclic trimer is lower than the open trimer by 5 kJ mol^{-1} whilst the cyclic and open tetramers have similar energies per bond within the limitations of these calculations. Clearly these are small changes at the 1 in 10^6 level and cannot be treated with confidence although the consistency over limited basis sets is striking. These studies support the greater stability of the cyclic forms over the open form in the case of the trimer. In the case of the tetramer the greater size is likely to reduce the tendency of four methanol molecules to hydrogen bond to form a ring.

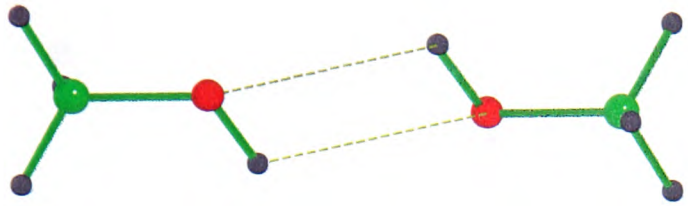

Methanol Cyclic Dimer

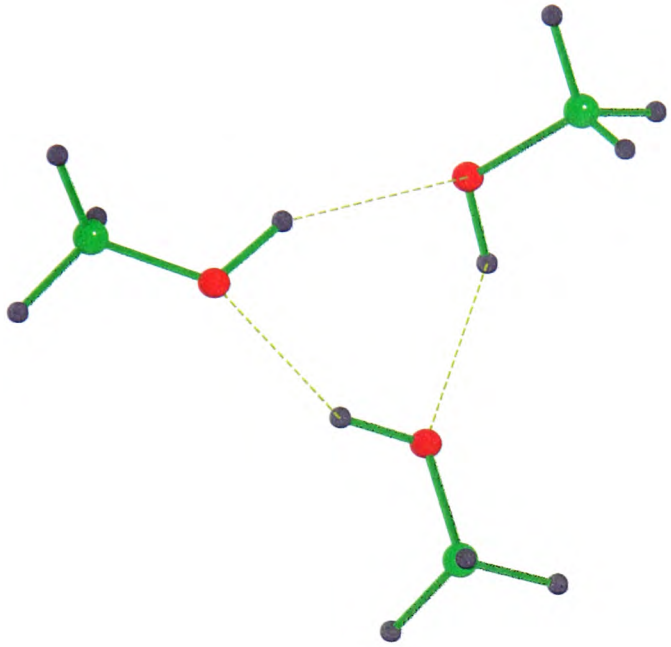

Methanol Cyclic Trimer

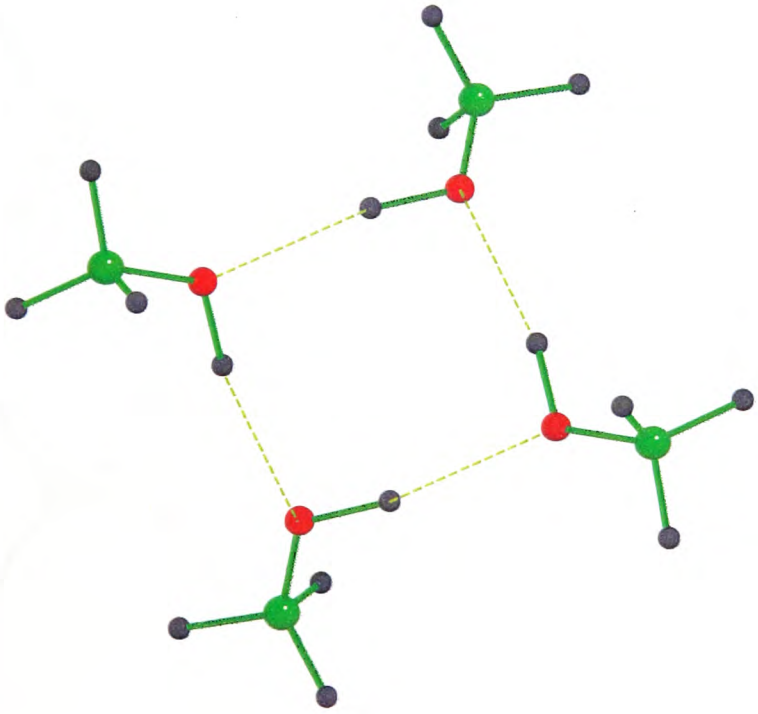

Methanol Cyclic Tetramer

Fig. 5.4(a) - Hydrogen Bonded Forms of Methanol - Cyclic Structure.

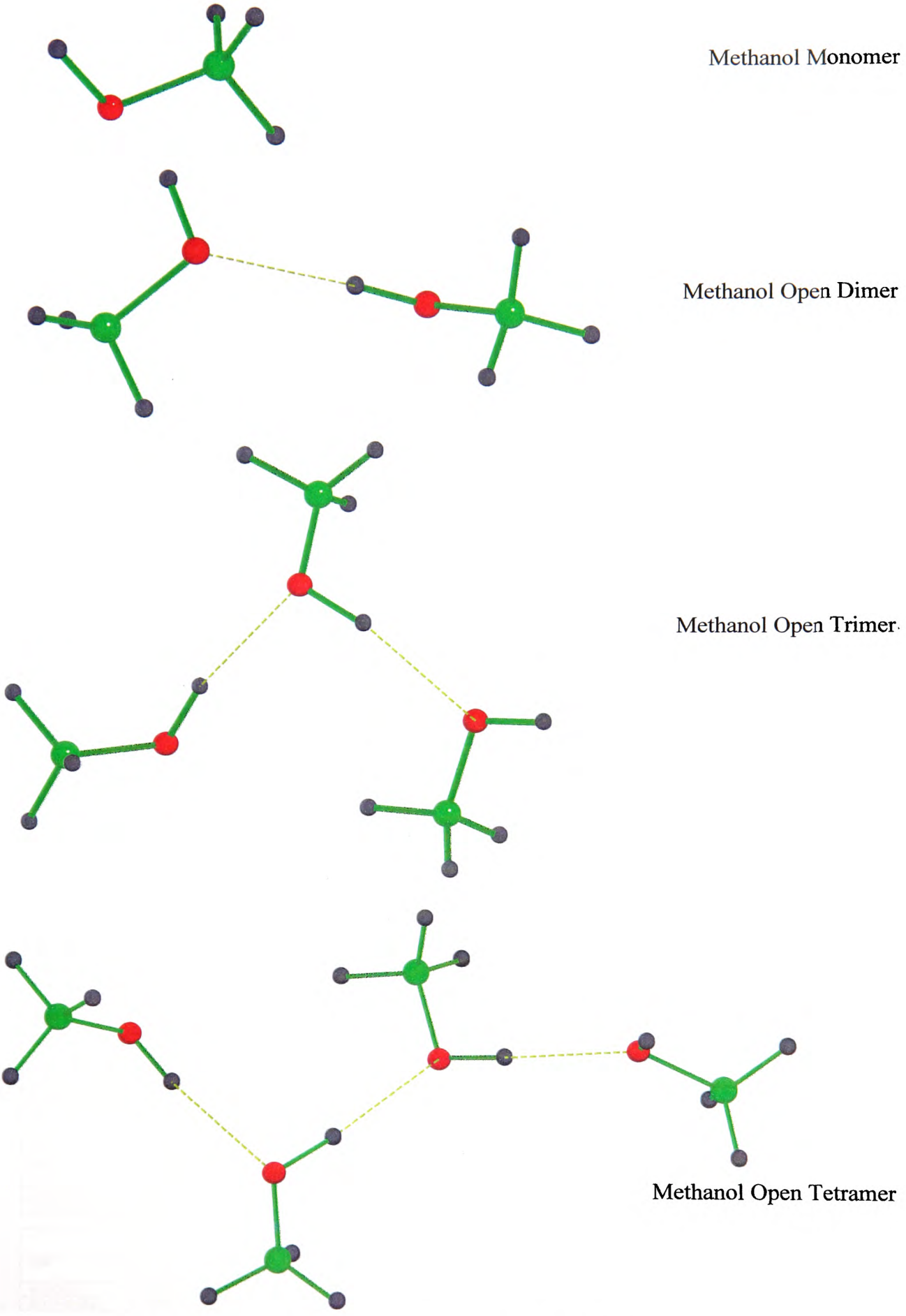

Fig. 5.4(b) - Hydrogen Bonded Forms of Methanol - Open Structure.

Table 5.2 - Comparison of *ab initio* calculated parameters using different basis sets for methanol monomer

Basis Set	ν(C-O)/ cm^{-1}	ν(O-H)/ cm^{-1}	E_{ZP}/E_h	$E_{Thermal}/E_h$	$E_{Electronic}/E_h$	Dipole Moment/*D*
RHF 6-31G(d)	1189(78)	4117(41)	0.055340	0.058596	-115.035418	1.8662
RHF 6-31++G(d,p)	1176(107)	4196(55)	0.054984	0.058272	-115.052514	1.9670
RHF 6-311+G(d)	1179(132)	4171(33)	0.055070	0.058348	-115.068333	2.0180
RHF 6-311++G(d,p)	1175(112)	4190(57)	0.054763	0.058057	-115.080508	1.9362
RHF 6-311++G(2d,2p)	1163(49)	4196(58)	0.054820	0.058133	-115.085651	1.7977
RHF 6-311++G(3df,3pd)	1174(87)	4181(55)	0.054681	0.057990	-115.090567	1.7394

$E_h = 4.3597482 \times 10^{-18}$ J; $D \approx 3.33564 \times 10^{-30}$ C m (relative intensities of infrared bands)

Table 5.3 - Calculated O-H stretching modes/cm^{-1} (relative intensities) in free and hydrogen bonded forms methanol - cyclic structure

Basis Set	Monomer	Dimer		Trimer			Tetramer			
RHF	Free	Bonded	Bonded	Bonded	Bonded	Bonded	Bonded	Bonded	Bonded	Bonded
6-31G (d)	3676(41)	3656(0)	3664(189)	3580(522)	3578(559)	3545(7)	3535(178)	3514(111)	3514(111)	3469(0)
Shift	0	-20	-12	- 94	-98	-131	-141	-162	-162	-207
6-31++G (d,p)	3747(55)	3717(0)	3724(213)	3648(517)	3644(529)	3618(17)	3598(131)	3581(1076)	3581(1076)	3545(0)
Shift	0	-30	-23	-99	-103	-129	-149	-166	-166	-172
6-311+G (d)	3724(33)	3704(0)	3707(157)							
Shift	0	-20	-20							
6-311++G (d,p)	3741(57)	3711(0)	3718(211)							
Shift	0	-30	-23							

Table 5.4 - Calculated O-H stretching modes/cm^{-1} (relative intensities) in free and hydrogen bonded forms of methanol - open structure

Basis Set	Monomer	Dimer		Trimer			Tetramer			
RHF	Free	Free	Bonded	Free	Bonded	Bonded	Free	Bonded	Bonded	Bonded
6-31G (d)	3676(41)	3673(57)	3620(361)	3681(57)	3590(461)	3564(381)	3676(61)	3600(422)	3574(421)	3531(639)
Shift	0	- 3	-56	+5	-86	-112	0	- 76	-102	-145
6-31++G (d,p)	3747(55)	3744(68)	3678(377)	3748(69)	3645(461)	3623(406)	3743(73)	3656(421)	3633(409)	3591(674)
Shift	0	- 3	-69	+1	-102	-124	-4	-91	-114	-156
6-311+G (d)	3724(33)	3728(47)	3665(318)							
Shift	0	+4	-59							
6-311++G (d,p)	3741(57)	3735(69)	3674(370)							
Shift	0	-6	-67							

Table 5.5 - Calculated hydrogen bonded distances and energies for free and hydrogen bonded methanol - cyclic structures.

Basis Set	Monomer	Dimer				
RHF	$E_{Electronic}$/kJ mol^{-1}	R1(H···0)/Å	R2(H···0)/Å	$E_{Electronic}$/kJ mol^{-1}	$E_{H\ Bond}$/kJ mol^{-1}	BSSE/kJ mol^{-1}
6-31G (d)	-302025.5	2.281	2.281	-604071.8	-20.8	7.22
6-31++G (d,p)	-302070.4	2.352	2.352	-604157.3	-16.5	1.48
6-311+G (d)	-302111.9	2.332	2.332	-604242.4	-18.6	2.06
6-311++G (d,p)	-302143.9	2.370	2.371	-604303.4	-15.6	1.16

	Trimer					
RHF	R1(0···H)/Å	R2(0···H)/Å	R3(H···0)/Å	$E_{Electronic}$/kJ mol^{-1}	$E_{H\ Bond}$/kJ mol^{-1}	BSSE/kJ mol^{-1}
6-31G(d)	1.772	1.778	1.757	-906146.9	-70.4	14.71
6-31++G(d,p)	2.047	2.026	2.024	-906270.3	-59.1	5.36

	Tetramer						
RHF	R1(H···0)/Å	R2(H···0)/Å	R3(H···0)/Å	R4(H···0)/Å	$E_{Electronic}$/kJ mol^{-1}	$E_{H\ Bond}$/kJ mol^{-1}	BSSE/kJ mol^{-1}
6-31G (d)	1.883	1.883	1.883	1.883	-1208220.9	-118.9	18.72
6-31++G (d,p)	1.919	1.919	1.919	1.919	-1208384.4	-102.8	10.20

Table 5.6 - Calculated hydrogen bonded distances and energies for free and hydrogen bonded methanol - open structures.

Basis Set	Monomer	Dimer		
RHF	$E_{Electronic}$/kJ mol^{-1}	R1(H···O)/Å	$E_{Electronic}$/kJ mol^{-1}	$E_{H\ Bond}$/kJ mol^{-1}
6-31G (d)	-302025.5	2.001	-604074.1	-23.1
6-31++G (d,p)	-302070.4	2.021	-604161.6	-20.8
6-311+G (d)	-302111.9	1.990	-604247.1	-23.3
6-311++G (d,p)	-302143.9	2.029	-604307.7	-19.9

Basis Set	Trimer			
RHF	R1(O···H)/Å	R2(O···H)/Å	$E_{Electronic}$/kJ mol^{-1}	$E_{H\ Bond}$/kJ mol^{-1}
	1.939	1.950	-906133.7	-57.2
	1.966	1.974	-906259.9	-48.7

Basis Set	Tetramer				
RHF	R1(H···O)/Å	R2(O···H)/Å	R3(O···H)/Å	$E_{Electronic}$/kJ mol^{-1}	$E_{H\ Bond}$/kJ mol^{-1}
6-31G (d)	1.951	1.944	1.886	-1208186.9	-84.9
6-31++G (d,p)	1.912	1.977	1.967	-1208355.1	-73.5

5.4 Discussion.

5.4.1 O-H stretching region.

A broad feature centred near 3300 cm^{-1} had been identified at 3438 cm^{-1} and curve resolution used to estimate integrated absorbance values and determine approximate amounts of hydrogen-bonded species. The best fit was obtained using a combined Gaussian-Lorentzian linear function at an initial band half-width of 45 cm^{-1}. These bands were tentatively assigned to a tetramer and/or another trimer. Smaller initial half-band widths suggested increasing numbers of component bands and the possibility cannot be ruled out that there are a number of hydrogen bonded forms with closely overlapping bands in all alcohol spectra under these conditions in this region. In the absence of detailed experimental or theoretical supporting evidence it was decided to limit curve resolution to the three most prominent features only.

However the recent results described by Kristiansson[111] suggest the tetramer band may give rise to shifts of -650 to -850 cm^{-1} from the monomer value. The *ab initio* calculated shifts give support for a much larger shift for the tetramers than the trimers. In the C_3 trimer the most intense IR bands in this region are the degenerate e species with a calculated shift of -112 cm^{-1} for methanol ; the C_1 species has near accidental degeneracy and the corresponding band is further shifted by -(3-7) cm^{-1}. The third band corresponds to a breathing type vibration with a larger shift but a lower IR intensity. The most intense

bands calculated for the tetramers are also e vibrations for the S_4 point group and are shifted by -162. It may be noted that the calculated shift at the HF/6-31G(d) level for the dimer (-56 cm^{-1}) and trimer (-97 cm^{-1}) underestimate the shift assigned to these bands for the dimer (-127 cm^{-1}) and trimer (-286 cm^{-1}) by a magnitude of 2 - 3. It is therefore possible that the calculated shift for the tetramer is consistent with an actual shift of -300 to -450 cm^{-1}. A larger shift for the tetramer would be consistent with a stable strongly hydrogen bonded structure similar in stability to those of carboxylic acid dimers. The likely greater strength of cyclic hydrogen bonded forms of alcohols was first discussed by Bellamy and Pace[112,113]. This possibility would appear to merit further experimental and theoretical studies.

The application of *ab initio* calculations using the Gaussian package in the study of alcohols and their associated hydrogen bonded structures is illustrated in Tables 5.2 and 5.3. Tables 5.2 and 5.3 present detailed new calculations for the methanol monomer. Table 5.2 compares values for ten basis sets using the Hartree Fock method for the angle and length of the O-H group, for the wavenumber value of the C-O and O-H stretching modes together with the relative intensities in the infrared and in the Raman, the thermodynamic values for zero point (zp), thermal (th), and electronic (e) energies and the dipole moment values. It should be noted that the wavenumber values are unscaled and harmonic. The major limitation of the Hartree Fock method is that it fails to allow for electron correlation, that is the interaction between two electrons as a function of electron separation. These effects are taken into account to some extent in the Moller Plesset, MP2 method and more so in the Density Functional Theory (B3LYP) method. Calculations by all three methods are included in Table 5.3 at the lowest and highest basis sets listed in Table 5.2 (6-31G(d) and 6-311++G(3df,3pd). These provide all 12 normal modes and compare wavenumber values with those measured for methanol in the gas and matrix isolated phase by Serrallach, Meyer and Gunthard [110]. Here the value of the O-H stretch included in Table 5.3 is corrected for anharmonicity which is reported as -75 cm^{-1} by Peron and Sandorfy [114].

These Tables indicate that the average difference between measured and calculated wavenumber decreases by 12% between the lowest and highest basis set used in Hartree Fock but by about 30% by the two methods which allow for electron correlation. However this average difference reduces dramatically between HF (-205.6), MP2 (-120.5) and B3LYP (-64.2) at the 6-31G(d) level and is significantly smaller (-181.7, -85.5,and –44.8) at the 6-311++G(3df,3pd) level.

It is therefore clear that more accurate structural and other information is gained by using higher basis sets and methods which take electron correlation into account. These higher level calculations make a considerable demand on computing power. Careful judgement must therefore be exercised in determining when new science requires this resource. Greater ease of transfer of information and data in standard file protocol format should facilitate this process which is illustrated by the problem of the structures and properties of hydrogen bonded forms of alcohols. The calculation of these properties should be in parallel with experimental measurements since mutual stimulation between experiment and theory is the essence of better scientific knowledge

5.5 Conclusions.

1. The evidence from infrared spectra and other physical methods for hydrogen bonding in alcohols is summarised and differences in interpretation discussed.
2. Measurement of infrared spectra of methanol 1 in solution in CCl_4 and vapour phase, and *ab initio* computations are reported over a range of basis sets and provide information on the range of hydrogen bonded species present including cyclic trimers and cyclic tetramers of different symmetries.
3. New information is provided on the effect of basis sets and *ab initio* methods used for methanol. The average difference between measured and calculated wavenumber deceases by 12% between the lowest and highest basis set used in Hartree Fock but by about 30% by the Moller Plesset and Density Functional methods which allow for electron correlation.

4. The average difference between measured and calculated wavenumber reduces dramatically between HF (-205.6), MP2 (-120.5) and B3LYP (-64.2) at the 6-31G(d) level and is significantly smaller (-181.7, -85.5,and –44.8) at the 6-311++G(3df,3pd) level.

Chapter 6

An *Ab Initio* Study of medium strength Hydrogen Bonding of Mono- and Bi-Functional Carbonyl and Nitrile Complexes with Hydrogen Chloride.

6.1 Introduction.

The structure of the simple carbonyl complex, $H_2CO\cdots HCl$ has been studied by rotational spectroscopy,[115,116,117] leading to the conclusion that the structure is planar with the HCl group bent by 20.3° from the O···H axis towards the adjacent aldehydic H. Calculated properties of this system,[118,119] have been related to IR measurements within a nitrogen matrix.[120] These studies reveal significant bending of the hydrogen bond which was the subject of further detailed calculations[121] The thermodynamic and spectroscopic properties of $(CH_3)_2CO\cdots HCl$,[122,123] and $CH_3HCO\cdots HCl$,[122] have been measured by IR spectroscopy and computed by *ab initio* methods. IR measurements and calculations for the corresponding nitrile complex, $HCN\cdots HCl$ and $CH_3CN\cdots HCl$ have also been summarised by Del Bene et al.[124] These studies are within a wider group of systems as are recent summaries of structural information from microwave measurements on these complexes by Page et al.[125] IR measurements have been carried out on $C_2H_5CN\cdots HCl$ complexes in the gas and by matrix isolation,[126] enabling shifts in group modes adjacent to the hydrogen bond to be compared with similar systems. Measurements and calculations on carbonyl and nitrile complexes are consistent with hydrogen bonding of HCl to lone pair electrons either to one of the two planar trigonal sp^3 type lone pairs on the oxygen (at an angle of approximately 120 degree) or to the single linear sp type lone pair on the nitrogen (leading to an approximately linear bond).

Density function theory (DFT) in hybrid (B3LYP) form has been used on HF and HCl complexes of acceptors including HCN and CH_3CN to show that energy, structures and spectroscopic properties can be similar to MP2 methods at higher basis sets in some but not all cases[124]. Comparisons of the formaldehyde (CH_2CO) complex with HCl using MP2, B3LYP, HF and other methods suggests that DFT methods do not accurately

determine properties from secondary interactions leading to bending of the hydrogen bond,[121] as measured by microwave spectroscopy[116]. Tuma et al.[127] compared a series of DFT methods applied to nine hydrogen bonded complexes containing from four to seven atoms, including $(HCl)_2$ and $H_3N\cdots HCl$ and showed improved calculated binding energies using a new functional, HCTH38 compared with those for the B3LYP method. The relationship between vibrational spectra and *ab initio* calculations has recently been reviewed,[128] including calculation of anharmonic vibrations and with examples of medium strength $H_3N\cdots HCl$ complexes and strong complexes of charged halogen anion complexes. Following these descriptions, it is convenient to describe hydrogen bonds between compounds containing lone pairs such as carbonyls and nitriles as of medium strength.

The present work compares information on hydrogen bonding with HCl in the mono-functional compounds H_2CO, CH_3HCO, $(CH_3)_2CO$, HCN, CH_3CN and CH_3CH_2CN and in two bi-functional compounds, HCOCN and CH_3COCN. There have been no studies reported for the complexes of the bi-functional compounds with HCl although their monomers, formyl nitrile and acetyl nitrile, have been characterised. Csaszar predicted,[129] the vibrational and rotational spectra of formyl nitrile observed by Lewis-Bevan et al.[130] These workers were able to measure the IR spectrum of formyl nitrile gas prepared by flash vacuum pyrolysis of cinnamyloxyacetonitrile to form a relatively stable species characterised by six of the fundamental vibrations. *Ab initio* calculations on formyl nitrile at the MP2/6-31G* and MP2/D95** level compared geometries and frequencies of this and related compounds.[131] Further *ab initio* calculations for the unimolecular dissociation of formyl nitrile by three routes showed that at room temperature all three rates of decomposition were minute.[132] Measurement of the Far IR spectrum of acetyl nitrile provided thermodynamic, spectroscopic and structural information supported by Hartree-Fock *ab initio* calculations.[133] The IR spectra of a series of nitriles were measured, frozen in argon and water in the region 2050 - 2320 cm^{-1} because of the recent accessibility of this region to astronomical observation and a larger shift between Ar and H_2O for acetyl

cyanide and other bi-functionals over mono-functionals was noted.[134] The decomposition of acetyl cyanide by various paths has been predicted theoretically to indicate that although certain paths were exothermic they were kinetically unfavourable.[135]

It is therefore of value to compare experimental (where known) and calculated thermodynamic, structural and spectroscopic properties of the three carbonyl and three nitrile complexes and to predict these properties for the two bi-functional complexes. For systems of this complexity the B3LYP method is likely to have some advantages and is explored with a range of high-level basis sets. It should be noted that for the 1:1 complex of HCl with acetaldehyde there are two possible isomers whilst for each of the two bi-functional compounds there are three possible isomers.

6.2 *Ab Initio* Results.

Previous work used both the self-consistent field, HF, and the electron correlated, B3LYP, methods with ten different basis sets in a study of the monomers of formaldehyde, acetaldehyde and acetone.[136] In the present work the latter method only is used, and, as before, smaller calculations were carried out on a PC whilst larger calculations were carried out on the Columbus super computer facility at Rutherford Appleton Laboratory, Didcot, UK. Harmonic wavenumber values had been determined for formaldehyde.[137] and acetaldehyde,[138] from which the harmonic values for acetone were estimated. Comparison of experimental and computed values of harmonic wavenumber values for all three carbonyls suggested that the accuracy of the B3LYP method was significantly greater than that of the HF method and the B3LYP/6-311++G(2d,2p) basis set provided best agreement with the experimental valued in this context.

The most probable molecular structure of the HCl complexes with carbonyls and nitriles were modelled using ChemX,[74] and the co-ordinates adjusted to achieve a plane of symmetry in each case other than for the acetone···HCl complex. In this case the most stable structure contained a methyl group twisted from the plane of the six heavy atoms. All model systems were optimised initially at the B3LYP/6-31G(d) level and the co-

ordinates from this calculation used for subsequent computations. The model of each proton acceptor and the HCl proton donor was systematically determined in each case by deleting the co-ordinates of the other component from each complex and adjusting the co-ordinates of each acceptor to the required symmetry. This determination of optimised complexes and components is analogous to the counterpoise method of determination of basis set superposition error (BSSE).[72]

The existence of many *ab initio* methods and the considerable choice of basis sets within each method has led to a profusion of publications in which the efficacy of the parameters used is measured by the degree of co-incidence with selected experimental parameters. To investigate these relationships ten basis sets within the B3LYP methods were applied to complexes of HCl for which a number of experimentally determined parameters are available. Table 1 lists the basis sets used together with the number of basis functions including the number within each symmetry species. The difference between the calculated and experimental values of hydrogen bonded energy, HCl wavenumber shifts and bond lengths as a function of these ten basis sets have been computed for the HCl complexes with, CH_2CO, CH_3HCO, HCN and CH_3CN. It should be noted that the experimental and calculated parameters are not necessarily comparable; in particular the calculated wavenumber shift of the four complexes is based on the harmonic approximation whilst the measured values are normally anharmonic. However harmonic values estimated from measured spectra were used in this case. There are also differences between considerations of measured and calculated values of bond length and angles since measured geometries are determined for anharmonic systems from B_0 as rotational constants normally with insufficient information to determine B_e values. Calculated geometries for harmonic systems require $B_0 = B_e$ and the calculated values of bond lengths in the equilibrium state ($V = -1/2$) are expected to be smaller than the measured anharmonic values in the $V = 0$ state where V is the vibrational quantum number.

6.2.1 Electronic energy and hydrogen bond energy.

Fig 6.1 shows the values of the electronic energies of the four complexes for each selected basis set less that for B3LYP/6-31G(d) defined as (E_n - E_1). The variational theorem requires that these energies converge towards a minimum with increasing number of basis functions, (Table 6.1 lists those used in the present work). The true value would be given by the exact wave function that is inaccessible for even the simplest molecules or ions. Fig. 6.1 reveals that the split double valence basis sets with two sizes of basis set per valence orbital (1-6) leads to little change in energy (from 3 to 4 or 5 to 6) with additional diffuse functions (permitting s and p orbitals to occupy more space). The addition of a polarisation function adding p functions to hydrogen atoms, (4 to 5) makes a significant difference. The change (6 to 7) from a double to a triple valence function (using three sizes of functions for each orbital type) leads to a considerable lowering in energy which then further reduces with additional polarisation and diffuse functions.

Care is needed in the definition of hydrogen bond energy since there are several different experimental and theoretical descriptions in the literature which will not be reviewed here. The equilibrium value is the depth of the well ($\Delta E_e = E_e - E_\infty$) for the potential energy function for the hydrogen bond B···HCl at absolute zero treated as a two body system with separation $r_{B\cdots H}$ for which r_e is the minimum and r_∞ corresponds to complete dissociation into the proton acceptor base, B and the donor, HCl. The more frequently quoted value is the equilibrium value corrected for zero point energy and BSSE and is defined here as $\Delta E_0 = E_0 - E_\infty$. This leads to a value relative to the lowest vibrational states and since the zero point energy is significantly greater in the complex than that for the sum of the components, ΔE_e is greater in magnitude than ΔE_0. These definitions leads to the hydrogen bond energy as a negative quantity and is alternatively defined as the binding energy, D_e or D_0 and is variously expressed in the literature as positive or negative according to conventions used and with magnitude (irrespective of sign) a measure of hydrogen bond strength. At any temperature thermal energy corresponding to rotational,

vibrational and translational energy is readily calculated and may be included. It is conventional to also include the zero point energy within the value of thermal energy which is included in Table 6.2 for clarity. Estimated experimentally based values of hydrogen bond energy back corrected to give ΔE_e have been reviewed,[122,124] for $CH_3HCO\cdots HCl$ (20.5 kJ mol^{-1}), $HCN\cdots HCl$ (23.0 kJ mol^{-1}) and $CH3CN\cdots HCl$ (28.5 kJ mol^{-1}). These values are compared with calculated values at ten basis sets in Fig 2. Here our calculated hydrogen bond energy is for electronic energy only and gives identical results with Del Bene et al.,[124] at the level B3LYP/6-31G(d,p) and B3LYP/6-31+G(d.p) which are numbers 2 and 5 respectively in Table 6.1. It appears that there is no measured value for H_2CO.

6.2.2 Shift in HCl mode in complex.

The anharmonic wavenumber shifts in the stretching mode of HCl (and other proton donors) in complexes with a wide range of proton acceptors (electron donors) have been summarised by Barnes[139] for complexes in the gaseous phase and by matrix isolation in argon at cryogenic temperatures. No gas value appears to be reported for complexes of H_2CO and CH_3HCO (possibly because of instability) but for HCN and CH_3CN the values were measured by Thomas and Thompson,[140] as 2806 cm^{-1} and 2731 cm^{-1} respectively and the latter value was confirmed by Ballard and Henderson.[141] The corresponding harmonic values may be estimated assuming the harmonic to anharmonic ratio in these complexes is that of HCl (2991/2886) to give 2908 and 2830 cm^{-1} Estimates of the harmonic wavenumber shift in the complex of H_2CO were made,[119] by scaling the matrix value by the ratio v(HCl harmonic gas) to v(HCl anharmonic matrix) ie (2991/2871). The anharmonic matrix values were taken as 2641 cm^{-1} for $H_2CO\cdots HCl$,[120] 2493 for $CH_3HCO\cdots HCl$,[142] 2703 cm^{-1} for $HCN\cdots HCl$,[143] and 2569 cm^{-1} for $CH_3CN\cdots HCl$.[144]. It is noted that the shifts for the nitrile complexes are greater in the matrix than the gas by 103 and 162 cm^{-1}. This relationship is discussed for a large number of base-hydrogen halide complexes in terms of correlation with proton affinity of the base, hydrogen bond

stretching force constant and dissociation energy of the complex.[139] In the present work the matrix isolated values of shift in HCl modes for complexes are used because of availability of values for all four complexes. These measured values lead to estimates of harmonic values as 2751 ($H_2CO\cdots HCl$), 2597 $CH_3HCO\cdots HCl$), 2816 ($HCN\cdots HCl$) and 2676 cm^{-1} ($CH_3CN\ldots HCl$). Fig 6.3 provides the plots of the difference between the estimated shift to lower wavenumber from the harmonic value of HCl against basis set.

6.2.3 Inter-nuclear distances in complexes.

An important inter-nuclear distance in complexes is that between the heavy atoms (N, O or C and Cl in the present work). Del Bene et al.[124] have summarised earlier measurements of the distances ($R(HCN\cdots Cl)$ = 3.402 Å, $R(CH_3CN\cdots Cl)$ = 3.291 Å). More recently these have been reported as 3.405 Å and 3.310 Å respectively.[125] The value for $R(O\cdots Cl)$ for $CH_2CO\cdots HCl$ is reported as 3.21 Å by microwave measurements.[115] The corresponding $R(C\cdots Cl)$ has been determined as 3.627 Å by Legon,[116,117] No measurement appears to have been reported for acetaldehyde. Fig 6.4 reports the difference between the calculated (R_e) and experimental (R_0) values. In the case of HCl R_e and R_0 values have long been known,[145] $R_e(H\text{-}Cl)$ = 1.2746 Å, $R_0(H\text{-}Cl)$ = 1.2838 Å. and the difference between the calculated and measured R_e value is also included in Fig 6.4.

6.2.4 Choice of basis set.

Figs 6.1-6.4 provide objective information on the selection of basis sets. Fig 6.1 demonstrates the convergence of electronic energy towards a minimum and reveals the improved energy values of the split triple valence (7 - 10 in Table 6.1) over the split double valence basis sets (1 - 6) for the four compounds studied. As described earlier the comparisons of many calculated and measured parameters are based on approximations that prevent direct comparisons of like with like. The hydrogen bonded energy differences in Fig 6.2 for the three accessible compounds conveys that the simplest split level valence basis set with one polarisation and diffusion function (7 in Table 6.1) provides the best agreement between theory and experiment. The measured shift in the HCl mode is

potentially an excellent test of theory subject to the determination of the harmonic values. The approximation used in the present work does suggest that the overall best agreement is that for 9 in Table 6.1 with the complexes of HCN and CH_3HCO showing agreement with $\pm$ 10 cm^{-1} whilst CH_3CN and H_2CO show agreement within $\pm$ 70 cm^{-1}. It is known that CN groups and CO groups are shifted to higher and lower wavenumber values respectively in higher nitriles,[126] and carbonyls,[146] but information on the lower members is limited to a matrix isolation study,[142] of HCN···HCl in which the nitrile band moves to higher wavenumber by 24 cm^{-1}. A systematic comparison of calculated and experimental study of proton acceptors is not yet available but would be of value. Fig. 6.4 shows little systematic variation in difference with basis set for the inter-nuclear separations X···Cl for X = N or O for the three complexes. The R_e value for HCl is accurately known and 9 and 10 in Table 6.1 provide nearest calculated values.

Although there is variation with basis set for a number of the comparisons of calculated and measured properties the present results support the choice of 9 [B3LYP/6-311++G(2d,2p)] in Table 1 for wider calculation of parameters associated with hydrogen bonding as also determined for simple carbonyl compounds in our earlier work.[126] Calculated structures using this basis set are shown in Fig. 6.5 for the four mono-carbonyls (including two forms of the acetaldehyde complex), and in Fig 6.6 for the three mono-nitriles. Fig 6.7 and 6.8 show the calculated structures for the three forms of formyl nitrile and acetyl nitrile respectively. Selected bond lengths and bond angles are shown in Tables 6.3 and 6.4 for mono-functional complexes for which experimental information is available for some of these parameters. Tables 6.5 and 6.6 compare bond lengths and bond angles for all eight carbonyl complexes and all five nitrile complexes considered together with their components at the selected basis set.

6.3 Discussion.

6.3.1 Calculated electronic and hydrogen bond energies of mono-functional complexes.

Table 6.2 provides the zero point energy and the sum of zero point energy with thermal and with electronic energy for all complexes and their components. This allows the hydrogen bond energy to be calculated as the difference between the electronic energy corrected for zero point energy of the complex and the sum of the components similarly corrected. The counterpoise method of calculation of BSSE,[72] calculates the electronic energy of each components within the complex but with the nuclei of the other components switched off or treated as ghost atoms to determine a BSSE error for which hydrogen bond energy is corrected to give ΔE_0. Table 6.2 also includes the equilibrium hydrogen bond energy corrected for BSSE (ΔE_e) as defined earlier. For consistency with most other literature the former will be discussed. For the mono-functional carbonyl compounds the hydrogen bond energy increases with additional methyl substitution in the sequence, -12.55, -18.09 and -20.87 kJ mol^{-1} suggesting the inductive supply of electrons from each methyl increases the stability of the hydrogen bond. Here the acetaldehyde complex with HCl *cis* to the aldehydic H is taken as the lower energy and hence more stable of the two possible isomers (Fig 6.5) ie -614.669070 compared with -614.668539 Hartrees. The higher energy form of the acetaldehyde complex has lower hydrogen bond energy than the lower energy form (-16.36 compared with –18.09 kJ mol^{-1})). No experimental information has so far been advanced to our knowledge for this species but our calculations suggest it is likely to be present in significant proportions when acetaldehyde and HCl are able to form hydrogen bonds. The three mono-nitriles included in Table 6.2 also show systematic increase in hydrogen bond energy with increasing alkyl substitution. The effect being less marked between methyl and ethyl (-10.92, -16.61 and –17.77 kJ mol^{-1}).

6.3.2 Calculated wavenumber shifts of mono-functional complexes.

Fig 6.3 compares, for various basis sets, calculated shifts in HCl stretching modes on complexation with estimated harmonic values derived from measurement of anharmonic values in the four simplest complexes. In Table 6.2 these calculated values and shifts are included for the basis set selected as providing best overall agreement (B3LYP/6-311++G(2d,2p) together with those for the CO and CN harmonic stretching modes for all thirteen complexes studied of which the mono-functional compounds are first considered. The HCl shift, well established as a measure of the hydrogen bond strength, increases systematically in the series of alkyl complexes with increased methyl substitution, -301.9, -393.6 and -407.7 cm^{-1}. Here the acetaldehyde complex is taken as the low energy form in which the hydrogen bond is *cis* to the aldehydic hydrogen. The *trans* complex is shown in which the CO is *cis* to the methyl group has higher energy and the calculated HCl shift is smaller (-347.5 cm^{-1}) than in the *cis* complex (-393.6 cm^{-1}) proving further evidence that the hydrogen bond is weaker in this complex. The shift in the carbonyl band is also smaller (-24.0 compared with -26.8 cm^{-1}). The shift in CO mode for alkyl substituents shows a general reduction of 20-30 cm^{-1} on hydrogen bonding, which as previously mentioned has not been systematically studied. This effect has important implications for analytical measurement when the carbonyl group is used as a probe for qualitative and quantitative analysis of systems in which proton donor molecules are present as a source of interference.

The alkyl nitrile complexes, as with the alkyl carbonyl complexes, show an increase in the shift in the HCl mode with increasing alkyl substitutions (-165, -236.4 and -244.2 cm^{-1}) but differ from the carbonyl complexes by showing an increase in the CN stretching mode on complexation (17.4, 15.45 and 14.5 cm^{-1}). The difference in the behaviour of the CO and CN functions on hydrogen bonding leading to decrease and increase in wavenumber value respectively is an interesting reflection of the contrasting bonding. The carbonyl double bond comprises planar trigonal sp^3 hybridised orbitals on

the C and O atoms with hydrogen bonding to one or other of the lone pair electrons on the O atom. The CO bond is weakened by electron withdrawal of bonding electrons by HCl. The nitrile bond is strengthened by withdrawal of anti- bonding electrons, associated with the bond formed by the linear sp hybridised N and C atoms, by the bonded HCl molecule.

6.3.3 Calculated bond lengths and bond angles in mono-functional complexes.

The significant bond lengths in relation to hydrogen bonds are those of the proton acceptor groups (CO and CN), the donor group (HCl) and the hydrogen bond itself (CO···HCl) and CN···HCl). The calculated values are included in Table 6.3 together with the heavy atom separations C···Cl and N···Cl for which experimental values have been reported in some cases. The calculated values of the bond angles COH and CNH determine the angle between the axes of the these bonds and the axis of the HCl bond (θ) which measure the bend towards an electron attracting hydrogen on an adjacent R-group are also included in Table 6.3. The structures of the mono-functional compounds based on these parameters are given in Fig. 6.5 for the complexes of carbonyl compounds and in Fig. 6.6 for those of the nitrile compounds. These will be discussed in comparison with experimental values in carbonyl complexes (Table 6.3) and nitrile complexes (Table 6.4). Overall comparisons of changes in mono- and bi-functional complexes are described (Table 6.5, Figs 6.9 and 6.10).

6.3.4 Comparison of measured and calculated energy, spectroscopic and structural parameters.

Methods with increased electron correlation and using higher basis sets are likely to provide more accurate molecular parameters than those reported in the present work. However, the earlier arguments suggest calculations with B3LYP/6-311++G(2d,2p) are a reasonable compromise between accuracy and computing power for the moderate size complexes reported. In the case of the mono-functional compounds studied measured and calculated values are compared in Table 6.3 for the simple carbonyl compounds.

Experimentally determined values of the hydrogen bond energy of $CH_2CO\cdots HCl$ do not appear to be reported but calculated values vary from -10 to -19 kJ mol^{-1} according to the method and assumptions used. The measured anharmonic shift (-242 cm^{-1})for the HCl stretching mode is based on matrix isolation measurements,[146] Nowek and Leszczynski estimated the harmonic HCl shift as -302 cm^{-1} which is close to their calculated value (-292 cm^{-1}), significantly larger than the value calculated by Rice et al [118], (151 cm^{-1}) and exactly the same as our value. The length of the hydrogen bond determined by microwave spectroscopy,[117] (1.968(10) Å) is somewhat larger than all calculated values of which those of Kang,[121] are nearest (1.9415 Å). The length of the HCl bond determined,[117] as 1.2839 Å is calculated as larger in most cases, the nearest value being that of Rice et al.[118] (1.283 Å). Best agreement for the COH angle,[118] is 106.8° compared with measured value[116] 107.1° and best agreement,[119] for θ is 20.2° compared with the measured,[117] value of 20.3 for the bend in the O···H-Cl bond towards the aldehydic hydrogen. The C···Cl distance is also determined from microwave measurements as 3.627Å which is overestimated in the three calculations listed in Table 6.5 by 2.5% for the presented work and by a larger and smaller amount,[121] by the B3LYP and MP2 methods respectively under a smaller basis set.

Measured information for $CH_3HCO\cdots HCl$ and $(CH_3)_2CO\cdots HCl$ is sparse. The hydrogen bond energy is measured,[122,123] for $(CH_3)_2CO\cdots HCl$ in the range -18 to -22 kJ mol^{-1} leading to an estimate.[122] for the corresponding value in $CH_3HCO\cdots HCl$ as –20.5 kJ mol^{-1}. These values are consistent with our calculated values of –20.87 –18.09 and –16.36 kJ mol^{-1} for the complexes of acetone and the low and high energy complexes of acetaldehyde respectively. The shift in the HCl mode is measured as –378 and –300 cm^{-1} in matrix and gas states for $CH_3HCO\cdots HCl$,[142] and $(CH_3)_2CO\cdots HCl$,[123] respectively which compare with the calculated values of –408 to –394 cm^{-1} in the present work. This predicts the value for the high-energy form of the acetaldehyde complex to be 333 cm^{-1} in a matrix. No accurate values of the geometrical parameters of these complexes have yet been

reported but the present calculations give an approximate indication of their detailed structure. For the $(CH_3)_2CO\cdots HCl$ complex a temperature dependent measurement on the bonded (1731 cm^{-1}) and free (1765 cm^{-1}) carbonyl stretching modes was used to determine thermodynamic properties of the equilibria.[122] The shift of -34 cm^{-1} for these anharmonic modes may be compared with the calculated harmonic values of -23.1 cm^{-1} in the present work. Dudis et al.[123] measured the anharmonic HCl mode in the complex of acetone with HCl at 2690 cm^{-1} leading to a shift of approximately -300 cm^{-1} compared with the larger calculated harmonic value of -407.7 cm^{-1} reported in Table 6.2. Other shifts were only accessible in matrix isolation and the CO, CC and HCl modes have reported shifts of -11, 7.8 and -280 cm^{-1} in this phase consistent with the shortening of the CO and HCl bonds and the lengthening of the CC bond on formation of the complex.

Comparison of measured and calculated parameters of simple nitriles is given in Table 6.4. The measured hydrogen bond energy of HCN···HCl is reported as –23.0 kJ mol^{-1} with no details of the method used.[124] The calculations have been repeated,[124] leading to the values of –22.15 and –19.23 kJ mol^{-1} using the same methods and basis sets for electronic energy only. The reported (-10.92 kJ mol^{-1}) is for a higher basis set and also corrected for zero point energy and BSSE. The experimental hydrogen bond energy for CH3CN···HCl is reported,[124] as –28.50 kJ mol^{-1} and also[141] as 22 ± 1.7 kJ mol^{-1} by variable temperature IR measurements. As in the HCN complex the same values (-28.4 and –25.1 kJ mol^{-1}) were calculated using the methods and basis set described,[124] but reported calculations by the chosen method and basis set are consistent with the wider results. The measured HCl shift in HCN···HCl is –80 cm^{-1} gas,[140] and –68 cm^{-1} in an argon matrix.[143] In $CH_3CN\cdots HCl$ and $C_2H_5CN\cdots HCl$ the HCl shift is very much greater in the matrix (–302 and –241 cm^{-1} respectively) than in the gas (-155 and –241 cm^{-1} respectively). The hydrogen bond length has been measured,[148] for HCN···HCl as 2.121 Å and for CH3CN···HCl as 2.007 Å by Legon et al.[149] The calculated values respectively underestimate these values as 2.0629 Å and 1.9792 Å by 6% and 3%. As previously

reported[126] the HCl anharmonic shifts for the propiontrile complex with HCl is -160 and -241 cm^{-1} in the vapour and argon matrix respectively compared with the present calculated harmonic value of -244.2 cm^{-1}. Experimental assignments of propionitrile have been reported by Klaboe and Grundnes.[147] No measured value for the length of the hydrogen bond or associated bond angles exist for $C_2H_5CN\cdots HCl$ but it is likely that our calculated value of 1.9688 Å underestimates the length by up to 6 % leading to an actual value of between 1.969 Å and 2.087 Å and that the CNH and NHCl angles are distorted from the linear positions to 181.1° and 180.3° towards the methyl group.

No experimental information has been reported for complexes of HCl with the bi-functional compounds but the anharmonic CN and CO stretching modes of HCOCN have been reported at 2230 and 1716 cm^{-1} respectively. (Lewis-Bevan)[130] These compare with the calculated harmonic modes at 2321.2 and 1775.1 cm^{-1} reported in Table 6.2. The experimental information is incomplete in a number of cases and some of the measured data are not directly comparable with calculated results. Nevertheless the calculated information gives useful relative values and is valuable towards predicting molecular parameters hitherto un-measured.

6.3.5 Calculated hydrogen bond energies and wavenumber shift for bi-functional complexes

The three isomers of the HCl complex with formyl nitrile are shown to have calculated properties that indicate that the hydrogen bond energy of each form is less than those of mono-functional counterparts. The isomer of the formyl nitrile complex with the highest hydrogen bond energy is shown to be that in which bonding to the nitrile occurs in which the hydrogen bond energy is –8.50 kJ mol^{-1} which is 48% of the value for the propionitrile complex, shown to be the strongest nitrile as acceptor considered here. The shift in HCl mode is -130.9 cm^{-1} which is 54% of that in propionitrile showing consistency between these parameters as indicators of hydrogen bond strength with a mean value of 51%. Hydrogen bonding to the carbonyl is shown to be stronger when *trans* rather *cis* to

the nitrile group. The hydrogen bond energy is –6.66 kJ mol^{-1} and shift in HCl mode -163.6 cm^{-1} in the former compared with –4.45 kJ mol^{-1} and -97.8 cm^{-1} in the latter. Taking the mean of the two indicators the hydrogen bond strength of complex NCHCO···HCl *cis* and *trans* is 22.5% and 36% respectively relative to the strength in $(CH3)_2CO$···HCl. This reflects the lower steric interactions from hydrogen than from the nitrile substituent and is parallel to the calculated values for the acetaldehyde complexes. The greater than expected (from bond energy considerations) shift in the HCl mode for complexes with carbonyls compared with complexes of nitriles has been noted previously.[126]

Calculations on complexes of acetyl nitrile for all three isomers show increased hydrogen bond strengths compared with those in formyl nitrile. The hydrogen bond energy for isomers of decreasing stability (compared with equivalent forms of formyl nitrile) are – $ClH\cdots NCCH_3CO$,10.79 (-8.50) kJ mol^{-1}; $NCCH_3CO\cdots HCl$ *cis* -9.25(-6.66) kJ mol^{-1}, NCCH3CO...HCl *trans*, -7.43 (-4.45) kJ mol^{-1}. The shifts in the HCl modes are similarly compared as -159.7 (-130.9), -196.0 (-163.6) and -134.1 (-97.8) cm^{-1}. This greater strength is consistent with the inductive supply of electron density to the nitrile and carbonyl group by the methyl group. A semi quantitative measure of the stability of the three complexes of acetyl cyanide can be made as follows; $ClH\cdots NCCH_3CO$ has 61% of the hydrogen bond energy and 65% of the shift in the HCl mode compared with the complex with propionitrile; *trans* $NCCH_3CO\cdots HCl$ has 44% hydrogen bond energy and 48% of the shift in the HCl mode, *cis* $NCCH_3CO\cdots HCl$ has 41% of the hydrogen bond energy and 33% of the HCl shift. Hence the strength of hydrogen bonding for the three forms of complexes of acetyl cyanide (mean values, 63, 46 and 37.5%) are estimated and shown to be stronger than the equivalent forms in formyl cyanide (mean values 51, 36 and 22.5%) but weaker than the counterparts of these forms in the mono-functional complexes which are 67 to 100% for the carbonyl complexes and 64 to 100% for the nitrile complexes. There is reasonable consistency among the calculated hydrogen bond strengths between hydrogen bond energies and shift in HCl stretching modes

As mentioned earlier the shift in the HCl mode as a proton donor is better characterised than the shift in the CO or CN groups modes as proton acceptors. In the case of the bi-functional complexes the calculated value of the nitrile shift to higher wavenumbers is 14-15 cm^{-1}. The calculated shift of the carbonyl group to lower wavenumbers is 10-20 cm^{-1}. These shifts are all lower than the corresponding shifts in mono-functionals and further reflects the weaker hydrogen bonding strength in all six complexes. In HCOCN and CH_3COCN the carbonyl and nitrile groups are conjugated leading to reduction in electron density of both proton acceptor groups consistent with weaker hydrogen bonding than in the equivalent mono-functional compounds.

6.3.6 Calculated structural parameters for mono- and bi-functional compounds.

The full geometrical structure for all seven isomers of the mono-functional complexes and all six isomers of the bi-functional isomers shown in Figs. 6.5-6.8 have been calculated at the selected method and basis set. The most significant values in relation to hydrogen bonding are reported in Table 6.5 and 6.6 grouped by the carbonyl and nitrile proton acceptor functions. Those selected are the lengths of the C-X, X···H and H-Cl bonds and the angle of the C-X-H bond where X = O or N. The value of θ is also included as the angle of departure from linearity of the X···HCl hydrogen bond.

The eight carbonyl complexes considered are listed in Table 6.5. It is noted that the hydrogen bond length is inversely related to the length of the CO and HCl bonds. This provides quantitative information on the link between greater hydrogen bond strength, reduction in hydrogen bond length and increase in lengths of adjacent proton acceptor (CO) and donor (HCl) groups. Table 6.5 lists the eight complexes in reducing strengths of hydrogen bond according to this correlation which is illustrated in Fig 6.9 showing the change in bond lengths relative to those in the formaldehyde complex for all complexes.

Table 6.5 shows that relative to the hydrogen bond length in the formaldehyde complex (1.8775 Å) the effect of adjacent methyl groups is to shorten this bond (1.7929, 1.8090, 1.8453 Å) whereas the effect of an adjacent nitrile is to lengthen the bond (2.0184,

2.0879 Å). When nitrile and methyl are both present the nitrile has greater effect (1.9696, 2.0266 Å respectively). The greater effect of nitrile over methyl also shows on the bond length of the complexed H-Cl. Relative to the formaldehyde complex (1.3023 Å), CN with H or CH_3 is least (1.2877, 1.2903, 1.2923, 1.2947 Å) whilst the effect of one CH_3 and one H, or two CH_3 groups is greatest (1.3059, 1.3096, 1.3120 Å). The length of a carbonyl group is shortened by an adjacent CN group (1.2028, 1.2044 Å) relative to the value in the formaldehyde complex (1.2057 Å) but lengthened by one or more adjacent methyl groups (1.2110, 1.2119, 1.2181 Å). When nitrile and methyl are both present the effects largely cancel each other (1.2079, 1.2090 Å respectively).

Table 6.6 reports parameters for the complexes with HCl via the nitrile group. This also shows an inverse relationship between the length of the RCN···HCl hydrogen bond (C_2H_5-, 1.9688; CH_3-, 1.9782; H-, 2.0629; CH_3CO-, 2.0740; HCO-, 2.1129 Å)) and length of the H-Cl bond (HCO-, 1.2902; CH3CO-, 1.2923; H-, 1.2928; CH_3-, 1.2987; C_2H_5-, 1.2996 Å). Here the calculated nitrile bond lengths are less affected than carbonyl bond lengths by these substituents and are in a narrower range (1.1441 - 1.1491 Å). Fig 6.10 shows the correlation of increase of hydrogen bond length with decrease in bond length of adjacent proton acceptor (CN) and proton donor (HCl) groups. It is notable in Figs. 6.9 and 6.10 that the considerable change in H···X bond length is accompanied by a significant lengthening of the HCl bond but little change in the acceptor group. This is because the small mass of the H atom is more easily displaced than that of the heavier O or N atoms in line with the relative change in wavenumber values of the stretching mode. Similarly the CO length does reduce slightly and the CN group increases slightly also in line with changes in the vibrational spectrum as discussed earlier.

Tables 6.5 and 6.6 demonstrate the enhancement of hydrogen bond strength by H and CH_3 groups relative to CN groups for all carbonyl complexes studied and that of the H and CH_3 groups relative to the CO groups on all nitrile complexes studied.

The calculated structures reveal varying deviations from linear hydrogen bonds for all nitriles and carbonyls studied. The angle, θ, between the axes of the linear RCN atoms and the axis of HCl is zero for R = H and CH_3 but the chlorine atom is bent towards hydrogen within R for R = C_2H_5, HCO and CH_3CO leading to θ values of 1.4, 2.1 and 4.4° respectively reflecting increasing attraction between the Cl atom and the most sterically favoured hydrogen. Within the eight carbonyls studied the value of θ is greatest for the three compounds for which R1 = H (R2 = CN, θ = 19.1°; R2 = H, θ = 11.8°; R2 = CH_3, θ = 9.4°). For the three compounds for which R1 = CH_3 smaller values of θ are determined and in the same sequence of R2 groups as for R1 = H to give θ = 8.6°, 4, and 2° respectively. The angle θ is smallest for R1 = CN and for R2 = H, θ = 0.2° whereas for R2 = CH_3, the HCl is bent away from the nitrile group to give θ = - 2.3 °. The values of θ therefore reflect attractions across space between the chlorine atom and hydrogen atoms in the most favoured steric position. The nitrile group is shown to have a repulsive affect on the chlorine atom arising from high electron density on both groups.

No information has so far been reported to our knowledge of complexes between these bi-functional compounds and HCl. The properties calculated for these complexes in the present work suggest three pairs of isomers should exist but bonding to the nitrile function is favoured and all hydrogen bonding is weaker than in corresponding mono-functional carbonyl and nitrile complexes.

6.4 Conclusions.

1. *Ab initio* calculations are reported for complexes of H_2CO, CH_3HCO, HCN and CH_3CN with HCl using ten basis sets between B3LYP/6-31G(d) and B3LYP/6-311++G(3df,3pd). Comparison with experimentally determined values of hydrogen bond energy, shift in the estimated harmonic HCl stretching mode of the complex and the N···Cl and O···Cl interatomic distances suggest an adequate basis is B3LYP/6-311++G(2d,2p) in the context of the present work.

2. In the case of CH_3HCO there are two possible isomers in which the HCl is *cis* and *trans* to the aldehydic H atom (low and high energy forms respectively). Using the basis set determined as optimal further *ab initio* calculations are reported for these complexes together with those of $(CH_3)_2CO$, C_2H_5CN, HCOCN and CH_3COCN. The two bi-functional complexes each have three possible isomers; HCl may bond to the nitrile or to the carbonyl group in either *cis* or *trans* conformation to the nitrile group.
3. A comparison is made of calculated values of zero point energy and the sum of zero point energy with thermal energy and with electronic energy; HCl, CO and CN harmonic stretching modes; selected geometrical structural parameters of all seven mono-functional complexes and of all six bi-functional complexes together with their components. These are used to calculate the hydrogen bond energy, ΔE_o, corrected for zero point energy and BSSE; shift in the harmonic stretching modes of the HCl, CO and CN groups and changes in geometrical structures of all forms on forming hydrogen bonded complexes.
4. The calculated ΔE_o values of HCl complexes of carbonyl compounds are:

H_2CO	CH_3HCO(high energy)	CH_3HCO(low energy)	$(CH_3)_2CO$
-12.55	-16.36	-18.09	-20.87 kJ mol^{-1}

The calculated hydrogen bond energies in HCl complexes of nitrile complexes are:

HCN	CH_3CN	C_2H_5CN
-10.92	-16.51	-17.71 kJ mol^{-1}

These changes are attributed to the inductive supply of electrons by alkyl groups and steric factors. In the bi-functional compounds hydrogen bond energies are smaller than in mono-functionals; the bonding to carbonyls with a *cis* nitrile is less than that with a *trans* nitrile and is greatest when bonded to the nitrile. The three respective values for each complex are:

formyl nitrile (HCOCN)	-4.45	-6.66	-8.50	kJ mol^{-1}
acetyl nitrile (CH3COCN)	-7.43	-9.25	-10.79	kJ mol^{-1}

These changes are attributed to effects of alkyl groups and delocalisation of electrons in conjugated CO and CN systems.

5. The shift in the harmonic HCl stretching mode in the HCl complexes are:

H_2CO	CH_3HCO(low energy)	CH_3HCO(high energy)	$(CH_3)_2CO$
-301.9	-347.5	-393.6	-407.7 cm^{-1}

HCN	CH_3CN	C_2H_5CN
-165.3	-236.4	-244.2 cm^{-1}

HCOCN to CO *cis* to CN	HCOCN to CO *trans* to CN	HCOCN to CN
-163.6	-97.8	-130.9 cm^{-1}

CH_3COCN to CO *cis* to CN	CH_3COCNtoCO *trans* to CN
-196.0	-134.1 cm^{-1}

CH_3COCNtoCN

-159.7 cm^{-1}

The shift in the CO and CN stretching modes in the complexes are also reported and are between -10 and -24 cm^{-1} (i.e. to lower value) for HCl complexes to the CO group and between 14 and 18 cm^{-1} (i.e. to higher value) to the CN group. The explanation for increase is a result of the antibonding properties of the free lone pair of electrons on the nitrogen atom. When the complex is formed, the antibonding electrons are effectively removed from any interaction with the triple CN bond. This causes the bond to strengthen, and thus the frequency of the CN stretch increases (See Appendix C).

6. The mean of the % of each ΔE_o value and the harmonic HCl shift of those in the acetone or propionitrile complexes are taken as an approximate measure of the hydrogen bond strength in the bifunctional complexes, These are:

ClH···NCHCO	51%	*trans* NCCHCO···HCl	36%
cis NCCHCO···HCl	22.5%.		
ClH···$NCCH_3CO$	61%	*trans* $NCCH_3CO$···HCl	46%
cis $NCCH_3CO$···HCl	37.5%.		

7. Calculated structures are shown for all eleven complexes studied. The interatomic distances and angles are reported for the C-X, X···H and H-Cl bonds and for the C-X···H and X···H-Cl angles for X = O and X = N. The length of the hydrogen bond varies between 2.0879 Å (weak) and 1.7929 Å (strong) for the carbonyl compounds and 2.1129 Å (weak) and 1.9688 Å (strong) for the nitrile compounds. The length of the HCl and CX bonds are correlated with those of the hydrogen bond. The calculated values of the bend in the hydrogen bonds are reported and related to interactions across space.

8. The calculated thermodynamic, spectroscopic and structural properties are compared with experimental information when available and predicted in other cases including the properties of a newly described high energy form of an acetaldehyde complex and those of three newly described isomers of complexes of formyl nitrile and acetyl nitrile with hydrogen chloride.

6.5 List of figures for Chapter 6.

Fig. 6.1 - Electronic energy values of complexes.

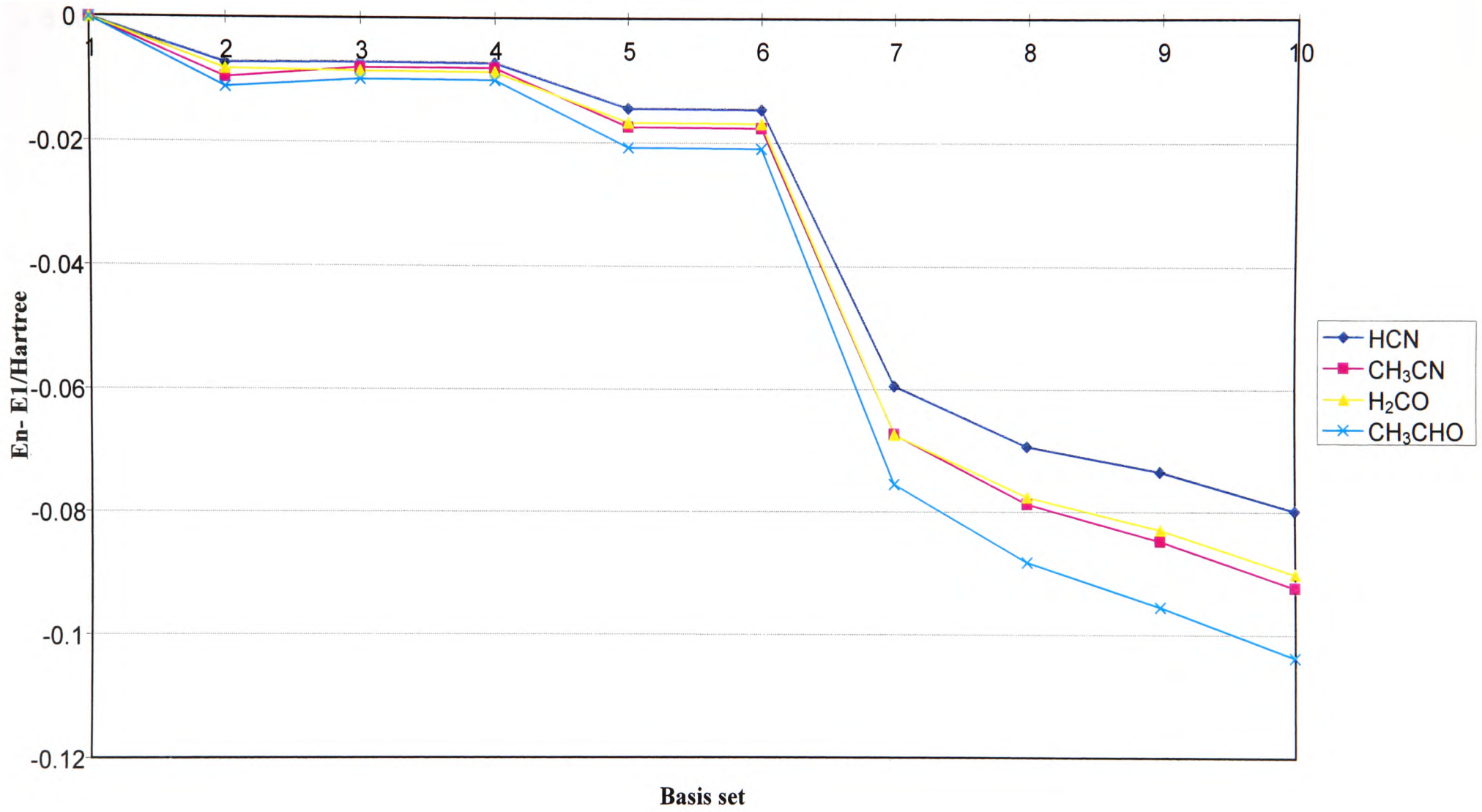

Fig. 6.2 - Difference between calculated and measured hydrogen bonded energies of complexes.

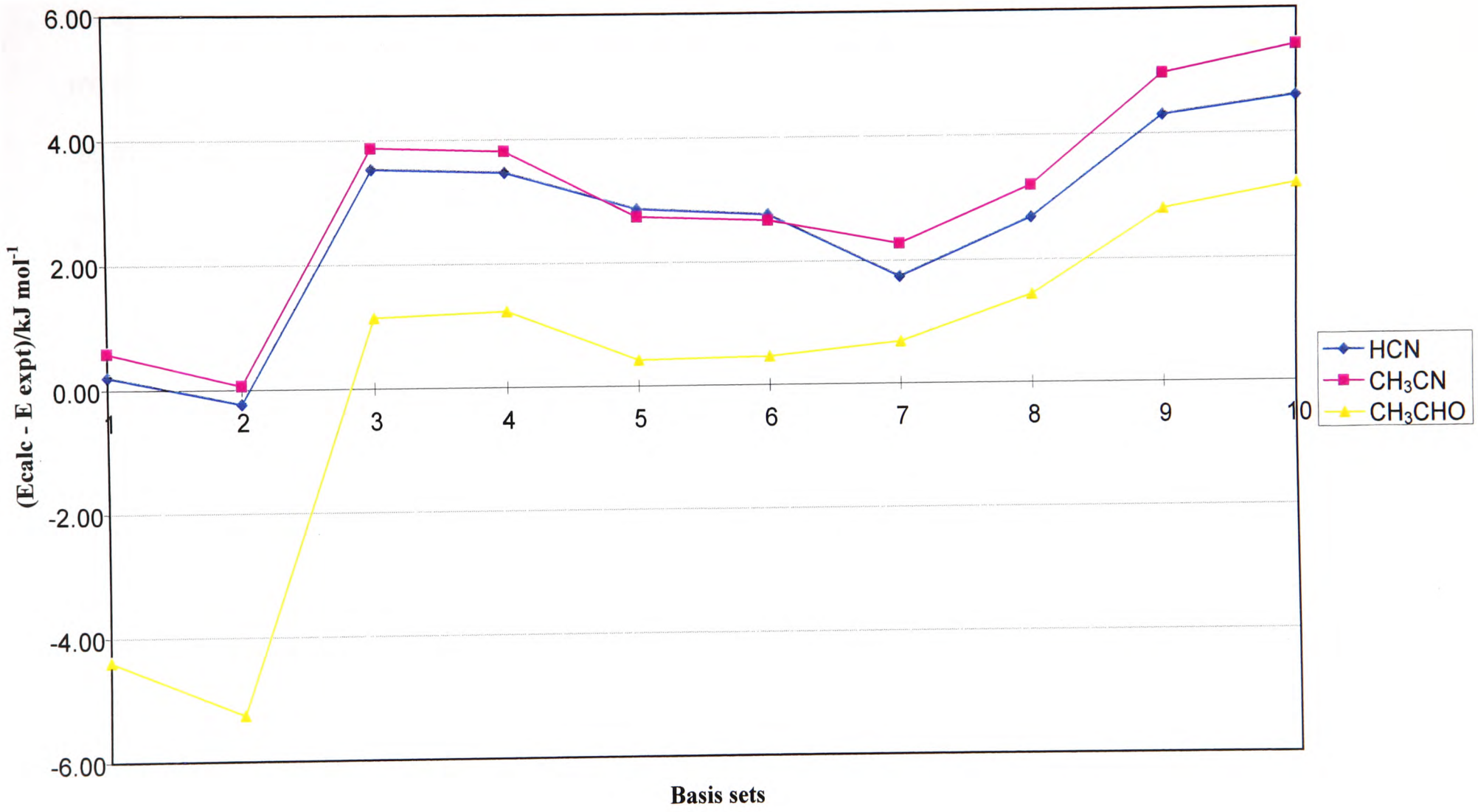

Fig. 6.3 - Difference between calculated and observed HCl shifts in complexes.

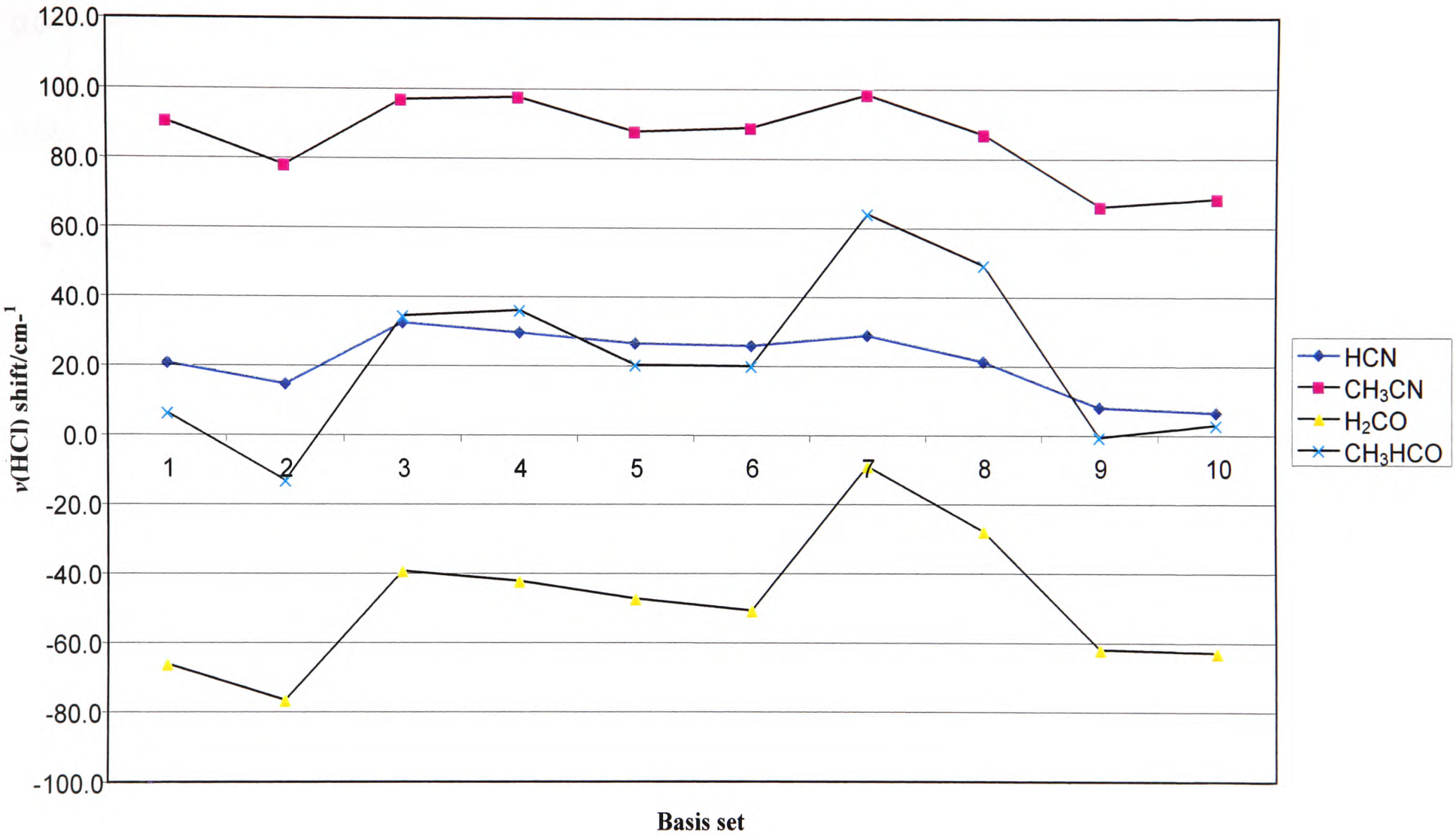

Fig. 6.4 - Difference between calculated and measured internuclear separations X...Cl of complexes with HCl.

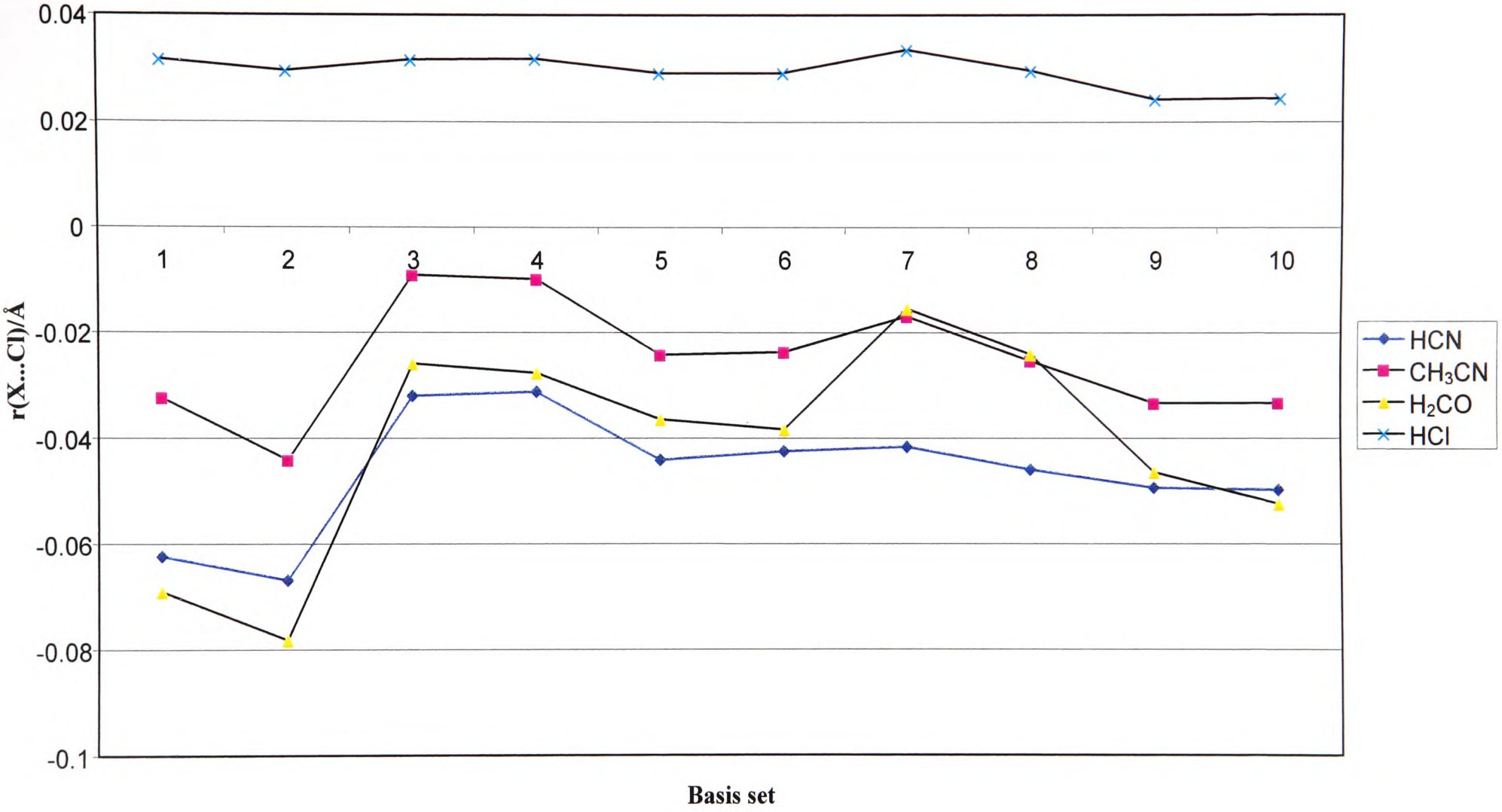

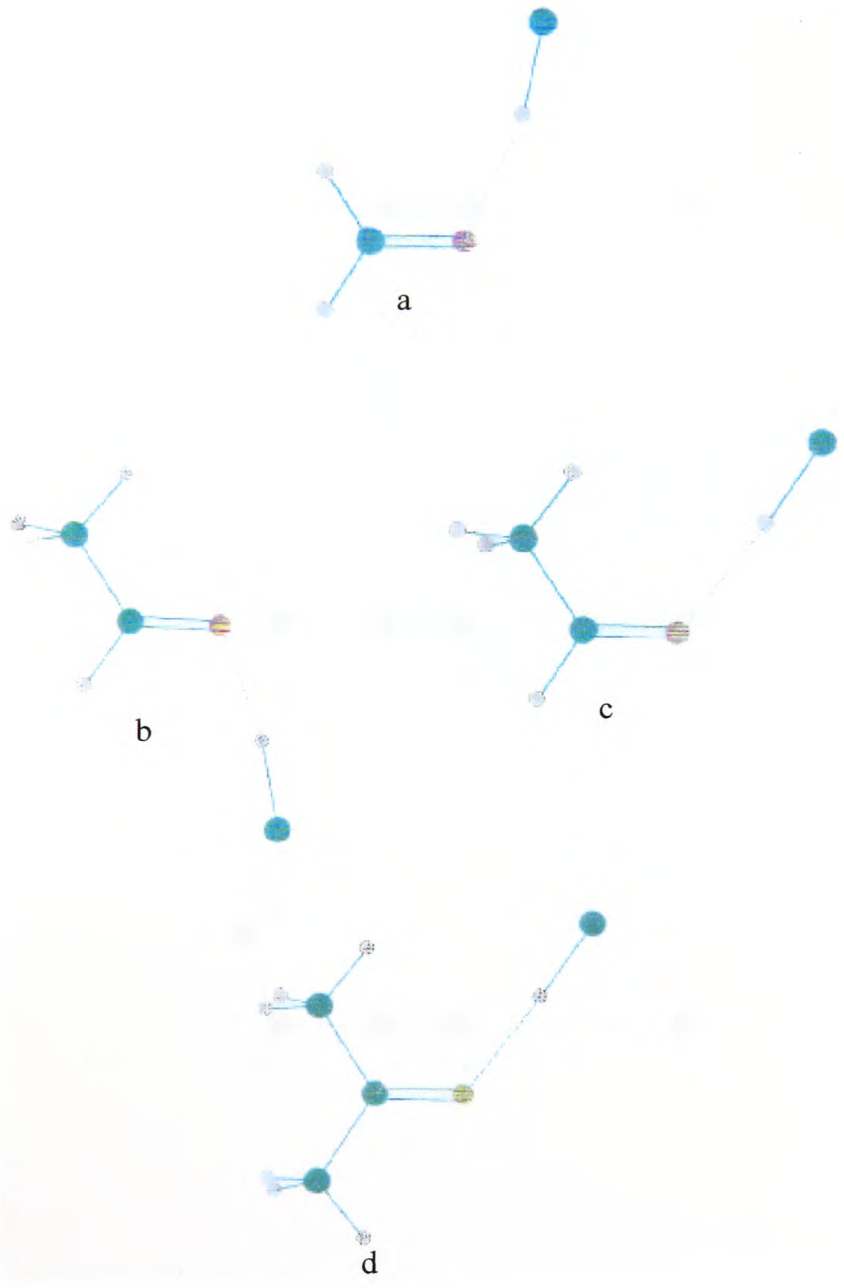

Fig. 6.5 – The calculated structures of the carbonyl···HCl complexes at the B3LYP/6 311++G(2d,2p) level. ((a) – formaldehyde, (b) – acetaldehyde (low energy), (c) – acetaldhyde (high energy), (d) – acetone).

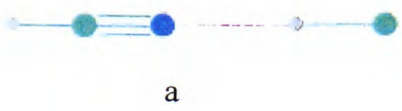

a

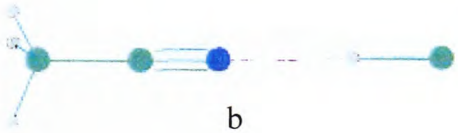

b

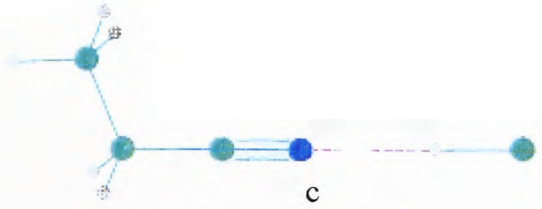

c

Fig. 6.6 – The calculated structures of the nitrile···HCl complexes at the B3LYP/6-311++G(2d,2p) level. ((a) – hydrogen cyanide, (b) – acetonitrile, (c) – propionitrile).

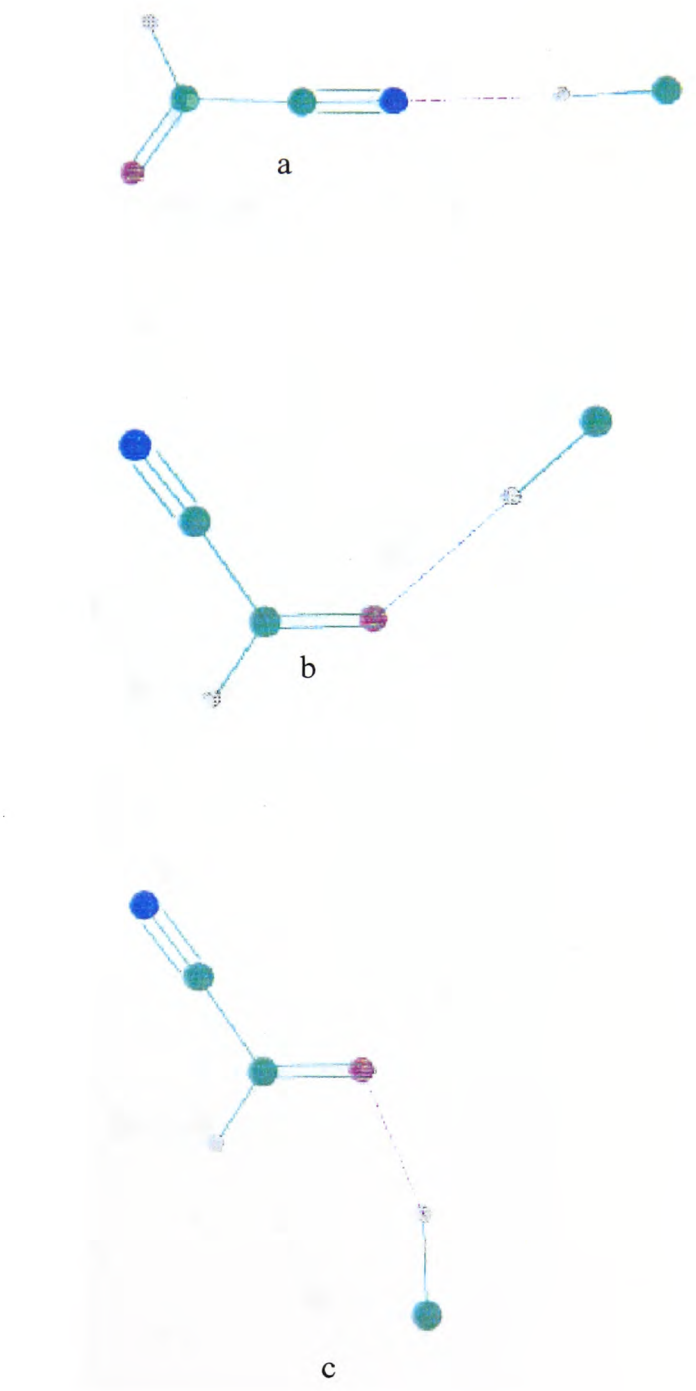

Fig. 6.7 – The calculated structures of the formyl nitrile···HCl complexes at the B3LYP/6-311++G(2d,2p) level. ((a) – bonded to nitrile, (b) – bonded to carbonyl cis to nitrile, (c) – bonded to carbonyl trans to nitrile).

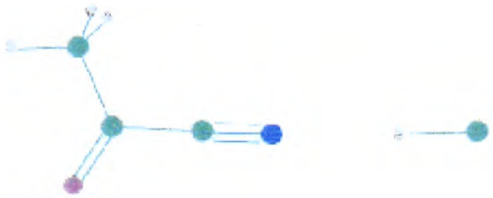

a

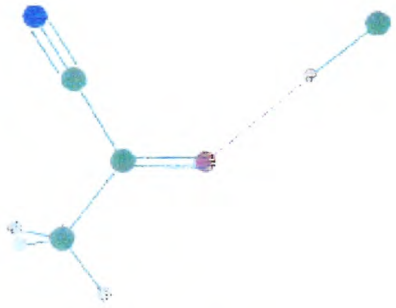

b

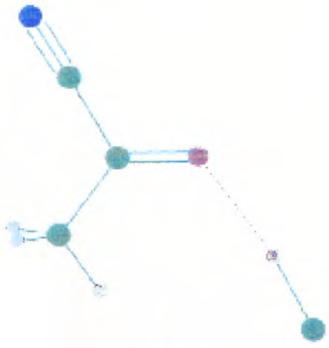

c

Fig. 6.8 – The calculated structures of the acetyl nitrile···HCl complexes at the B3LYP/6-311++G(2d,2p) level. ((a) – bonded to nitrile, (b) – bonded to carbonyl cis to nitrile, (c) – bonded to carbonyl trans to nitrile).

Fig. 6.9 - Change in bond length of carbonyl with substituent.

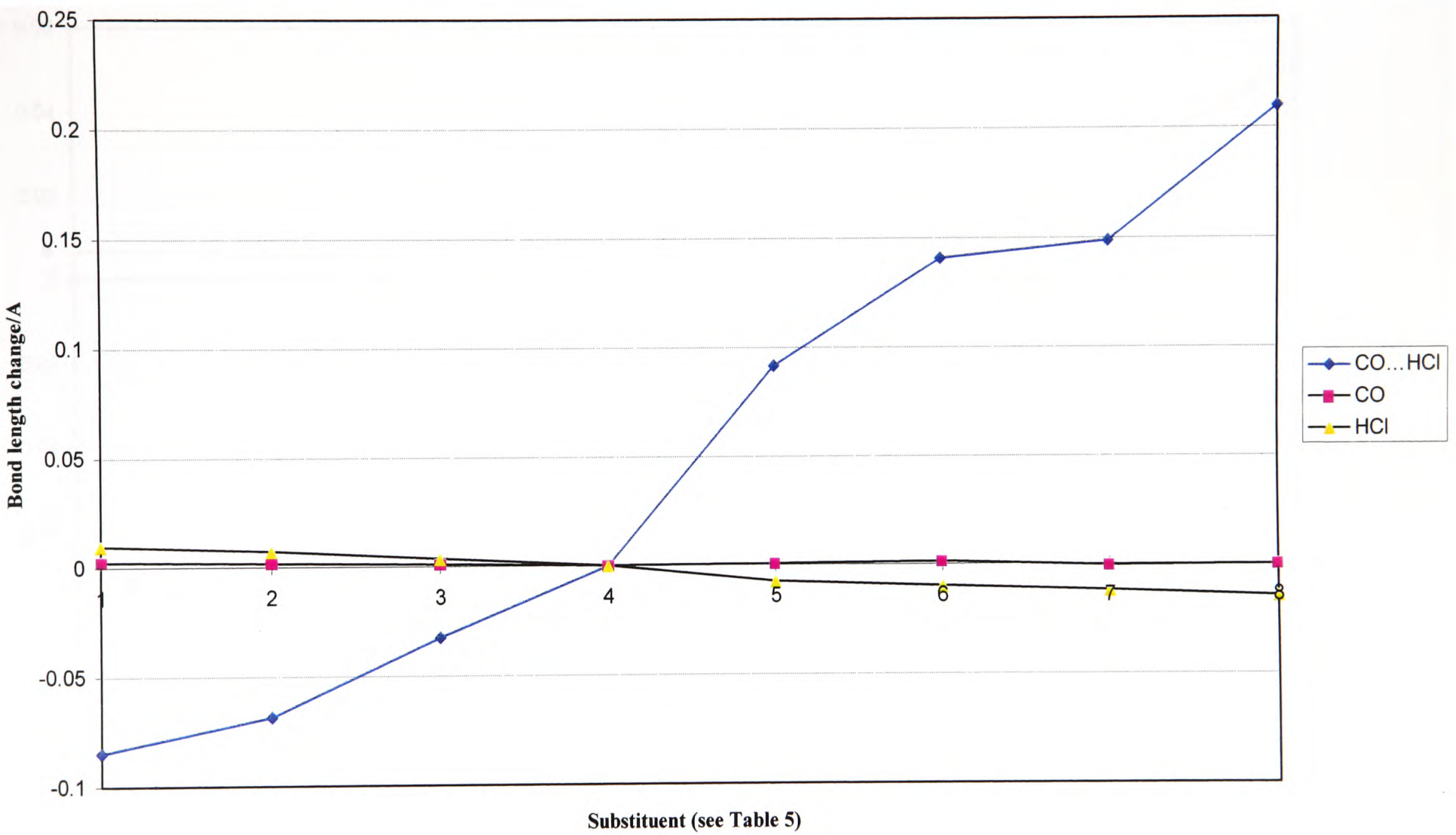

Fig. 6.10 - Change in bond length of nitrile with substituents.

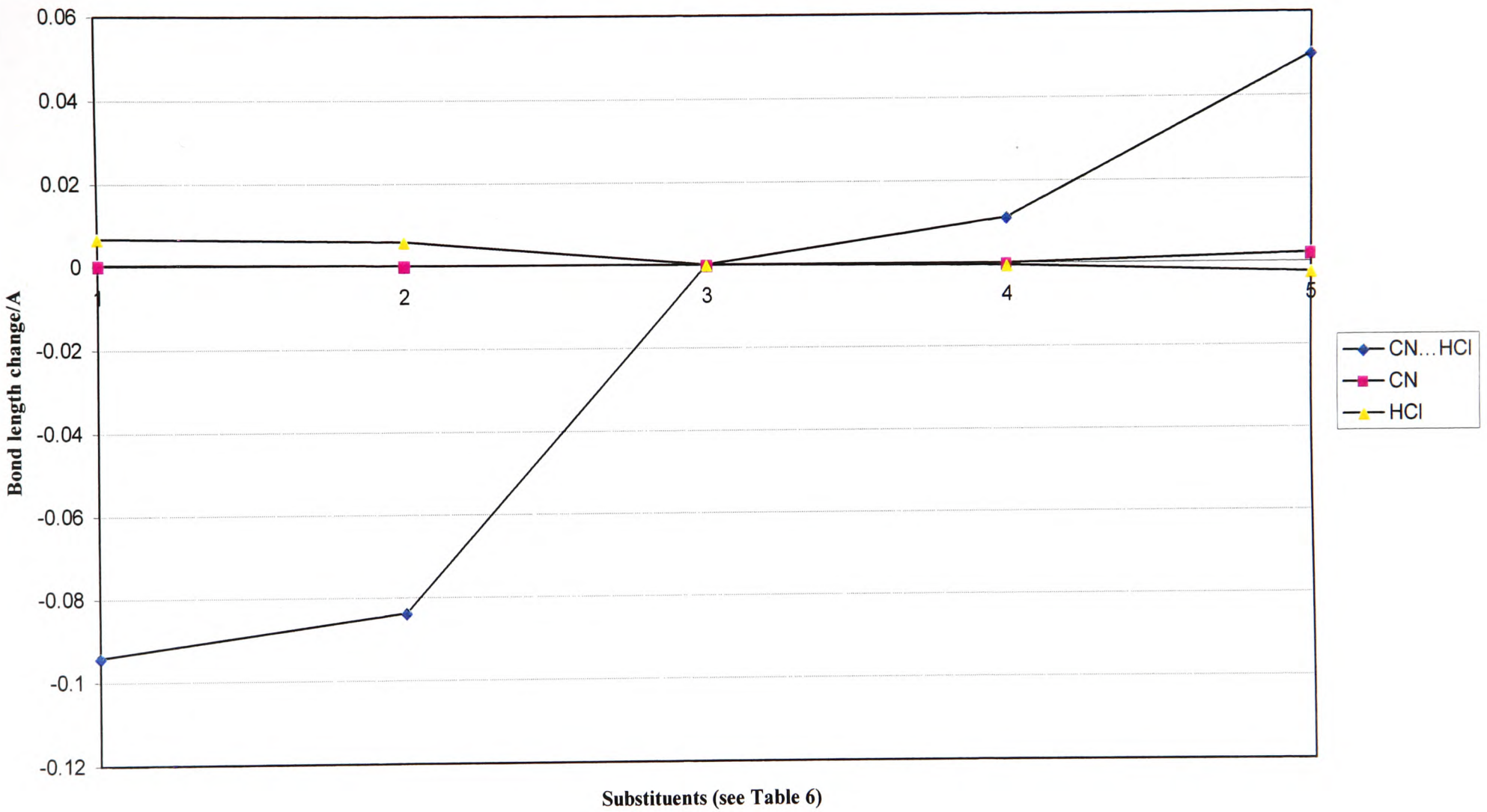

6.6 List of tables for Chapter 6.

Table 6.1 - Basis sets and number of basis functions used for hydrogen bonded carbonyl and nitrile complexes.

	Complex	formaldehyde...HCl			acetaldehyde...HCl			hydrogen cyanide...HCl			acetonitrile...HCl				
	Point group	C_s			C_s			$C_{\infty v}$			C_{3v}				
	Species	A'	A"	Total	A'	A"	Total	A1	A2	Total	B1	B2	A'	A"	Total
Number	Basis sets at B3LYP/														
1	6-31G(d)	42	13	55	55	19	74	30	3	33	10	10	37	14	71
2	6-31G(d,p)	48	16	64	64	25	89	32	3	35	12	12	42	18	84
3	6-31+G(d)	51	16	67	67	23	90	36	3	39	13	13	46	17	89
4	6-31++G(d)	54	16	70	71	24	95	38	3	41	13	13	48	18	92
5	6-31+G(d,p)	57	19	76	76	29	105	38	3	41	15	15	51	21	102
6	6-31++G(d,p)	60	19	79	80	30	110	40	3	43	15	15	53	22	105
7	6-311+G(d)	63	20	83	82	29	111	43	3	46	17	17	54	21	109
8	6-311++G(d,p)	72	23	95	95	36	131	47	3	50	19	19	61	26	125
9	6-311++G(2d,2p)	87	32	119	116	15	131	55	6	61	24	24	75	36	159
10	6-311++G(3df,3pd)	123	56	179	167	87	254	73	14	87	37	37	109	62	245

Table 6.2 - Comparison of hydrogen bonding in mono- and bi-functional carbonyl and nitrile complexes

	Formaldehyde			Acetaldehyde			Acetone		
	$H_2CO...HCl$			cis $(CH_3)HCO...HCl$			$(CH_3)_2CO...HCl$		
B3LYP/6-311++G(2d,2p)	Ezp	Eth+Ezp	Eelec+Ezp	Ezp	Eth+Ezp	Eelec+Ezp	Ezp	Eth+Ezp	Eelec+Ezp
HCl/Hartrees	0.006664	0.009025	-460.829789	0.006664	0.009025	-460.829789	0.006664	0.009025	-460.829789
carbonyl/Hartrees	0.026532	0.029399	-114.518649	0.055316	0.059206	-153.832304	0.083499	0.088856	-193.142189
carbonyl...HCl/hartrees	0.036059	0.041345	-575.35347	0.0646	0.071094	-614.66907	0.09257	0.100618	-653.979967
H bond energy/kJ mol-1			-13.21			-18.32			-20.98
BSSE Error/kJ mol-1			0.67			0.22			0.10
Corrected for BSSE/kJ mol-1			ΔEo = -12.55			ΔEo = -18.09			ΔEo = -20.87
			ΔEe=-20.06			ΔEe=-24.97			ΔEe=-27.19
Calc. harmonic mode/cm-1	Value	Shift		Value	Shift		Value	Shift	
ν(HCl) free	2918.1			2918.1			2918.1		
ν(CO) free	1811.4			1801.6			1771.7		
ν(CO) complex	1791.3	-20.1		1774.8	-26.8		1748.6	-23.1	
ν(HCl) complex	2616.2	-301.9		2524.5	-393.6		2510.4	-407.7	
				trans $(CH_3)HCO...HCl$					
B3LYP/6-311++G(2d,2p)				Ezp	Eth+Ezp	Eelec+Ezp			
HCl/Hartrees				0.006664	0.009025	-460.829789			
carbonyl/Hartrees				0.055322	0.059209	-153.832298			
carbonyl...HCl/hartrees				0.06459	0.071063	-614.668539			
H bond energy/kJ mol-1						-16.94			
BSSE Error/kJ mol-1						0.58			
Corrected for BSSE/kJ mol-1						ΔEo = -16.36			
						ΔEe=-23.20			
Calc. harmonic mode/cm-1				Value	Shift				
ν(HCl) free				2918.1					
ν(CO) free				1802.3					
ν(CO) complex				1778.3	-24.0				
ν(HCl) complex				2570.7	-347.5				

	Hydrogen cyanide			Acetonitrile			Propionitrile		
	HCN...HCl			CH_3CN...HCl			C_2H_5CN...HCl		
B3LYP/6-311++G(2d,2p)	Ezp	Eth+Ezp	Eelec+Ezp	Ezp	Eth+Ezp	Eelec+Ezp	Ezp	Eth+Ezp	Eelec+Ezp
HCl/Hartrees	0.006664	0.009025	-460.829789	0.006664	0.009025	-460.829789	0.006664	0.009025	-460.829789
nitrile/Hartrees	0.01626	0.018808	-93.440536	0.045206	0.048825	-132.755292	0.074186	0.078881	-172.052369
nitrile...HCl/Hartrees	0.025177	0.030584	-554.274866	0.054128	0.06061	-593.591752	0.08307	0.090662	-632.889123
H bond energy/kJ mol-1			-11.92			-17.51			-18.29
BSSE Error/kJ mol-1			1.00			0.90			0.52
Corrected for BSSE/kJ mol-1			ΔEo = -10.92			ΔEo = -16.61			ΔEo = -17.77
			ΔEe = -16.84			ΔEe = -22.54			ΔEe = -23.59
Calc. harmonic mode/cm-1				Value	Shift		Value	Shift	
ν(HCl) free	2918.1			2918.1			2918.1		
ν(CN) free	2192.9			2353.1			2342.1		
ν(CN) complex	2210.3	17.4		2368.6	15.5		2356.6	14.5	
ν(HCl) complex	2752.8	-165.3		2681.7	-236.4		2673.9	-244.2	

	Formyl nitrile			Acetyl nitrile		
	HCOCN...HCl			CH_3COCN...HCl		
B3LYP/6-311++G(2d,2p)	Ezp	Eth+Ezp	Eelec+Ezp	Ezp	Eth+Ezp	Eelec+Ezp
HCl/Hartrees	0.006664	0.009025	-460.829789	0.006664	0.009025	-460.829789
nitrile/Hartrees	0.026344	0.030366	-206.778198	0.054338	0.059746	-246.093078
nitrile...HCl/Hartrees	0.034966	0.042082	-667.611653	0.062953	0.07144	-706.927378
H bond energy/kJ mol-1			-9.63			-11.84
BSSE Error/kJ mol-1			1.12			1.06
Corrected for BSSE/kJ mol-1			ΔEo = -8.50			ΔEo = -10.79
			ΔEe = -13.64			ΔEe = -15.91
Calc. harmonic mode/cm-1						
ν(HCl) free	2918.1			2918.1		
ν(CN) free	2321.2			2317.5		
ν(CN) complex	2335.3	14.1		2332.2	14.6	
ν(HCl) complex	2787.2	-130.9		2758.4	-159.7	

	cis CNHCO...HCl		
B3LYP/6-311++G(2d,2p)	Ezp	Eth+Ezp	Eelec+Ezp
HCl/Hartrees	0.006664	0.009025	-460.829789
carbonyl/Hartrees	0.026338	0.030361	-206.778203
carbonyl...HCl/hartrees	0.034888	0.042053	-667.610086
H bond energy/kJ mol-1			-5.50
BSSE Error/kJ mol-1			1.05
Corrected for BSSE/kJ mol-1			ΔEo = -4.45
			ΔEe = -9.40
Calc. harmonic mode/cm-1	Value	Shift	
ν(HCl) free	2918.1		
ν(CO) free	1775.1		
ν(CO) complex	1764.7	-10.4	
ν(HCl) complex	2820.3	-97.8	

	trans CNHCO...HCl		
B3LYP/6-311++G(2d,2p)	Ezp	Eth+Ezp	Eelec+Ezp
HCl/Hartrees	0.006664	0.009025	-460.829789
carbonyl/Hartrees	0.026338	0.030361	-206.778203
carbonyl...HCl/hartrees	0.035076	0.042096	-667.610927
H bond energy/kJ mol-1			-7.71
BSSE Error/kJ mol-1			1.05
Corrected for BSSE/kJ mol-1			ΔEo = -6.66
			ΔEe = -12.10
Calc. harmonic mode/cm-1			
ν(HCl) free	2918.1		
ν(CO) free	1775.1		
ν(CO) complex	1758.2	-17.0	
ν(HCl) complex	2754.5	-163.6	

	cis $CNCH_3CO$...HCl		
	Ezp	Eth+Ezp	Eelec+Ezp
	0.006664	0.009025	-460.829789
	0.054338	0.059748	-246.093079
	0.062887	0.071423	-706.926113
			-8.52
			1.09
			ΔEo = -7.43
			ΔEe = --12.37
	Value	Shift	
	2918.1		
	1778.6		
	1762.6	-16.0	
	2784.0	-134.1	

	trans $CNCH_3CO$...HCl		
	Ezp	Eth+Ezp	Eelec+Ezp
	0.006664	0.009025	-460.829789
	0.054341	0.059749	-246.093075
	0.063108	0.071465	-706.926796
			-10.32
			1.07
			ΔEo = -9.25
			ΔEe = -14.77
	2918.1		
	1777.3		
	1758.0	-19.3	
	2722.1	-196.0	

Table 6.3 - Comparison of calculated and experimental values of molecular parameters of carbonyl complexes.

R1	R2	Shift/cm^{-1}		Bond lengths/Å				Angles/°			Expt method/ phase	Ab initio method/ basis set
		HCl	CO	C...Cl	CO	O...H	HCl	COH	q	Reference		
H	H			3.627	1.2051	1.968(10)	1.2839	107.1	20.3	116,117	MW/Gas	
		-242	-12							120,146	IR/MI	
		-302	-20	3.7169	1.2057	1.8775	1.3023	112.8	11.8	This work		B3LYP/6-311++G(2d,2p)
		-151	-11		1.211		1.283	121.3	17	118		CPF/TZZP
		-292	-36		1.215	1.848	1.291	106.8	14.7	119		MP2/6-311++G(2df,2pd)
					1.208		1.287	109.2	13.2	119		CCSD(T)/6-311G(2d,2p)
				3.7095		1.9415	1.2868		15.5	121		MP2/6-311+G(d,p)
				3.8577		1.8918	1.3203		20.2	121		B3LYP/6-311++G(d,p)
H	CH_3	-378								142	IR/MI	
		-394	-27	3.6829	1.2119	1.809	1.3096	112.8	9.4	This work		B3LYP/6-311++G(2d,2p)
CH_3	H	-348	-24	3.9385	1.211	1.8453	1.3059	124.2	4	This work		B3LYP/6-311++G(2d,2p)
CH_3	CH_3	-300	-34							122,123	IR/Gas	
		-479								139	IR/MI	
		-408	-23	3.9178	1.2181	1.7929	1.312	125	2	This work		B3LYP/6-311++G(2d,2p)
H	CN	-164	-17		1.2044	2.0184	1.2923	111.2	19.1	This work		B3LYP/6-311++G(2d,2p)
CN	H	-98	-10		1.2028	2.0879	1.2877	137	0.2	This work		B3LYP/6-311++G(2d,2p)
CH_3	CN	-196	-19		1.209	1.9696	1.2947	124.7	8.6	This work		B3LYP/6-311++G(2d,2p)
CN	CH_3	-134	-16		1.2079	2.0266	1.2903	137.1	-2.3	This work		B3LYP/6-311++G(2d,2p)

R1 is *cis* to the O...H-Cl group
R2 is *trans* to the O...H-Cl group

Table 6.4 - Comparison of calculated and experimental values of molecular parameters of nitrile complexes.

R-	Shift/cm^{-1}		Bond lengths/Å				Bond angles/°				
	HCl	CN	N...Cl	CN	N...H	HCl	CNH	NHCl	Reference	Expt method/ phase	Ab initio method/ basis set
H-	-80								140	IR/Gas	
	-183								143	IR/MI	
			3.4045		2.121				148,149	MW/Gas	
	-165	17.4	3.357	1.1441	2.0629	1.2928	180	180	This work		B3LYP/6-311++G(2d,2p)
	-153		3.334						124		B3LYP/6-31G(d,p)
	-140		3.361						124		B3LYP/6-31+G(d,p)
	-113		3.376						124		MP2/6-31+Gd,p)
CH_3-	-155								140	IR/Gas	
	-302								144	IR/MI	
			3.301(4)		2.0070				150	MW/Gas	
	-236	15.5	3.278	1.1478	1.9792	1.2987	180	180	This work		B3LYP/6-311++G(2d,2p)
	-227		3.266						124		B3LYP/6-31G(d,p)
	-218		3.286						124		B3LYP/6-31+G(d,p)
	-167		3.316						124		MP2/6-31+Gd,p)
C_2H_5-	-160	4.5							126	IR/Gas	
	-241	9							126	IR/MI	
	-244	14.5	3.268	1.1485	1.9688	1.2996	181.1	180.3	This work		B3LYP/6-311++G(2d,2p)
HCO-	-131	14.1	3.403	1.1492	2.1129	1.2903	180.7	181.4	This work		B3LYP/6-311++G(2d,2p)
CH_3CO-	-160	14.6	3.366	1.1491	2.074	1.2923	182	177.6	This work		B3LYP/6-311++G(2d,2p)

Table 6.5 - *Ab initio* calculated bond lengths and angles of carbonyl complexes.
(B3LYP/6-311++G(2d.2p))

	carbonyl complex		components						
No.	R1	R2	Bond lengths/Å		Bond angles/°			Bond lengths/Å	
			CO	O...H	HCl	COH	θ	CO	HCl
1	CH_3	CH_3	1.2181	1.7929	1.312	125	2	1.2107	1.2802
2	H	CH_3	1.2119	1.809	1.3096	112.8	9.4	1.205	1.2802
3	CH_3	H	1.211	1.8453	1.3059	124.2	4	1.205	1.2802
4	H	H	1.2057	1.8775	1.3023	112.8	11.8	1.2006	1.2802
5	CH_3	CN	1.209	1.9696	1.2947	124.7	8.6	1.2035	1.2802
6	H	CN	1.2044	2.0184	1.2923	111.2	19.1	1.198	1.2802
7	CN	CH_3	1.2079	2.0266	1.2903	137.1	-2.3	1.2035	1.2802
8	CN	H	1.2028	2.0879	1.2877	137	0.2	1.198	1.2802

Table 6.6 - Ab initio calculated bond lengths and angles of nitrile complexes.
(B3LYP/6-311++G(2d,2p))

nitrile complex		component							
No.	R-	Bond lengths/Å			Bond angles/°			Bond length/Å	
		CN	N...H	HCl	CNH	NHCl	Theta	CN	HCl
1	C_2H_5-	1.1485	1.9688	1.2996	181.1	180.3	1.4	1.1503	1.2802
2	CH_3-	1.1478	1.9792	1.2987	180	180	0	1.1498	1.2802
3	H-	1.1441	2.0629	1.2928	180	180	0	1.1463	1.2802
4	CH_3CO-	1.1491	2.074	1.2923	182	177.6	4.4	1.1512	1.2802
5	HCO-	1.1492	2.1129	1.2903	180.7	181.4	2.1	1.1492	1.2802

Chapter 7

Conclusions and Suggested Further Work.

7.1 Conclusion.

In this Thesis, the general phenomenon of hydrogen bonding has been studied. The first part of the work (Chapter 5), has focussed largely on the computational calculations of molecular and spectroscopic quantities and how these quantities may be used to identify the type of hydrogen bonding present, using methanol as the subject molecule.

Calculations for methanol were carried out using three calculation methods and ten basis sets and the properties determined. The stable model was taken as that in which the methyl hydrogen atoms are staggered with respect to the O-H group. This corresponds to the C_s point group and the 12 vibrations split into 9 a′ and 3a′ vibrations. The basis sets correspond to different levels of approximation for molecular orbitals and higher basis sets are composed of greater numbers of basis functions. The O-H and C-O stretching vibrations are the most characteristic of alcohols, and for all three methods, HF, MP2 and B3LYP and ten basis sets, have been calculated. The calculated wavenumber values are comparable with the measured values reported by Serrallach, Meyer and Gunthard [110].

It was found that the average difference between measured and calculated wavenumber decreases by 12% between the lowest and highest basis set used in Hartree Fock but by about 30% by the two methods which allow for electron correlation. However this average difference reduces dramatically between HF (-205.6), MP2 (-120.5) and B3LYP (-64.2) at the 6-31G(d) level and is significantly smaller (-181.7, -85.5,and -44-8) at the 6-311++G(3df,3pd) level. It is therefore clear that more accurate structural and other information is gained by using higher basis sets and methods that take electron correlation into account.

Also, the measurement of infrared spectra of methanol in solution in CCl_4 and vapour phase, and the *ab initio* computations provide information on the range of hydrogen bonded species present including cyclic trimers and cyclic tetramers of different

symmetries. The structures and properties of the hydrogen bonded forms of methanol were determined by *ab initio* calculations carried out over a range of basis sets and provided information on cyclic and open dimer, trimer and tetramer together with vibrational spectra and hydrogen bond energies. The calculated wavenumber and intensity values are reported for free and bonded 0-H groups together with hydrogen bonded O–H···O distances and energy values. The dimer is shown to form a stable open structure but forms an unstable transition state in the cyclic structure. The trimer and tetramer are shown to have hydrogen bond energies, which are greater by 12 and 32 kJ mol^{-1} in the cyclic form than in the open form. This reflects the great number of H-bonds in this cyclic form.

Evidence is provided that methanol can exist in two distinct cyclic trimeric forms for which the structure and properties of each form are computed by *ab initio* methods at the RHF/6-3 1 G(d,p) level. High and low energy forms have approximate C_3 and C_1 symmetry respectively and hydrogen bonding energies are determined for the methanol trimers as -46.0 kJ mol^{-1} for the C_3 form and -48.5 kJ mol^{-1} for the C_1 form. More accurate energy values would require high-level electron correlation methods but energy differences are found to highly consistent. The H-bonding of the C_1 form is 2-3 kJ mol^{-1} greater than that of the C_3 form, which can be attributed to steric interaction from alkyl groups when all on the same side of the ring as in C_3. The difference in molecular properties is small, but provides the basis for experimental verification, and recent work[152, 153, 154] has already made some headway into this, analyzing the methanol trimer, and good agreement between experimental and theoretical work has been found.

The second part of this work concentrated on medium strength hydrogen bonding.

The *ab initio* calculations reported for complexes of H_2CO, CH_3HCO, HCN and CH_3CN with HCl suggest an adequate basis is B3LYP/6-311++G(2d,2p) in the context of the present work.

In the case of CH_3HCO there are two possible isomers in which the HCl is *cis* and *trans* to the aldehydic H atom (low and high energy forms respectively). Using the basis

set determined as optimal further *ab initio* calculations have been made, together with those of $(CH_3)_2CO$, C_2H_5CN, HCOCN and CH_3COCN. The two bi-functional complexes each have three possible isomers; HCl may bond to the nitrile or to the carbonyl group in either *cis* or *trans* conformation to the nitrile group.

A comparison has been made of calculated values of zero point energy and the sum of zero point energy with thermal energy and with electronic energy; HCl, CO and CN harmonic stretching modes; selected geometrical structural parameters of all seven mono-functional complexes and of all six bi-functional complexes together with their components. These were used to calculate the hydrogen bond energy, ΔE_o, corrected for zero point energy and BSSE; shift in the harmonic stretching modes of the HCl, CO and CN groups and changes in geometrical structures of all forms on forming hydrogen bonded complexes.

The calculated ΔE_o values of HCl complexes of carbonyl compounds are:

H_2CO	CH_3HCO(high energy)	CH_3HCO(low energy)	$(CH_3)_2CO$
-12.55	-16.36	-18.09	-20.87 kJ mol^{-1}

The calculated hydrogen bond energies in HCl complexes of nitrile complexes are:

HCN	CH_3CN	C_2H_5CN
-10.92	-16.51	-17.71 kJ mol^{-1}

These changes are attributed to the inductive supply of electrons by alkyl groups and steric factors. In the bi-functional compounds hydrogen bond energies are smaller than in mono-functionals; the bonding to carbonyls with a *cis* nitrile is less than that with a *trans* nitrile and is greatest when bonded to the nitrile. The three respective values for each complex are:

formyl nitrile (HCOCN)	-4.45	-6.66	-8.50	kJ mol^{-1}
acetyl nitrile (CH3COCN)	-7.43	-9.25	-10.79	kJ mol^{-1}

These changes are attributed to effects of alkyl groups and delocalisation of electrons in conjugated CO and CN systems.

The shift in the harmonic HCl stretching mode in the HCl complexes are:

H_2CO	CH_3HCO(low energy)	CH_3HCO(high energy)	$(CH_3)_2CO$
-301.9	-347.5	-393.6	-407.7 cm^{-1}

HCN	CH_3CN	C_2H_5CN
-165.3	-236.4	-244.2 cm^{-1}

HCOCN to CO *cis* to CN	HCOCN to CO *trans* to CN	HCOCN to CN
-163.6	-97.8	-130.9 cm^{-1}

CH_3COCN to CO *cis* to CN	CH_3COCNtoCO *trans* to CN
-196.0	-134.1 cm^{-1}

CH_3COCNtoCN

-159.7 cm^{-1}

The shift in the CO and CN stretching modes in the complexes are between -10 and -24 cm-1 (i.e. to lower value) for HCl complexes to the CO group and between 14 and 18 cm-1 (i.e. to higher value) to the CN group. The explanation for increase is a result of the antibonding properties of the free lone pair of electrons on the nitrogen atom. When the complex is formed, the antibonding electrons are effectively removed from any interaction with the triple CN bond. This causes the bond to strengthen, and thus the frequency of the CN stretch increases.

The mean of the % of each ΔE_o value and the harmonic HCl shift of those in the acetone or propionitrile complexes are taken as an approximate measure of the hydrogen bond strength in the bifunctional complexes, These are:

ClH···NCHCO	51%	*trans* NCCHCO···HCl	36%
cis NCCHCO···HCl	22.5%.		
ClH···$NCCH_3CO$	61%	*trans* $NCCH_3CO$···HCl	46%
cis $NCCH_3CO$···HCl	37.5%.		

The length of the hydrogen bond varies between 2.0879 Å (weak) and 1.7929 Å (strong) for the carbonyl compounds and 2.1129 Å (weak) and 1.9688 Å (strong) for the

nitrile compounds. The length of the HCl and CX bonds are correlated with those of the hydrogen bond.

It is therefore clear that more accurate structural and other information is gained by using higher basis sets and methods, which take electron correlation into account. These higher-level calculations make a considerable demand on computing power. Careful judgement must therefore be exercised in determining when new science requires this resource. Greater ease of transfer of information and data in standard file protocol format should facilitate this process, which is illustrated by the problem of the structures, and properties of hydrogen bonded forms of alcohols. The calculation of these properties should be in parallel with experimental measurements since mutual stimulation between experiment and theory is the essence of better scientific knowledge.

7.2 Suggested Further Work.

For a more realistic picture of the methanol complexes, a study using the B3LYP/6-311++G(2d,2p) basis set would provide more consistent and, perhaps, plausible results.

For the carbonyl and nitrile complexes, there is clear scope to extend this work to the weak and strong forms of hydrogen bonding, to provide an overall view of hydrogen bonded complexes. Such work could be carried out with the ESPRC funded research programme at the Rutherford Appleton Laboratories, utilising the Columbus supercomputer.

References

1 A, Werner, *Liesbigs Ann*, 1902, **322**, 261, Ber. 1903, 36,147.

2 L. Knorr, *Ber*, 1911, **44**, 1138.

3 P. Pfeiffer, *Ber*,1914, **47**, 1580

4 P. Schuster (Editor), *The Hydrogen Bond*, Vol I, North Holland, 1985.

5 W. M. Latimer and W. H. Rodebush, *J. Am. Chem. Soc.*, 1920, **42**, 1419.

6 R. P. Bell, *Acids and Bases: Their Quantitative Behaviour*, Methuen,1969, Ch 8.

7 J. Tomkinson, *Spectrochimica Acta*, 1992, **48A**, No 3, 329.

8 S. N. Vinogradov and R. H. Linnel, *Hydrogen Bonding*, Van Nostrad,1971,Ch 1, Sec 5.

9 G. C. Pimentel and A. L. McClellan, *The Hydrogen Bond*, W. H. Freeman and Co. 1960,

10 M. M. Davies, *Rep. Prog. Chem.*, 1946, **43**, 5.

11 W. S. Fyfe, *J. Chem. Phys.*, 1953, **21**, 2.

12 G. L. Miessler and D. A. Tarr, *Inorganic Chemistry*, Prentice-Hall International Editions, 1991, Ch. 3.

13 A. C. Legon, *Chem. Soc. Rev.*, 1990, **19**, 197.

14 J. E. Huheey, *Inorganic Chemistry:Principles of Structure and Reactivity*, Harper and Row Publishing Co., 1983, Ch 6, p269.

15 D. F. Shriver et al., *Inorganic Chemistry*, 1990, Ch 9, p291, Oxford University Press

16 M. D. Joesten and L. J. Schaad, *Hydrogen Bonding*, 1974, Ch 1, p35, Marcel Dekker Inc

17 P. Schuster (Editor), *The Hydrogen Bond*, North Holland, 1985, Vol II, Ch 8, p395

18 D. J. Millen, *J. Mol. Struct.*, 1978, **45**, 1.

19 Ref. 5

20 M. D. Joesten, *J. Chem. Educ.*, 1982, **59**, 5, 362.

21 J. T. Arnold and M. E. Packard, *J. Chem. Phys.*, 1951, **19**, 1608.

22 J. T. Arnold and M. E. Packard, *Phys. Rev.*, 1951, **83**, 210.

23 E. D. Becker, U. Liddel and J. N. Shoolery, *J. Mol. Spect.*, 1958, **2**, 1

24 N. B. Colthup, L. H. Daly and S. E. Wiberley, *Introduction to Infrared and Raman Spectroscopy*, Third Ed., Academic Press, Boston, 1990.

25 J. S. Craw et al, *Spectrochimica Acta*, 1991, **47A**,1, 69.

26 A. C. Legon and D. J. Millen, *Chem. Rev.*, 1986, **86**, 3, 636.

27 W. C. Hamilton and J. A. Ibers, *Hydrogen Bonding in Solids*, W. A. Benjamin Inc. 1968, Ch 3 p85.

28 C. M. Huggins and G. C. Pimentel, *J. Chem. Phys.*, 1956, **60**,1615.

29 G. M. Barrow, *J. Chem. Phys.*, 1955, **59**, 1129.

30 D. J. Millen, *J. Mol. Struct.*, 1983, **100**, 351.

31 J. E. Bertie and D. J. Millen, *J. Chem. Soc.*, 1965, 497.

32 J. E. Bertie and M. V. Falk, *Can. J. Chem.*, 1973, **51**,1713.

33 N. Sheppard, *Hydrogen Bonding*, Ed. D. Hadzi, Perggamon Press 1959, p101.

34 D. J. Millen and J. Zabicky, *J. Chem. Soc.*, 1965, 3080.

35 L. Al-Adhami and D. J. Millen, *Nature*,1966, **211**,1291.

36 C. N. Banwell, *Fundamentals of Molecular Spectroscopy*, McGraw-Hill, 1972, Ch 2, p54,

37 A. Rauk, *Orbital Interaction Theory of Organic Chemistry*, Wiley 1994, pp 160-162.

38 D. J. Millen, *Croatica Chemica Acta*, 1982, **55**, 133.

39 W. O. George and P. S. McIntyre, *Infrared Spectroscopy*, Wiley, 1987, Ch 2, p 54,

40 P. R. Griffiths, *Chemical Infrared Fourier Transform Spectroscopy*, Wiley, 1975.

41 P. R. Griffiths and J. A. deHaseth, *Fourier Transform Infrared Spectroscopy*, Wiley, 1986.

42 M. L. Boas, *Mathematical Methods in the Physical Sciences*, Wiley, 1983, Ch 7.

43 P. Jacquinot et al., *J. Rech. C. N. R. S.*, 1948, **6**, 91.

44 J. Connes et al., *NOUV. Rev. Appl.*, 1970, **1**, 3.

45 W. O. George and D. Steele (Eds), *Computing Applications in Molecular Spectroscopy*, Royal Society of Chemistry, 1995

46 A. P. French and M. G. Ebison, *Introduction to Classical Mechanics*, Chapman and Hall, 1990, p 141.

47 Ref. 46, p 134.

48 Ref. 46, p 144.

49 Ref. 42, p 397.

50 Ref. 42, p 398.

51 Ref. 46, p 63.

52 A. Beiser, *Concepts of Modern Physics*, McGraw-Hill, 1987, p 167.

53 E. F. H. Brittain, W. O. George and C. H. J. Wells, *Introduction to Molecular Spectroscopy Theory and Experiment*, Academic Press, 1970, p 120.

54 Ref. 4, p 29.

55 R. N. Dixon (senior reporter), *A Specialist Periodical Report, Theoretical Chemistry*, The Chemical Society, 1983, **1**, 7.

56 M. Born and R. Oppenheimer, *Ann. Physik.*, 1927, **84**, 457.

57 Ref. 52, p 174.

58 Ref. 4, p 31.

59 W. J. Hehre, L. Radom, J. A. Pople and P. V. R. Schleyer, *Ab initio Molecular Orbital Theory*, John Wiley & Sons, 1986, p15.

60 Ref. 59, p 11.

61 R. Eisberg, R. Resnick, *Quantum Physics of Atoms, Molecules, Solids, Nuclei, and Particles*, John Wiley & Sons, 1985, p 305.

62 Ref. 59, p 20.

63 Ref. 4, p 31.

64 Ref. 59, p 17.

65 Ref. 59, p 18.

66 Ref. 59, p 19.

67 Ref. 61, p 245.

68 Ref. 61, p 100.

69 J. B. Foresman and A Frisch, *Exploring Chemistry with Electronic Structure Methods*, Gaussian Inc. 1995-96, p 64.

70 Ref. 4, p 65.

71 Ref. 4, p 200.

72 S. F. Boys and F. Bernardi, *Mol. Phys.*, 1970, **19**, 553.

73 *Animol User's Guide*, 1995, p 54.

74 *Chem-X Reference Guide*, 1995, **2**, 23.

75 Ref. 74, p 17.

76 Ref. 74, p 16.

77 Ref. 74, p 26.

78 Ref. 74, p 28.

79 *Gaussian 94 User's Reference*, Gaussian Inc.1995, p 182.

80 Ref. 79, p 26.

81 Ref. 69, p 80.

82 Ref. 79, p 29.

83 Ref. 59, p 68.

84 Ref. 59, p 76.

85 Ref. 79, p 26.

86 Ref 79, p 24.

87 Ref 79, p 26.

88 *Grams/386 and Grams/32 User's Guide*, Galactic Industries Corporation.

89 D. W. Marquardt, *J. Soc. Ind. Appl. Math.*, 1963, **11**,431.

90 R. S. McDonald, P. A. Wilks, *App Spectrosc*, 1988, **42**, p151.

91 R. S. McDonald, *Pittcom Communication*,1995.

92 Ref. 91.

93 U. Liddel and E.D. Becker, *Spectrochimica Acta (Part A)*, 1975, **10**, 70.

94 L.J. Bellamy and R.J. Pace, *Spectrochimica Acta (Part A)*, 1966, **22**, 525.

95 R.G. Lee, R.H. Hunt, E.K. Plyler and D.M. Dennison, *J. Mol.Spect.*, 1975, **57**, 138.

96 A.J. Barnes, H.E. Hallam and D. Jones, *Proc R. Soc. London. A.* 1973, **335**, 97.

97 L.A. Curtiss and M. Blander, *Chem Rev*, 1988, **88**, 827.

98 R.G. Inskeep, J.M. Kelliher, P.E. McMahon and B.G. Somers, *J. Chem Phys*, 1958, **28**, 1033. R. G. Inskeep, F. E. Dickson and H. M. Olson, *J. Mol. Spectr.*, 1960, **5**, 284.

99 M. Van Thiel, E.D. Becker and G. C. Pimentel, *J. Chem. Phys.*, 1957, **27**, 95.

100 A.J. Barnes and H.E. Hallam, *Trans Faraday Soc.*, 1970, **66**, 1920

101 V. Cheam, S.B. Farnham and S.D. Christian, *J. Phys Chem.*, 1970, **74**, 23.

102 F. Huisken and M. Stemmler, *Chemical Physics Letters*, 1988, **144**, 391.

103 G. Brink and L. Glasser, *J. Phys. Chem.*, 1978, **82**, 1000.

104 K. Shinomiya and T. Shinomiya, *Bull. Chem. Soc. Japan*, 1990, **63**, 1093.

105 S. Perez-Casas, L.M. Trejo and M. Costas, *J. Chem Soc., Faraday Trans*, 1991, **87**(11), 1733.

106 M. Iwahashi, Y. Hayashi, N. Hachiya, H. Matsuzawa and H. Kobayashi, *J. Chem Soc., Faraday Trans*, 1993, **89**(4), 707.

107 G.M. Forland, F.O. Libnau, O.M. Kvalheim and H. Hoiland, *Applied Spectroscopy*, 1996, **50**(10), 10.

108 L.A. Curtiss, *J. Chem. Phys.*, 67, **1144**, 1977.

109 O. Mo, M. Yanez and J. Elguero, *Journal of Molecular Structure (Theochem)*, 1994, **314**, 73.

110 A. Serralach, R. Meyer and Hs. H. Gunthard, *J. Mol. Spect.*, 1974, **52**, 94

111 O. Kristiansson, *J. Mol. Struct.*, 1999, **477**, 105.

112 L.J. Bellamy and R.J. Pace, *Spectrochimica Acta (Part A)*, 1966, **22**, 525.

113 L.J. Bellamy K. J. Morgan and R.J. Pace, *Spectrochimica Acta (Part A)*, 1966 **22**, 535.

114 J. J. Peron and C. Sandorfy, *J. Chem. Phys.*, 1976, **65**(8), 3153

115 G. T. Fraser, C. W. Gillies, J. Zozom, F. J. Lovas and R. D. Suenram, *J. Mol.Struct.*, 1987, **126**, 200.

116 A. C. Legon, *Faraday Discuss. Chem. Soc.*, 1994, **97**,19.

117 A. C. Legon, *J. Chem. Soc., Faraday Transactions*, 1996, **92(15)** 2677.

118 J. E. Rice, T. J. Lee and N. C. Handy, *J. Chem. Phys.*, 1988, **11**, 7011.

119 A. Nowek and J. Leszczynski, *J. Chem. Phys.*, 1996, **104(4)**, 1441.

120 L. Strandman-Long, B. Nelander and L. Nord, *J. Mol. Struct.*, 1984, **117**, 217.

121 H. C. Kang, *J. Mol. Struct. (Theochem),* 1997, **401**, 127.

122 H. D. Mettee, J. E. Del Bene and S. I. Hauck, *J. Phys. Chem.*, 1982, **86**, 5048.

123 D. S. Dudis, J. B. Everhart, T. M. Branch and S. S. Hunnicutt, *J. Phys. Chem.*, 1996, **100**, 2083.

124 J. E. Del Bene, W. B. Person and K Szczepaniak, *J. Phys. Chem.*, 1995, **99**, 10705.

125 M. D. Page, E. R. Waclawik, J. H. Holloway and A. C. Legon, *J. Mol. Struct.*, 1999, **509**, 55.

126 W. O George, P. E. Hirani, E. N. Lewis, W. F. Maddams and D. A. Williams, *J. Mol. Struct.*, 1986, **141**, 227.

127 C. Tuma, A. D. Boese and N. C. Handy, *Phys. Chem. Chem. Phys.* 1999, **1**, 3939.

128 J. E. Del Bene and M. J. T. Jordan, *Int. Rev. in Physical Chem.*, 1999, ***18(1)***, 119.

129 A. G. Csaszar, *Chemical Physics Letters*, 1989, **162(4-5)**, 361.

130 W. Lewis-Bevan, R. D. Gustan, J. Tyrrell, W. D. Stork and G. L. Salmon, *J. Am. Chem. Soc.*, 1992, **114(6)**, 1993.

131 J. Tyrrell, *J Mol. Struct(Theochem)*, 1991, **77**, 87.

132 N. Chang and C. Yu, *Chem. Phys. Letters,* 1995, **242**(1,2), 232

133 S. Bell, G. A. Guirgis, J. Lin and J. R. Durig, *J. Mol. Struct.*, 1990, **238**, 183

134 M. P. Bernstein, S. A. Sandford and I. J. Allamandola, *Astrophysical Journal*, 1997, **476(2)**, 932.

135 R. Sumathi and M. T. Nguyen, *J. Mol. Struct.*, 1990, **238**, 183

136 W. O. George, B. F. Jones, Rh. Lewis and J. M. Price, *Int. J. Vibr. Spec., [www.ijvs.com]* 1999. **3**, 2, 5.

137 S. Carter, N. Pinnavaia and N. C. Handy, *Chem. Phys. Letters*, 1995, **240**, 400.

138 K. B. Wiberg, Y. Thiel, L. Goodman and J. Leszczynski, *J. Phys. Chem.*, 1995, **99**, 13, 850.

139 A. J. Barnes, *J. Mol. Struct.*, 1983, **100**, 259.

140 R. K. Thomas and H. W. Thompson, *Proc. R. Soc. London A*, 1870, **316**, 303.

141 L. Ballard and G. Henderson, *J. Phys. Chem.*, 1991, **95**, 660

142 Rh Lewis, PhD Thesis 1990

143 G. L. Johnson and L Andrews, *J. Amer. Chem. Soc.*, 1983, **105**, 163.

144 A. Burneau, A. Loutellier and L. Schriver, *J. Mol. Struct.*, 1980, **61**, 397.

145 G. Herzberg, *Spectra of Diatomic Molecules*, D. Van Nostrand, Princeton, 1965, p 534

146 S. B. H. Bach and B. S. Ault, *J. Phys. Chem.*, 1984, **88**, 3600.

147 P. Klaboe and J. Grundnes, *Spectrochim. Acta*, 1968, **24A**, 1905.

148 A. C. Legon and D. J. Millen, *Chem. Phys. Letters*, 1988, **147**, 484.

149 A. C. Legon, E. Campbell and W. H. Flygare, *J. Chem. Phys.*, 1982, **76**, 2267.

150 A. C. Legon, D. J. Millen and H. M. North, *J. Phys. Chem.*, 1987, **91**, 5310.

151 J. R. Dixon, W.O. George and Rh. Lewis, "*The Networking of Infrared Spectrometers and Computers*" in "*Computing Applications in Molecular Spectroscopy*" W.O. George and D. Steele (Eds), Royal Society of Chemistry 1995, p. 61. This uses *ChemX*, Chemical Design Ltd, Oxford Molecular Group, The Medawar Centre, Oxford Science Park, Oxford OXA 4GA, UK.

152 R. A. Provencal et al, *J. Chem. Phys.*, 1999, **110**(9), 4258.

153 O. Mo and M. Yanez, *J. Chem. Phys.*, 1997, **107**(9), 3592.

154 G. S. Tschumper, J. M. Gonzales and H. F. Schaefer, *J. Chem. Phys.*, 1999, **111**(7),3027.

References for Appendix C

C1 A. McIntosh, A. M. Gallegos, R. R. Cucchese and J. W. Bevan, *J. Chem. Phys.*, 1997, 107(20), 8327.

C2 S. L. A. Adebayo, A. C. Legon and D. J. Millen, *J. Chem. Soc., Faraday Transactions,* 1991, 87(3) 443.

C3 Gaussian 94 User's Reference, Gaussian Inc Pittsburgh PA, page 23.

C4 Animol Useres Guide, 1995, page 54.

C5 Gaussian 94 User's Reference, Gaussian Inc Pittsburgh PA, page 68.

C6 J. R. Durig, P. Klaeboe, G. A. Guirgis, L. Wang and J. Lui, *Zeitschrift fur Physikalische Chemie Bd.*, 1995, 191(S), 23.

C7 D. A. Dixon, B. E. Smart, *J Phys. Chem.*, 1991, 95, 1609.

C8 G. L. Johnson, L. Andrews, *J. Am. Chem. Soc.*, 1983, 105, 163.

C9 W. O. George, P. Hirani, E. N. Lewis, W. F. Maddams and D. A. Williams, *J Mol. Struct.*, 1986, 141, 227.

Appendix A

Solving the Time Independent Schrödinger Equation for a Simple Harmonic Oscillator Potential.

A.1 Recap of chapter 2.

In chapter 2 a brief summary of the quantum mechanical treatment of the diatomic molecule was presented. Here, a fuller solution is offered.

We considered two coupled masses, m_1 and m_2, and treated them as a reduced mass system, with reduced mass, μ, such that:

$$\mu = \frac{m_1 m_2}{m_1 + m_2} \qquad \text{Eq. A.1}$$

And this mass was bound, via a spring of force constant k, in a potential energy well, V_0:

$$V_0 = \frac{kx^2}{2} \qquad \text{Eq. A.2}$$

where x is the displacement of the mass from the equilibrium position.

The resulting motion was described to be simple harmonic with a classical frequency, ν_μ, given by:

$$\nu_\mu = \frac{1}{2\pi}\sqrt{\frac{k}{\mu}} \qquad \text{Eq. A.3}$$

The time independent Schrödinger Equation was thus described as:

$$\frac{d^2\psi}{dx^2} + \frac{2\mu}{\hbar^2}(E - V_0)\psi = 0 \qquad \text{Eq. A.4}$$

where ψ is an eigenfunction of the equation to be determined.

A.2 Parameterising the equation.

Combining equations A.2, A.3 and A.4, we get:

$$\frac{d^2\psi}{dx^2} + \left[\frac{2\mu E}{\hbar^2} - \left(\frac{2\pi m \nu_\mu}{\hbar}\right)x^2\right]\psi = 0 \qquad \text{Eq. A.5}$$

If we now introduce toe parameters, α and β, such that:

$$\alpha = \frac{2\pi\mu\nu_\mu}{\hbar} \quad \text{and} \quad \beta = \frac{2\mu E}{\hbar^2} \qquad \text{Eq. A.6}$$

Then clearly equation A.5 becomes the more compact form:

$$\frac{d^2\psi}{dx^2} + (\beta - \alpha^2 x^2)\psi = 0 \qquad \text{Eq. A.7}$$

Now, if we express this in terms of a dimensionless variable, $u = \sqrt{\alpha} \cdot x$, then:

$$u = \sqrt{\frac{2\pi\mu}{2\pi\hbar}\left(\frac{k}{\mu}\right)^{\frac{1}{2}}} \cdot x = \frac{(k\mu)^{1/4}}{\hbar^{1/2}} \cdot x \qquad \text{Eq. A.8}$$

Thus:

$$\frac{d^2\psi}{dx^2} = \frac{du}{dx} \cdot \frac{d}{du}\left(\frac{d\psi}{du}\right) = \alpha \frac{d^2\psi}{du^2} \qquad \text{Eq. A.9}$$

Therefore, equation A.7 becomes:

$$\frac{d^2\psi}{du^2} + \left(\frac{\beta}{\alpha} - u^2\right)\psi = 0 \qquad \text{Eq. A.10}$$

It is the solutions to this equation that we must find.

We must find solutions for which $\psi(u)$ and its first derivative are singles valued, continuous and finite, for all u from $-\infty$ to $+\infty$. The first two conditions will automatically be satisfied by the solutions we obtain. However, it will be necessary to take care to ensure that $\psi(u)$ remains finite as $|u| \to \infty$. We shall thus consider $\psi(u)$ for large values of $|u|$. Now for any finite value of the total energy, E, the quantity β/α becomes negligible compared to u^2, for large $|u|$. Thus equation A.10 may be written as:

$$\frac{d^2\psi}{du^2} = u^2\psi \qquad |u| \to \infty \qquad \text{Eq. A.11}$$

The general solution to this differential equation is of the form:

$$\psi = Ae^{-u^2/2} + Be^{u^2/2} \qquad \text{Eq. A.12}$$

where A and B are arbitrary constants. We verify this by differentiating ψ twice with respect to u:

$$\frac{d^2\psi}{du^2} = A\left(u^2 - 1\right)e^{-u^2/2} + B\left(u^2 + 1\right)e^{u^2/2} \qquad \text{Eq. A.13}$$

But as $|u| \to \infty$, this is essentially:

$$\frac{d^2\psi}{du^2} = Au^2 e^{-u^2/2} + Bu^2 e^{u^2/2} \qquad \text{Eq. A.14}$$

And substituting this into equation A.11 gives:

$$Au^2 e^{-u^2/2} + Bu^2 e^{u^2/2} = u^2\psi \qquad \text{Eq. A.15}$$

and this clearly satisfies equation A.11 identically.

Now, for the condition that $\psi(u)$ remains finite as $|u| \to \infty$, it is apparent from equation A.12 that we must set B=0. Hence the form of the eigenfunctions for large $|u|$ are of the form:

$$\psi = Ae^{-u^2/2} \qquad |u| \to \infty \qquad \text{Eq. A.16}$$

This suggests that the general solution to equation A.10 can be written in the form:

$$\psi(u) = Ae^{-u^2/2} \cdot H(u) \qquad \text{Eq. A.17}$$

These solutions are to be valid *for all* u, so $H(u)$ mut be functions that vary slowly compared to $e^{-u^2/2}$ as $|u| \to \infty$, in order that equations A.17 and A.16. Elsewhere, $H(u)$ must have the correct forms to generate to correct eigenfunctions, $\psi(u)$.

A.3 A power series solution.

To evaluate the functions described by $H(u)$, we must differentiate equation A.17 twice with respect to u:

$$\frac{d^2\psi}{du^2} = Ae^{-u^2/2}\left(-H + u^2 H - 2u\frac{dH}{du} + \frac{d^2H}{du^2}\right) \qquad \text{Eq. A.18}$$

Substituting this into equation A.10 and simplifying, we are left with a differential equation in H, which will determine the functions $H(u)$:

$$\frac{d^2H}{du^2} - 2u\frac{dH}{du} + \left(\frac{\beta}{\alpha} - 1\right)H = 0 \qquad \text{Eq. A.19}$$

The most general technique available for the analytical solution of this form of differential equation is to assume that the solution can be written in terms of a power series of the independent variable:

$$H(u) = \sum_{l=0}^{l=\infty} a_l u^l \equiv a_0 + a_1 u + a_2 u^2 + a_3 u^3 + \cdots \qquad \text{Eq. A.20}$$

Calculating the 1st and 2nd derivatives of equation A.20 ,we have:

$$\frac{dH}{du} = \sum_{l=1}^{l=\infty} l a_l u^{l-1} \equiv 1a_1 + 2a_2 u + 3a_3 u^2 + \cdots \qquad \text{Eq. A.21}$$

$$\frac{dH}{du} = \sum_{l=2}^{l=\infty} l(l-1) a_l u^{l-2} \equiv 1\cdot 2a_2 + 2\cdot 3a_3 u + 3\cdot 4a_4 u^2 \cdots \qquad \text{Eq. A.22}$$

And substituting equations A.20, A.21 and A.22 into A.19, we obtain:

$$\begin{aligned} &1\cdot 2a_2 + 2.3a_3 u + 3\cdot 4a_4 u^2 + 4\cdot 5a_5 u^3 + \cdots - 2\cdot 1a_1 u - 2\cdot 2a_2 u^2 - 2\cdot 3a_3 u^3 - \cdots \\ &+(\beta/\alpha - 1)a_0 + (\beta/\alpha - 1)a_1 u + (\beta/\alpha - 1)a_2 u^2 + (\beta/\alpha - 1)a_3 u^3 + \cdots = 0 \end{aligned} \qquad \text{Eq. A.23}$$

Since this is to be true for all values of u, then the coefficients of each term of u must equal zero:

For:

$$\begin{aligned} u^0 &: \quad 1\cdot 2a_2 + (\beta/\alpha - 1)a_0 = 0 \\ u^1 &: \quad 2\cdot 3a_3 + (\beta/\alpha - 1 - 2\cdot 1)a_1 = 0 \\ u^2 &: \quad 3\cdot 4a_4 + (\beta/\alpha - 1 - 2\cdot 2)a_2 = 0 \\ u^3 &: \quad 3\cdot 4a_5 + (\beta/\alpha - 1 - 2\cdot 3)a_3 = 0 \end{aligned} \qquad \text{Eq. A.24}$$

Clearly, for the l^{th} power of u, the relationship is:

$$u^l : \quad (l+1)(l+2)a_{l+2} + (\beta/\alpha - 1 - 2l)a_l = 0 \qquad \text{Eq. A.25}$$

i.e.

$$a_{l+2} = -\frac{(\beta/\alpha - 1 - 2l)}{(l+1)(l+2)} a_l \qquad \text{Eq. A.26}$$

This recursive relationship will calculate, successively, the coefficients a_2, a_4, a_6 etc in terms of a_0, and the coefficients a_3, a_5, a_7 etc in terms of a_1. The terms a_0 and a_1 are not specified in the recursive relationship, but they are defined as the two arbitrary constants

needed to satisfy the general solution of the second order differential equation of $H(u)$. We see, then, that the general solution for equation A.19 splits into two separate series, which we write as:

$$H(u) = a_0\left(1+\frac{a_2}{a_0}u^2+\frac{a_4}{a_2}\cdot\frac{a_2}{a_0}u^4+\frac{a_6}{a_4}\cdot\frac{a_4}{a_2}\cdot\frac{a_2}{a_0}u^6+\cdots\right) + a_1\left(u+\frac{a_3}{a_1}u^3+\frac{a_5}{a_3}\cdot\frac{a_3}{a_1}u^5+\frac{a_7}{a_5}\cdot\frac{a_5}{a_3}\cdot\frac{a_3}{a_1}u^7+\cdots\right) \qquad \text{Eq. A.27}$$

The ratios a_{l+2}/a_l are found via equation A.26. Note that the first series is an even function of u and the second is an odd function of u. For an arbitrary value of β/α, both series in equation A.27 will contain an infinite number of terms. However, this will not lead to acceptable eigenfunctions.

Consider either series. For large l:

$$\frac{a_{l+2}}{a_l} = \frac{(\beta/\alpha - 1 - 2l)}{(l+1)(l+2)} \simeq \frac{2l}{l^2} = \frac{2}{l} \qquad \text{Eq. A.28}$$

Now consider the expansion of e^{u^2}:

$$e^{u^2} = 1+u^2+\frac{u^4}{2!}+\frac{u^6}{3!}+\cdots+\frac{u^l}{(l/2)!}+\frac{u^{l+2}}{(l/2+1)!}+\cdots \qquad \text{Eq. A.29}$$

For large l, the ratio of the coefficients of successive powers of u is:

$$\frac{1/(l/2+1)!}{1/(l/2)!} = \frac{(l/2)!}{(l/2+1)!} = \frac{(l/2)!}{(l/2+1)(l/2)1} = \frac{1}{l/2+1} \simeq \frac{1}{l/2} = \frac{2}{l} \qquad \text{Eq. A.30}$$

The two ratios are the same, implying that the terms of high power in u for e^{u^2} can differ from the corresponding terms in the even series of $H(u)$ by nothing more than a multiplicative constant K, and similarly can only differ from the corresponding terms in the odd series of $H(u)$ by another constant K'.

Now, for $|u| \to \infty$ the low power terms of u are not important, and so we can conclude that:

$$H(u) = a_0 K e^{u^2} + a_1 u K' e^{u^2} \qquad |u| \to \infty \qquad \text{Eq. A.31}$$

And according to equation A.17:

$$\psi(u) = Ae^{-u^2/2} \cdot H(u)$$

So therefore:

$$Ae^{-u^2/2}H(u) = a_0 AKe^{u^2/2} + a_1 AK'ue^{u^2/2} \qquad |u| \to \infty \qquad \text{Eq. A.32}$$

However, this increases without limit as $|u| \to \infty$, which is not acceptable for an eigenfunction. Acceptable eigenfunctions are obtainable for certain values of β/α. We set either a_0=0 or a_1=0, and we force the remaining series of $H(u)$ to terminate by setting:

$$\beta/\alpha = 2n+1 \qquad \text{Eq. A.33}$$

where:

$$n = 1,3,5,\ldots \qquad \text{if } a_0 = 0$$
$$n = 2,4,6,\ldots \qquad \text{if } a_1 = 0$$

It is clear from equation A.26 that such a choice of β/α will cause the series to terminate, since at the n^{th} term, l=n:

$$a_{n+2} = -\frac{(\beta/\alpha - 1 - 2n)}{(n+1)(n+2)} a_n = -\frac{(2n+1-1-2n)}{(n+1)(n+2)} a_n = 0 \qquad \text{Eq. A.34}$$

The coefficients a_{n+4}, a_{n+6}, a_{n+8}, ... will also be zero, since they are proportional to a_{n+2}.

A.4 Hermite polynomials.

The resulting solutions, $H_n(u)$ are polynomials of order u^n and are called Hermite polynomials. Each Hermite polynomial can be generated from equation A.27 by calculating the coefficients from the recursion relation with β/α given by equation A.33, for a particular value on n.

In general, they are calculated from the relationship:

$$H_n(u) = 2u \cdot H_{n-1}(u) - (2n-2) \cdot H_{n-2}(u) \qquad n = 2,3,4,\ldots \qquad \text{Eq. A.35}$$

where:

$$H_0(u) = 1$$
$$H_1(u) = 2u$$

Table A.1 lists the first few Hermite polynomials.

n	$H_n(u)$
0	1
1	$2u$
2	$4u^2 - 2$
3	$8u^3 - 12u$
4	$16u^4 - 48u^2 + 12$
5	$32u^5 - 160u^3 + 120u$

Table A.1 – The first six Hermite polynomials.

Thus the eigenfunctions we require are of the form:

$$\psi_n(u) = A_n e^{-u^2/2} \cdot H_n(u) \qquad \text{Eq. A.36}$$

Evaluating α and β from equations A.6 and A.33, we see that:

$$\frac{2\mu E}{\hbar^2} \cdot \frac{\hbar}{2\pi\mu\nu_\mu} = \frac{2E}{h\nu_\mu} = 2n+1$$

i.e.

$$E = \left(n + \frac{1}{2}\right) h\nu_\mu \qquad n = 0,1,2,\ldots \qquad \text{Eq. A.37}$$

This is the total eigenfunction for the reduced mass system, where ν_μ is the classical vibrational frequency of the system.

Appendix B

Sample input and output Gaussian 94/92 file types.

B.1 A sample input file.

Fig B.1 shows a typical Gaussian input file for formyl nitrile···HCl. The format is as described in chapter 4, section 4.1.2. The molecule was built using Chem-X and saved as a PDB (Protein Database) file. This file was then converted by Gaussian 94 into a Z-matrix using the NEWZMAT utility, so that the molecular information could be read by Gaussian. Initially, the data was optimised using the B3LYP/6-31G* basis set, before applying the B3LYP/6-311++G(2d,2p) basis set to optimise the structure and calculate the IR frequencies. Note the inclusion of a description of the file in the second line, and that the molecular geometry is described by Cartesian coordinates. The calculations were performed on the Columbus supercomputer at the Rutherford Appleton Laboratory. The data was sent, and the output received, via FTP over the Internet, and the job submitted via TELNET. Fig B.2 is the molecular representation of the Z-Matrix information.

```
#B3LYP/6-311++G(2d,2p) opt freq

formyl nitrile...HCl ( CON...HCl) opt B3lyp/6-31G*

0 1
6            1.351702     2.452380     0.000000
6            0.599876     1.180939     0.000000
7            0.000000     0.188733     0.000000
1            0.718491     3.355772     0.000000
1           -1.121144    -1.568911     0.000000
8            2.557153     2.477381     0.000000
```

Fig B.1 – A typical Gaussian input file. The information describes the formyl nitrile···HCl complex.

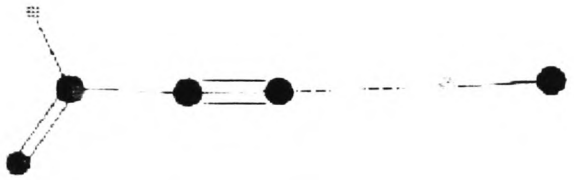

Fig B.2 – The molecular representation of the Z-Matrix information for the formyl nitrile$\cdots$HCl complex.

B.2 A sample output file.

Overleaf is the output generated by Gaussian from the information entered in the Z-Matrix of the input file. For the sake of brevity, some of the iterations of the calculation have been deleted. Note that this calculation took 10 hours, 52 minutes, 28.63 seconds.

```
Sender: LSF System <operator@columbus.rl.ac.uk>
Subject: Job 6202: <Jhnconb9> Done

Job <Jhnconb9> was submitted from host <columbus.rl.ac.uk> by user
<wog>.
Job was executed on host(s) <columbus.rl.ac.uk>, in queue <e3>, as user
<wog>.
</home/columbus_chem/wog> was used as the home directory.
</home/columbus_chem/wog> was used as the working directory.
Started at Sun May 30 16:59:39 1999
Results reported at Mon May 31 03:53:22 1999

Your job looked like:

------------------------------------------------------------
# LSBATCH: User input
# @$-r Jhnconb9
# @$-q e3
# @$-lm 50000000
# @$-eo
rung94 <<EOF
# B3LYP/6-311++G(2d,2p) opt freq

formyl nitrile...HCl  ( CON...HCl)  opt at B3lyp/6-31G*

0 1
             6           1.351702    2.452380    0.000000
             6           0.599876    1.180939    0.000000
             7           0.000000    0.188733    0.000000
             1           0.718491    3.355772    0.000000
             1          -1.121144   -1.568911    0.000000
             8           2.557153    2.477381    0.000000
            17          -1.868473   -2.630998    0.000000

EOF

------------------------------------------------------------

Successfully completed.

Resource usage summary:

    CPU time   :  39148.63 sec.
    Max Memory :        36 MB
    Max Swap   :        80 MB

Max Processes  :         7

The output (if any) follows:

 Entering Gaussian System, Link 0=/usr/local/g94/g94
OSF1 columbus.rl.ac.uk V4.0 878 alpha
 Initial command:
 /usr/local/g94/l1.exe /tmp/g94-339.inp -scrdir=/tmp/
 Entering Link 1 = /usr/local/g94/l1.exe PID=       963.

       Copyright (c) 1988,1990,1992,1993,1995 Gaussian, Inc.
                     All Rights Reserved.

 This is part of the Gaussian 94(TM) system of programs. It is
```

Cite this work as:
Gaussian 94, Revision E.3,
M. J. Frisch, G. W. Trucks, H. B. Schlegel, P. M. W. Gill,
B. G. Johnson, M. A. Robb, J. R. Cheeseman, T. Keith,
G. A. Petersson, J. A. Montgomery, K. Raghavachari,
M. A. Al-Laham, V. G. Zakrzewski, J. V. Ortiz, J. B. Foresman,
J. Cioslowski, B. B. Stefanov, A. Nanayakkara, M. Challacombe,
C. Y. Peng, P. Y. Ayala, W. Chen, M. W. Wong, J. L. Andres,

```
 E. S. Replogle, R. Gomperts, R. L. Martin, D. J. Fox,
 J. S. Binkley, D. J. Defrees, J. Baker, J. P. Stewart,
 M. Head-Gordon, C. Gonzalez, and J. A. Pople,
 Gaussian, Inc., Pittsburgh PA, 1995.

 ************************************************
 Gaussian 94:  DEC-AXP-OSF/1-G94RevE.3 1-Dec-1997
                30-May-1999
 ************************************************
 -------------------------------
 # B3LYP/6-311++G(2d,2p) opt freq
 -------------------------------
 1/14=-1,18=20,26=3,38=1/1,3;
 2/9=110,12=2,17=6,18=5/2;
 3/5=4,6=6,7=1212,11=2,25=1,30=1/1,2,3;
 4//1;
 5/5=2,38=4,42=-5/2;
 6/7=2,8=2,9=2,10=2,28=1/1;
 7//1,2,3,16;
 1/14=-1/3(1);
 99//99;
 2/9=110/2;
 3/5=4,6=6,7=1212,11=2,25=1,30=1/1,2,3;
 4/5=5,16=2/1;
 5/5=2,38=4,42=-5/2;
 7//1,2,3,16;
 1/14=-1/3(-5);
 2/9=110/2;
 3/5=4,6=6,7=1212,11=2,25=1,30=1,39=1/1,3;
 6/7=2,8=2,9=2,10=2,28=1/1;
 99/9=1/99;
 -----------------------------------------------------
 formyl nitrile...HCl ( CON...HCl) opt at B3lyp/6-31G*
 -----------------------------------------------------
 Symbolic Z-matrix:
    Charge = 0 Multiplicity = 1
 6      1.3517     2.45238    0.
 6      0.59988    1.18094    0.
 7      0.         0.18873    0.
 1      0.71849    3.35577    0.
 1      -1.12114   -1.56891   0.
 8      2.55715    2.47738    0.
 17     -1.86847   -2.631     0.


GradGradGradGradGradGradGradGradGradGradGradGradGradGradGradGradGrad
 Berny optimization.
 Initialization pass.
                          ----------------------------
                          !    Initial Parameters    !
                          ! (Angstroms and Degrees)  !
 -------------------------                            -------------------
------
 ! Name  Definition              Value          Derivative Info.
!
 ---------------------------------------------------------------------------
------
 ! R1    R(2,1)                  1.4771         estimate D2E/DX2
!
```

```
 ! R2    R(3,2)                  1.1594         estimate D2E/DX2
!
 ! R3    R(4,1)                  1.1032         estimate D2E/DX2
!
 ! R4    R(5,3)                  2.0848         estimate D2E/DX2
!
 ! R5    R(6,1)                  1.2057         estimate D2E/DX2
!
 ! R6    R(7,5)                  1.2987         estimate D2E/DX2
!
 ! A1    L(1,2,3)              180.             estimate D2E/DX2
!
 ! A2    L(1,2,3)              180.5601         estimate D2E/DX2
!
 ! A3    A(2,1,4)              114.3758         estimate D2E/DX2
!
 ! A4    L(2,3,5)              180.             estimate D2E/DX2
!
 ! A5    L(2,3,5)              181.3758         estimate D2E/DX2
!
 ! A6    A(2,1,6)              121.7847         estimate D2E/DX2
!
 ! A7    A(4,1,6)              123.8395         estimate D2E/DX2
!
 ! A8    L(3,5,7)              180.             estimate D2E/DX2
!
 ! A9    L(3,5,7)              182.5993         estimate D2E/DX2
!
 ! D1    D(2,6,1,4)            180.             estimate D2E/DX2
!
 ---------------------------------------------------------------------
------
 Trust Radius=3.00D-01 FncErr=1.00D-07 GrdErr=1.00D-06
 Number of steps in this run=  26 maximum allowed number of steps= 100.

GradGradGradGradGradGradGradGradGradGradGradGradGradGradGradGradGradGrad

                     Input orientation:
 ---------------------------------------------------------------------
 Center     Atomic                   Coordinates (Angstroms)
 Number     Number              X           Y           Z
 ---------------------------------------------------------------------
    1          6           1.351702    2.452380    0.000000
    2          6           0.599876    1.180939    0.000000
    3          7           0.000000    0.188733    0.000000
    4          1           0.718491    3.355772    0.000000
    5          1          -1.121144   -1.568911    0.000000
    6          8           2.557153    2.477381    0.000000
    7         17          -1.868473   -2.630998    0.000000
 ---------------------------------------------------------------------

                     Distance matrix (angstroms):
                     1          2          3          4          5
 1  C    0.000000
 2  C    1.477093   0.000000
 3  N    2.636512   1.159450   0.000000
 4  H    1.103210   2.178065   3.247517   0.000000
 5  H    4.720778   3.244008   2.084772   5.257068   0.000000
 6  O    1.205710   2.347700   3.431755   2.037707   5.468304
 7  Cl   6.017496   4.541323   3.382614   6.521794   1.298664
                6          7
```

```
 6  O     0.000000
 7  Cl    6.758824    0.000000
Stoichiometry    C2H2ClNO
Framework group  CS[SG(C2H2ClNO)]
Deg. of freedom   11
Full point group                 CS      NOp   2
Largest Abelian subgroup         CS      NOp   2
Largest concise Abelian subgroup C1      NOp   1
                  Standard orientation:
---------------------------------------------------------------------
Center     Atomic                   Coordinates (Angstroms)
Number     Number              X           Y           Z
---------------------------------------------------------------------
   1          6           1.351701    2.452381    0.000000
   2          6           0.599876    1.180939    0.000000
   3          7           0.000000    0.188733    0.000000
   4          1           0.718490    3.355772    0.000000
   5          1          -1.121144   -1.568911    0.000000
   6          8           2.557152    2.477382    0.000000
   7         17          -1.868472   -2.630998    0.000000
---------------------------------------------------------------------
 Rotational constants (GHZ):     50.8138040      0.7345715
0.7241038
 Isotopes: C-12,C-12,N-14,H-1,H-1,O-16,Cl-35
 Standard basis: 6-311++G(2d,2p) (5D, 7F)
 There are   117 symmetry adapted basis functions of A'  symmetry.
 There are    46 symmetry adapted basis functions of A"  symmetry.
 Crude estimate of integral set expansion from redundant
integrals=1.000.
 Integral buffers will be    131072 words long.
 Raffenetti 2 integral format.
 Two-electron integral symmetry is turned on.
   163 basis functions      241 primitive gaussians
    23 alpha electrons       23 beta electrons
       nuclear repulsion energy       151.3006347548 Hartrees.
 One-electron integrals computed using PRISM.
 The smallest eigenvalue of the overlap matrix is  2.800D-05
 Projected CNDO Guess.
 Initial guess orbital symmetries:
      Occupied  (A') (A') (A') (A') (A') (A') (A') (A") (A')
                (A') (A') (A') (A') (A') (A") (A') (A') (A') (A")
                (A') (A") (A')
      Virtual   (A") (A') (A') (A') (A') (A') (A') (A") (A') (A')
                (A') (A") (A') (A') (A') (A") (A') (A') (A') (A")
                (A') (A') (A') (A") (A') (A") (A") (A') (A') (A')
                (A") (A") (A') (A') (A') (A') (A') (A') (A") (A')
                (A') (A') (A") (A') (A') (A') (A") (A') (A') (A')
                (A") (A') (A") (A") (A') (A') (A') (A") (A") (A')
                (A') (A') (A') (A') (A") (A') (A') (A') (A") (A')
                (A') (A') (A") (A') (A') (A') (A") (A') (A") (A")
                (A') (A') (A') (A") (A") (A') (A') (A') (A') (A')
                (A') (A') (A") (A') (A") (A') (A') (A') (A') (A')
                (A') (A") (A') (A') (A") (A') (A') (A') (A") (A')
                (A') (A') (A") (A') (A") (A') (A") (A") (A') (A')
                (A') (A") (A') (A') (A') (A') (A') (A') (A") (A')
                (A') (A") (A') (A") (A') (A") (A") (A') (A') (A")
 Requested convergence on RMS density matrix=1.00D-08 within  64 cycles.
 Requested convergence on MAX density matrix=1.00D-06.
 Integral accuracy reduced to 1.0D-05 until final iterations.
 Initial convergence to 1.0D-05 achieved.  Increase integral accuracy.
```

```
SCF Done:  E(RB+HF-LYP) =  -667.646215958     A.U. after   15 cycles
            Convg  =    0.4594D-08             -V/T =  2.0029
            S**2   =   0.0000

 **********************************************************************

           Population analysis using the SCF density.

 **********************************************************************

 Orbital Symmetries:
       Occupied  (A') (A') (A') (A') (A') (A') (A') (A") (A') (A')
                 (A') (A') (A') (A') (A') (A") (A') (A') (A') (A")
                 (A') (A") (A')
       Virtual   (A") (A') (A') (A') (A") (A') (A') (A") (A') (A')
                 (A") (A') (A') (A') (A") (A') (A') (A') (A') (A')
                 (A") (A") (A') (A') (A') (A') (A') (A') (A') (A")
                 (A') (A") (A') (A") (A') (A") (A') (A') (A') (A")
                 (A') (A') (A") (A') (A') (A') (A") (A') (A') (A')
                 (A") (A') (A") (A') (A') (A") (A') (A") (A') (A')
                 (A') (A") (A') (A') (A") (A') (A") (A') (A') (A')
                 (A') (A') (A') (A") (A') (A') (A") (A") (A') (A')
                 (A') (A") (A') (A') (A') (A") (A") (A') (A') (A')
                 (A') (A') (A') (A") (A") (A') (A') (A") (A") (A')
                 (A') (A") (A') (A') (A") (A') (A') (A') (A") (A')
                 (A") (A') (A") (A') (A') (A') (A') (A") (A') (A")
                 (A') (A') (A") (A') (A') (A') (A") (A') (A") (A')
                 (A') (A') (A') (A') (A") (A') (A') (A') (A') (A')
  The electronic state is 1-A'.
 Alpha  occ. eigenvalues -- -101.53686 -19.20534 -14.38893 -10.35498 -
10.27514
 Alpha  occ. eigenvalues --   -9.45212  -7.21580  -7.20726  -7.20726  -
1.13184
 Alpha  occ. eigenvalues --   -0.97476  -0.82481  -0.75967  -0.59696  -
0.52590
 Alpha  occ. eigenvalues --   -0.48354  -0.47771  -0.42277  -0.40647  -
0.40287
 Alpha  occ. eigenvalues --   -0.34576  -0.31562  -0.31559
 Alpha virt. eigenvalues --   -0.14381  -0.04423  -0.02227   0.00895
0.02761
 Alpha virt. eigenvalues --    0.02808   0.03784   0.04190   0.06209
0.06677
 Alpha virt. eigenvalues --    0.06900   0.08462   0.09361   0.10305
0.10766
 Alpha virt. eigenvalues --    0.11737   0.13593   0.15768   0.18685
0.19197
 Alpha virt. eigenvalues --    0.19404   0.20484   0.20810   0.23872
0.26239
 Alpha virt. eigenvalues --    0.27353   0.28568   0.33717   0.36052
0.41057
 Alpha virt. eigenvalues --    0.41353   0.45054   0.45431   0.47067
0.47439
 Alpha virt. eigenvalues --    0.47440   0.47526   0.48316   0.49620
0.51430
 Alpha virt. eigenvalues --    0.53796   0.56145   0.56789   0.58004
0.61124
 Alpha virt. eigenvalues --    0.66087   0.66123   0.66873   0.71333
0.73599
 Alpha virt. eigenvalues --    0.74715   0.78828   0.79160   0.87471
0.93262
```

```
 Alpha virt. eigenvalues --    0.95144   0.95251   0.95738   0.99615
0.99844
 Alpha virt. eigenvalues --    1.03115   1.03946   1.08067   1.12552
1.16750
 Alpha virt. eigenvalues --    1.17607   1.22010   1.23945   1.27512
1.38818
 Alpha virt. eigenvalues --    1.43634   1.48741   1.53259   1.59082
1.60940
 Alpha virt. eigenvalues --    1.71881   1.78079   1.93224   1.95170
2.06624
 Alpha virt. eigenvalues --    2.16742   2.25678   2.25798   2.29345
2.35444
 Alpha virt. eigenvalues --    2.35444   2.42912   2.43030   2.45090
2.48334
 Alpha virt. eigenvalues --    2.64679   2.66522   2.71316   2.74574
2.75621
 Alpha virt. eigenvalues --    2.90578   3.10574   3.13065   3.18818
3.20782
 Alpha virt. eigenvalues --    3.22764   3.25046   3.28486   3.37041
3.37922
 Alpha virt. eigenvalues --    3.46495   3.64727   3.73171   3.76108
3.77167
 Alpha virt. eigenvalues --    3.85758   3.93734   3.98338   3.99147
4.09955
 Alpha virt. eigenvalues --    4.21678   4.67661   4.73534   4.73881
4.94423
 Alpha virt. eigenvalues --    4.99802   5.04386   5.05493   5.19182
5.60321
 Alpha virt. eigenvalues --    5.92765   6.72416   6.76592   6.92160
7.12181
 Alpha virt. eigenvalues --    7.15383   9.84428  23.95579  24.11554
25.79146
 Alpha virt. eigenvalues --   25.79948  26.85799  35.72468  49.89139
215.83878
          Condensed to atoms (all electrons):
               1          2          3          4          5          6
  1  C    5.499219  -0.778010   0.255085   0.432983   0.011657
0.471359
  2  C   -0.778010   6.870385   0.002773  -0.116160  -0.006627  -
0.137991
  3  N    0.255085   0.002773   6.827563   0.012675  -0.005020
0.020208
  4  H    0.432983  -0.116160   0.012675   0.592867   0.000627  -
0.041709
  5  H    0.011657  -0.006627  -0.005020   0.000627   0.479824
0.000878
  6  O    0.471359  -0.137991   0.020208  -0.041709   0.000878
7.954032
  7  Cl  -0.005704  -0.010617   0.040376  -0.000060   0.259897  -
0.000050
               7
  1  C   -0.005704
  2  C   -0.010617
  3  N    0.040376
  4  H   -0.000060
  5  H    0.259897
  6  O   -0.000050
  7  Cl  16.962971
 Total atomic charges:
               1
```

```
 1  C     0.113411
 2  C     0.176247
 3  N    -0.153659
 4  H     0.118777
 5  H     0.258764
 6  O    -0.266726
 7  Cl   -0.246813
Sum of Mulliken charges=   0.00000
Atomic charges with hydrogens summed into heavy atoms:
                1
 1  C     0.232188
 2  C     0.176247
 3  N    -0.153659
 4  H     0.000000
 5  H     0.000000
 6  O    -0.266726
 7  Cl    0.011951
Sum of Mulliken charges=   0.00000
Electronic spatial extent (au):  <R**2>=  1340.8145
Charge=      0.0000 electrons
Dipole moment (Debye):
   X=      0.4673    Y=      4.2557    Z=      0.0000  Tot=      4.2813
Quadrupole moment (Debye-Ang):
  XX=    -44.6992   YY=    -33.6060   ZZ=    -35.5716
  XY=     -5.6148   XZ=      0.0000   YZ=      0.0000
Octapole moment (Debye-Ang**2):
 XXX=    -11.8980  YYY=     32.8836  ZZZ=      0.0000  XYY=     -0.6286
 XXY=    -10.9234  XXZ=      0.0000  XZZ=      3.3447  YZZ=      3.5288
 YYZ=      0.0000  XYZ=      0.0000
Hexadecapole moment (Debye-Ang**3):
XXXX=   -669.0787 YYYY= -1010.8673 ZZZZ=    -37.6708 XXXY=   -423.9440
XXXZ=      0.0000 YYYX=   -388.5772 YYYZ=      0.0000 ZZZX=      0.0000
ZZZY=      0.0000 XXYY=   -323.0629 XXZZ=   -105.8310 YYZZ=   -183.6343
XXYZ=      0.0000 YYXZ=      0.0000 ZZXY=   -121.6400
N-N= 1.513006347548D+02 E-N=-1.882126767190D+03  KE= 6.657269981443D+02
Symmetry A'    KE= 6.134419915254D+02
Symmetry A"    KE= 5.228500661889D+01
***** Axes restored to original set *****
-------------------------------------------------------------------
Center     Atomic                   Forces (Hartrees/Bohr)
Number     Number              X              Y              Z
-------------------------------------------------------------------
   1          6           0.008970812    0.001066735    0.000000000
   2          6          -0.009909154   -0.019322107    0.000000000
   3          7           0.011772832    0.020621411    0.000000000
   4          1           0.002133836   -0.002027893    0.000000000
   5          1          -0.002689194   -0.003623695    0.000000000
   6          8          -0.012764326   -0.000133116    0.000000000
   7         17           0.002485194    0.003418665    0.000000000
-------------------------------------------------------------------
Cartesian Forces:  Max     0.020621411 RMS     0.007948730
Internal  Forces:  Max     0.023456896 RMS     0.006827207


GradGradGradGradGradGradGradGradGradGradGradGradGradGradGradGradGrad
 Berny optimization.
 Search for a local minimum.
 Step number   1 out of a maximum of  26
 All quantities printed in internal units (Hartrees-Bohrs-Radians)
 Second derivative matrix not updated -- first step.
```

The second derivative matrix:

	R1	R2	R3	R4	R5
R1	0.34905				
R2	0.00000	1.28154			
R3	0.00000	0.00000	0.33330		
R4	0.00000	0.00000	0.00000	0.00622	
R5	0.00000	0.00000	0.00000	0.00000	1.02005
R6	0.00000	0.00000	0.00000	0.00000	0.00000
A1	0.00000	0.00000	0.00000	0.00000	0.00000
A2	0.00000	0.00000	0.00000	0.00000	0.00000
A3	0.00000	0.00000	0.00000	0.00000	0.00000
A4	0.00000	0.00000	0.00000	0.00000	0.00000
A5	0.00000	0.00000	0.00000	0.00000	0.00000
A6	0.00000	0.00000	0.00000	0.00000	0.00000
A7	0.00000	0.00000	0.00000	0.00000	0.00000
A8	0.00000	0.00000	0.00000	0.00000	0.00000
A9	0.00000	0.00000	0.00000	0.00000	0.00000
D1	0.00000	0.00000	0.00000	0.00000	0.00000

	R6	A1	A2	A3	A4
R6	0.30026				
A1	0.00000	0.25000			
A2	0.00000	0.00000	0.25000		
A3	0.00000	0.00000	0.00000	0.16000	
A4	0.00000	0.00000	0.00000	0.00000	0.16000
A5	0.00000	0.00000	0.00000	0.00000	0.00000
A6	0.00000	0.00000	0.00000	0.00000	0.00000
A7	0.00000	0.00000	0.00000	0.00000	0.00000
A8	0.00000	0.00000	0.00000	0.00000	0.00000
A9	0.00000	0.00000	0.00000	0.00000	0.00000
D1	0.00000	0.00000	0.00000	0.00000	0.00000

	A5	A6	A7	A8	A9
A5	0.16000				
A6	0.00000	0.25000			
A7	0.00000	0.00000	0.16000		
A8	0.00000	0.00000	0.00000	0.25000	
A9	0.00000	0.00000	0.00000	0.00000	0.25000
D1	0.00000	0.00000	0.00000	0.00000	0.00000

	D1
D1	0.04262

Eigenvalues ---	0.00622	0.04262	0.16000	0.16000	0.16000
Eigenvalues ---	0.22000	0.25000	0.25000	0.25000	0.25000
Eigenvalues ---	0.30026	0.33330	0.34905	1.02005	1.28154
Eigenvalues ---	1000.00000				

RFO step: Lambda=-7.07910325D-04.
Linear search not attempted -- first point.
Iteration 1 RMS(Cart)= 0.00932262 RMS(Int)= 0.00001669
Iteration 2 RMS(Cart)= 0.00002113 RMS(Int)= 0.00000007
Iteration 3 RMS(Cart)= 0.00000013 RMS(Int)= 0.00000000
TrRot= 0.000000 0.000000 0.000000 0.000000 0.000000 0.000000

Variable	Old X	-DE/DX	Delta X (Linear)	Delta X (Quad)	Delta X (Total)	New X
R1	2.79130	-0.00179	0.00000	-0.00511	-0.00511	2.78619
R2	2.19104	-0.02346	0.00000	-0.01829	-0.01829	2.17275
R3	2.08477	-0.00288	0.00000	-0.00864	-0.00864	2.07613
R4	3.93965	0.00028	0.00000	0.04078	0.04078	3.98043
R5	2.27846	-0.01276	0.00000	-0.01251	-0.01251	2.26596
R6	2.45412	-0.00423	0.00000	-0.01404	-0.01404	2.44008
A1	3.14159	0.00000	0.00000	0.00000	0.00000	3.14159
A2	3.15137	0.00152	0.00000	0.00608	0.00608	3.15744
A3	1.99623	0.00071	0.00000	0.00424	0.00424	2.00048

```
   A4          3.14159   0.00000   0.00000   0.00000   0.00000   3.14159
   A5          3.16561   0.00007   0.00000   0.00046   0.00046   3.16607
   A6          2.12554  -0.00020   0.00000  -0.00093  -0.00093   2.12462
   A7          2.16141  -0.00051   0.00000  -0.00332  -0.00332   2.15809
   A8          3.14159   0.00000   0.00000   0.00000   0.00000   3.14159
   A9          3.18696  -0.00016   0.00000  -0.00065  -0.00065   3.18631
   D1          3.14159   0.00000   0.00000   0.00000   0.00000   3.14159
        Item               Value     Threshold  Converged?
Maximum Force            0.023457     0.000450     NO
RMS     Force            0.006827     0.000300     NO
Maximum Displacement     0.017895     0.001800     NO
RMS     Displacement     0.009324     0.001200     NO
Predicted change in Energy=-3.530659D-04

Iteration  1 RMS(Cart)=  0.00189063 RMS(Int)=  0.00000023
Iteration  2 RMS(Cart)=  0.00000029 RMS(Int)=  0.00000000
TrRot=  0.000000  0.000000  0.000000  0.000000  0.000000  0.000000
Variable       Old X    -DE/DX   Delta X   Delta X   Delta X     New X
                                 (Linear)    (Quad)   (Total)
   R1          2.78925  -0.00002  -0.00006  -0.00003  -0.00009   2.78916
   R2          2.17174  -0.00001   0.00001   0.00000   0.00001   2.17175
   R3          2.07730   0.00000   0.00001   0.00001   0.00001   2.07731
   R4          3.98667   0.00004   0.00608   0.00000   0.00608   3.99274
   R5          2.26387   0.00001   0.00002   0.00001   0.00003   2.26390
   R6          2.43850  -0.00001  -0.00018   0.00000  -0.00019   2.43831
   A1          3.14159   0.00000   0.00000   0.00000   0.00000   3.14159
   A2          3.17534   0.00000   0.00000   0.00002   0.00001   3.17535
   A3          1.99505   0.00000   0.00002   0.00002   0.00004   1.99509
   A4          3.14159   0.00000   0.00000   0.00000   0.00000   3.14159
   A5          3.15368  -0.00001  -0.00042  -0.00006  -0.00048   3.15320
   A6          2.12946   0.00000   0.00002   0.00000   0.00003   2.12948
   A7          2.15868   0.00000  -0.00004  -0.00002  -0.00006   2.15861
   A8          3.14159   0.00000   0.00000   0.00000   0.00000   3.14159
   A9          3.16583   0.00000  -0.00066   0.00004  -0.00062   3.16522
   D1          3.14159   0.00000   0.00000   0.00000   0.00000   3.14159
        Item               Value     Threshold  Converged?
Maximum Force            0.000037     0.000450     YES
RMS     Force            0.000011     0.000300     YES
Maximum Displacement     0.004339     0.001800     NO
RMS     Displacement     0.001890     0.001200     NO
Predicted change in Energy=-1.143284D-07

GradGradGradGradGradGradGradGradGradGradGradGradGradGradGradGradGradGrad

                     Input orientation:
---------------------------------------------------------------------
Center     Atomic                   Coordinates (Angstroms)
Number     Number                X           Y           Z
---------------------------------------------------------------------
   1          6             1.353620    2.451751    0.000000
   2          6             0.611228    1.176086    0.000000
   3          7            -0.000019    0.202882    0.000000
   4          1             0.715397    3.346769    0.000000
   5          1            -1.144486   -1.573185    0.000000
   6          8             2.551025    2.489644    0.000000
   7         17            -1.868821   -2.640991    0.000000
---------------------------------------------------------------------
                     Distance matrix (angstroms):
                1          2          3          4          5
 1  C    0.000000
```

```
 2  C     1.475963   0.000000
 3  N     2.624834   1.149239   0.000000
 4  H     1.099266   2.173181   3.224260   0.000000
 5  H     4.737156   3.262059   2.112869   5.259764   0.000000
 6  O     1.198005   2.342700   3.425946   2.025881   5.492120
 7  Cl    6.026620   4.552002   3.402944   6.521615   1.290299
            6          7
 6  O     0.000000
 7  Cl    6.771887   0.000000
 Stoichiometry    C2H2ClNO
 Framework group  CS[SG(C2H2ClNO)]
 Deg. of freedom   11
 Full point group                 CS      NOp   2
 Largest Abelian subgroup         CS      NOp   2
 Largest concise Abelian subgroup C1      NOp   1
                  Standard orientation:
 ---------------------------------------------------------------------
 Center     Atomic              Coordinates (Angstroms)
 Number     Number              X           Y           Z
 ---------------------------------------------------------------------
    1          6           1.353396    2.452309    0.000000
    2          6           0.611142    1.176564    0.000000
    3          7           0.000000    0.203293    0.000000
    4          1           0.715077    3.347258    0.000000
    5          1          -1.144275   -1.572897    0.000000
    6          8           2.550797    2.490331    0.000000
    7         17          -1.868494   -2.640782    0.000000
 ---------------------------------------------------------------------
 Rotational constants (GHZ):     52.1063746      0.7316603
0.7215288
 Isotopes: C-12,C-12,N-14,H-1,H-1,O-16,Cl-35
 Standard basis: 6-311++G(2d,2p) (5D, 7F)
 There are   117 symmetry adapted basis functions of A'  symmetry.
 There are    46 symmetry adapted basis functions of A"  symmetry.
 Crude estimate of integral set expansion from redundant
integrals=1.000.
 Integral buffers will be    131072 words long.
 Raffenetti 2 integral format.
 Two-electron integral symmetry is turned on.
   163 basis functions      241 primitive gaussians
    23 alpha electrons       23 beta electrons
       nuclear repulsion energy       151.5624690340 Hartrees.
 One-electron integrals computed using PRISM.
 The smallest eigenvalue of the overlap matrix is  2.788D-05
 Initial guess read from the read-write file:
 Initial guess orbital symmetries:
       Occupied  (A') (A') (A') (A') (A') (A') (A') (A") (A') (A')
                 (A') (A') (A') (A') (A') (A") (A') (A') (A') (A")
                 (A') (A") (A')
       Virtual   (A") (A') (A') (A') (A') (A") (A') (A") (A') (A')
                 (A") (A') (A') (A') (A") (A') (A') (A') (A') (A')
                 (A") (A") (A') (A') (A') (A') (A') (A') (A') (A")
                 (A') (A") (A') (A") (A') (A") (A') (A') (A') (A")
                 (A') (A') (A") (A') (A') (A') (A") (A') (A') (A')
                 (A") (A') (A") (A') (A') (A") (A') (A") (A') (A')
                 (A') (A") (A') (A') (A") (A') (A') (A') (A') (A')
                 (A') (A') (A') (A") (A') (A') (A") (A") (A') (A')
                 (A') (A") (A') (A') (A') (A") (A") (A') (A') (A')
                 (A') (A') (A') (A") (A") (A') (A') (A') (A") (A')
                 (A') (A") (A') (A') (A") (A') (A') (A') (A") (A')
```

```
                (A")  (A')  (A')  (A")  (A')  (A')  (A')  (A")  (A')  (A")
                (A')  (A')  (A")  (A')  (A')  (A')  (A")  (A')  (A")  (A')
                (A')  (A')  (A')  (A')  (A")  (A')  (A')  (A')  (A')  (A')
Requested convergence on RMS density matrix=1.00D-08 within  64 cycles.
Requested convergence on MAX density matrix=1.00D-06.
SCF Done:  E(RB+HF-LYP) =  -667.646611884     A.U. after    7 cycles
             Convg  =    0.7921D-08             -V/T =  2.0027
             S**2   =    0.0000
***** Axes restored to original set *****
-------------------------------------------------------------------
Center     Atomic                     Forces (Hartrees/Bohr)
Number     Number              X              Y              Z
-------------------------------------------------------------------
   1          6          -0.000005100   -0.000002526    0.000000000
   2          6           0.000005654   -0.000001290    0.000000000
   3          7          -0.000007364    0.000005934    0.000000000
   4          1          -0.000001519    0.000000859    0.000000000
   5          1           0.000007446   -0.000006699    0.000000000
   6          8           0.000000804    0.000001992    0.000000000
   7         17           0.000000079    0.000001731    0.000000000
-------------------------------------------------------------------
Cartesian Forces:  Max     0.000007446 RMS     0.000003562
Internal  Forces:  Max     0.000009567 RMS     0.000003400


GradGradGradGradGradGradGradGradGradGradGradGradGradGradGradGradGradGrad
 Berny optimization.
 Search for a local minimum.
 Step number  24 out of a maximum of  26
 All quantities printed in internal units (Hartrees-Bohrs-Radians)
 Update second derivatives using information from points  8  9 10 11 12
                                                         13 14 15 16 17

                                                         18 20 21 24
 Trust test= 9.26D-01 RLast= 6.13D-03 DXMaxT set to 5.00D-02
 The second derivative matrix:
                       R1        R2        R3        R4        R5
          R1          0.28668
          R2         -0.00482   1.25292
          R3          0.00854  -0.00262   0.34664
          R4          0.00196  -0.00278   0.00032   0.00564
          R5          0.10034  -0.03057   0.02363  -0.00240   0.89858
          R6         -0.00408  -0.00309  -0.00395   0.00903  -0.00432
          A1          0.00000   0.00000   0.00000   0.00000   0.00000
          A2          0.00109  -0.00545   0.00010   0.00030   0.00018
          A3          0.01980  -0.00024  -0.00191  -0.00013  -0.03097
          A4          0.00000   0.00000   0.00000   0.00000   0.00000
          A5          0.02512   0.01179   0.00082  -0.00252  -0.02022
          A6         -0.00285   0.00188   0.00133  -0.00045   0.02000
          A7         -0.02919   0.00155  -0.01421   0.00062   0.01382
          A8          0.00000   0.00000   0.00000   0.00000   0.00000
          A9         -0.02266  -0.00930   0.00007   0.00274   0.01758
          D1          0.00000   0.00000   0.00000   0.00000   0.00000
                       R6        A1        A2        A3        A4
          R6          0.31604
          A1          0.00000   0.25000
          A2         -0.00309   0.00000   0.07070
          A3          0.00141   0.00000   0.02114   0.15119
          A4          0.00000   0.00000   0.00000   0.00000   0.16000
          A5          0.00977   0.00000  -0.00752  -0.00548   0.00000
```

```
          A6            0.00188   0.00000  -0.03097   0.00429   0.00000
          A7            0.00600   0.00000  -0.00109   0.00764   0.00000
          A8            0.00000   0.00000   0.00000   0.00000   0.00000
          A9           -0.00720   0.00000   0.01307   0.00468   0.00000
          D1            0.00000   0.00000   0.00000   0.00000   0.00000
                          A5        A6        A7        A8        A9
          A5            0.09476
          A6           -0.00045   0.24073
          A7            0.00436  -0.00747   0.16322
          A8            0.00000   0.00000   0.00000   0.25000
          A9           -0.06733   0.00196  -0.00484   0.00000   0.07692
          D1            0.00000   0.00000   0.00000   0.00000   0.00000
                          D1
          D1            0.04262
     Eigenvalues ---    0.00519   0.01734   0.04262   0.05893   0.12013
     Eigenvalues ---    0.16000   0.16503   0.22436   0.25000   0.25000
     Eigenvalues ---    0.28942   0.31680   0.34775   0.91503   1.25605
     Eigenvalues --- 1000.00000
 RFO step:  Lambda= 0.00000000D+00.
 Quartic linear search produced a step of  0.00461.
 Iteration  1 RMS(Cart)=  0.00002918 RMS(Int)=  0.00000000
 Iteration  2 RMS(Cart)=  0.00000000 RMS(Int)=  0.00000000
 TrRot=  0.000000  0.000000  0.000000  0.000000  0.000000  0.000000
 Variable       Old X    -DE/DX   Delta X   Delta X   Delta X     New X
                                  (Linear)    (Quad)   (Total)
    R1         2.78916   0.00000   0.00000   0.00000   0.00000   2.78917
    R2         2.17175   0.00000   0.00000   0.00000   0.00000   2.17175
    R3         2.07731   0.00000   0.00000   0.00000   0.00000   2.07731
    R4         3.99274   0.00000   0.00003  -0.00006  -0.00003   3.99272
    R5         2.26390   0.00000   0.00000   0.00000   0.00000   2.26390
    R6         2.43831   0.00000   0.00000   0.00000   0.00000   2.43831
    A1         3.14159   0.00000   0.00000   0.00000   0.00000   3.14159
    A2         3.17535   0.00000   0.00000   0.00001   0.00001   3.17536
    A3         1.99509   0.00000   0.00000   0.00000   0.00000   1.99508
    A4         3.14159   0.00000   0.00000   0.00000   0.00000   3.14159
    A5         3.15320  -0.00001   0.00000  -0.00006  -0.00006   3.15314
    A6         2.12948   0.00000   0.00000   0.00000   0.00000   2.12949
    A7         2.15861   0.00000   0.00000   0.00000   0.00000   2.15861
    A8         3.14159   0.00000   0.00000   0.00000   0.00000   3.14159
    A9         3.16522   0.00001   0.00000   0.00006   0.00006   3.16528
    D1         3.14159   0.00000   0.00000   0.00000   0.00000   3.14159
         Item               Value     Threshold  Converged?
 Maximum Force            0.000010     0.000450     YES
 RMS     Force            0.000003     0.000300     YES
 Maximum Displacement     0.000073     0.001800     YES
 RMS     Displacement     0.000029     0.001200     YES
 Predicted change in Energy=-5.592960D-10
 Optimization completed.
    -- Stationary point found.
                          ----------------------------
                          !   Optimized Parameters   !
                          ! (Angstroms and Degrees)  !
 --------------------------                          --------------------
------
 ! Name  Definition              Value          Derivative Info.
!
 ---------------------------------------------------------------------------
------
 ! R1    R(2,1)                  1.476          -DE/DX =    0.
!
```

```
 ! R2    R(3,2)                  1.1492          -DE/DX =    0.
!
 ! R3    R(4,1)                  1.0993          -DE/DX =    0.
!
 ! R4    R(5,3)                  2.1129          -DE/DX =    0.
!
 ! R5    R(6,1)                  1.198           -DE/DX =    0.
!
 ! R6    R(7,5)                  1.2903          -DE/DX =    0.
!
 ! A1    L(1,2,3)              180.              -DE/DX =    0.
!
 ! A2    L(1,2,3)              181.9341          -DE/DX =    0.
!
 ! A3    A(2,1,4)              114.3101          -DE/DX =    0.
!
 ! A4    L(2,3,5)              180.              -DE/DX =    0.
!
 ! A5    L(2,3,5)              180.6651          -DE/DX =    0.
!
 ! A6    A(2,1,6)              122.0104          -DE/DX =    0.
!
 ! A7    A(4,1,6)              123.6795          -DE/DX =    0.
!
 ! A8    L(3,5,7)              180.              -DE/DX =    0.
!
 ! A9    L(3,5,7)              181.3535          -DE/DX =    0.
!
 ! D1    D(2,6,1,4)            180.              -DE/DX =    0.
!
 ---------------------------------------------------------------------
------

GradGradGradGradGradGradGradGradGradGradGradGradGradGradGradGradGradGrad

                    Input orientation:
 ---------------------------------------------------------------------
 Center     Atomic                   Coordinates (Angstroms)
 Number     Number                X           Y           Z
 ---------------------------------------------------------------------
    1          6             1.353661    2.452162    0.000000
    2          6             0.611269    1.176498    0.000000
    3          7             0.000022    0.203293    0.000000
    4          1             0.715439    3.347181    0.000000
    5          1            -1.144445   -1.572774    0.000000
    6          8             2.551066    2.490055    0.000000
    7         17            -1.868780   -2.640580    0.000000
 ---------------------------------------------------------------------
                    Distance matrix (angstroms):
                    1          2          3          4          5
  1  C     0.000000
  2  C     1.475963   0.000000
  3  N     2.624834   1.149239   0.000000
  4  H     1.099266   2.173181   3.224260   0.000000
  5  H     4.737156   3.262059   2.112869   5.259764   0.000000
  6  O     1.198005   2.342700   3.425946   2.025881   5.492120
  7  Cl    6.026620   4.552002   3.402944   6.521615   1.290299
                    6          7
  6  O     0.000000
  7  Cl    6.771887   0.000000
```

```
Stoichiometry    C2H2ClNO
Framework group  CS[SG(C2H2ClNO)]
Deg. of freedom   11
Full point group                 CS      NOp   2
Largest Abelian subgroup         CS      NOp   2
Largest concise Abelian subgroup C1      NOp   1
                  Standard orientation:
---------------------------------------------------------------------
Center     Atomic                   Coordinates (Angstroms)
Number     Number                X           Y           Z
---------------------------------------------------------------------
   1          6             1.353396    2.452309    0.000000
   2          6             0.611142    1.176564    0.000000
   3          7             0.000000    0.203293    0.000000
   4          1             0.715077    3.347258    0.000000
   5          1            -1.144275   -1.572897    0.000000
   6          8             2.550797    2.490331    0.000000
   7         17            -1.868494   -2.640782    0.000000
---------------------------------------------------------------------
 Rotational constants (GHZ):      52.1063746      0.7316603
0.7215288
 Isotopes: C-12,C-12,N-14,H-1,H-1,O-16,Cl-35
 Standard basis: 6-311++G(2d,2p) (5D, 7F)
 There are   117 symmetry adapted basis functions of A'  symmetry.
 There are    46 symmetry adapted basis functions of A"  symmetry.
 Crude estimate of integral set expansion from redundant
integrals=1.000.
 Integral buffers will be    131072 words long.
 Raffenetti 2 integral format.
 Two-electron integral symmetry is turned on.
   163 basis functions      241 primitive gaussians
    23 alpha electrons       23 beta electrons
       nuclear repulsion energy       151.5624690340 Hartrees.

 ***********************************************************************

            Population analysis using the SCF density.

 ***********************************************************************

 Orbital Symmetries:
       Occupied  (A') (A') (A') (A') (A') (A') (A") (A') (A')
                 (A') (A') (A') (A') (A') (A") (A') (A') (A') (A")
                 (A') (A") (A')
       Virtual   (A") (A') (A') (A') (A') (A") (A') (A") (A') (A')
                 (A") (A') (A') (A') (A") (A') (A') (A') (A') (A')
                 (A") (A") (A') (A') (A') (A') (A') (A') (A') (A")
                 (A') (A") (A') (A") (A') (A") (A') (A') (A') (A")
                 (A') (A') (A") (A') (A') (A') (A") (A') (A') (A')
                 (A") (A') (A") (A') (A') (A") (A') (A") (A') (A')
                 (A') (A") (A') (A') (A") (A') (A") (A') (A') (A')
                 (A') (A') (A') (A") (A') (A') (A") (A") (A') (A')
                 (A') (A") (A') (A') (A') (A") (A") (A') (A') (A')
                 (A') (A') (A') (A") (A") (A') (A') (A") (A") (A')
                 (A') (A") (A') (A') (A") (A') (A') (A') (A") (A')
                 (A") (A') (A') (A") (A') (A') (A') (A") (A') (A")
                 (A') (A') (A") (A') (A') (A') (A") (A') (A") (A')
                 (A') (A') (A') (A') (A") (A') (A') (A') (A') (A')
  The electronic state is 1-A'.
```

```
 Alpha  occ. eigenvalues -- -101.53725 -19.20404 -14.38512 -10.35278 -
10.27093
 Alpha  occ. eigenvalues --   -9.45270  -7.21637  -7.20781  -7.20781  -
1.13542
 Alpha  occ. eigenvalues --   -0.97753  -0.82662  -0.75858  -0.59775  -
0.52622
 Alpha  occ. eigenvalues --   -0.48535  -0.47632  -0.42369  -0.40789  -
0.40439
 Alpha  occ. eigenvalues --   -0.34511  -0.31636  -0.31634
 Alpha virt. eigenvalues --   -0.14078  -0.04160  -0.01989   0.00916
0.02840
 Alpha virt. eigenvalues --    0.03063   0.03789   0.04316   0.06254
0.06728
 Alpha virt. eigenvalues --    0.06894   0.08550   0.09360   0.10317
0.10758
 Alpha virt. eigenvalues --    0.11791   0.13637   0.15945   0.18763
0.19346
 Alpha virt. eigenvalues --    0.19538   0.20469   0.20818   0.23937
0.26279
 Alpha virt. eigenvalues --    0.27520   0.28689   0.33640   0.36373
0.40927
 Alpha virt. eigenvalues --    0.41220   0.45107   0.45373   0.47028
0.47370
 Alpha virt. eigenvalues --    0.47371   0.47442   0.48686   0.49875
0.51460
 Alpha virt. eigenvalues --    0.53970   0.56205   0.56997   0.58378
0.61143
 Alpha virt. eigenvalues --    0.66066   0.66087   0.66693   0.71722
0.73792
 Alpha virt. eigenvalues --    0.75178   0.78994   0.79394   0.87951
0.93816
 Alpha virt. eigenvalues --    0.94981   0.95246   0.95915   0.99529
1.00017
 Alpha virt. eigenvalues --    1.03528   1.03981   1.08233   1.13273
1.16745
 Alpha virt. eigenvalues --    1.17297   1.23004   1.23542   1.27994
1.39091
 Alpha virt. eigenvalues --    1.43936   1.49439   1.53097   1.59490
1.61721
 Alpha virt. eigenvalues --    1.72623   1.78601   1.93626   1.96037
2.07066
 Alpha virt. eigenvalues --    2.16276   2.25612   2.25795   2.30121
2.35375
 Alpha virt. eigenvalues --    2.35376   2.42811   2.42954   2.45547
2.47779
 Alpha virt. eigenvalues --    2.64886   2.66241   2.69845   2.75266
2.75759
 Alpha virt. eigenvalues --    2.90782   3.10200   3.12910   3.18908
3.21179
 Alpha virt. eigenvalues --    3.22914   3.25148   3.28404   3.37733
3.37843
 Alpha virt. eigenvalues --    3.46360   3.65456   3.74590   3.75723
3.76678
 Alpha virt. eigenvalues --    3.86169   3.92975   3.99262   3.99308
4.11152
 Alpha virt. eigenvalues --    4.21438   4.68321   4.73862   4.74263
4.94669
 Alpha virt. eigenvalues --    4.99536   5.04987   5.06386   5.20256
5.62648
```

```
 Alpha virt. eigenvalues --    5.94385   6.72658   6.76873   6.92442
7.12389
 Alpha virt. eigenvalues --    7.16103   9.84513  23.97399  24.13761
25.79094
 Alpha virt. eigenvalues --   25.79833  26.86718  35.74920  49.89876
215.83953
          Condensed to atoms (all electrons):
               1          2          3          4          5          6
  1  C    5.488700  -0.785240   0.265202   0.433448   0.011637
0.474541
  2  C   -0.785240   6.921118  -0.021772  -0.118907  -0.006817  -
0.146834
  3  N    0.265202  -0.021772   6.835858   0.014805  -0.003789
0.022439
  4  H    0.433448  -0.118907   0.014805   0.594341   0.000768  -
0.043134
  5  H    0.011637  -0.006817  -0.003789   0.000768   0.480519
0.000895
  6  O    0.474541  -0.146834   0.022439  -0.043134   0.000895
7.957487
  7  Cl  -0.005889  -0.010403   0.038671  -0.000100   0.263394  -
0.000055
               7
  1  C   -0.005889
  2  C   -0.010403
  3  N    0.038671
  4  H   -0.000100
  5  H    0.263394
  6  O   -0.000055
  7  Cl  16.956255
 Total atomic charges:
               1
  1  C    0.117601
  2  C    0.168855
  3  N   -0.151414
  4  H    0.118779
  5  H    0.253392
  6  O   -0.265340
  7  Cl  -0.241873
 Sum of Mulliken charges=   0.00000
 Atomic charges with hydrogens summed into heavy atoms:
               1
  1  C    0.236379
  2  C    0.168855
  3  N   -0.151414
  4  H    0.000000
  5  H    0.000000
  6  O   -0.265340
  7  Cl   0.011519
 Sum of Mulliken charges=   0.00000
 Electronic spatial extent (au):  <R**2>=  1345.0445
 Charge=     0.0000 electrons
 Dipole moment (Debye):
    X=     0.4583    Y=     4.1926    Z=     0.0000  Tot=     4.2176
 Quadrupole moment (Debye-Ang):
   XX=   -44.5324   YY=   -33.6665   ZZ=   -35.5011
   XY=    -5.5740   XZ=     0.0000   YZ=     0.0000
 Octapole moment (Debye-Ang**2):
  XXX=   -11.7408  YYY=    31.9755  ZZZ=     0.0000  XYY=    -0.9242
  XXY=   -10.9037  XXZ=     0.0000  XZZ=     3.3655  YZZ=     3.6004
```

```
 YYZ=      0.0000  XYZ=      0.0000
Hexadecapole moment (Debye-Ang**3):
XXXX=   -668.3208 YYYY= -1016.6513 ZZZZ=    -37.5243 XXXY=   -425.1981
XXXZ=      0.0000 YYYX=   -389.8161 YYYZ=      0.0000 ZZZX=      0.0000
ZZZY=      0.0000 XXYY=   -324.0589 XXZZ=   -105.6096 YYZZ=   -184.2877
XXYZ=      0.0000 YYXZ=      0.0000 ZZXY=   -121.8771
N-N= 1.515624690340D+02 E-N=-1.882730140498D+03  KE= 6.658270457823D+02
Symmetry A'    KE= 6.135286703558D+02
Symmetry A"    KE= 5.229837542655D+01
1\1\GINC-COLUMBUS\FOpt\RB3LYP\6-311++G(2d,2p)\C2H2Cl1N1O1\WOG\31-May-1
999\0\\# B3LYP/6-311++G(2D,2P) OPT FREQ\\formyl nitrile...HCl ( CON...
HCl) opt at B3lyp/6-31G*\\0,1\C,1.3536608789,2.452162262,0.\C,0.611269
4305,1.1764975152,0.\N,0.000021977,0.203292768,0.\H,0.7154385683,3.347
1806272,0.\H,-1.1444451619,-1.5727736553,0.\O,2.5510660093,2.490055038
2,0.\Cl,-1.8687798339,-2.6405797245,0.\\Version=DEC-AXP-OSF/1-G94RevE.
3\State=1-A'\HF=-667.6466119\RMSD=7.921e-09\RMSF=3.562e-06\Dipole=0.18
04679,1.6494811,0.\PG=CS [SG(C2H2Cl1N1O1)]\\@


 THERE IS NO CURE FOR BIRTH AND DEATH SAVE TO ENJOY THE INTERVAL.

                                -- GEORGE SANTAYANA
 Job cpu time:  0 days  7 hours 30 minutes 32.7 seconds.
 File lengths (MBytes):  RWF=    34 Int=     0 D2E=     0 Chk=     3 Scr=
1
 Normal termination of Gaussian 94
 Link1:  Proceeding to internal job step number  2.
 ----------------------------------------------------------
 #N Geom=AllCheck Guess=Read RB3LYP/6-311++G(2d,2p) Freq
 ----------------------------------------------------------
 1/10=4,29=7,30=1,38=1/1,3;
 2/12=2/2;
 3/5=4,6=6,7=1212,11=2,25=1,30=1/1,2,3;
 4/5=1,7=1/1;
 5/5=2,42=-5/2;
 8/6=4,11=11,23=2/1;
 11/6=1,8=1,9=11,15=111,16=11/1,2,10;
 10/6=1/2;
 7/8=1,10=1,25=1/1,2,3,16;
 1/10=4,30=1/3;
 6/7=2,8=2,9=2,10=2,18=1,28=1/1;
 99//99;
 ----------------------------------------------------------
 formyl nitrile...HCl ( CON...HCl) opt at B3lyp/6-31G*
 ----------------------------------------------------------
 Redundant internal coordinates taken from checkpointfile:
 /tmp/g94-963.chk
    Charge = 0 Multiplicity = 1
 C,0,1.3536608789,2.452162262,0.
 C,0,0.6112694305,1.1764975152,0.
 N,0,0.000021977,0.203292768,0.
 H,0,0.7154385683,3.3471806272,0.
 H,0,-1.1444451619,-1.5727736553,0.
 O,0,2.5510660093,2.4900550382,0.
 Cl,0,-1.8687798339,-2.6405797245,0.


GradGradGradGradGradGradGradGradGradGradGradGradGradGradGradGradGradGrad
 Berny optimization.
 Initialization pass.
```

```
                          ----------------------------
                          !    Initial Parameters    !
                          ! (Angstroms and Degrees)  !
 -------------------------                            --------------------
------
 ! Name  Definition                Value          Derivative Info.
!
 ------------------------------------------------------------------------
------
 ! R1    R(2,1)                    1.476          calculate D2E/DX2
analytical!
 ! R2    R(3,2)                    1.1492         calculate D2E/DX2
analytical!
 ! R3    R(4,1)                    1.0993         calculate D2E/DX2
analytical!
 ! R4    R(5,3)                    2.1129         calculate D2E/DX2
analytical!
 ! R5    R(6,1)                    1.198          calculate D2E/DX2
analytical!
 ! R6    R(7,5)                    1.2903         calculate D2E/DX2
analytical!
 ! A1    L(1,2,3)                  180.           calculate D2E/DX2
analytical!
 ! A2    L(1,2,3)                  181.9341       calculate D2E/DX2
analytical!
 ! A3    A(2,1,4)                  114.3101       calculate D2E/DX2
analytical!
 ! A4    L(2,3,5)                  180.           calculate D2E/DX2
analytical!
 ! A5    L(2,3,5)                  180.6651       calculate D2E/DX2
analytical!
 ! A6    A(2,1,6)                  122.0104       calculate D2E/DX2
analytical!
 ! A7    A(4,1,6)                  123.6795       calculate D2E/DX2
analytical!
 ! A8    L(3,5,7)                  180.           calculate D2E/DX2
analytical!
 ! A9    L(3,5,7)                  181.3535       calculate D2E/DX2
analytical!
 ! D1    D(2,6,1,4)                180.           calculate D2E/DX2
analytical!
 ------------------------------------------------------------------------
------
 Trust Radius=3.00D-01 FncErr=1.00D-07 GrdErr=1.00D-07
 Number of steps in this run=  26 maximum allowed number of steps= 100.

GradGradGradGradGradGradGradGradGradGradGradGradGradGradGradGradGradGrad

                     Input orientation:
 ---------------------------------------------------------------------
 Center     Atomic                   Coordinates (Angstroms)
 Number     Number                X           Y           Z
 ---------------------------------------------------------------------
    1          6             1.353661    2.452162    0.000000
    2          6             0.611269    1.176498    0.000000
    3          7             0.000022    0.203293    0.000000
    4          1             0.715439    3.347181    0.000000
    5          1            -1.144445   -1.572774    0.000000
    6          8             2.551066    2.490055    0.000000
    7         17            -1.868780   -2.640580    0.000000
```

```
---------------------------------------------------------------
                    Distance matrix (angstroms):
                    1          2          3          4          5
 1  C     0.000000
 2  C     1.475963   0.000000
 3  N     2.624834   1.149239   0.000000
 4  H     1.099266   2.173181   3.224260   0.000000
 5  H     4.737156   3.262059   2.112869   5.259764   0.000000
 6  O     1.198005   2.342700   3.425946   2.025881   5.492120
 7  Cl    6.026620   4.552002   3.402944   6.521615   1.290299
                    6          7
 6  O     0.000000
 7  Cl    6.771887   0.000000
                         Interatomic angles:
      C1-C2-N3=178.0659        C2-C1-H4=114.3101        N3-C1-H4=113.4634
      N3-C2-H4=150.6155        C1-N3-H5=178.2475        C2-N3-H5=179.3349
      C2-C1-O6=122.0104        N3-C1-O6=122.8571        N3-C2-O6=156.2364
      H4-C1-O6=123.6795        C2-H4-O6= 67.7178       N3-H5-Cl7=178.6465
 Stoichiometry    C2H2ClNO
 Framework group  CS[SG(C2H2ClNO)]
 Deg. of freedom   11
 Full point group                 CS      NOp   2
 Largest Abelian subgroup         CS      NOp   2
 Largest concise Abelian subgroup C1      NOp   1
                   Standard orientation:
 ---------------------------------------------------------------
 Center     Atomic                 Coordinates (Angstroms)
 Number     Number              X           Y           Z
 ---------------------------------------------------------------
    1          6           1.353396    2.452309    0.000000
    2          6           0.611142    1.176564    0.000000
    3          7           0.000000    0.203293    0.000000
    4          1           0.715077    3.347258    0.000000
    5          1          -1.144275   -1.572897    0.000000
    6          8           2.550797    2.490331    0.000000
    7         17          -1.868494   -2.640782    0.000000
 ---------------------------------------------------------------
 Rotational constants (GHZ):     52.1063746      0.7316603
0.7215288
 Isotopes: C-12,C-12,N-14,H-1,H-1,O-16,Cl-35
 Standard basis: 6-311++G(2d,2p) (5D, 7F)
 There are   117 symmetry adapted basis functions of A'  symmetry.
 There are    46 symmetry adapted basis functions of A"  symmetry.
 Crude estimate of integral set expansion from redundant
integrals=1.000.
 Integral buffers will be    131072 words long.
 Raffenetti 2 integral format.
 Two-electron integral symmetry is turned on.
   163 basis functions      241 primitive gaussians
    23 alpha electrons       23 beta electrons
       nuclear repulsion energy       151.5624690340 Hartrees.
 One-electron integrals computed using PRISM.
 The smallest eigenvalue of the overlap matrix is  2.788D-05
 Initial guess read from the checkpoint file:
 /tmp/g94-963.chk
 Initial guess orbital symmetries:
       Occupied  (A') (A') (A') (A') (A') (A') (A') (A") (A') (A')
                 (A') (A') (A') (A') (A') (A") (A') (A') (A') (A")
                 (A') (A") (A')
       Virtual   (A") (A') (A') (A') (A') (A") (A') (A") (A') (A')
```

```
                (A")  (A')  (A')  (A')  (A")  (A')  (A')  (A')  (A')  (A')
                (A")  (A")  (A')  (A')  (A')  (A')  (A')  (A')  (A')  (A")
                (A')  (A")  (A')  (A")  (A')  (A")  (A')  (A')  (A')  (A")
                (A')  (A')  (A")  (A')  (A')  (A')  (A")  (A')  (A')  (A')
                (A")  (A')  (A")  (A')  (A')  (A")  (A')  (A")  (A')  (A')
                (A')  (A")  (A')  (A')  (A")  (A')  (A")  (A')  (A')  (A')
                (A')  (A')  (A')  (A")  (A')  (A')  (A")  (A")  (A')  (A')
                (A')  (A")  (A')  (A')  (A')  (A")  (A")  (A')  (A')  (A')
                (A')  (A')  (A')  (A")  (A")  (A')  (A')  (A")  (A")  (A')
                (A')  (A")  (A')  (A')  (A")  (A')  (A')  (A')  (A")  (A')
                (A")  (A')  (A')  (A")  (A')  (A')  (A')  (A")  (A')  (A")
                (A')  (A')  (A")  (A')  (A')  (A')  (A")  (A')  (A")  (A')
                (A')  (A')  (A')  (A')  (A")  (A')  (A')  (A')  (A')  (A')
 Requested convergence on RMS density matrix=1.00D-08 within  64 cycles.
 Requested convergence on MAX density matrix=1.00D-06.
 SCF Done:  E(RB+HF-LYP) =  -667.646611884     A.U. after    1 cycles
             Convg  =    0.2731D-08             -V/T =  2.0027
             S**2   =    0.0000
 Range of M.O.s used for correlation:     1   163
 NBasis=   163 NAE=    23 NBE=    23 NFC=     0 NFV=     0
 NROrb=    163 NOA=    23 NOB=    23 NVA=   140 NVB=   140

 **** Warning!!: The largest alpha MO coefficient is  0.68324089D+02

 G2DrvN: can do   7 atoms at a time, so will make   1 passes doing
MaxLOS=2.
 FoFDir used for L=0 through L=2.
          Differentiating once with respect to electric field.
                with respect to dipole field.
          Differentiating once with respect to nuclear coordinates.
 Integrals replicated using symmetry in FoFDir.
 MinBra= 0 MaxBra= 2 MinRaf= 0 MaxRaf= 2.
 IRaf=       0 NMat=  24 IRICut=      24 DoRegI=T DoRafI=T ISym2E= 2
JSym2E=2.
          There are  24 degrees of freedom in the 1st order CPHF.
  21 vectors were produced by pass  0.
 AX will form  21 AO Fock derivatives at one time.
  21 vectors were produced by pass  1.
  21 vectors were produced by pass  2.
  21 vectors were produced by pass  3.
  21 vectors were produced by pass  4.
  18 vectors were produced by pass  5.
   7 vectors were produced by pass  6.
   2 vectors were produced by pass  7.
 Inv2:  IOpt= 1 Iter= 1 AM= 1.26D-15 Conv= 1.00D-12.
 Inverted reduced A of dimension 132 with in-core refinement.
 Full mass-weighted force constant matrix:
 Low frequencies ---  -15.9036  -11.5040   -9.1718   -0.0033   -0.0020
0.0028
 Low frequencies ---   19.7755   22.2348   87.1175
 Harmonic frequencies (cm**-1), IR intensities (KM/Mole),
 Raman scattering activities (A**4/AMU), Raman depolarization ratios,
 reduced masses (AMU), force constants (mDyne/A) and normal coordinates:
                      1                      2                      3
                     A'                     A"                     A'
 Frequencies --    18.7230               20.2574               87.1174
 Red. masses --    10.7691                5.4608               14.0695
 Frc consts  --     0.0022                0.0013                0.0629
 IR Inten    --     1.4338                3.5914                3.3310
 Raman Activ --     0.0000                0.0000                0.0000
```

Depolar	--	0.0000			0.0000				0.0000
Atom	AN	X	Y	Z	X	Y	Z	X	Y
Z									
1	6	-0.13	0.01	0.00	0.00	0.00	-0.26	0.21	0.25
0.00									
2	6	0.24	-0.21	0.00	0.00	0.00	0.17	0.17	0.26
0.00									
3	7	0.50	-0.38	0.00	0.00	0.00	0.47	0.10	0.30
0.00									
4	1	-0.40	-0.18	0.00	0.00	0.00	-0.75	0.22	0.26
0.00									
5	1	0.26	-0.22	0.00	0.00	0.00	0.32	-0.32	-0.37
0.00									
6	8	-0.14	0.36	0.00	0.00	0.00	-0.08	0.21	0.25
0.00									
7	17	-0.17	0.07	0.00	0.00	0.00	-0.11	-0.26	-0.40
0.00									

			4			5			6
			A'			A"			A'
Frequencies	--		227.8679			295.0476			382.4409
Red. masses	--		6.8818			3.6303			1.0754
Frc consts	--		0.2105			0.1862			0.0927
IR Inten	--		6.9400			0.2672			31.6452
Raman Activ	--		0.0000			0.0000			0.0000
Depolar	--		0.0000			0.0000			0.0000
Atom	AN	X	Y	Z	X	Y	Z	X	Y
Z									
1	6	-0.08	0.19	0.00	0.00	0.00	-0.06	0.01	-0.01
0.00									
2	6	-0.28	0.33	0.00	0.00	0.00	0.43	0.01	-0.01
0.00									
3	7	0.37	-0.08	0.00	0.00	0.00	-0.20	-0.06	0.03
0.00									
4	1	0.26	0.43	0.00	0.00	0.00	-0.63	0.00	-0.02
0.00									
5	1	0.43	-0.31	0.00	0.00	0.00	-0.61	0.83	-0.56
0.00									
6	8	-0.06	-0.31	0.00	0.00	0.00	-0.05	0.01	0.02
0.00									
7	17	-0.02	-0.01	0.00	0.00	0.00	0.01	-0.01	0.01
0.00									

			7			8			9
			A"			A'			A'
Frequencies	--		387.2119			619.8487			910.1334
Red. masses	--		1.1518			11.4738			6.4230
Frc consts	--		0.1017			2.5973			3.1347
IR Inten	--		30.5637			3.9450			134.1310
Raman Activ	--		0.0000			0.0000			0.0000
Depolar	--		0.0000			0.0000			0.0000
Atom	AN	X	Y	Z	X	Y	Z	X	Y
Z									
1	6	0.00	0.00	0.00	-0.30	-0.02	0.00	0.03	0.56
0.00									
2	6	0.00	0.00	0.06	0.63	-0.01	0.00	0.13	-0.27
0.00									
3	7	0.00	0.00	-0.08	0.10	0.40	0.00	-0.16	-0.18
0.00									
4	1	0.00	0.00	-0.07	-0.38	-0.06	0.00	0.21	0.69
0.00									

5	1	0.00	0.00	0.99	0.04	-0.04	0.00	0.01	0.01	0.00
6	8	0.00	0.00	-0.01	-0.31	-0.32	0.00	0.01	-0.11	0.00
7	17	0.00	0.00	-0.01	0.00	0.00	0.00	0.00	0.00	0.00

	10	11	12
	A"	A'	A'
Frequencies --	1000.8866	1408.9137	1778.2450
Red. masses --	1.7485	1.1594	10.3547
Frc consts --	1.0320	1.3560	19.2918
IR Inten --	0.2897	10.3417	165.2264
Raman Activ --	0.0000	0.0000	0.0000
Depolar --	0.0000	0.0000	0.0000

Atom	AN	X	Y	Z	X	Y	Z	X	Y	Z
1	6	0.00	0.00	0.23	-0.02	-0.08	0.00	0.70	0.05	0.00
2	6	0.00	0.00	-0.09	0.02	-0.02	0.00	-0.03	0.01	0.00
3	7	0.00	0.00	0.01	0.00	0.00	0.00	0.02	0.01	0.00
4	1	0.00	0.00	-0.97	0.85	0.51	0.00	-0.02	-0.50	0.00
5	1	0.00	0.00	0.00	0.00	0.00	0.00	0.01	0.01	0.00
6	8	0.00	0.00	-0.06	-0.06	0.04	0.00	-0.51	-0.02	0.00
7	17	0.00	0.00	0.00	0.00	0.00	0.00	0.00	0.00	0.00

	13	14	15
	A'	A'	A'
Frequencies --	2335.7135	2790.2385	2997.8152
Red. masses --	12.5928	1.0371	1.0882
Frc consts --	40.4773	4.7574	5.7617
IR Inten --	26.6252	599.3244	25.8265
Raman Activ --	0.0000	0.0000	0.0000
Depolar --	0.0000	0.0000	0.0000

Atom	AN	X	Y	Z	X	Y	Z	X	Y	Z
1	6	0.00	-0.07	0.00	0.00	0.00	0.00	0.05	-0.07	0.00
2	6	0.41	0.67	0.00	0.00	0.01	0.00	0.00	0.00	0.00
3	7	-0.32	-0.51	0.00	0.00	0.00	0.00	0.00	0.00	0.00
4	1	-0.02	-0.07	0.00	0.01	-0.01	0.00	-0.56	0.82	0.00
5	1	-0.05	-0.07	0.00	0.56	0.83	0.00	0.00	0.01	0.00
6	8	-0.03	0.00	0.00	0.00	0.00	0.00	0.00	0.00	0.00
7	17	0.00	0.00	0.00	-0.02	-0.02	0.00	0.00	0.00	0.00

```
 -------------------
 - Thermochemistry -
 -------------------
 Temperature   298.150 Kelvin.  Pressure   1.00000 Atm.
 Atom  1 has atomic number  6 and mass  12.00000
```

```
Atom  2 has atomic number  6 and mass  12.00000
Atom  3 has atomic number  7 and mass  14.00307
Atom  4 has atomic number  1 and mass   1.00783
Atom  5 has atomic number  1 and mass   1.00783
Atom  6 has atomic number  8 and mass  15.99491
Atom  7 has atomic number 17 and mass  34.96885
Molecular mass:    90.98249 amu.
Principal axes and moments of inertia in atomic units:
                          1         2         3
    EIGENVALUES --    34.63571  466.63816  2501.27387
          X            0.59947   0.80040   0.00000
          Y            0.80040  -0.59947   0.00000
          Z            0.00000   0.00000   1.00000
THIS MOLECULE IS AN ASYMMETRIC TOP.
ROTATIONAL SYMMETRY NUMBER  1.
ROTATIONAL TEMPERATURES (KELVIN)       2.50070      0.03511      0.03463
ROTATIONAL CONSTANTS (GHZ)            52.10637      0.73166      0.72153
Zero-point vibrational energy      91277.8 (Joules/Mol)
                                   21.81593 (Kcal/Mol)
WARNING-- EXPLICIT CONSIDERATION OF   8 DEGREES OF FREEDOM AS
          VIBRATIONS MAY CAUSE SIGNIFICANT ERROR
VIBRATIONAL TEMPERATURES:     26.94    29.15   125.34   327.85   424.51
          (KELVIN)           550.24   557.11   891.82  1309.47  1440.04
                            2027.10  2558.48  3360.55  4014.51  4313.16

 Zero-point correction=                           0.034766
(Hartree/Particle)
 Thermal correction to Energy=                    0.041999
 Thermal correction to Enthalpy=                  0.042944
 Thermal correction to Gibbs Free Energy=         0.000447
 Sum of electronic and zero-point Energies=          -667.611846
 Sum of electronic and thermal Energies=             -667.604612
 Sum of electronic and thermal Enthalpies=           -667.603668
 Sum of electronic and thermal Free Energies=        -667.646165

                     E (Thermal)             CV                S
                      KCAL/MOL        CAL/MOL-KELVIN    CAL/MOL-KELVIN
TOTAL                    26.355            20.365            89.441
ELECTRONIC                0.000             0.000             0.000
TRANSLATIONAL             0.889             2.981            39.437
ROTATIONAL                0.889             2.981            26.860
VIBRATIONAL              24.578            14.403            23.144
VIBRATION  1              0.593             1.986             6.765
VIBRATION  2              0.593             1.986             6.609
VIBRATION  3              0.601             1.958             3.724
VIBRATION  4              0.651             1.799             1.896
VIBRATION  5              0.689             1.683             1.445
VIBRATION  6              0.752             1.508             1.030
VIBRATION  7              0.756             1.498             1.011
VIBRATION  8              0.980             0.990             0.417
                              Q            LOG10(Q)           LN(Q)
TOTAL BOT          0.622681D+00          -0.205734         -7.459109
TOTAL V=0          0.610039D+16          15.785357         29.361741
VIB (BOT)          0.110312D-12         -12.957376        -29.835462
VIB (BOT)  1       0.110642D+02           1.043922          2.403718
VIB (BOT)  2       0.102255D+02           1.009686          2.324889
VIB (BOT)  3       0.236127D+01           0.373145          0.859199
VIB (BOT)  4       0.865161D+00          -0.062903         -0.144840
VIB (BOT)  5       0.646352D+00          -0.189531         -0.436412
VIB (BOT)  6       0.471962D+00          -0.326093         -0.750857
```

VIB (BOT)	7	0.464577D+00	-0.332943	-0.766629
VIB (BOT)	8	0.235969D+00	-0.627145	-1.444054
VIB (V=0)		0.108073D+04	3.033715	6.985388
VIB (V=0)	1	0.115755D+02	1.063541	2.448893
VIB (V=0)	2	0.107378D+02	1.030914	2.373766
VIB (V=0)	3	0.291363D+01	0.464434	1.069398
VIB (V=0)	4	0.149925D+01	0.175874	0.404966
VIB (V=0)	5	0.131717D+01	0.119643	0.275487
VIB (V=0)	6	0.118757D+01	0.074658	0.171906
VIB (V=0)	7	0.118252D+01	0.072808	0.167646
VIB (V=0)	8	0.105288D+01	0.022381	0.051534
ELECTRONIC		0.100000D+01	0.000000	0.000000
TRANSLATIONAL		0.341112D+08	7.532897	17.345137
ROTATIONAL		0.165480D+06	5.218745	12.016604

***** Axes restored to original set *****

Center Number	Atomic Number	Forces (Hartrees/Bohr) X	Y	Z
1	6	-0.000005076	-0.000002531	0.000000000
2	6	0.000005657	-0.000001306	0.000000000
3	7	-0.000007380	0.000005942	0.000000000
4	1	-0.000001526	0.000000865	0.000000000
5	1	0.000007434	-0.000006706	0.000000000
6	8	0.000000797	0.000001997	0.000000000
7	17	0.000000093	0.000001739	0.000000000

Cartesian Forces: Max 0.000007434 RMS 0.000003563
Internal Forces: Max 0.000009593 RMS 0.000003402

GradGradGradGradGradGradGradGradGradGradGradGradGradGradGradGradGrad
Berny optimization.
Search for a local minimum.
Step number 1 out of a maximum of 26
All quantities printed in internal units (Hartrees-Bohrs-Radians)
Second derivative matrix not updated -- analytic derivatives used.
The second derivative matrix:

	R1	R2	R3	R4	R5
R1	0.26326				
R2	0.00500	1.24929			
R3	0.01377	0.00001	0.31826		
R4	0.00090	-0.00263	-0.00012	0.00637	
R5	0.08730	-0.00554	0.03084	-0.00102	0.87258
R6	-0.00107	0.00304	0.00013	0.00844	0.00114
A1	0.00000	0.00000	0.00000	0.00000	0.00000
A2	0.00227	-0.00201	-0.00036	0.00002	-0.00511
A3	0.01419	0.00263	0.00851	0.00012	-0.03993
A4	0.00000	0.00000	0.00000	0.00000	0.00000
A5	-0.00004	0.00016	-0.00002	0.00015	-0.00015
A6	0.01252	0.00051	-0.00969	-0.00073	0.02511
A7	-0.02671	-0.00313	0.00118	0.00061	0.01482
A8	0.00000	0.00000	0.00000	0.00000	0.00000
A9	0.00008	0.00004	-0.00004	-0.00016	-0.00011
D1	0.00000	0.00000	0.00000	0.00000	0.00000

	R6	A1	A2	A3	A4
R6	0.29894				
A1	0.00000	0.05227			
A2	0.00000	0.00000	0.06436		
A3	-0.00012	0.00000	0.02112	0.09672	

```
             A4            0.00000   0.00107   0.00000   0.00000   0.00549
             A5           -0.00006   0.00000   0.00117   0.00054   0.00000
             A6            0.00075   0.00000  -0.02605  -0.05640   0.00000
             A7           -0.00063   0.00000   0.00493  -0.04032   0.00000
             A8            0.00000  -0.00224   0.00000   0.00000  -0.00550
             A9           -0.00028   0.00000  -0.00212   0.00000   0.00000
             D1            0.00000  -0.00808   0.00000   0.00000  -0.00034
                             A5         A6        A7        A8        A9
             A5            0.00470
             A6           -0.00059   0.13084
             A7            0.00005  -0.07445   0.11477
             A8            0.00000   0.00000   0.00000   0.00678
             A9           -0.00474   0.00014  -0.00014   0.00000   0.00760
             D1            0.00000   0.00000   0.00000  -0.00007   0.00000
                             D1
             D1            0.06241
     Eigenvalues ---       0.00059   0.00118   0.00610   0.01100   0.01153
     Eigenvalues ---       0.04792   0.05461   0.06691   0.13473   0.19900
     Eigenvalues ---       0.26325   0.29920   0.31953   0.88964   1.24943
     Eigenvalues --- 1000.00000
 Angle between quadratic step and forces=  52.26 degrees.
 Linear search not attempted -- first point.
 Iteration  1 RMS(Cart)=  0.00196099 RMS(Int)=  0.00000132
 Iteration  2 RMS(Cart)=  0.00000238 RMS(Int)=  0.00000000
 TrRot=  0.000000  0.000000  0.000000  0.000000  0.000000  0.000000
 Variable       Old X    -DE/DX   Delta X   Delta X   Delta X     New X
                                  (Linear)    (Quad)   (Total)
    R1         2.78916   0.00000   0.00000  -0.00001  -0.00001   2.78915
    R2         2.17175   0.00000   0.00000   0.00000   0.00000   2.17175
    R3         2.07731   0.00000   0.00000   0.00000   0.00000   2.07731
    R4         3.99274   0.00000   0.00000   0.00008   0.00008   3.99283
    R5         2.26390   0.00000   0.00000   0.00000   0.00000   2.26390
    R6         2.43831   0.00000   0.00000  -0.00001  -0.00001   2.43830
    A1         3.14159   0.00000   0.00000   0.00000   0.00000   3.14159
    A2         3.17535   0.00000   0.00000   0.00006   0.00006   3.17541
    A3         1.99509   0.00000   0.00000   0.00000   0.00000   1.99509
    A4         3.14159   0.00000   0.00000   0.00000   0.00000   3.14159
    A5         3.15320  -0.00001   0.00000  -0.00241  -0.00241   3.15079
    A6         2.12948   0.00000   0.00000   0.00000   0.00000   2.12949
    A7         2.15861   0.00000   0.00000  -0.00001  -0.00001   2.15861
    A8         3.14159   0.00000   0.00000   0.00000   0.00000   3.14159
    A9         3.16522   0.00001   0.00000  -0.00035  -0.00035   3.16487
    D1         3.14159   0.00000   0.00000   0.00000   0.00000   3.14159
         Item               Value     Threshold  Converged?
 Maximum Force            0.000010     0.000450     YES
 RMS     Force            0.000003     0.000300     YES
 Maximum Displacement     0.004277     0.001800     NO
 RMS     Displacement     0.001961     0.001200     NO
 Predicted change in Energy=-1.016359D-08

GradGradGradGradGradGradGradGradGradGradGradGradGradGradGradGradGrad

 ***********************************************************************

            Population analysis using the SCF density.

 ***********************************************************************

 Orbital Symmetries:
```

```
      Occupied  (A') (A') (A') (A') (A') (A') (A') (A") (A') (A')
                (A') (A') (A') (A') (A') (A") (A') (A') (A') (A")
                (A') (A") (A')
      Virtual   (A") (A') (A') (A') (A') (A") (A') (A") (A') (A')
                (A") (A') (A') (A') (A") (A') (A') (A') (A') (A')
                (A") (A") (A') (A') (A') (A') (A') (A') (A') (A")
                (A') (A") (A') (A") (A') (A") (A') (A') (A') (A")
                (A') (A') (A") (A') (A') (A') (A") (A') (A') (A')
                (A") (A') (A") (A') (A') (A") (A') (A") (A') (A')
                (A') (A") (A') (A') (A") (A') (A") (A') (A') (A')
                (A') (A') (A') (A") (A') (A') (A") (A") (A') (A')
                (A') (A") (A') (A') (A') (A") (A") (A') (A') (A')
                (A') (A') (A') (A") (A") (A') (A') (A") (A") (A')
                (A') (A") (A') (A') (A") (A') (A') (A') (A") (A')
                (A") (A') (A') (A") (A') (A') (A') (A") (A') (A")
                (A') (A') (A") (A') (A') (A') (A") (A') (A") (A')
                (A') (A') (A') (A') (A") (A') (A') (A') (A') (A')
 The electronic state is 1-A'.
 Alpha  occ. eigenvalues -- -101.53725 -19.20404 -14.38512 -10.35278 -
10.27093
 Alpha  occ. eigenvalues --   -9.45270  -7.21637  -7.20781  -7.20781  -
1.13542
 Alpha  occ. eigenvalues --   -0.97753  -0.82662  -0.75858  -0.59775  -
0.52622
 Alpha  occ. eigenvalues --   -0.48535  -0.47632  -0.42369  -0.40789  -
0.40439
 Alpha  occ. eigenvalues --   -0.34511  -0.31636  -0.31634
 Alpha virt. eigenvalues --   -0.14078  -0.04160  -0.01989   0.00916
0.02840
 Alpha virt. eigenvalues --    0.03063   0.03789   0.04316   0.06254
0.06728
 Alpha virt. eigenvalues --    0.06894   0.08550   0.09360   0.10317
0.10758
 Alpha virt. eigenvalues --    0.11791   0.13637   0.15945   0.18763
0.19346
 Alpha virt. eigenvalues --    0.19538   0.20469   0.20818   0.23937
0.26279
 Alpha virt. eigenvalues --    0.27520   0.28689   0.33640   0.36373
0.40927
 Alpha virt. eigenvalues --    0.41220   0.45107   0.45373   0.47028
0.47370
 Alpha virt. eigenvalues --    0.47371   0.47442   0.48686   0.49875
0.51460
 Alpha virt. eigenvalues --    0.53970   0.56205   0.56997   0.58378
0.61143
 Alpha virt. eigenvalues --    0.66066   0.66087   0.66693   0.71722
0.73792
 Alpha virt. eigenvalues --    0.75178   0.78994   0.79394   0.87951
0.93816
 Alpha virt. eigenvalues --    0.94981   0.95246   0.95915   0.99529
1.00017
 Alpha virt. eigenvalues --    1.03528   1.03981   1.08233   1.13273
1.16745
 Alpha virt. eigenvalues --    1.17297   1.23004   1.23542   1.27994
1.39091
 Alpha virt. eigenvalues --    1.43936   1.49439   1.53097   1.59490
1.61721
 Alpha virt. eigenvalues --    1.72623   1.78601   1.93626   1.96037
2.07066
```

```
 Alpha virt. eigenvalues --    2.16276   2.25612   2.25795   2.30121
2.35375
 Alpha virt. eigenvalues --    2.35376   2.42811   2.42954   2.45547
2.47779
 Alpha virt. eigenvalues --    2.64886   2.66241   2.69845   2.75266
2.75759
 Alpha virt. eigenvalues --    2.90782   3.10200   3.12910   3.18908
3.21179
 Alpha virt. eigenvalues --    3.22914   3.25148   3.28404   3.37733
3.37843
 Alpha virt. eigenvalues --    3.46360   3.65456   3.74590   3.75723
3.76678
 Alpha virt. eigenvalues --    3.86169   3.92975   3.99262   3.99308
4.11152
 Alpha virt. eigenvalues --    4.21438   4.68321   4.73862   4.74263
4.94669
 Alpha virt. eigenvalues --    4.99536   5.04987   5.06386   5.20256
5.62648
 Alpha virt. eigenvalues --    5.94385   6.72658   6.76873   6.92442
7.12389
 Alpha virt. eigenvalues --    7.16103   9.84513  23.97399  24.13761
25.79094
 Alpha virt. eigenvalues --   25.79833  26.86718  35.74920  49.89876
215.83953
          Condensed to atoms (all electrons):
               1         2         3         4         5          6
  1  C    5.488701  -0.785240   0.265202   0.433448   0.011637
0.474541
  2  C   -0.785240   6.921117  -0.021772  -0.118907  -0.006817  -
0.146834
  3  N    0.265202  -0.021772   6.835858   0.014805  -0.003789
0.022439
  4  H    0.433448  -0.118907   0.014805   0.594341   0.000768  -
0.043134
  5  H    0.011637  -0.006817  -0.003789   0.000768   0.480519
0.000895
  6  O    0.474541  -0.146834   0.022439  -0.043134   0.000895
7.957487
  7  Cl  -0.005888  -0.010403   0.038671  -0.000100   0.263394  -
0.000055
               7
  1  C   -0.005888
  2  C   -0.010403
  3  N    0.038671
  4  H   -0.000100
  5  H    0.263394
  6  O   -0.000055
  7  Cl  16.956255
 Total atomic charges:
               1
  1  C    0.117601
  2  C    0.168855
  3  N   -0.151414
  4  H    0.118779
  5  H    0.253392
  6  O   -0.265339
  7  Cl  -0.241873
 Sum of Mulliken charges=   0.00000
 Atomic charges with hydrogens summed into heavy atoms:
               1
```

```
 1  C     0.236379
 2  C     0.168855
 3  N    -0.151414
 4  H     0.000000
 5  H     0.000000
 6  O    -0.265339
 7  Cl    0.011519
Sum of Mulliken charges=   0.00000
Electronic spatial extent (au):  <R**2>=  1345.0445
Charge=      0.0000 electrons
Dipole moment (Debye):
   X=      0.4583    Y=      4.1926    Z=      0.0000  Tot=      4.2176
Quadrupole moment (Debye-Ang):
  XX=    -44.5324   YY=    -33.6665   ZZ=    -35.5011
  XY=     -5.5740   XZ=      0.0000   YZ=      0.0000
Octapole moment (Debye-Ang**2):
 XXX=    -11.7408  YYY=     31.9755  ZZZ=      0.0000  XYY=     -0.9242
 XXY=    -10.9037  XXZ=      0.0000  XZZ=      3.3655  YZZ=      3.6004
 YYZ=      0.0000  XYZ=      0.0000
Hexadecapole moment (Debye-Ang**3):
XXXX=   -668.3207 YYYY= -1016.6514 ZZZZ=    -37.5243 XXXY=   -425.1980
XXXZ=      0.0000 YYYX=   -389.8162 YYYZ=      0.0000 ZZZX=      0.0000
ZZZY=      0.0000 XXYY=   -324.0589 XXZZ=   -105.6096 YYZZ=   -184.2877
XXYZ=      0.0000 YYXZ=      0.0000 ZZXY=   -121.8771
N-N= 1.515624690340D+02 E-N=-1.882730145640D+03  KE= 6.658270481781D+02
Symmetry A'    KE= 6.135286722777D+02
Symmetry A"    KE= 5.229837590047D+01
 Exact polarizability:  51.131  15.829  57.218   0.000   0.000  30.953
Approx polarizability:  79.266  24.119  80.055   0.000   0.000  43.767
1\1\GINC-COLUMBUS\Freq\RB3LYP\6-311++G(2d,2p)\C2H2Cl1N1O1\WOG\31-May-1
999\0\\#N GEOM=ALLCHECK GUESS=READ RB3LYP/6-311++G(2D,2P) FREQ\\formyl
 nitrile...HCl ( CON...HCl) opt at B3lyp/6-31G*\\0,1\C,1.3536608789,2.
452162262,0.\C,0.6112694305,1.1764975152,0.\N,0.000021977,0.203292768,
0.\H,0.7154385683,3.3471806272,0.\H,-1.1444451619,-1.5727736553,0.\O,2
.5510660093,2.4900550382,0.\Cl,-1.8687798339,-2.6405797245,0.\\Version
=DEC-AXP-OSF/1-G94RevE.3\State=1-A'\HF=-667.6466119\RMSD=2.731e-09\RMS
F=3.563e-06\Dipole=0.1804688,1.6494826,0.\DipoleDeriv=1.1719525,0.2974
904,0.,0.2869252,1.2102208,0.,0.,0.,0.3161547,-0.1087972,-0.2728602,0.
,-0.3975686,-0.5834844,0.,0.,0.,0.1907392,-0.2284123,-0.0001648,0.,-0.
0117107,-0.2120044,0.,0.,0.,-0.2515716,-0.0232856,0.0376026,0.,0.05056
59,-0.0655606,0.,0.,0.,0.0967836,0.3529271,0.2864732,0.,0.2960587,0.59
73009,0.,0.,0.,0.1591744,-0.8527777,-0.2106437,0.,-0.0834868,-0.520608
4,0.,0.,0.,-0.292239,-0.3116068,-0.1378975,0.,-0.1407837,-0.4258638,0.
,0.,0.,-0.2190413\Polar=51.1342016,15.829656,57.2144132,0.,0.,30.95327
11\PG=CS [SG(C2H2Cl1N1O1)]\NImag=0\\0.94268432,-0.07905513,0.51308519,
0.,0.,0.17002197,-0.06856915,-0.03253474,0.,0.49879471,0.00508225,-0.1
9477010,0.,0.62086437,1.11816350,0.,0.,-0.06802299,0.,0.,0.05204210,0.
01073691,-0.01164310,0.,-0.37514376,-0.54662177,0.,0.36811229,-0.01205
855,0.00790701,0.,-0.54703279,-0.90517413,0.,0.55994692,0.90974983,0.,
0.,0.01364434,0.,0.,-0.02231487,0.,0.,0.01502542,-0.11759770,0.1004288
6,0.,0.01283481,-0.01428828,0.,-0.00371370,-0.00046998,0.,0.14882112,0
.10322305,-0.22589332,0.,0.00728080,-0.02864021,0.,-0.00256522,-0.0005
7883,0.,-0.11729514,0.23713467,0.,0.,-0.05869293,0.,0.,0.01941682,0.,0
.,-0.00224360,0.,0.,0.02094458,-0.00100267,-0.00244148,0.,0.00223557,0
.00347111,0.,-0.00376203,0.00009052,0.,0.00009630,0.00025427,0.,0.0945
9794,-0.00272247,-0.00290895,0.,0.00276289,0.00582296,0.,0.00010879,-0
.00365906,0.,0.00023350,0.00041024,0.,0.13157017,0.19911501,0.,0.,0.00
062808,0.,0.,0.00084074,0.,0.,-0.00419960,0.,0.,-0.00005566,0.,0.,0.00
527247,-0.76685785,0.02400125,0.,-0.06899309,-0.06655956,0.,0.00419250
,0.00278381,0.,-0.04038340,0.00924673,0.,0.00110542,0.00180850,0.,0.87
```

```
149994,-0.01588879,-0.09895928,0.,-0.04982879,0.00767108,0.,0.00409535
,-0.00500664,0.,0.03149963,0.01776998,0.,0.00087335,0.00095468,0.,0.02
968551,0.07806133,0.,0.,-0.05734099,0.,0.,0.01833634,0.,0.,-0.00177863
,0.,0.,0.02061713,0.,0.,-0.00012895,0.,0.,0.02022832,0.00060614,0.0012
4436,0.,-0.00115909,-0.00194812,0.,-0.00042221,-0.00325994,0.,-0.00005
742,-0.00014448,0.,-0.09327053,-0.13376138,0.,-0.00056352,-0.00043626,
0.,0.09486662,0.00141964,0.00153945,0.,-0.00151173,-0.00307309,0.,-0.0
0332096,-0.00323818,0.,-0.00010859,-0.00020253,0.,-0.13381794,-0.19973
487,0.,-0.00096624,-0.00049115,0.,0.13830582,0.20520037,0.,0.,-0.00023
748,0.,0.,-0.00029814,0.,0.,0.00186695,0.,0.,0.00001366,0.,0.,-0.00235
707,0.,0.,0.00006679,0.,0.,0.00094529\\0.00000508,0.00000253,0.,-0.000
00566,0.00000131,0.,0.00000738,-0.00000594,0.,0.00000153,-0.00000086,0
.,-0.00000743,0.00000671,0.,-0.00000080,-0.00000200,0.,-0.00000009,-0.
00000174,0.\\\@


 I DO NOT KNOW WHAT I MAY APPEAR TO THE WORLD; BUT TO MYSELF
 I SEEM TO HAVE BEEN ONLY LIKE A BOY PLAYING ON THE SEASHORE,
 AND DIVERTING MYSELF IN NOW AND THEN FINDING A SMOOTHER PEBBLE
 OR A PRETTIER SHELL THAN ORDINARY, WHILST THE GREAT OCEAN OF
 TRUTH LAY ALL UNDISCOVERED BEFORE ME.
                                             -- NEWTON (1642-1726)
 Job cpu time:  0 days  3 hours 21 minutes 55.1 seconds.
 File lengths (MBytes):  RWF=   34 Int=    0 D2E=    0 Chk=    4 Scr=
1
 Normal termination of Gaussian 94
```

Output from Gaussian 94 inputted into Gaussian 98 for final calculated values

```
!    Initial Parameters    !
                           ! (Angstroms and Degrees)  !
 -------------------------                             -------------------
------
 ! Name  Definition              Value          Derivative Info.
!
 --------------------------------------------------------------------------
------
 ! R1    R(1,2)                  1.476          calculate D2E/DX2
analytical!
 ! R2    R(1,4)                  1.0993         calculate D2E/DX2
analytical!
 ! R3    R(1,6)                  1.198          calculate D2E/DX2
analytical!
 ! R4    R(2,3)                  1.1492         calculate D2E/DX2
analytical!
 ! R5    R(3,5)                  2.1129         calculate D2E/DX2
analytical!
 ! R6    R(5,7)                  1.2903         calculate D2E/DX2
analytical!
 ! A1    A(2,1,4)              114.3101         calculate D2E/DX2
analytical!
 ! A2    A(2,1,6)              122.0104         calculate D2E/DX2
analytical!
 ! A3    A(4,1,6)              123.6795         calculate D2E/DX2
analytical!
 ! A4    L(2,3,5,-3,-1)        180.6651         calculate D2E/DX2
analytical!
 ! A5    L(3,5,7,-3,-1)        181.3535         calculate D2E/DX2
analytical!
```

```
 ! A6    L(2,3,5,-1,-2)          180.              calculate D2E/DX2
analyticall!
 ! A7    L(3,5,7,-1,-2)          180.              calculate D2E/DX2
analyticall!
 ! A8    L(1,2,3,4,-1)           178.0659          calculate D2E/DX2
analyticall!
 ! A9    L(1,2,3,4,-2)           180.              calculate D2E/DX2
analyticall!
 ---------------------------------------------------------------------
------
 Trust Radius=3.00D-01 FncErr=1.00D-07 GrdErr=1.00D-07
 Number of steps in this run=  25 maximum allowed number of steps= 100.

GradGradGradGradGradGradGradGradGradGradGradGradGradGradGradGradGradGrad

                         Input orientation:
 ---------------------------------------------------------------------
 Center     Atomic     Atomic              Coordinates (Angstroms)
 Number     Number      Type              X           Y           Z
 ---------------------------------------------------------------------
    1          6          0        1.353394    2.452310    0.000000
    2          6          0        0.611141    1.176564    0.000000
    3          7          0        0.000000    0.203293    0.000000
    4          1          0        0.715074    3.347259    0.000000
    5          1          0       -1.144274   -1.572898    0.000000
    6          8          0        2.550795    2.490333    0.000000
    7         17          0       -1.868492   -2.640784    0.000000
 ---------------------------------------------------------------------
                  Distance matrix (angstroms):
                       1          2          3          4          5
     1  C    0.000000
     2  C    1.475963   0.000000
     3  N    2.624834   1.149239   0.000000
     4  H    1.099266   2.173181   3.224260   0.000000
     5  H    4.737156   3.262058   2.112869   5.259764   0.000000
     6  O    1.198005   2.342700   3.425946   2.025881   5.492120
     7  Cl   6.026620   4.552002   3.402945   6.521615   1.290299
                       6          7
     6  O    0.000000
     7  Cl   6.771887   0.000000
                    Interatomic angles:
       C1-C2-N3=178.0659        C2-C1-H4=114.3101        N3-C1-H4=113.4634
       N3-C2-H4=150.6155        C1-N3-H5=178.2475        C2-N3-H5=179.3349
       C2-C1-O6=122.0104        N3-C1-O6=122.8571        N3-C2-O6=156.2363
       H4-C1-O6=123.6795        C2-H4-O6= 67.7178        N3-H5-Cl7=178.6465

                      1                      2                      3
                     A'                     A"                     A'
 Frequencies --    28.9835                34.8121                87.2008
 Red. masses --    11.1988                 5.6149                14.0356
 Frc consts  --     0.0055                 0.0040                 0.0629
 IR Inten    --     1.4474                 4.2197                 3.3057
 Raman Activ --     0.0000                 0.0000                 0.0000
 Depolar     --     0.0000                 0.0000                 0.0000
 Atom AN      X      Y      Z        X      Y      Z        X      Y
Z
   1   6    -0.13   0.01   0.00     0.00   0.00  -0.26     0.21   0.25
0.00
   2   6     0.25  -0.21   0.00     0.00   0.00   0.17     0.17   0.26
0.00
```

3	7	0.51	-0.38	0.00	0.00	0.00	0.48	0.10	0.30
0.00									
4	1	-0.40	-0.19	0.00	0.00	0.00	-0.76	0.22	0.26
0.00									
5	1	0.20	-0.19	0.00	0.00	0.00	0.26	-0.31	-0.38
0.00									
6	8	-0.15	0.37	0.00	0.00	0.00	-0.08	0.21	0.24
0.00									
7	17	-0.17	0.07	0.00	0.00	0.00	-0.11	-0.26	-0.40
0.00									

	4	5	6
	A'	A"	A'
Frequencies --	229.4370	298.4490	409.3439
Red. masses --	7.5304	4.3551	1.0574
Frc consts --	0.2336	0.2286	0.1044
IR Inten --	7.8629	0.0028	30.7792
Raman Activ --	0.0000	0.0000	0.0000
Depolar --	0.0000	0.0000	0.0000

Atom	AN	X	Y	Z	X	Y	Z	X	Y
Z									
1	6	-0.09	0.20	0.00	0.00	0.00	-0.06	0.01	-0.01
0.00									
2	6	-0.29	0.34	0.00	0.00	0.00	0.48	0.00	-0.01
0.00									
3	7	0.40	-0.09	0.00	0.00	0.00	-0.24	-0.05	0.02
0.00									
4	1	0.27	0.45	0.00	0.00	0.00	-0.69	0.00	-0.02
0.00									
5	1	0.36	-0.27	0.00	0.00	0.00	-0.48	0.83	-0.56
0.00									
6	8	-0.07	-0.32	0.00	0.00	0.00	-0.05	0.01	0.01
0.00									
7	17	-0.02	-0.01	0.00	0.00	0.00	0.01	-0.01	0.01
0.00									

	7	8	9
	A"	A'	A'
Frequencies --	417.9812	619.8753	910.3577
Red. masses --	1.0883	11.4699	6.4232
Frc consts --	0.1120	2.5967	3.1363
IR Inten --	30.2301	3.9433	134.3952
Raman Activ --	0.0000	0.0000	0.0000
Depolar --	0.0000	0.0000	0.0000

Atom	AN	X	Y	Z	X	Y	Z	X	Y
Z									
1	6	0.00	0.00	0.00	-0.30	-0.01	0.00	0.03	0.56
0.00									
2	6	0.00	0.00	0.04	0.63	-0.01	0.00	0.13	-0.27
0.00									
3	7	0.00	0.00	-0.06	0.10	0.40	0.00	-0.16	-0.18
0.00									
4	1	0.00	0.00	-0.04	-0.38	-0.05	0.00	0.21	0.69
0.00									
5	1	0.00	0.00	1.00	0.04	-0.04	0.00	0.01	0.01
0.00									
6	8	0.00	0.00	0.00	-0.31	-0.32	0.00	0.01	-0.11
0.00									
7	17	0.00	0.00	-0.02	0.00	0.00	0.00	0.00	0.00
0.00									

	10	11	12
	A"	A'	A'

Frequencies --		1001.2931			1409.2878			1778.9121		
Red. masses --		1.7478			1.1594			10.3534		
Frc consts --		1.0324			1.3567			19.3038		
IR Inten --		0.2898			10.3420			165.5255		
Raman Activ --		0.0000			0.0000			0.0000		
Depolar --		0.0000			0.0000			0.0000		
Atom	AN	X	Y	Z	X	Y	Z	X	Y	Z
1	6	0.00	0.00	0.23	-0.02	-0.08	0.00	0.70	0.05	0.00
2	6	0.00	0.00	-0.09	0.02	-0.02	0.00	-0.03	0.01	0.00
3	7	0.00	0.00	0.01	0.00	0.00	0.00	0.02	0.01	0.00
4	1	0.00	0.00	-0.97	0.85	0.51	0.00	-0.02	-0.50	0.00
5	1	0.00	0.00	0.00	0.00	0.00	0.00	0.02	0.01	0.00
6	8	0.00	0.00	-0.06	-0.06	0.04	0.00	-0.51	-0.02	0.00
7	17	0.00	0.00	0.00	0.00	0.00	0.00	0.00	0.00	0.00

		13			14			15		
		A'			A'			A'		
Frequencies --		2335.3006			2787.1527			2999.7142		
Red. masses --		12.5909			1.0372			1.0881		
Frc consts --		40.4570			4.7470			5.7690		
IR Inten --		27.1179			601.3638			25.4431		
Raman Activ --		0.0000			0.0000			0.0000		
Depolar --		0.0000			0.0000			0.0000		
Atom	AN	X	Y	Z	X	Y	Z	X	Y	Z
1	6	0.00	-0.07	0.00	0.00	0.00	0.00	0.05	-0.07	0.00
2	6	0.41	0.67	0.00	0.00	0.01	0.00	0.00	0.00	0.00
3	7	-0.32	-0.51	0.00	0.00	0.00	0.00	0.00	0.00	0.00
4	1	-0.02	-0.06	0.00	0.01	-0.01	0.00	-0.56	0.82	0.00
5	1	-0.05	-0.07	0.00	0.56	0.83	0.00	0.00	0.01	0.00
6	8	-0.03	0.00	0.00	0.00	0.00	0.00	0.00	0.00	0.00
7	17	0.00	0.00	0.00	-0.02	-0.02	0.00	0.00	0.00	0.00

- Thermochemistry -

Temperature 298.150 Kelvin. Pressure 1.00000 Atm.
Atom 1 has atomic number 6 and mass 12.00000
Atom 2 has atomic number 6 and mass 12.00000
Atom 3 has atomic number 7 and mass 14.00307
Atom 4 has atomic number 1 and mass 1.00783
Atom 5 has atomic number 1 and mass 1.00783
Atom 6 has atomic number 8 and mass 15.99491
Atom 7 has atomic number 17 and mass 34.96885
Molecular mass: 90.98249 amu.
Principal axes and moments of inertia in atomic units:

```
                       1         2         3
    EIGENVALUES --    34.63573  2466.63840  2501.27413
          X            0.59947   0.80040   0.00000
          Y            0.80040  -0.59947   0.00000
          Z            0.00000   0.00000   1.00000
 THIS MOLECULE IS AN ASYMMETRIC TOP.
 ROTATIONAL SYMMETRY NUMBER  1.
 ROTATIONAL TEMPERATURES (KELVIN)       2.50070      0.03511      0.03463
 ROTATIONAL CONSTANTS (GHZ)            52.10634      0.73166      0.72153
 Zero-point vibrational energy      91802.0 (Joules/Mol)
                                   21.94121 (Kcal/Mol)
 WARNING-- EXPLICIT CONSIDERATION OF   8 DEGREES OF FREEDOM AS
           VIBRATIONS MAY CAUSE SIGNIFICANT ERROR
 VIBRATIONAL TEMPERATURES:     41.70    50.09   125.46   330.11   429.40
          (KELVIN)            588.95   601.38   891.86  1309.79  1440.63
                             2027.64  2559.44  3359.96  4010.07  4315.89

 Zero-point correction=                           0.034966
(Hartree/Particle)
 Thermal correction to Energy=                    0.042082
 Thermal correction to Enthalpy=                  0.043026
 Thermal correction to Gibbs Free Energy=         0.001569
 Sum of electronic and zero-point Energies=          -667.611654
 Sum of electronic and thermal Energies=             -667.604537
 Sum of electronic and thermal Enthalpies=           -667.603593
 Sum of electronic and thermal Free Energies=        -667.645050
```

Appendix C

Preliminary results.

C.1 A Comparison of Different Basis Sets and Calculation Methods for HCN and HF

The experimentally determined structural parameters and IR frequencies of both HCN and HF are well documented[C1,C2], and therefore provide a good bench mark for testing the accuracy of Gaussian calculations at different levels. The following Z-Matrices were used for the optimisation of the geometries of HCN and HF:

HF OPT Z-MATRIX

#<calc method>/<basis set> OPT
0,1
F
H,1,R

R=0.90209

HCN OPT Z-MATRIX

#<calc method>/<basis set> OPT
0,1
N
C,1,CN
H,2,CH,1,HCN

CN=1.164
CH=1.05
HCN=180.0

Where the calculation method was selected from HF and MP2, and the basis set from 3-21G, 3-21G*, 3-21G**, 3-21+G*, 6-31G*, 6-31+G*, 6-311++G**, STO-3G, STO-4G. These were chosen from the documented calculation methods and basis sets[C3].

The resulting optimised geometry was then submitted again, but this time the IR frequencies were calculated - i.e. OPT was changed to FREQ=ANAL. The resulting Gaussian output files were then fed into Animol [C4] so that the resulting spectra could be analysed. Animol applies a default frequency correction factor of 0.8929[C5] to any imported Gaussian spectrum, which might be regarded as an empirical correction for vibrational anharmonicity as well as overestimation of the force constants in the theory

Table C.1 shows the results of this comparison.

C.1.1 Comments

Considering the overall discrepancies between the results for all calculation methods and basis sets used, deciding which to use appears entirely arbitrary - what seems to give good results for one molecule, provides quite erroneous results for an other (eg. HF/STO-3G provides a 0.53% difference between calculated and experimental frequencies for the HF stretch, but an 18.9% difference for the CH bend). Also a suitable cut-off point must be established when deciding the difference between good and bad results. When selecting a basis set/calculation method, not only must the calculation time be a point of consideration, but also the molecule in question - do we really need to be able to perform calculations for elements up to xenon, when our molecule only consists of atoms up to nitrogen? Taking all of this into account, the HF calculation method and 3-21G, or possibly 6-31G basis sets provide a suitable compromise for further calculations.

C.2 Intramolecular Hydrogen Bonding - 2-Fluoroethanol

The 2-fluoroethanol molecule is an ideal molecule for intramolecular hydrogen bond studies. It has the fluorine and oxygen atoms at opposite ends of the molecule so any H-bonding that occurs is subjected to a torsional strain across the C–C bond, and this allows conformational analysis to be achieved. The non-interacting atoms, the hydrogen atoms bonded to the carbon atoms (two hydrogen atoms per carbon atom), are small and provide a negligible effect on any weakly bound interactions that might occur.

C.2.1 Chem-X Results

The molecule, 2-fluoroethanol, generated has the structure shown in Fig. C.1, and the structural parameters shown in Table C.2. Clearly, Chem-X has decided that the cis-conformer is the lowest energy form. The Van der Waals and Molecular Mechanics energies were calculated to be 7.0549 kcals and 6.5418 kcals respectively. This structure was then optimised using the MM Optimisation function, with the VdW Minimisation as a precursor. The resulting changes in structure and parameters are shown in Fig. C.2 and Table C.3 respectively. The new VdW and MM Energies were then calculated to be 6.7233

kcals and 6.2436 kcals, showing a decrease in energy of 0.3316 kcals and 0.2972 kcals respectively.

The optimised structure was then subjected to a conformation study. The O1–C2 and C2–C3 bonds were chosen, because they are the only bonds with torsional properties. Each bond was allowed 72 steps through the 360° rotation, giving an energy reading every 5°. This provided a database with 72^2 (5184) conformers, from which the lowest energy conformer can be chosen. The plots in Fig. C.3 and Fig. C.4 show the energy change of the molecule as the O1–C2 and C2–C3 bonds are rotated through 360°. From these plots it is possible to find the global minimum energy value, and thus view the structure from the database of conformers. Fig. C.5 shows the superposition of Fig. C.3 and Fig. C.4 providing an overall energy plot for the 2-fluoroethanol molecule, undergoing simultaneous rotations of the O1–C2 and C2–C3 bonds.

From the conformer generation, it was found that number 22 in the database had the lowest energy. The VdW energy was calculated as 5.9971 kcals, and the MM energy as 5.5283 kcals. Fig. C.6 shows this conformer, with the structural parameters in Table C.4, with the fluorine (F4) and the OH (O1,H5) atoms spread as far apart as possible. This is as expected, since the atoms repel to produce the most stable, lowest energy structure available. Note that Chem-X did not allow a hydrogen bond between F4 and H5. This has to be performed manually by setting the O1C2C3F4 and H5O1C2C3 torsion angles to 0°, to form the cis- conformer, and then creating the H-bond. After this manipulation, but before the H-bond was inserted, the VdW and MM energies were calculated to be 24.6709 kcals and 25.6735 kcals respectively. After the H-bond addition these energies were reduced to 14.9159 and 12.2905 kcals respectively. Thus the Chem-X H-bond is not a purely cosmetic feature, and does affect the energy calculation of the molecule. The molecule is shown in Fig. C.7.

When this H-bonded molecule was subjected to a conformational analysis, the results are very surprising. The same bonds were specified for the torsional analysis (O1–

C2 and C2–C3) and were also given the same number of steps (72). The structure with the minimum energy was found to be number 2629 (out of 5184) in the database. It had a VdW energy of 6.0006 kcals and a MM energy of 5.5337 kcals. However, the structure has now reverted back to that of the result obtained by the initial conformer study - i.e. the trans- conformer, and the H-bond is stretched across the molecule apparently dissecting the C2–C3 bond, which is clearly erroneous (Fig. C.7). Figs. C.8, C.9 and C.10 show the VdW energy plots for the bond rotations as before.

C.2.2 Gaussian 94

The optimised molecule in Fig. C.2 (trans-conformer) provides a good starting point for *ab initio* calculations, since the molecular parameters are close to the actual ones. This will reduce the calculation time and also reduce the likelihood of the calculation converging on a local minimum instead of the desired global minimum.

Fig. C.10 shows the Z-Matrix for 2-fluoroethanol after the PDB structure file for Fig. C.2 had been successfully converted by Gaussian 94. The basis set chosen was a standard 3-21G and the calculation method, RHF, is the spin-restricted Hartree-Fock Theory. The resulting optimised parameters (from the output file) are then fed into a Chem-X representation of the molecule. Fig. C.12 shows this molecule, and Table C.5 displays the structural parameters.

If the cis- conformer is then optimised by Gaussian (by setting the torsional angles O1-C2 and C2-C3 to zero), and the results fed into Chem-X, the molecule remains in the cis- conformation as shown in Fig C.13, together with the structural parameters in Table C.6.

Fig. C.14 shows the Gaussian generated IR spectrum for the cis and trans conformers of the molecule, with Table C.7 out lining some of the main peak frequencies, together with the corresponding experimental values.

C.2.3 Comments

From these results, it appears that Chem-X cannot decide whether H-bonding affects the stability of the molecular conformers. When a conformation generation is performed, Chem-X clearly rotates both torsional bonds completely, and only considers the global energy minimum, which is decided to be the only stable conformer, and this is why the H-bonded cis- conformer reverted back to the trans- conformer, even though a H-bond had been created between the fluorine atom and the OH hydrogen atom. To find other stable conformers, one must look for energy minima in the generated plots, and decide on the validity of the structures at these points.

Gaussian, however, is able to distinguish between stable conformers, providing that the starting geometry specified in the Z-Matrix is within the boundaries of a local minimum. Gaussian then minimises the energy towards this local minimum, adjusting the structure as it does so. But this means that Gaussian will not find the global energy minimum if the starting geometry is not within the confines of the global minimum.

Table C.8 provides experimental data on some of the structural parameters of 2-Fluoroethanol[C6,C7]. Both the Chem-X and Gaussian results are reasonably consistent with these, however, it is felt that while the Chem-X parameters are based upon in-built values, the Gaussian parameters are the result of quantum mechanical calculations, and so their validity is not as questionable.

The optimisation of the cis conformer also reveals the overlapping of the Van der Waals radii of the F and H atoms that constitute the expected H-bond (Fig. C.17). Since the F and O atoms are in close proximity, we would expect a repulsion due their high electroegativities, resulting in the molecule reverting back to the trans conformer. This implies that Gaussian has calculated that the electronic orbitals of the F and H atoms overlap sufficiently for an association to occur, which is stronger than the repulsion. Thus it appears that Gaussian has predicted the formation of a H-bond for the cis conformer in agreement with experimental results

C.3 Intermolecular Hydrogen Bonding - HCN · · · HF

The simplicity of the HCN···HF dimer provides a good reference point for molecular modelling, and it is also a well documented system[C1,C2,].

The following Z-Matrix was used to generate the optimised structure for the dimer after it had been built in Chem-X:

```
# HF/3-21G OPT

HCN...HF DIMER 30/11/95

0,1
X1
N2,1,X1N2
C3,2,N2C3,1,90.0
H4,3,C3H4,2,180.0,1,0.0,0
F5,4,H4F5,3,180.0,2,0.0,0
H6,5,F5H6,4,180.0,3,0.0,0

X1N2=1.0
N2C3=1.1378
C3H4=1.0542
H4F5=1.88
F5H6=0.9370
```

Table C.9 compares the generated structural parameters with those obtained experimentally.

The IR frequencies for HF, HCN, and the dimer were then calculated from the optimised geometries (for HF and HCN, the geometries calculated in C.1 were used) and Fig C.16 shows the resulting spectra as extracted from the output files by Animol, with Table C.10 detailing the bands, together with the experimental values[C6,C7].

C.3.1 Comments

Gaussian is able to predict with a reasonable degree of accuracy (~10% maximum deviation) between the experimental[C8] IR spectroscopic frequencies of HF, HCN and the HCN...HF dimer and the calculated ones. Some discrepancy in the CH stretches can be attributed to anharmonicity, which Gaussian does not take into account, since it calculates the frequencies assuming harmonic vibrations.

It must be noted that Gaussian also appears to correctly calculate the way in which the vibrational frequencies shift due to H-bonding. Normally, there is a decrease in the vibrational frequency of the covalent bonds of the atoms involved in the H-bonding, as the shift in frequency of the HF stretch shows. However, the CN stretch increases in frequency (see Table C.9). This has been documented by George et al.[C9] in both matrix isolation and gas phase. The explanation for this is assumed to be a result of the anti-bonding properties of the free lone pair of electrons on the nitrogen atom. When the complex is formed, the anti-bonding electrons are effectively removed from any interaction with the triple CN bond. This causes the bond to strengthen, and thus the frequency of the CN stretch increases.

Nevertheless, further calculations on other cyanides must be performed to verify that this is correct prediction by Gaussian, and not just an anomaly of this particular system.

C.4 Figures for Appendix C.

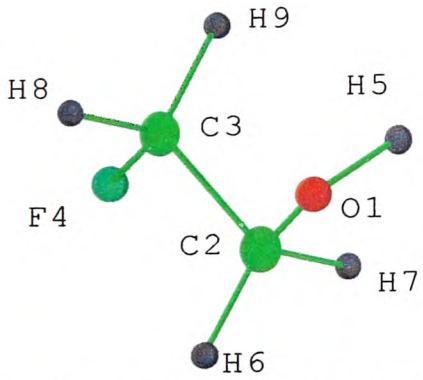

Fig C.1 - Structure of 2-fluoroethanol as generated by Chem-X.

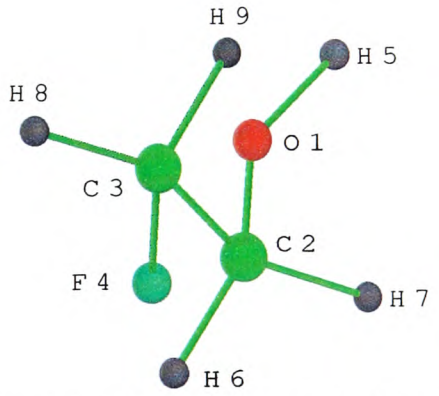

Fig C.2. 2-fluoroethanol after VdW minimisation and MM optimisation.

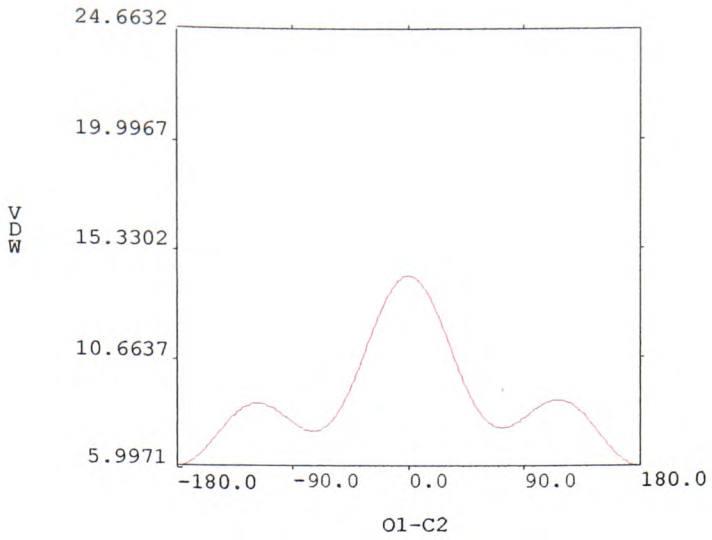

Fig C.3 - Plot of VdW energy for 2-fluoroethanol as a function of the O1C2 torsion angle.

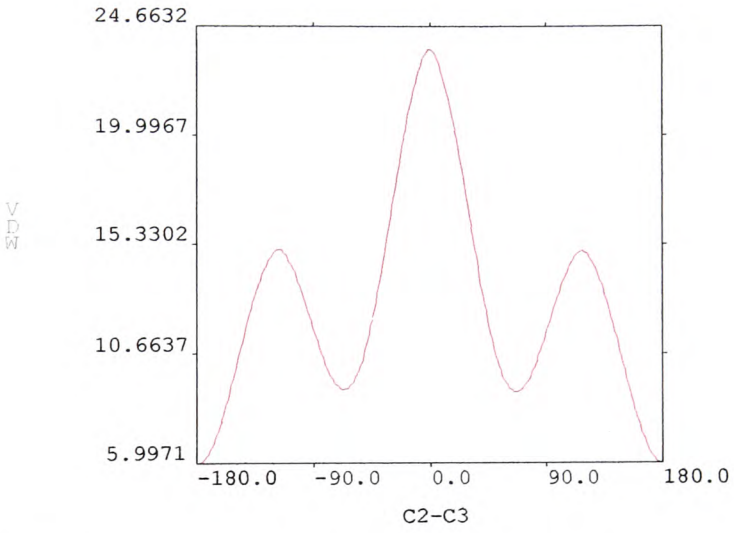

Fig C.4 - Plot of VdW energy for 2-fluoroethanol as a function of the C2C3 torsion angle.

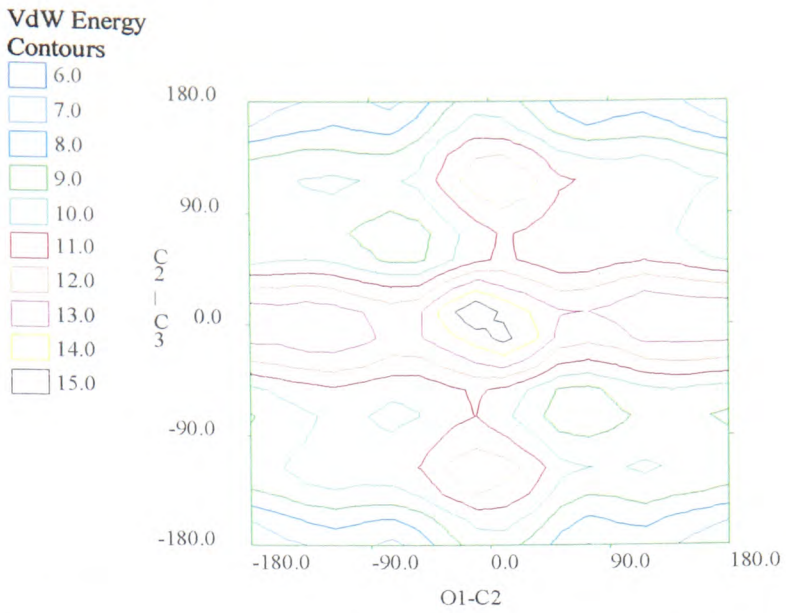

Fig C.5 - A VdW energy contour plot for the simultaneous rotation of the O1C2 and C2C3 bonds in 2-fluoroethanol.

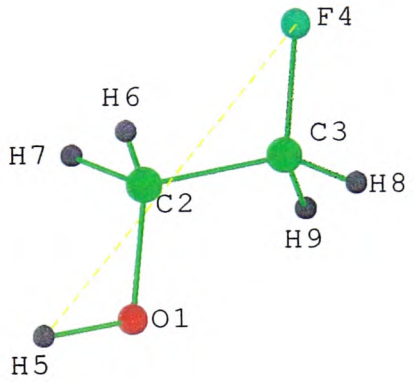

Fig C.6 - Lowest energy conformer

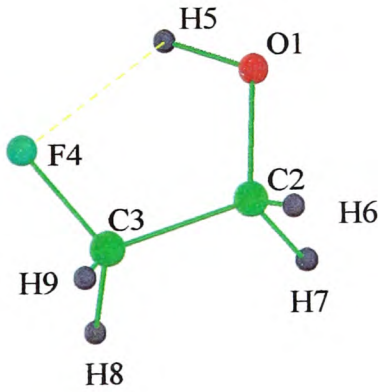

Fig C.7 - H-bonded cis conformer

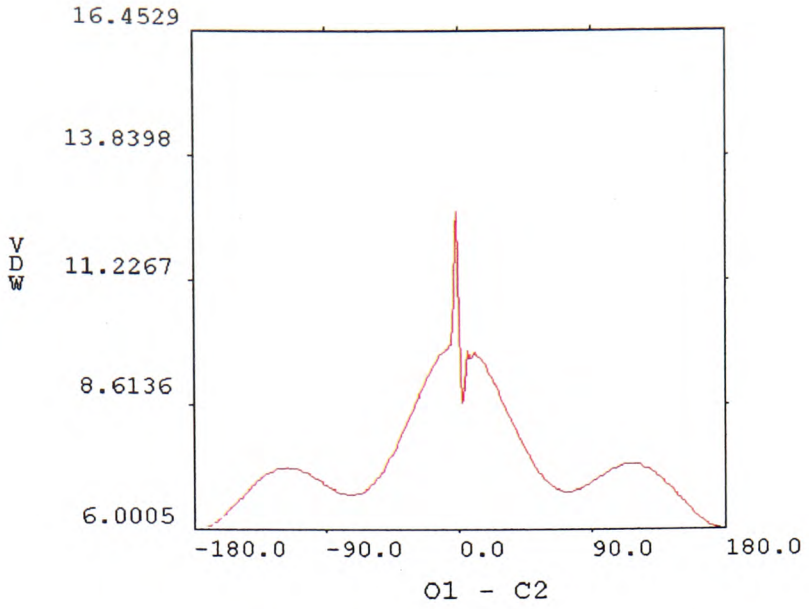

Fig C.8 - VdW energy plot for the O1-C2 torsion for the cis H-bonded conformer.

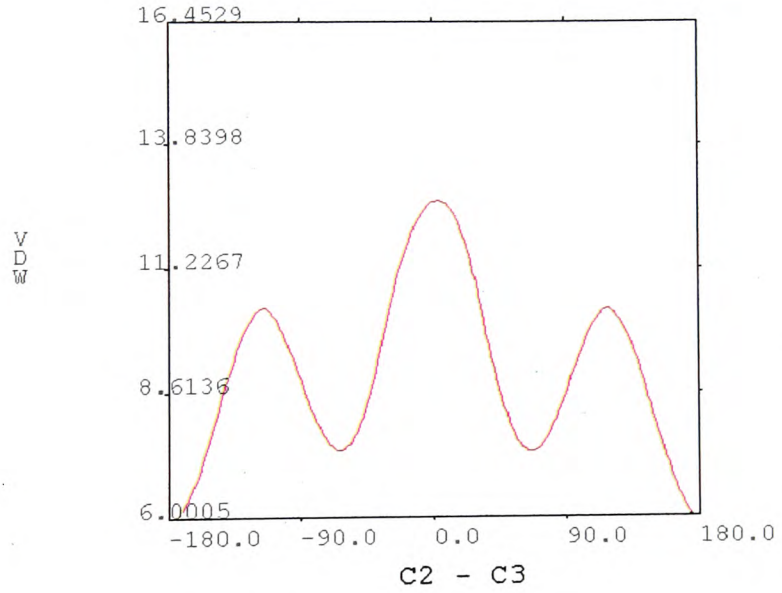

Fig C.9 - VdW energy plot for the C2-C3 torsion for the cis H-bonded conformer.

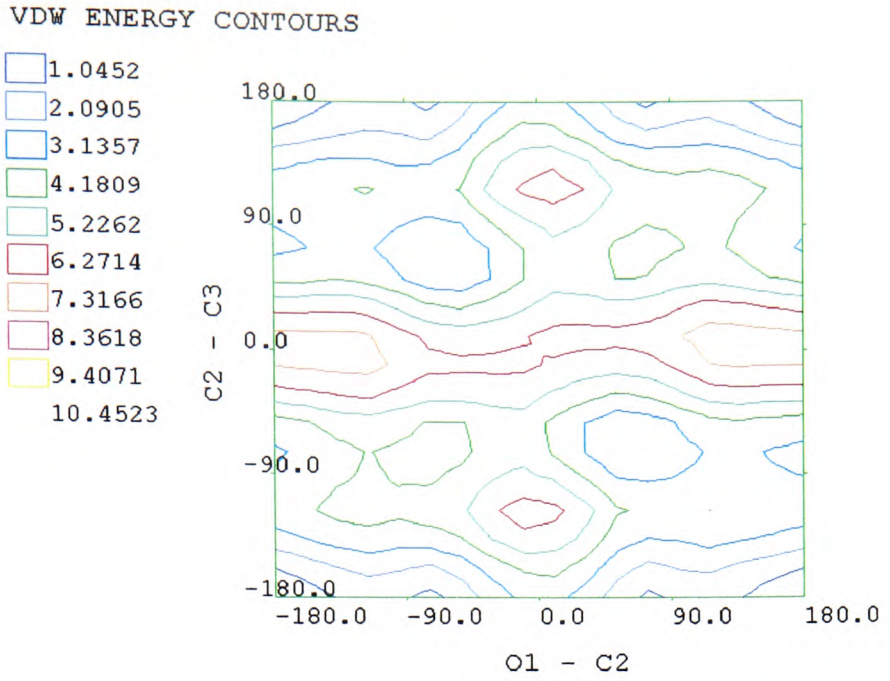

Fig C.10 - VdW energy plot for the O1-C2 and C2-C3 torsional rotations for the cis H-bonded conformer

#RHF/3-21G OPT

2-fluoroethanol optimisation.

0 1
F
C,1,R2
C,2,R3,1,A3
O,2,R4,1,A4,3,0.,0
H,2,R5,1,A5,3,0.,0
H,2,R6,1,A6,3,D6,0
H,3,R7,2,A7,1,D7,0
H,6,R8,2,A8,1,D8,0
H,3,R9,2,A9,1,D9,0
Variables:
R2=1.38
R3=1.52272388
R4=2.40033685
R5=3.21834771
R6=1.07968977
R7=2.13351025
R8=2.46735547
R9=1.08009675
A3=109.96788007
A4=143.39870406
A5=133.41748456
A6=109.9844341
A7=28.59751515
A8=60.29002652
A9=110.04921018
D6=-119.97764876
D7=120.60738402
D8=96.2405868
D9=60.02582697

Fig C.11 - The 2-fluoroethanol Z-Matrix imported to Gaussian 94 from the Chem-X PDB file (formatted into two columns to save space).

Fig C.12 - The Gaussian optimised trans conformer of 2-fluoroethanol.

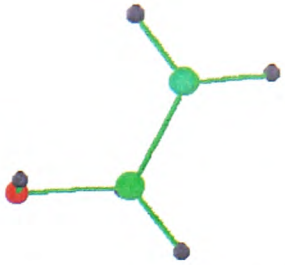

Fig C.13 - The Gaussian optimised cis conformer of 2-fluoroethanol.

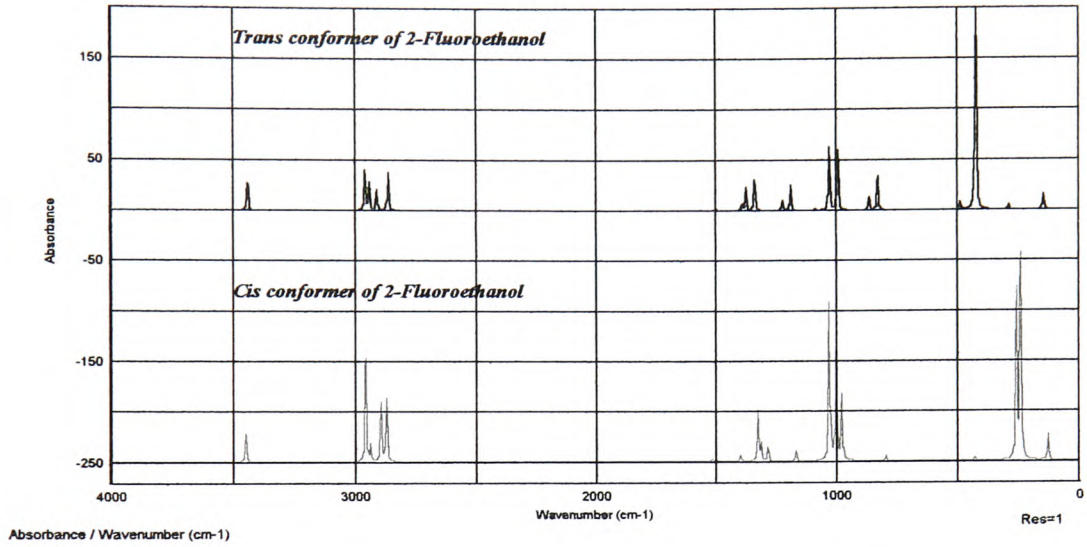

Fig C.14 - The Calculated spectra for the trans and cis conformers of 2-fluoroethanol.

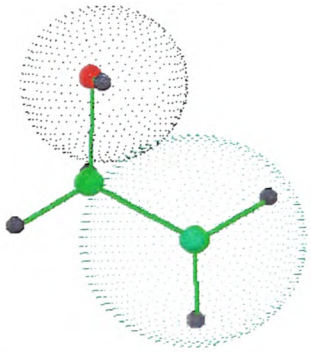

Fig C.15 - The optimised cis conformer of 2-fluoroethanol showing the overlapping Van der Waals radii.

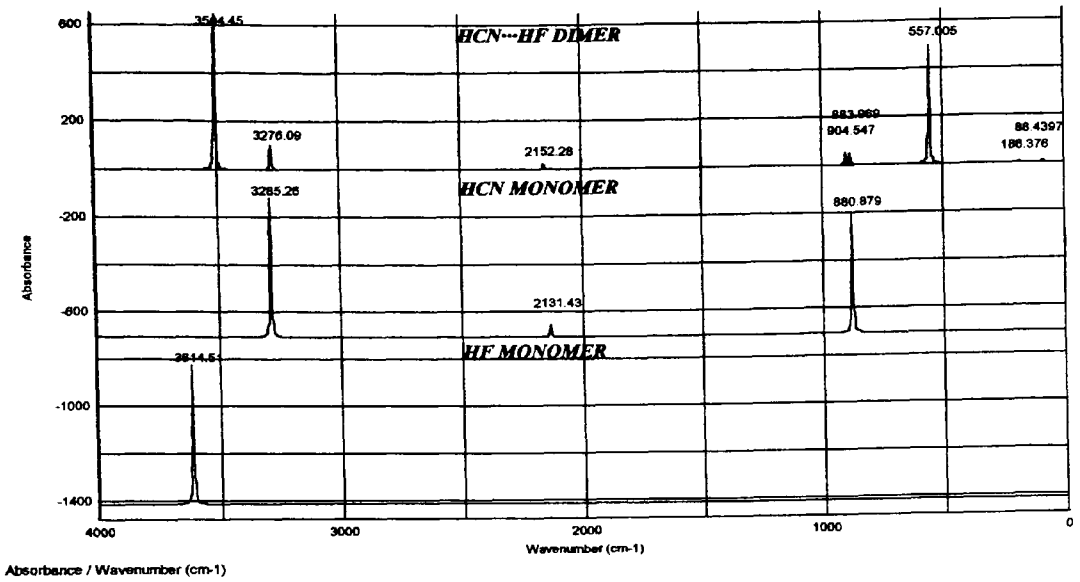

Fig C.16 - Calculated spectra of HCN...HF, HCN, HF, showing the frequencies of each peak.

C.5 Tables for Appendix C.

Basis Set	*H–F Length*	*H–F Stretch*	*Thry:Expt*	*×Animol Factor*	*C≡N Length*	*C≡N Stretch*	*Thry:Expt*	*×Animol Factor*
RHF/3-21G	0.93745	4061.26	1.0251565	0.9123893	1.13718	2394.56	1.1419796	1.0163619
RHF/3-21G*	0.93744	4061.41	1.0251944	0.912423	1.13718	2394.54	1.1419701	1.0163534
RHF/3-21G**	0.90209	4313.92	1.0889338	0.9691511	1.13716	2397.67	1.1434628	1.0176819
RHF/3-21+G*	0.94154	4040.52	1.0199212	0.9077299	1.13922	2360.6	1.1257839	1.0019477
RHF/6-31G*	0.91106	4356.17	1.0995986	0.9786428	1.13249	2438.6	1.1629826	1.0350545
RHF/6-31+G*	0.91345	4314.07	1.0889716	0.9691847	1.13302	2426.29	1.1571119	1.0298296
RHF/6-311G**	0.8961	4510.29	1.1385021	1.0132669	1.12651	2413.37	1.1509502	1.0243457
RHF/6-311++G**	0.89729	4493.84	1.1343498	1.0095713	1.12708	2406.53	1.1476882	1.0214425
RHF/STO-3G	0.95546	4474.97	1.1295865	1.005332	1.15292	2541.96	1.2122756	1.0789252
RHF/STO-4G	0.95452	4412.59	1.1138404	0.9913179	1.1544	2519.88	1.2017455	1.0695535
MP2/3-21G	0.9586	3759.08	0.9488792	0.8445025	1.18621	1942.26	0.9262751	0.8243849
MP2/3-21+G*	0.97016	3671.4	0.9267468	0.8248046	1.18915	2031.43	0.9688008	0.8622327
MP2/6-31G*	0.93397	4039.56	1.0196789	0.9075142	1.17283	2071.71	0.9880106	0.8793294
MP2/6-31+G*	0.94091	3941.39	0.9948985	0.8854597	1.17814	2030.05	0.9681427	0.861647
MP2/6-311**	0.91281	4251.77	1.0732457	0.9551886	1.17069	2020.98	0.9638172	0.8577973
MP2/6-311++G**	0.91662	4198.73	1.0598571	0.9432728	1.17143	2015.51	0.9612085	0.8554755
MP2/STO-3G	0.97518	4145.34	1.0463803	0.9312784	1.22359	1900.11	0.9061735	0.8064945
MP2/STO-4G	0.97471	4084.63	1.0310556	0.9176395	1.22744	1876.59	0.8949567	0.7965115
HF/3-21G	0.93752	4060.32	1.0249192	0.9121781	1.13718	2394.54	1.1419701	1.0163534
HF/6-31G*	0.91106	4356.17	1.0995986	0.9786428	1.13249	2438.6	1.1629826	1.0350545
HF/6-311++G**	0.89744	4491.32	1.1337137	1.0090051	1.12705	2406.74	1.1477883	1.0215316
HF/STO-4G	0.95452	4412.59	1.1138404	0.9913179	1.1544	2265.86	1.0806019	0.9617357

Basis Set	*C–H Length*	*C–H Stretch*	*Thry:Expt*	*×Animol Factor*	*C–H Bend (×2)*	*Thry:Expt*	*×Animol Factor*	*HCN Angle*
RHF/3-21G	1.05012	3692.37	1.115048	0.9923927	989.22	1.389393	1.2365597	180
RHF/3-21G*	1.05012	3692.37	1.115048	0.9923927	989.22	1.389393	1.2365597	180
RHF/3-21G**	1.04658	3787.6	1.1438062	1.0179876	958.64	1.3464423	1.1983337	180
RHF/3-21+G*	1.05246	3660.97	1.1055656	0.9839534	976.93	1.3721312	1.2211968	180
RHF/6-31G*	1.05893	3680.6	1.1114936	0.9892293	888.75	1.2482794	1.1109687	180
RHF/6-31+G*	1.05994	3666.73	1.1073051	0.9855015	878.84	1.2343605	1.0985809	180
RHF/6-311G**	1.05773	3624.54	1.0945642	0.9741622	891.42	1.2520296	1.1143063	180
RHF/6-311++G**	1.05823	3620.5	1.0933442	0.9730763	877.67	1.2327172	1.0971183	180
RHF/STO-3G	1.06977	3918.4	1.1833062	1.0531425	951.15	1.3359224	1.1889709	180
RHF/STO-4G	1.06823	3903.68	1.1788609	1.0491862	949.28	1.3332959	1.1866333	180
MP2/3-21G	1.06445	3501.17	1.0573081	0.9410042	839.99	1.1797944	1.050017	180
MP2/3-21+G*	1.06861	3485.98	1.0527209	0.9369216	1036.41	1.4556729	1.2955489	180
MP2/6-31G*	1.06853	3521.82	1.0635441	0.9465543	717.84	1.0082306	0.8973252	180
MP2/6-31+G*	1.07098	3492.47	1.0546808	0.9386659	687.48	0.9655889	0.8593741	180
MP2/6-311**	1.0671	3492.54	1.0547019	0.9386847	757.05	1.0633023	0.9463391	180
MP2/6-311++G**	1.06789	3483.6	1.0520022	0.9362819	728.69	1.0234698	0.9108881	180
MP2/STO-3G	1.0876	3670.89	1.1085613	0.9866196	758.83	1.0658024	0.9485641	180
MP2/STO-4G	1.08612	3655.08	1.1037869	0.9823704	754.07	1.0591168	0.942614	180
HF/3-21G	1.05012	3692.37	1.115048	0.9923927	989.22	1.389393	1.2365597	180
HF/6-31G*	1.05893	3680.6	1.1114936	0.9892293	888.75	1.2482794	1.1109687	180
HF/6-311++G**	1.05823	3620.52	1.0933502	0.9730817	877.68	1.2327313	1.0971308	180
HF/STO-4G	1.06823	3506.4	1.0588875	0.9424099	1056.47	1.4838479	1.3206246	180

Notes: The experimental values used are: HF Stretch=3961.6cm^{-1}; CN Stretch=2096.85 cm^{-1}; CH Stretch=3311.40 cm^{-1}; CH Bend=711.98 cm-1; CH bond length=1.07A; CN bond length=1.15 A; HF bond length=0.91A; Animol correction factor=0.89

Table C.1 - The comparison of results produced by different basis sets/calculation methods for HCN and HF.

Bond Length	Value (A)	Bond Angle	Value (Degs)	Torsional Angle	Value (Degs)
O1C2	1.407	O1C2C3	110	O1C2C3F4	180
C2C3	1.523	C2C3F4	110	H5O1C2C3	-90
C3F4	1.38	C2O1H5	107.5		
O1H5	0.95	C3C2H6	108.9		
C2H6	1.08	C3C2H7	108.9		
C2H7	1.08	C2C3H8	110		
C3H8	1.08	C2C3H9	110		
C3H9	1.08				

Table C.2 - Structural parameters for 2-fluoroethanol as generated by Chem-X.

Bond Length	Value (A)	Bond Angle	Value (Degs)	Torsional Angle	Value (Degs)
O1C2	1.412	O1C2C3	109.9	O1C2C3F4	179.6
C2C3	1.526	C2C3F4	109.8	H5O1C2C3	-74.2
C3F4	1.381	C2O1H5	108.6		
O1H5	0.953	C3C2H6	109		
C2H6	1.081	C3C2H7	109.6		
C2H7	1.082	C2C3H8	109.4		
C3H8	1.08	C2C3H9	109.4		
C3H9	1.08				

Table C.3 - Structural parameters after VdW minimisation and MM optimisation.

Bond Length	Value (A)	Bond Angle	Value (Degs)	Torsional Angle	Value (Degs)
O1C2	1.412	O1C2C3	109.9	O1C2C3F4	179.6
C2C3	1.526	C2C3F4	109.8	H5O1C2C3	-179.2
C3F4	1.381	C2O1H5	108.6		
O1H5	0.953	C3C2H6	109		
C2H6	1.081	C3C2H7	109.6		
C2H7	1.082	C2C3H8	109.4		
C3H8	1.08	C2C3H9	109.4		
C3H9	1.08				

Table C.4 - Structural parameters of the lowest energy conformer.

Bond Length	Value (A)	Bond Angle	Value (Degs)	Torsional Angle	Value (Degs)
O1C2	1.438	O1C2C3	104.3	O1C2C3F4	179.9
C2C3	1.514	C2C3F4	108.1	H5O1C2C3	-179.1
C3F4	1.408	C2O1H5	111.5		
O1H5	0.965	C3C2H6	109.6		
C2H6	1.083	C3C2H7	109.5		
C2H7	1.083	C2C3H8	110		
C3H8	1.078	C2C3H9	110.1		
C3H9	1.077				

Table C.5 - Gaussian optimised parameters for the trans conformer.

Bond Length	Value (A)	Bond Angle	Value (Degs)	Torsional Angle	Value (Degs)
O1C2	1.437	O1C2C3	109.1	O1C2C3F4	58.4
C2C3	1.513	C2C3F4	106.1	H5O1C2C3	-52.8
C3F4	1.418	C2O1H5	108.2		
O1H5	0.968	C3C2H6	109.5		
C2H6	1.084	C3C2H7	110.7		
C2H7	1.078	C2C3H8	112.5		
C3H8	1.078	C2C3H9	110.5		
C3H9	1.077				

Table C.6 - Gaussian optimised parameters for the cis conformer.

Assignment	Experimental	Trans Conformer	Cis Conformer
OH Stretch	3653	3446.8	3438.4
COH in plane bending	1351	1328	1340.7
CO stretch	1113	1002	1086.8
CF stretch	1039	1031.1	1030
CC stretch	888	797	862.59
CCO bend	516	428.73	486

Table C.7 - Comparison of the experimental IR and calculated frequencies for some of the main bands in the 2-fluoroethanol spectrum.

Bond Length	Value (A)	Bond Angle	Value (Degs)	Torsional Angle	Value (Degs)
O1C2	1.411	O1C2C3	112.8	O1C2C3F4	62.2
C2C3	1.503	C2C3F4	109	H5O1C2C3	55.5
C3F4	1.395	C2O1H5	105.8		
O1H5	1.008	C3C2H6	111.4		
C2H6	1.093	C3C2H7	111.4		
C2H7	1.093	C2C3H8	111.4		
C3H8	1.093	C2C3H9	111.4		
C3H9	1.093				

Table C.8 - Experimental parameters for 2-fluoroethanol from microwave data.

PARAMETER	EXPERIMENTAL VALUE	CALCULATED VALUE
HF Bond length	0.906 A	0.9420 A
CN Bond length	1.131 A	1.1351 A
CH Bond length	1.060 A	1.0511 A
HCN Angle	180.0 Degs	180.0 Degs
CNH Angle	180.0 Degs	180.0 Degs
NH Hydrogen bond distance	2.012 A	1.8662 A

Table C.9 - Comparison of the experimental and theoretical structural parameters for the HCN...HF dimer.

CALCULATED FREQUENCIES (cm^{-1})			
Species	Monomer	Dimer	Difference
HF stretch	3614.51	3504.45	-110.06
CH stretch	3285.26	3276.09	-9.17
CN stretch	2131.43	2152.28	20.85
HCN bend x2	2x 880.879	904.547/883.969	23.668/3.09
EXPERIMENTAL FREQUENCIES (cm^{-1})[C2]			
Species	Monomer	Dimer	Difference
HF stretch	3961.6	3716.2	-245.4
CH stretch	3311.4	3310.329	-1.071
CN stretch	2096.85	2120.933	24.083
HCN bend x2	2x711.98	2x726.531	14.551

Table C.10 - Calculated and experimental IR frequencies for HF, HCN and the HCN···HF dimer.